Studies on subcellular localization of dengue virus protease, consequential effects on cell homeostasis and evaluation of anti-protease molecules

Thesis submitted to the University of Hyderabad for the degree of Doctor of Philosophy

Submitted By
Lekha Gandhi
Enrollment No. 16 LTPH08



UNDER THE GUIDANCE OF

Dr. Musturi Venkataramana

Dept. of Biotechnology and Bioinformatics

School of Life Sciences

University of Hyderabad

Gachibowli, Hyderabad, Telangana -500046

CERTIFICATE

This is to certify that this thesis entitled "Studies on subcellular localization of dengue virus protease, consequential effects on cell homeostasis and evaluation of anti-protease molecules" submitted to the University of Hyderabad by Ms. Lekha Gandhi bearing registration number 16 LTPH08 for the degree of Doctor of Philosophy, is based on the studies carried out by her under my supervision.

This thesis is free from plagiarism and has not been submitted earlier in part or in full to this or any other University or Institution for the award of any degree or diploma.

Research Publications

- **1. Lekha Gandhi** and Musturi Venkataramana. Simultaneous detection of dual subcellular localized dengue virus protease by co-transfection. 2023. *STAR protocols* (Accepted, 2023).
- **2. Gandhi L**, Maisnam D, Rathore D, Chauhan P, Bonagiri A. and Venkataramana M, Differential localization of dengue virus protease affects cell homeostasis and triggers to thrombocytopenia. *iScience*. 2023. 26, (7): 10702. 10.1016/j.isci.2023.107024.
- **3. Gandhi L**, Maisnam, D, Rathore, Chauhan P, Bonagiri A, Venkataramana M. Respiratory illness virus infections with special emphasis on COVID-19. *Eur J Med Res*, 2022. 27: 236. 10.1186/s40001-022-00874-x.
- **4.** Gandikota C, **Gandhi L,** Maisnam D, Kesavulu MM, Billoria A, Prasad VSV, and Venkataramana M. A novel anti-NS2BNS3pro antibody-based indirect ELISA test for the diagnosis of dengue virus infections. *J Med Virol.* 2021. 93(6): 3312-3321. 10.1002/jmv.26024.

- **5**. Gandikota C, Mohammed F, **Gandhi L**, Maisnam D, Mattam U, Rathore D, Chatterjee A, Mallick K, Billoria A, Prasad VSV, Sepuri NBV, Venkataramana M. Mitochondrial Import of Dengue Virus NS3 Protease and Cleavage of GrpEL1, a Cochaperone of Mitochondrial Hsp70. *J Virol.* 2020. 17, 94(17): e01178-20. 10.1128/JVI.01178-20.
- **6.** Ganji L.R, **Gandhi L,** Venkataramana Musturi, Meena A. Kanyalkar. Design, synthesis, and evaluation of different scaffold derivatives against NS2B-NS3 protease of dengue virus. *Med Chem Res.* 2021. 30:285–301. 10.1007/s00044-020-02660-y.

B. Presented the research work at the following conferences:

- 1. International Conference on Virus Evolution, Infection and Disease Control-2022 (IVEIDC), 15th -17th December 2022. Dept. of Biotechnology and Bioinformatics, School of Life Sciences, University of Hyderabad (Oral Presentation). Awarded as one of the 'Best Oral presentation'.
- **2.** International Conference of Virology on Evolution of Viruses and Viral Diseases (VIROCON-2020), 18th-20th Feburary-2020, at the Indian National Science Academy, New Delhi, India (Poster Presentation).
- **3.** International Conference on Innovations in pharma and Biopharma Industry: Challenges and opportunities for academy and Industry. 20th -22nd December, 2017. School of LifeSciences, University of Hyderabad (Poster Presentation).
- **4.** Academia Sinica University of Hyderabad (AS-UoH) Joint Workshop on Frontiers in Life Sciences, 16th-17th, 2016, School of Life Sciences, University of Hyderabad.

Course Work Details

Course Code	Name	Pass/Fail
BT-801	Analytical Techniques	PASS

BT-802	Research Ethics, Data analysis	PASS
	and Biostatistics	
BT-803	Lab work and Seminar	PASS

Supervisor Head of the Department Dean of School



University of Hyderabad

Central University (P.O), Hyderabad-500046, India

DECLARATION

I hereby declare that the work presented in this thesis entitled "Studies on subcellular
localization of dengue virus protease, consequential effects on cell homeostasis and
evaluation of anti-protease molecules" is entirely original and was carried out by me in the
Department of Biotechnology & Bioinformatics, University of Hyderabad, under the
supervision of Dr. Musturi Venkataramana. I further declare that this work has not been
submitted earlier for the award of a degree or diploma from any other University or Institution.

Date: Ms. Lekha Gandhi

ACKNOWLEDGEMENTS

First and foremost, I would like to praise and thank God, for his countless blessings.

I would like to show my greatest appreciation to my supervisor Dr. Musturi Venkataramana for his continuous support, motivation and guidance throughout my research work.

I thank my doctoral committee members Dr. Kota Arun Kumar and Dr. N. Prakash Prabhu for timely suggestions and guidance.

I want to thank the present Head of the Department of Biotechnology and Bioinformatics, Prof. J. S. S. Prakash and former heads for providing good department facilities. I thank present Dean, Prof. N. Siva Kumar and former Deans of the School of Life Sciences for allowing me to use all the central facilities of department and school.

I would like to thank Prof. Naresh Babu V. Sepuri and Dr. Prasad Tammineni for allowing me to use the DBT-Builder School Facility- Agilent Seahorse Analyzer.

I would like to thank Prof. Rajagopala Subramanyam for allowing me to use their Plant Sciences Confocal Facility.

I would like to thank Dr. A. Bindu Maday Reddy for providing cell lines.

I would like to thank Dr. V.S.V Prasad, CEO, Lotus children's hospital, Lakdikapul and Dr. Arcy Billora for providing blood samples and Dr. Y. Ravi Kumar, Ramaiah College, Bangalore for providing the chemical compounds.

I would like to thank the funding bodies DBT, DST-SERB, STARS and ICMR for providing us the grant to accomplish our research.

I thank DBT-SERB *and* ICMR *for providing me SRF- Fellowships.*

I would like to thank Dasaradhaiah Kudali for helping me in confocal microscopy and Dr.

Monika for helping me in using Agilent Sea horse facility.

I would like to thanks Sandeep Dey from Dr. Arun Kota Kumar sir lab in helping me generating the confocal image graphs.

I would like to thank all the staff of Department Biotechnology and Bioinformatics, School of Life Sciences.

I thank my present lab mates Deepti, Deepika, Preeti, Anvesh, Soofiya, Poornima and Sakshi and past lab mates also. I thank all the M.Sc. and M. Tech students Prama, Jyoti, Mohit, Rohit, Shubhangi and Himaja and past students, Shubham and Sujhitha. I thank Sai and Balakrishna for doing support work in lab.

I would like to give special thanks to Mahati and Deepti for always supporting and encouraging me throughout my Ph.D.

I would like to thank my friends K Mahati, Neera Yadav and Arpita Sagar.

I also thank Subahan, Abhay, Navya and Anita for providing cells whenever needed.

I thank my parents, brother and Subhesh for always supporting me during my Ph.D. journey.

A special thanks to Sir and Ma'am for providing homely environment in lab.

Lekha Gandhi

	DEDICATION			
I dec	dicate this thesis wholeheartedly to God and my parents for givir			
me	e endless support, love and having faith in me to accomplish this			
	journey.			

TABLE OF CONTENTS

Acronyms	11-13
List of Figures and Tables	14
Chapter 1: Review of Literature.	15-16
1.1 Introduction.	17
1.2 Epidemiology	17-20
1.3 Dengue virus Clinical Manifestations	20-21
1.4 Dengue virus genome and its transmission life cycle	21-29
1.5 Host-Virus Interactions	29-31
1.6 Diagnosis, Antivirals and Vaccines	31-34
1.7 Significance of the study	35
1.8 Scope of the study	35-36
Chapter 2: Dengue Virus Protease Localization in Subcellular Organ	nelles37
2.1 Introduction	38-40
2.2 Materials and Methods	41-55
2.3 Results.	55-65
2.4 Discussion.	66-68
Chapter 3: Identification of Dengue Virus Protease Substrates	69
3.1 Introduction	70-72
3.2 Materials and Methods	72-78
3.3 Results	78-92
3.4 Discussion	93-95
Chapter 4: Effect of Dengue Protease on Cell Homeostasis	96
4.1 Introduction	97-99
4.2 Materials and Methods	99-102

4.3 Results.						102-106
4.4 Discuss	ion					107-109
Chapter	5:	Identification	and	Evaluation	of	anti-protease
molecules.	• • • • • • • • •	•••••	• • • • • • • • • • •	• • • • • • • • • • • • • • • • • • • •	• • • • • • • • • • • • • • • • • • • •	110
5.1 Introduc	etion					111-113
5.2 Materia	ls and M	lethods				113-121
5.3 Results.			• • • • • • • • • • • • • • • • • • • •			121-136
5.4 Discuss	ion		•••••		• • • • • • • • • • • • • • • • • • • •	137-139
Conclusion	1		• • • • • • • • • • • • • • • • • • • •			140-142
Bibliograp	hy				• • • • • • • • •	143-167
Publication	าร					168-170

ACRONYMS

• ATP Adenosine tri-phosphate

• a.a Amino acid

• bp Base pair

• B₄N Tetra-O-benzoylated NDGA

• CprM Capsid Pre-membrane

• DENV Dengue virus

• DF Dengue fever

• DHF Dengue Hemorrhagic fever

• DSS Dengue shock syndrome

• DMEM Dulbecco's Modified Eagle Medium

• ELISA Enzyme-Linked Immunosorbent Assay

• EDRF1 Erythroid Differentiation Regulatory Factor 1

• FBS Fetal Bovine Serum

• GAPDH Glyceraldehyde 3-phosphate dehydrogenase

• JEV Japanese Encephalitis Virus

• kDa Kilo Daltons

• LB Luria-Bertani

• MALIDI-TOF Matrix-assisted laser desorption/ionization- time-of-flight

• MFN Mitofusins

• mM Millimolar

• mg Milligram

MITA Mediator of IRF3 activation

• mtHSP70 Mitochondrial heat shock protein 70

• μg microgram

• µL microliter

• µM micromolar

• NCBI National Center for Biotechnology Information

• NDGA Nordihydroguaiaretic acid

NS Non Structural Protein

• NAP-1 Nucleosome Assembly Protein-1

• NAP1-L1 Nucleosome Assembly Protein1-Like 1

• nm nanometer

• ORF Open Reading Frame

• PAGE Polyacrylamide Gel Electrophoresis

• PBS Phosphate Buffer Saline

• pro Protease

• polyA poly Adenylate tail

• RIPA Radio Immunoprecipitation Assay

• ROS Reactive Oxygen Species

• RT Room temperature

• RT-PCR Reverse Transcriptase Polymerase chain reaction

• RdRp RNA-dependent RNA polymerase

• TAE Tris-Acetate-EDTA

• TM Transmembrane

• TBEV Tick-Borne Encephalitis Virus

• UTR Untranslated Region

• USUV Usutu virus

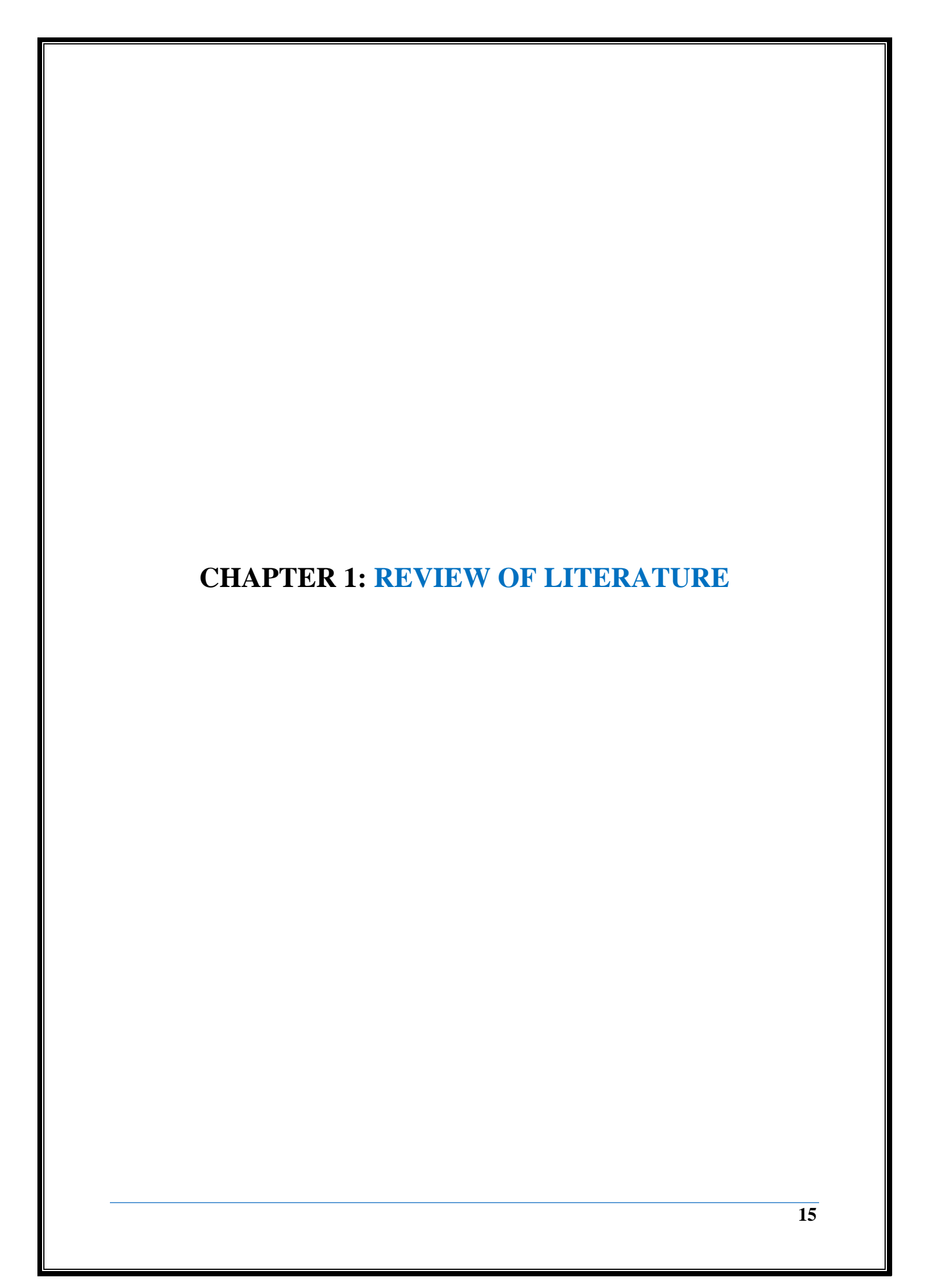
• YFV Yellow Fever Virus

• WHO World Health Organization

• WNV West Nile Virus

List of Figures and Tables

Chapters	1	2	3	4	5
Figures	1.2.1	2.1.1	3.2.1	4.2.1	5.2.1
	1.2.2	2.1.2	3.3.1	4.2.2	5.2.2
	1.2.3	2.1.3	3.3.2	4.3.1	5.2.3
	1.3	2.2.1	3.3.3	4.3.2	5.3.1
	1.4.1	2.2.2	3.3.4	4.4	5.3.2
	1.4.2	2.2.3	3.3.5		5.3.3
	1.6.1	2.2.4	3.3.6		5.3.4
		2.2.5	3.3.7		5.3.5
		2.3.1	3.3.8		5.3.6
		2.3.2	3.3.9		5.3.7
		2.3.3	3.4		5.3.8
		2.3.4			5.3.9
		2.3.5			5.3.10
		2.3.6			5.3.11
		2.3.7			5.4
		2.3.8			
		2.3.9			
Tables	1.6.1	-	3.3.1	_	5.3.1
	1.6.2				



REVIEW OF LITERATURE

- > INTRODUCTION
- ➤ EPIDEMIOLOGY
- > CLINICAL MANIFESTATIONS
- > DENGUE VIRUS LIFE CYCLE AND GENOME ORGANIZATION
- ➤ HOST-VIRUS INTERACTION
- > DIAGNOSIS, ANTIVIRALS AND VACCINES
- > SCOPE OF THE STUDY
- > SIGNIFICANCE OF THE STUDY

1.1 INTRODUCTION

Studies on viruses and their pathogenicity for the past few years led to the major advancement in the field of virology. This advancement led virologists to study the basic genome organization of viruses, their mode of action, pathogenesis, host-virus interactions and developing antiviral molecules and vaccines. In spite of the above studies, viruses are known to play a crucial role in the global ecosystem and pose a huge burden on host species [1]. Host-virus interaction results in the evolution of escape mechanisms in host species and alters the prey-predator relationship [2].

There are many different viruses, classified as RNA and DNA viruses, that infect multiple host species and are major threats to human lives. One such group of RNA viruses are the Flaviviruses of the family *Flaviviridae*. These are single-stranded RNA (ssRNA) viruses, that cause major disease illnesses, and few of them are transmitted by arthropods. These arthropodborne viruses, also termed as arboviruses, have evolved from common ancestors. These include the Japanese Encephalitis Virus (JEV), Yellow Fever Virus (YFV), Dengue Virus (DENV), Zika Virus, Tick-Borne Encephalitis Virus (TBEV), West Nile Virus (WNV) and Usutu virus (USUV) [3-5]. Among the above viruses, the dengue virus is the subject of this study.

1.2 EPIDEMIOLOGY

Dengue virus is a flavivirus of the family *Flaviviridae*. Over the past thousand years' dengue has been reported worldwide. Epidemiologically, dengue virus has been circulating for the past seven decades remarkably. The spread of dengue virus has been reported from tropical and subtropical regions of the world, and more than 130 countries are endemic to dengue virus infection. It has been reported that 400 million infections occur every year and half of the population is being affected worldwide [6-8]. The first dengue outbreak occurred in 1779 in

Jakarta, Indonesia [9]. Since then, there have been continuous outbreaks worldwide. The first strain of dengue virus was isolated in 1943, from an acutely ill patient. In 1944, dengue virus was isolated from India, New Guinea, and Hawaii [10]. These strains were identified as DENV1 serotypes. Another virus strain from New Guinea was reported as DENV 2. Later, in 1956, DENV 3 and 4 were isolated subsequently from hemorrhagic patients during an epidemic in Manila, the Philippines. Since the year 1980, till date, all the serotypes (DENV1-4) circulated globally, mainly covering the regions in Asia, South America and the Caribbean [10-12]. The World Health Organization (WHO) reported an eight-fold increase in dengue cases in the past two decades, with approximately 5.2 million cases in the year 2019 alone [7, 12]. According to the European Centre for Disease Prevention and Control Report-2023, the most affected regions were Bolivia, Argentina, Peru, and Brazil. All DENV 1-4 serotypes were circulated in America also (Figure 1.2.1) [13, 14].

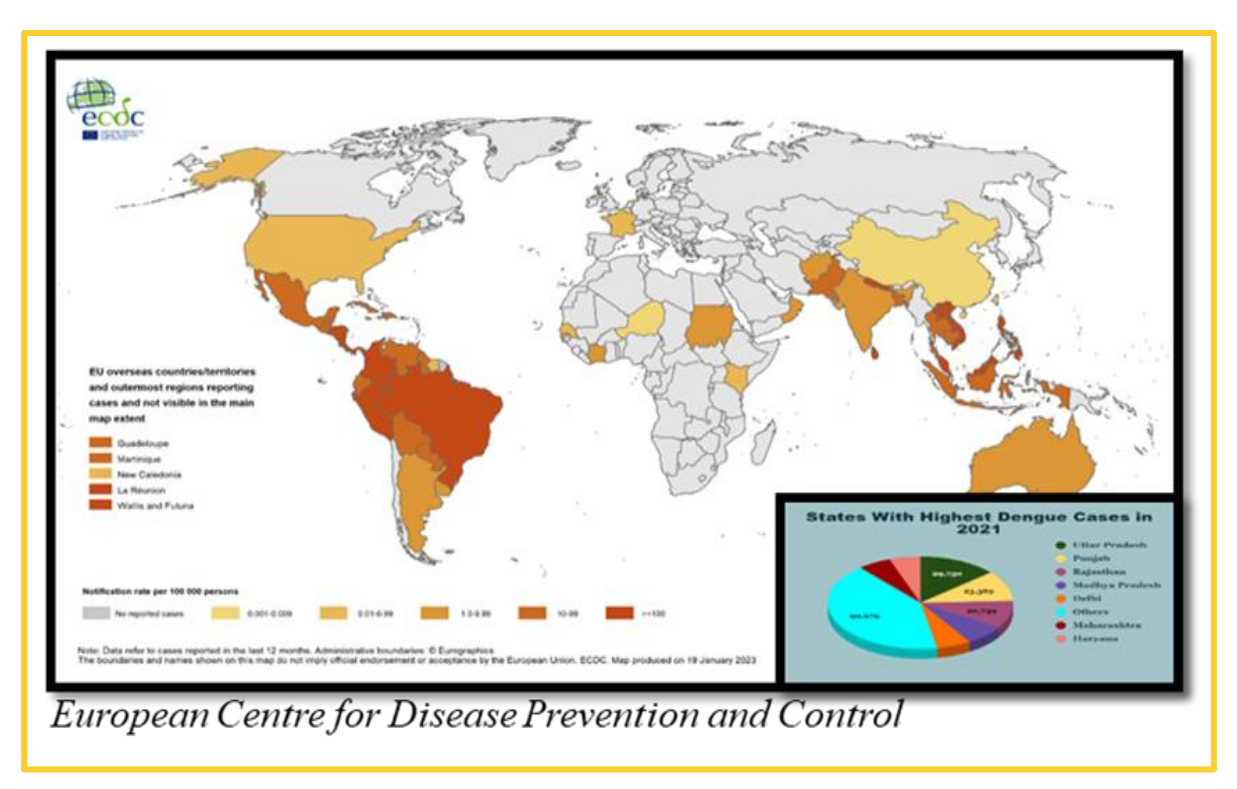


Figure 1.2.1: The world map showing the geographical distribution of dengue virus infections [14].

Reports also suggest an exponential increase in dengue virus infections worldwide.

Approximately, 400 million infections occur yearly, and 90 million infections have been reported clinically.

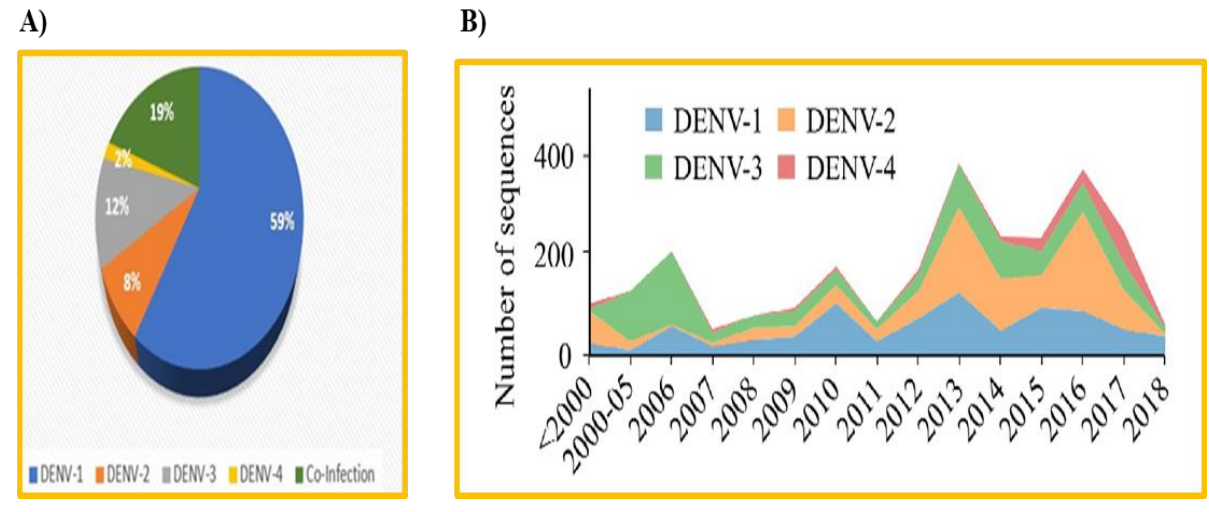


Figure 1.2.2: (**A**) The pie chart shows the percentage of serotype distribution in Telangana, India, during 2017-2020. DENV1 (59%) showed the major portion, followed by co-infection, DENV3, DENV4 and others [18]. (**B**) Graphical presentation of the number of sequences analyzed suggests the existence of all serotypes in a particular year [15].

India alone reports one-third of the above infections. India showed hyper endemicity with all the circulating serotypes causing infections and co-infections in North, South, East, West, and Central India and entitled as the hotspot of dengue virus infections. In North India, DENV-2 was the predominant serotype circulating in Delhi, and later the changes were observed in the serotype trend with DENV-1 & 3 [15]. In Southern India, DENV-1, 2 & 3 were found to be the pre-dominating serotypes until 2015, and DENV-4 appeared as one of the dominant serotype later on, as presented in (Figure 1.2.2) [16, 17].

Another report suggested that DENV-1 and 2 serotypes excelled in 2010 and 2013. DENV-3 was at its peak during the 2006 outbreak (Figure 1.2.3) [18]. DENV-4 emerged in Southern India in later years while, DENV2 showed dominancy in all parts of India [17-19].

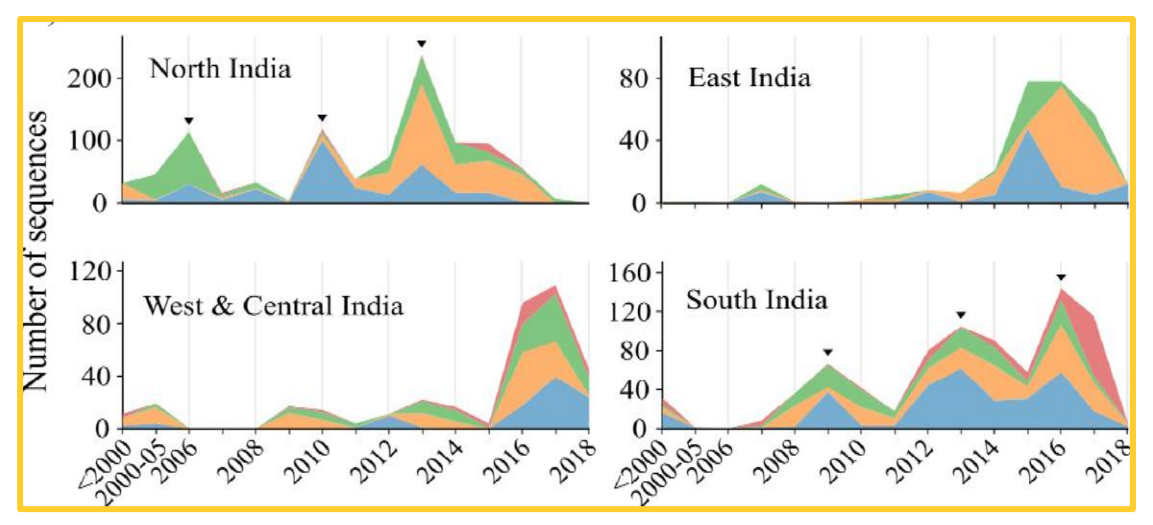


Figure 1.2.3: Representation of dengue virus distribution in different geographical regions of India during 2000-18 [15].

1.3 CLINICAL MANIFESTATIONS

Dengue is transmitted through the bite of female mosquito species *Aedes aegypti* and *Ades albopictus*. According to WHO, clinical symptoms of dengue virus infection have been classified as Dengue without warning signs, dengue with warning signs and severe dengue. Dengue shows acute illness during infection and manifests symptoms of Dengue Fever (DF), Dengue Hemorrhagic Fever (DHF) and Dengue Shock Syndrome (DSS) [20]. Dengue fever symptoms include rashes, headache, joint pain, muscle soreness, retro-orbital pain, and abdominal cramps. DHF is characterized by red or purple blisters on the skin, epistaxis, and gingival bleeding, circulatory failure. Some patients show symptoms of hypovolemic shock resulting in severe plasma leakage leading to dengue shock syndrome [21, 22]. Symptoms of dengue are characterized in patients by their immune system profile. In pediatric patients, primary infections or initial infections cause mild or unidentified symptoms like dengue fever. Secondary infections or co-infections with any of the serotypes may cause severe symptoms with acute illness and plasma leakage, leading to shock syndrome while subsequent infections in adults lead to severe hemorrhages and organ failure [21, 23].

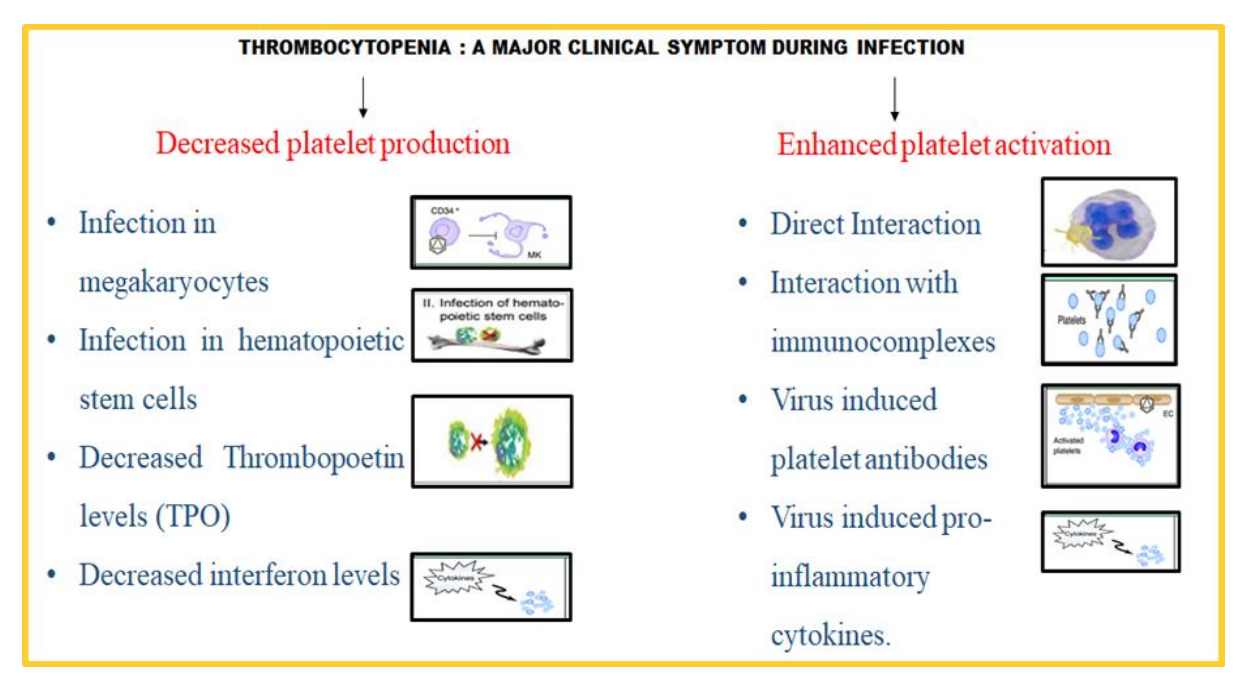


Figure 1.3: Schematic representation showing the causes of thrombocytopenia during virus infection [20, 24].

According to WHO, thrombocytopenia is the 'hallmark' symptom of dengue virus infection causing a rapid decline in the platelet count i.e. less than 1,50,000/µl of blood [20, 24]. There are several hypotheses proposed, but the mechanism behind the sudden decrease in platelet count has not yet been explained to date. Some hypothesized that thrombocytopenia is due to decreased platelet production and increased platelet activation [25]. DENV affects naive or progenitor bone marrow cells, thereby inhibiting their proliferation. In earlier reports, it is evident that during acute illness, dengue causes bone marrow suppression or hypoplasia. Another study reported direct interaction with platelets, platelet destruction, apoptosis, lysis by the complement system and generation of anti-platelet antibodies (Figure 1.3) [25-28].

1.4 DENGUE VIRUS STRUCTURE, GENOME ORGANIZATION AND ITS LIFE CYCLE

Dengue virus is roughly spherical with a size of 40-50 nm consisting of an outer envelope lipid bilayer membrane and inner nucleocapsid enclosing the viral genome. Dengue virus is

transmitted by the bite of female mosquito *Aedes aegypti* and by a few other species such as *Aedes albopictus*, *Aedes polynesiensis*, *Aedes scutellaris* [29].

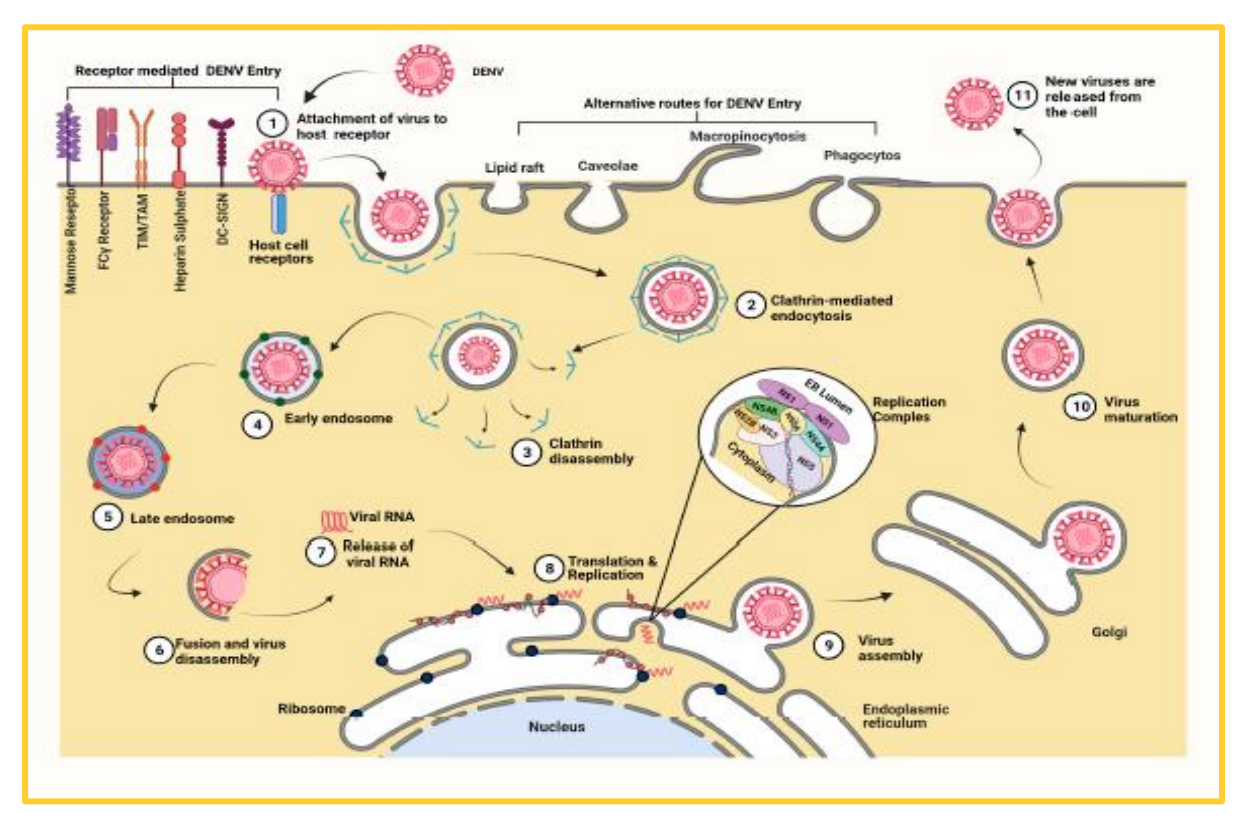


Figure 1.4.1: Dengue virus replication cycle: (1) DENV attaches and binds to its host receptors via receptor-mediated endocytosis, **(2)** Virus internalizes with the clathrin-coated vesicles, **(3)** The clathrin coated virus reaches to cytoplasm and fuses with the early endosomes, **(4)** The early endosome with pH ~ 6.5, are the site of virus maturation, **(5)** The mature endosome with lower pH, 5.5, causes conformational changes, **(6)** Due to low pH, fusion of the viral envelope begins, **(7)** In the cytoplasm, virus disassembles and releases the viral genome (capsid-bound RNA), **(8)** Viral RNA starts translation and replication in the ER, **(9)** In the ER, new viral proteins and genome are assembled forming new immature virus, **(10)** Immature virus undergoes furin-mediated maturation in the Trans-Golgi Network (TGN), **(11)** The mature virus progeny gets exocytosed from the infected cells [29].

When an infected mosquito bites, during the intake of blood, the virus gets transmitted to humans. Dengue virus is present in the saliva of the mosquitoes, which gets released into the skin of an individual. The virus starts its replication in the vector itself prior to transmission in hosts, thus transmitting virion progenies. This virus binds to different types of cells like fibroblast monocytes, epithelial cells, macrophages, hepatocytes, B & T-cells, dendritic and endothelial cells. This virus enters and binds to the host cell surface by surface attachment and

internalization process. DENV binds to numerous cell-type receptor molecules like the mannose receptor (MR) (monocytes, macrophages, fibroblast), glycosaminoglycan (GAG) (epithelial cells), the lipopolysaccharide (LPS)-(monocyte and macrophages) and c-type lectin, known as Dendritic cell-intercellular adhesion molecule 3-grabbing non-integrin (DC-SIGN) (dendritic cells). After attachment, the virus gets internalized into host cells via, a clathrincoated vesicle-like structure in the endosomes. Virus particle internalizes into host cells by the early endosome, later matures and fuses with the late endosomes. In the late endosomes due to acidic pH, the envelope and pr-membrane envelope protein encounters conformational changes and dissociate leading to the fusion of viral envelope with the host's endosomal membrane. Later, the nucleocapsid gets released into the cytoplasm. The viral RNA genome is transported to the endoplasmic reticulum (ER) for the replication of viral genome and synthesis of viral proteins. DENV replication commences with the formation of a replication complex in the ER lumen. The positive-sense RNA strand act as template for synthesizing viral proteins, as well as the complimentary negative strand. The translation and maturation of viral proteins form ER vesicle packets in ER membrane required for RNA replication. The new immature viral protein particles proceed for assembly of new viral particles in the Trans Golgi Network (TGN), followed by exocytosis of new virion progenies, thus completing its infection life cycle (Figure 1.4.1) [11, 21, 22, 29]. Dengue virus carries 11 kbp single-stranded RNA flanked by 5'UTR and 3'UTRs that encodes the polyprotein to yield mature functional proteins i.e. structural proteins (Capsid, Pre-Membrane and Envelope) and non-structural proteins (NS1, NS2A, NS2B, NS3, NS4A NS4B, NS5). 5' UTR is capped, followed by a 5'-AG-3' di nucleotide sequence, while 3'UTR lacks poly adenylate tail (poly-A), terminating with a 5'CU-OH-3 sequence. Both the 5' and 3' UTRs form a large stem-loop A structure (SLA) and 3'UTR forms stem-loop (3'SL) structure [21, 30-32].

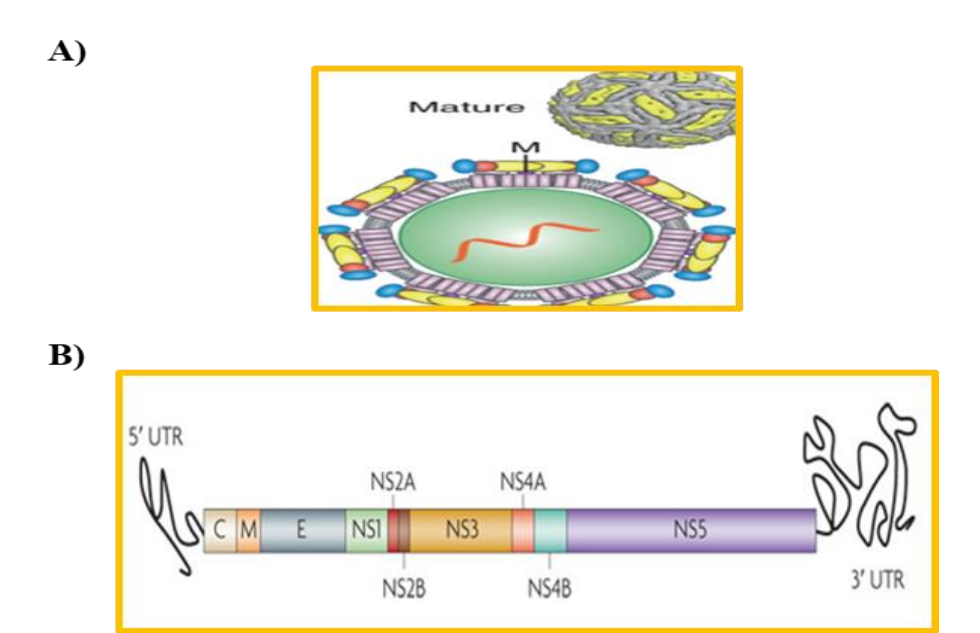


Figure 1.4.2: Dengue virus genome structure and organization. **(A)** Mature dengue virus structure showing the outer envelope and inner capsid oligomers enclosing the viral genome. **(B)** Virus subgenomic segments flanked by the 5' and 3' UTR sequences. Structural (Capsid, Membrane, Envelope) and non-structural (NS1- NS5) gene segments were also shown [30].

Structural proteins

Capsid, a 12 kDa, highly positively charged basic protein. This protein plays an important function in viral assembly during infection by encapsulating the viral genome. The capsid forms homo-oligomers with binding affinities to both nucleic acid and lipid membranes [33]. The three-dimensional structure of capsid was resolved using NMR and crystallography studies. The capsid form dimers which, shows unequal charge distribution i.e. basic amino acid residues residing on one face of the molecule and a hollow hydrophobic surface on the opposite side [34, 35]. These structural analyses helped researchers in studying the interactions with host proteins and functional studies contributed to understanding the viral assembly during infection. Based on these studies, it is reported that the hollow hydrophobic region allows the capsid protein to get associated with ER membranes. Moreover, it is reported that dengue capsid localizes to both cytoplasm and nucleus [36, 37]. Although it plays a role in virus assembly in cytoplasm, it was found to be distributed in the nucleus, majorly in nucleoli [38, 39]. However, the significance of its nuclear localization has not yet been understood. Several

shreds of evidences reported that capsid accumulates in lipid droplets that are necessary for particle formation during capsid assembly. Its interaction with lipid droplets might impact host lipid metabolism during infection [40, 41].

Pre-Membrane, an 8 kDa protein, containing 166- amino acid glycoprotein. During virus maturation, two subunits, pr and M constitute the prM protein, where the pr protein is cleaved by the host enzyme i.e. furin to release the pr peptide (1-91 amino acid residues) thereby releasing the mature M protein with ectodomain and a transmembrane region. Dengue virus particles occur in both mature and immature forms that have distinct morphology. In the immature virion, prM heterodimerizes with the envelope and inhibits the formation of a fusogenic envelope during virion secretion. A report showed the development of cell-based assay that detects pre-M processing during its classical secretory pathway [42, 43].

Envelope, ~55 kDa protein is a highly immunogenic structure present on the surface of dengue virus. The host cell receptors recognize these immunogenic structures which help in fusion with endosomal membrane for cell entry. It is reported that this protein occurs in dimeric form, when exposed to low pH, it rearranges to form trimers. Envelope protein is composed of β -strand organized into three domains: the central domain I, the dimerization domain II, and the C-terminal Ig G-like domain III. Two monomers direct itself in a head-to-tail orientation to form dimers. The fusion loop of the II domain interacts with the endosomal membrane during the fusion event. The fusion of envelope protein allows the internalization of the virus into the host cells [44-46].

Non-Structural Proteins

Non-structural protein 1 (NS1), ~48 kDa, mostly conserved among all the flaviviruses group. NS1 protein occurs in the monomeric form initially during infection. Later, during the post-translational modification in ER-lumen, it exists as homodimers [47]. NS1 is the only secretory

protein in hexameric form that is secreted constitutively during infection and enters into the bloodstream of the infected individuals [48]. It is reported that NS1 mimics the host lipoproteins and intervenes with the endogenous lipogenesis process. The levels of NS1 are more profound in the DHF and DSS infected cases compared to the dengue fever. NS1 mediates complement activation that leads to the generation of anaphylatoxins leading to vascular leakage [49]. Due to the early secretion of NS1, it has been reported as one of the potential diagnostic methods to detect dengue virus infections. A recent report showed the efficacy of NS1 protein by generating the anti-NS1 monoclonal antibodies as a safe and effective therapeutic against all serotypes during the infection [50].

Non-structural proteins 2A and 2B (NS2A & NS2B)

NS2A is ~22 kDa protein consisting of a hydrophobic transmembrane region. It is reported that NS2A behaves as viroporin. Due to the presence of hydrophobic regions, it interacts with host membranes and causes cytopathic effect. NS2A forms a crucial component during the viral particle formation. This protein interacts with the Capsid-prM and NS2B for the viral assembly. NS2A is known to inhibit innate immune signaling to enhance virus replication [51-53].

NS2B is the smallest \sim 14-15 kDa membrane-associated protein that acts as a catalytic factor for dengue viral NS3 protease. Structurally, NS2B possesses four hydrophobic transmembrane domains and a central hydrophilic domain [54]. Based on NMR and X-ray studies, it is reported that the N-terminal region of NS2B binds to the NS3 protease domain in a tightly regulated manner to allow NS3 to perform its proper catalytic activity. NS2B also possesses a C-terminal region with β -hairpin structure that binds to the substrate binding site of the protease domain. Such binding forms closed conformation resulting in the constitution of an active protease [55, 56]. Apart from performing co-factor function, NS2B also helps NS3 in sequestering to the cell membrane where NS3 can perform its function during the viral assembly. A recently published

study stated that NS2B solely can degrade the cyclic GMP-AMP Sensor (cGAS), a cytosolic DNA sensor, for type I Interferon signaling in the host, thereby inhibiting the host antigenic response and increasing the viral replication [55].

Non-structural protein 3 (NS3)

NS3 is a 70 kDa, a multifunctional protein that possesses protease, RNA helicase and 5' triphosphatase activities. The N-terminal domain of NS3 protein contains a serine protease (1-180 a.a) and C-terminal helicase domains (181-618 a.a). The protease and helicase domains are linked via linker conserved domain. NS3pro possesses a conserved catalytic triad (His-51, Asp-75, Ser-135) with enzyme-like catalytic activity. The C-terminal helicase domain possesses helicase and nucleoside triphosphatase activities. Many studies have reported that the central hydrophilic domain of NS2B (49-96 a.a) is necessary for efficient protease enzymatic activity [56] and cleaves off polyprotein at NS2A/NS2B, NS2B/NS3, NS3/NS4A, NS4B/NS5 junctions. During virus replication, NS3 helicase is also involved in unwinding the dsRNA which is driven by ATP hydrolysis [57]. Furthermore, recent studies have demonstrated its role in the formation of infectious virions during infection. NS3 interacts with multiple host cellular factors for well regulated virus replication.

Non-structural proteins 4A and 4B (NS4A & NS4B)

NS4A, a 16 kDa, highly hydrophobic integral membrane protein. Although very few studies have characterized this protein, it is reported that the N-terminal region of NS4A extrude out in the cytoplasm during proteolytic cleavage by NS2BNS3, whereas the C-terminal amino acid residues act as a signal sequence for the translocation of NS4B to the ER lumen [58-60]. Another study shows that NS4A interacts with NS1 and might have some role in viral replication complex which is still unclear. Further studies gave evidence that it alters the host

membrane and interacts with other viral proteins thus favoring the virus replication and replication organelle formation [61, 62].

NS4B, a 28 kDa protein, is an endoplasmic reticulum-associated membrane protein containing many conserved hydrophobic residues among all four DENV serotypes [63]. It has been reported that NS4B has relatively high similarity among the serotypes but low sequence similarity to other viruses such as JEV, WNV, ZIKA and hepatitis C (HCV) viruses [64]. Although the functions of membrane proteins are not yet clearly explained, a study showed that during the dengue virus infection, N-glycosylation of NS4B occurs which may play a role in viral replication. It is also reported that both NS4A and NS4B play a major role during IFN-α/β induced signal transduction via blocking the immune response pathway [65, 66]. To date, no crystal structure of NS4B has been developed because of its highly hydrophobic and complex nature. Other reports show that during dengue virus infections, NS4B forms homodimers. Another study reported NS4B interaction with the host protein, stress-associated ER protein 1(SERP1), which is essentially involved in antiviral response mechanism [67].

Non-structural protein 5 (NS5)

NS5, a 104 kDa protein, is the largest and highly conserved protein with 67% identity among the DENV serotypes. NS5 harbors two important functions i.e. methyltransferase activity performed (MTase) by the N-terminal domain and RNA-dependent RNA polymerase (RdRp) activity performed by the C-terminal domain [68]. MTase of NS5 acts as a capping enzyme that synthesizes 5' cap structure during the virus replication. It methylates at the N7 of guanine nucleotide and the 2'-O of ribose sugar unit of the first nucleotide using S-adenosyl-L-methionine (SAM) as methyl group donor and adds GMP to a 5' diphosphate end of the nascent RNA genome. NS5 RdRp synthesizes the viral RNA genome by *de novo* initiation mechanism, which requires both 5' and 3' ends [69, 70]. NS5 contains nuclear localization signals that aid

in translocation into the nucleus, although the functional significance remains unclear. Apart from the above functions, it is also reported that NS5 plays a major role in host-virus interactions [71-73].

1.5 HOST-VIRUS INTERACTIONS

Viruses impose pressure on the host using different advantages they possess in order to control the host's defense. These include the interference with the host's normal functions by the virus-coded proteins. In this direction, dengue virus protease is involved in viral polyprotein processing which is a crucial step in the virus life cycle. In addition to these functions, several reports suggest its non-canonical functions contribute towards disease pathogenesis, distribution of cellular components, and alterations in host survival mechanisms like dysregulating the host proteins and the immune system.

1.5.1 Disease Manifestations and Host Immune Response

Dengue protease contributes to severe complicacies like hemorrhagic stroke and shock syndrome conditions during infection. The role of dengue virus protease (NS2BNS3/NS3) is in the first line in triggering severe disease manifestations. Studies reported that both dengue NS3 and NS2BNS3 induce apoptosis. It was shown that it cleaves IkBα and IkBβ, thereby inducing NF-kB activation and resulting in apoptosis of endothelial cells, causing hemorrhage [74]. To escape the host immune response, dengue viral protease has evolved strategies by hijacking the host transcriptional and translation mechanisms. It is reported that dengue viral protease cleaves a key adaptor protein, Mediator of IRF3 activation (MITA), also known as Stimulator of interferon genes (STING). This protein is an ER-resident membrane spanning protein produced during the interferon production triggered by any pathogens [75]. It is reported that dengue virus protease also induces mitochondrial fragmentation by cleaving

mitofusins (MFN1 and MFN2), the mitochondrial outer membrane proteins, which are required for efficient antiviral responses and cell survival [76].

Thrombocytopenia is one of the earliest and consistently appearing clinical features to detect the dengue virus infection. A sudden decrease in low platelet count occurs immediately after infection, leading to hemorrhagic conditions. The most precautionary treatment adopted by hospital authorities is the platelet transfusion for patients suffering from thrombocytopenia. Due to increased side effects, it is suggested that platelet transfusion is not effective and must not be used routinely for controlling virus infections. As mentioned in reported studies, the mechanistic insights of thrombocytopenia are not yet explained clearly and need to be elucidated. In this direction, studies on basic research using computational and/or experimental approaches would give new directions in detailing the viral protease functions causing thrombocytopenia and aid in developing anti-viral drug therapeutics. In the present study we tried to understand the role of dengue virus protease, its functional characterization and its interaction with host proteins in the upcoming chapters. We hope that this study will explain the significant role of the viral protease hampering in cell homeostasis and contribute towards understanding the mechanism of thrombocytopenia.

1.5.2 Metabolic alterations

Dengue infection causes alterations in metabolic activities. It is reported that NS3 interacts directly with GAPDH leading to suppression in glycolytic activities and thereby resulting in alterations in hepatic functions that might cause fatal diseases during infection. Other studies show that it plays a role in lipid metabolism also [77, 78].

1.5.3 Redistribution of Host Proteins

Dengue NS3 protein interacts with host proteins by localizing into the subcellular organelles or by binding to the host membrane proteins. Several studies show that NS3 interacts with

nuclear receptor binding protein (NRBP), which allows its distribution from the cytoplasm to the perinuclear region [79]. Further, it has been reported that Caveolin-1 in the lipid rafts is associated with NS3 protein during virus polyprotein processing and replication. This process appears to regulate the recruitment of other cellular factors required for the sequestering of other proteins for infection [80].

1.6 DIAGNOSIS, ANTIVIRALS AND VACCINES

Dengue diagnosis is one of the very challenging aspects for clinicians and researchers. Early detection aids in the proper treatment of the infected individuals. The gold standard and most conventional diagnostic method is viral isolation. After virus isolation, confirmation is done by Reverse Transcriptase-Polymerase Chain Reaction (RT-PCR) or Immunofluorescence Assay (IFA) [81]. Other conventional methods used routinely are serological tests, rapid antigen/antibody detection tests, Nucleic Acid Amplification tests (NAAT), and DENV NS1 antigen based tests. Serological tests like Enzyme-Linked Immuno Sorbent Assay (Ig G/Ig M) and Hemagglutination Inhibition (HI) tests are simple and convenient to perform [82]. But sometimes in these tests, virus escapes the detection and show cross-reactivity. Many rapid diagnostic kits are available in markets and confirm the detection as early as 15 minutes thus helping immediately to diagnose the patients. However, these tests also show high cross reactivity towards other flaviviruses. NS1 antigen test is also one of the widely used laboratory diagnostic method as the levels of NS1 protein is relatively high during the early infection, which allows easy and rapid detection. The NS1 antigen test has been used as an alternative detection method for the virus culture [82, 83]. Apart from these tests, detecting biomarkers is another method of detection. In our previously published study, anti-NS2BNS3pro antibody based indirect ELISA test was developed as one of the diagnostic methods for detecting the dengue virus infection [84].

Another challenge to control the dengue virus pathogenesis is the non-availability of antivirals and vaccines. The major challenge in developing the vaccines and the antivirals is the existence of four distinct serotypes and their cross-reactivity toward other viruses. The Antibody Dependent Enhancement (ADE) phenomenon is one of the major obstacles to develop the vaccines. It is reported that the high mutation rates and drug resistance have been a global challenge to develop safe and effective vaccines. Thus, developing vaccine candidates, like tetravalent vaccine formulations, synthetic peptides, whole-virion, recombinant live vector, infectious cDNA clone-derived, and naked DNA-attenuated viral vaccines have been proposed for DENV infection (Table 1.6.1) [85, 86]. To date, there have been no licensed dengue vaccines approved. However, the first approved vaccine is Dengvaxia®, a tetravalent dengue vaccine-CYD-TDV, by Sanofi Pasteur, was licensed in Mexico in December 2015. Different therapeutics and strategies have been employed for developing the antivirals against all the serotypes (Figure 1.6.1) [85, 86].



Figure 1.6.1: Strategies for developing antivirals against dengue virus [85].

Table 1.6.1: List of vaccines developed [86].

Vaccine Type	Vaccine Name	Developer	Current Stage	Target Antigen	Strategy	Key Clinical Outcome
	Dengvaxia© (CYD- TDV) ^(87,88,89)	Sanofi Pasteur	Licensed	Live virus	DENV 1–4 genes substituted for the YF17D virus genes (prM/E).	Age limit; increased risk of severe dengue in seronegative subjects but high effectiveness and safe in seropositive individuals
	Tetravax; TV003/TV005 ^(90,91)	NIH (USA); Butantan Institute (Brazil); Panacea Biotec Ltd. (India)	Phase II/III	Live virus	Attenuation of DENV1, DENV3, DENV4, and a DENV2/DENV4 chimerical by excluding 30 nucleotides from the 3' UTR.	Well-tolerated; balanced immune response in subjects, effective with administration of a single dose. Adverse reaction (mild rash)
Live attenuated	TAK-003; DENVax ⁽⁹²⁾	Mahidol University; Inviragen; Takeda		DENV2 PDK-53 attenuated vaccine coding sequences are replaced with DENV1, DENV3, and DENV4 coding sequences.	Immunogenic and well- tolerated in multiple phase I and II clinical studies, independent of the participants' age or serostatus, safety profile not entirely known	
	TDEN F17/F19 ^(93,94)	WRAIR and GSK	Phase II	Live virus	Involving primary cells of dog kidney (PDK) and lung cells of fetal rhesus (FrhL) in serial passages	Proven to be a safe, well- tolerated, and immunogenic DENV vaccine candidate in phase II trial
Inactivated	TDEV-PIV ^(95,96)	GSK, Firocruz and WRAIR Merck	Phase I	Inactive virus	Employing adjuvants and purified formalin-inactivated virus	Well-tolerated, immunogenic in naive and seropositive individuals. No risk of re- activation and good immuno- logical balance
Recombinant subunit	V180 ^(97,98)	GSK, Firocruz and WRAIR Merck	Phase I/II	80% of the E protein	DEN-80E-containing recombinant truncated protein	Induce steady immune responses against all DENV serotypes, decreasing the likelihood of the ADE effect
Nucleic acid	TVDV ^(99,100)	U.S Naval Medical Research Centre	Phase I	prM and E proteins	prM/E proteins are encoded via a recombinant plasmid vector	immunogenicity. Plasmid modification required.
(DNA)	D1ME100 ⁽¹⁰¹⁾	US Naval Medical Research Center	Phase I	prM and E proteins	recombinant plasmid vector encoding prM/E	No neutralizing antibody response detected in individuals with low-dose immunization

Many antivirals have been reported for inhibiting the viral infection (Table 1.6.2). Repurposed drugs have been used in clinical trials to develop safe and effective antivirals. A report shows that the use of Ribavirin in combination was found to be effective in inhibiting dengue infections.

Table 1.6.2: List of Reported dengue virus inhibitors [85].

Target	Antiviral Name	Mechanism of Antiviral Action	Method
Envelope	MLH40 ⁽¹⁰²⁾	Inhibit virus entry	DENV inhibition assays, molecular docking
	DET4 ⁽¹⁰³⁾	Inhibit virus entry and binding	Molecular docking, molecular dynamics
	BP34610 ⁽¹⁰⁴⁾	Inhibit virus entry	HTS, cell-based assay
Capsid	Pep14-23 ⁽¹⁰⁵⁾	Inhibit interaction of C protein lipid droplets	Molecular docking
	VGTI-A3/VGTI-A3-03 ⁽¹⁰⁶⁾	Inhibit capsid protein	Cell-based assay
NS2B/NS3 pro	Nelfinavir ⁽¹⁰⁷⁾	Inhibit protease enzyme	Molecular modeling, cell-based assay, yield-reduction assay
	Diaryl (thio)ethers (Compound 7 and 8) ⁽¹⁰⁸⁾	Inhibit protease enzyme	Cell-based assay
	MB21 ⁽¹⁰⁸⁾	Inhibit protease enzyme	Protease inhibition assay, cell- based assay
	Policresulen ⁽¹⁰⁸⁾	Inhibit protease enzyme and destabilization	Cell-based assay
	Compound 45a ⁽¹⁰⁹⁾	Inhibit protease enzyme	Cell-based assay
	Compound 104 ⁽¹¹⁰⁾	Inhibit protease enzyme	Cell-based assay
	Compound 14 ⁽¹¹¹⁾	Inhibit protease enzyme	Molecular docking, Protease inhibition assay, cell-based flavivirus immune detection, cell viability assay
	Compound C ⁽¹¹²⁾	Inhibit protease enzyme	HTS, Molecular modeling, protease inhibition, cell-based assay
	Carnosine ⁽¹¹³⁾	Inhibit protease enzyme	Protease assay, molecular docking, cell-based assay
	A1-A5 ⁽¹¹⁴⁾	Inhibit protease enzyme	Molecular docking
	8 g and 8 h ⁽¹¹⁵⁾	Inhibit protease enzyme	Protease activity assay, protease inhibition assay, molecular docking
	Luteolin ⁽¹¹⁶⁾	Inhibit protease enzyme	Molecular docking
	Hesperetin ⁽¹¹⁷⁾	Inhibit protease enzyme	Protease assay activity, cell-based assay, molecular docking
	Epigallocatchin ⁽¹¹⁸⁾	Inhibit protease enzyme	Molecular docking
	CC 3 ⁽¹¹⁹⁾	Inhibit protease enzyme	Protease assay activity, cell-based assay
	4-hydroxy-6-(9,13,17-trimethyldodeca- 8,12,16-trienyl)2(3 H)-benzofuranone ⁽¹²⁰⁾	Inhibit protease enzyme	Protease assay activity, cell-based assay
	Dryobalanops aromatic(121)	Inhibit protease enzyme	Protease assay activity
	Diasarone-I ⁽¹²²⁾	Inhibit protease enzyme	Cell-based assay, molecular docking
	Isobiflorin ⁽¹²³⁾	Inhibit protease enzyme	Protease assay activity
	Compound I ⁽¹²⁴⁾	Inhibit protease enzyme	Protease inhibition assay, cell viability assay, western blot, RT- PCR, IF microscopy
NS4A	Compound-B ⁽¹²⁵⁾	Inhibit viral replication	Cell-based assay
NS4B	AM404 ⁽¹²⁶⁾	Inhibit NS4B	Cell-based assay
	NITD-688 ⁽¹²⁷⁾	Inhibit NS4B	HTS, in vivo study
	Compound 14a ^(127,128)	Inhibit NS4B	Cell-based assay
NS5 RdRp	2'-C-methylcytidine ⁽¹²⁷⁾	Inhibit viral replication	Cell-based assay
NS5 MTase	Azidothymidine-based triazoles (9a,11a,11b,11i,15i,17b,19b) ⁽¹²⁸⁾	Inhibit viral RNA capping	Cell-based assay, molecular modeling
	BG-323 ^(129,130) NSC 12155 ⁽¹³¹⁾	Inhibit viral RNA capping Inhibit viral RNA capping	Cell-based assay Molecular docking, cell-based assay

1.7 SIGNIFICANCE OF THE STUDY

For the last seventy years, dengue virus infection has emerged continuously with the higher multiplication rates. Most of the countries worldwide are suffering from serious dengue outbreaks which have an alarming impact on the public health care system. In order to control this alarming situation, virologists are conducting trials to understand the basis of disease severity. Many studies are under progress related to virus serotyping/genotyping characterization, developing methods for early diagnosis, high throughput screening methods for developing antiviral molecules, structural and immunological studies for designing vaccine candidates. Although there has been tremendous advancement in these areas of research but all these are progressing with considerable limitations. The escape of virus infection also takes place due to the availability of limited diagnostic methods and improper assessment of the disease severity which leads to the death of the patients. To reduce the global burden of a viral disease, vaccines are the most suitable approach. However, the limitations to develop a safe and effective vaccine is challenging for scientists. In context to dengue virus infections, Dengvaxia was licensed but the immunopathogenesis and cross-reactivity of the vaccine did not show a higher acceptance rate. Thus, taken into consideration, it is important to understand clearly the dengue virus replication and disease manifestation mechanisms.

1.8 SCOPE OF THE STUDY

With existing literature and considering the related aspects, we aimed to study the role of dengue virus non-structural protein- 3 (protease) in the disease pathogenesis, particularly in 'thrombocytopenia'. Our study focused on understanding the existing forms of viral protease during natural infections. For this, we have first set out to understand its localization sites in cells using localization studies, primarily focusing on the nuclear compartment. Then, we targeted to study the protease-host protein interactions for the identification of novel substrates.

Further, we identified a few plant derived (derivatives of NDGA) anti-protease molecules that could inhibit the virus protease function.

The following are the major questions we tried to address in the study:

- 1. What are the different existing forms of dengue virus protease?
- 2. Which form (NS2BNS3 and/or NS3) of dengue virus protease is existing during infection?
- 3. What is the subcellular localization site of the dengue virus protease?
- 4. Does the viral protease target any substrate in the nucleus during virus infection?
- 5. Does it play any functional role in the process of thrombocytopenia?
- 6. Is it possible to develop specific anti-protease molecules?

In order to address the above hypothetical questions, we have framed the following objectives and presented in chapters 2, 3, 4 and 5:

- 1. To understand the dengue virus protease localization in subcellular organelles.
- 2. Identification of dengue viral protease substrates.
- 3. Effect of protease on cellular homeostasis.
- 4. Identification of the specific anti-protease molecules.

		PROTEASE GANELLES

2.1 INTRODUCTION

Dengue virus non-structural proteins play significant roles during viral multiplication. NS3 alone or along with NS2B possess a crucial role and are the prime drug targets for developing anti-virals. NS2B (14 -15 kDa) possesses a hydrophobic domain and a hydrophilic central domain. In the hydrophilic region of NS2B, 40 amino acid residues linked with G4-S-G4 linker to the N-terminal part of NS3 and form the NS2BNS3pro active protease (Figure 2.1.1) [132, 133].

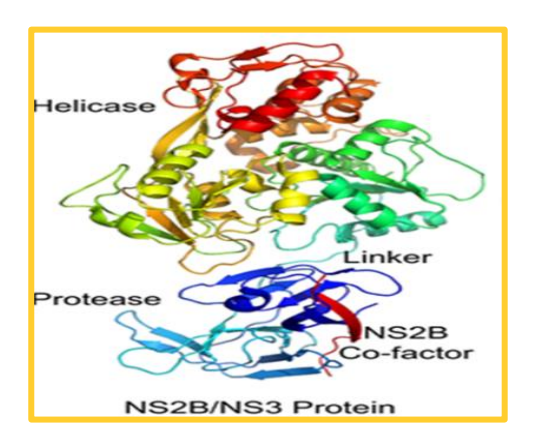


Figure 2.1.1: Dengue Virus protease scaffold structure with protease domain linked via a linker region to the helicase domain. NS2B acts as a co-factor in the NS2BNS3 protein complex [132].

NS3 is a 70 kDa, a multifunctional serine protease consisting of a conserved catalytic triad with Histidine (H-51), Aspartate (D-75), and Serine (S-135) (Figure 2.1.2). Its helicase and NTPase activities are required for unwinding the double-stranded form of RNA during the virus genome replication. The N-terminal region (1-180 residues) represents the protease domain. NS3 helicase (181-618 residues) belongs to the helical superfamily 2 domain. NS2BNS3pro complex processes the polyprotein into mature functional proteins which are required for virus assembly and replication [133, 134]. The C-terminal of NS3 forms a subdomain with essential motifs, subdomains 1 and 2: RecA-like fold and structural motifs required for ATP hydrolysis and RNA binding activities. The other subdomain 3 is involved in forming a single-stranded

DNA (ssDNA) binding tunnel during the formation of the replication complex. The viral protease shares 60-70% similarity among the four dengue serotypes [135].

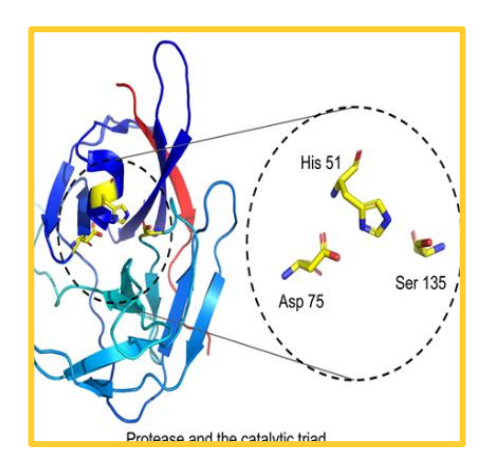


Figure 2.1.2: Folded structure of dengue viral protease carrying the catalytic triad H-51, D-75 and S-135 [80].

Unlike other proteases like trypsin (a serine protease), the binding pockets of dengue protease are shallow and superficial and therefore substrate binding is highly specific. The cleavage site for DENV protease is the dibasic amino acids (Lys-Arg, Arg-Arg, Arg-Lys, Gln-Arg) at P1/P2 followed by a small residue (Gly/Ala/Ser) at P1' position. Reports further support that the substrate cleavage site for dengue protease is Arg/Lys-Ser-Arg-Ile/Val-Leu at P1-P4 [136, 137, 138]. This protease cleaves at the juncture of C/prM, NS2A/NS2B, NS2B/NS3, NS3/NS4A, NS4B/NS5. Host proteases like furin mediated-cleavage occur at the junctions of (Cpr/M) and signal peptidase cleave at the remaining junctions i.e. C/prM, M/E, E/NS1, NS1/NS2, NS4A/NS5 [139-141]. It is reported that NS3 has self-proteolytic activity and cleaves itself at an internal cleavage site [459 a.a] within the helicase domain (Figure 2.1.3) [139].

In addition to being involved in the processing of self-polypeptide, DENV protease is known to cleave host cellular proteins like, FAM134B (Endoplasmic Receptor), Nucleoporins (Nups), thereby enhancing the viral replication and affecting host metabolism [142, 143]. During natural infections, the dengue virus primarily infects bone marrow cells, myeloid lineages, macrophages, dendritic cells, B and T cells, neuronal cells and hepatocytes [144, 145]. NS3

was found to accumulate in phagocytes of the spleen and lymph node, liver hepatocytes, and myeloid cells in bone marrow [146]. Among these cells, bone marrow megakaryocytes (MKs) are highly permissible to infection [145].

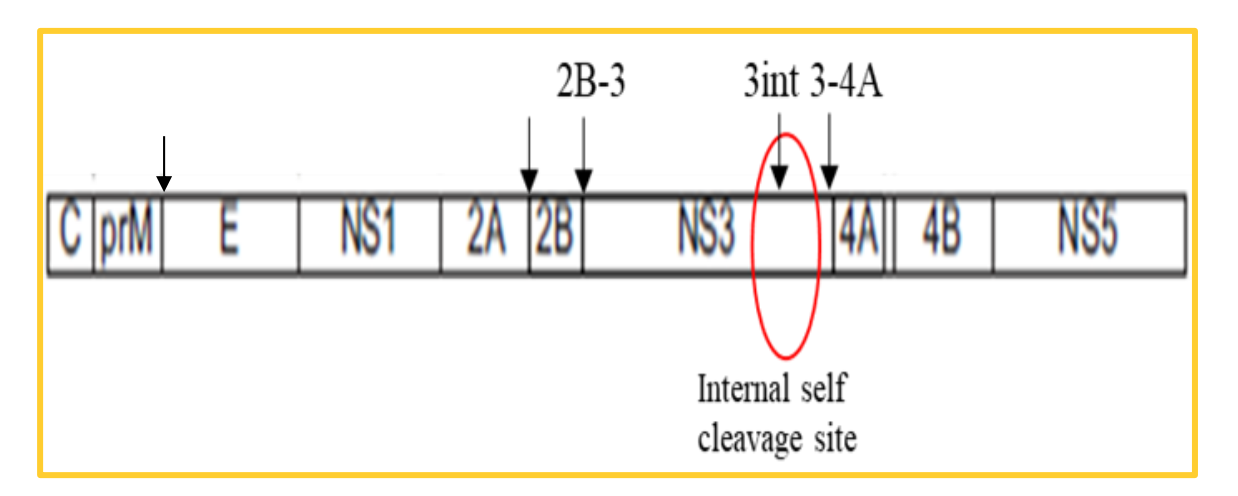


Figure 2.1.3: Dengue virus polypeptide showing viral protease cleavage sites. The black arrows represent the sites cleaved by proteases [141].

Virus-mitochondria interaction is being revealed in several reports suggesting mitochondrial dysfunction. Reports also indicate that the virus-coded proteases cleave the mitochondrial proteins. In the case of the dengue virus non-structural proteins like NS4B, NS2BNS3 target the mitochondrial membranes. The study from our laboratory reported NS3 targets the mitochondrial matrix and cleaves the GrpEL1, a co-chaperone of mitochondrial HSP70 (mtHSP70) [147]. Thus, the cleavage sites in the dengue virus polyprotein [141] and the nature of the protease activity appear to yield two forms of the protease i.e. NS2BNS3 and NS3 alone. In addition to the mitochondrial targeting by the dengue virus protease, it was also detected in the host nucleus. But, whether it is NS2BNS3 or NS3 or both is not known. Hence in this chapter, we made an attempt to understand the existing forms of dengue virus protease and to reveal the localization of NS2BNS3 and NS3 in subcellular organelles. In this context, we have generated different recombinant constructs of protease and dengue virus cultures and subcellular studies were carried out.

2.2 MATERIALS AND METHODS

Serotyping and genotyping analysis of dengue virus strains circulating in South India has been carried out in our laboratory for the past 15 years. Complete nucleotide sequences of serotypes 1, 2 and 4 characterized in our laboratory are deposited in the NCBI gene bank database [KX618706, KX845005, KX618706, MG560144]. The sub-genomic parts of serotype 1 (Figure 2.2.1) are used as templates for generating the recombinant constructs necessary in the present study.

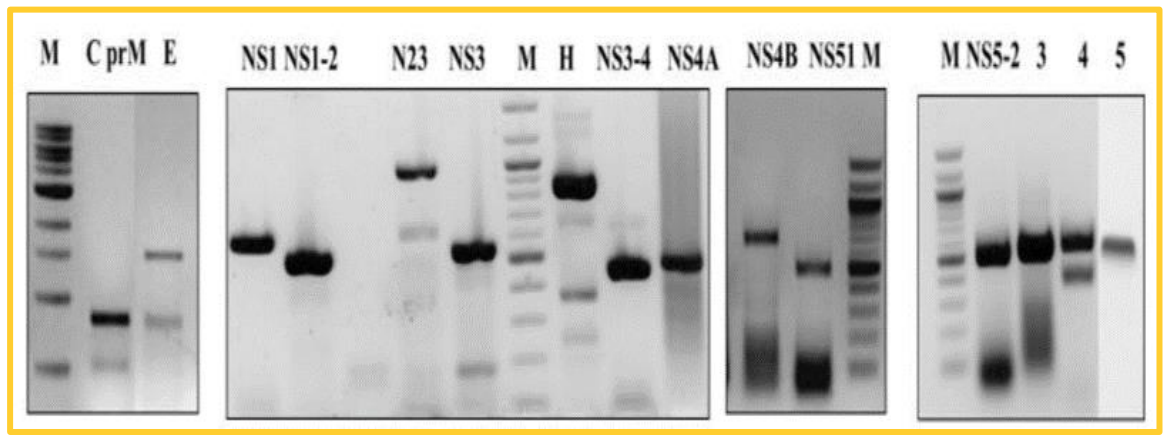


Figure 2.2.1: Agarose gel image depicting different sub-genomic parts of the genome of DENV1 serotype (Accession no: KX618706) characterized in-house.

2.2.1 Prediction of Nuclear Localization Signals (NLS)

To identify the nuclear localization signals in NS2BNS3 and NS3, the amino acid sequences were retrieved from the NCBI database of the in-house characterized DENV1 with Accession no. KX618706.1, Protein id. ASD49618.1. NLS in both the sequences were determined using the cNLS mapper software with a cutoff score of 0.4 and also identified the residues that show the monopartite and bipartite NLS sequences based on classical nuclear localization signal.

2.2.2 Generation of Dengue Virus Protease recombinant constructs

The following plasmid constructs were generated and used for the present study:

- 1. pRSET-A NS2BNS3pro.
- 2. pEGFP-N1 NS2BNS3pro.
- 3. pEGFP-N1 NS2BNS3pro (S135A) mutant.
- 4. pEGFP-N1 NS2BNS3.
- 5. pEGFP-N1 NS3pro-helicase (NS3).

Below is the description of cloning of each construct:

pRSET-A NS2BNS3pro (46+185 a. a.), clone was generated earlier in our previous study [84]. Briefly, NS2BNS3pro consists of the hydrophilic domain of NS2B (46 a.a) and the protease domain of (NS3 185 a.a) was linked via a G4-S-G4 linker sequence. NS2B was amplified using NS2B Forward- 5' TATGGGATCCGCTGATTTATCATTGGAGAAA and NS2B Reverse 5 3, NS3pro amplified NS3 Forwardprimers. using was 5'GGGGGGGGAGTAGTGGTGGAGGCGGAGAGCAGTTCTTGATGATGGTA and NS3 Reverse 5'ATCGAGAATTCTTACCTAAACACCTCGTCCTCAATC3' primers. The obtained gene products were used as templates with external primers (the above forward primer of NS2B and the reverse primer of NS3) for overlap extension PCR (OE PCR) to generate NS2B-G4-S-G4-NS3pro. This amplified DNA was digested with *EcoRI* and *BamHI* enzymes and then ligated to the similarly digested pRSET-A vector.

Ligation Reaction

The digested gel eluted products were ligated using the T4 ligase enzyme. The reactions were performed in a final volume of 15 µl with 1x T4 DNA Ligase Buffer, 100 ng of vector, 3 folds of

the insert, and 1 µl T4 DNA Ligase. The reaction was carried out at 22°C for 90 minutes and left at 4°C overnight.

Bacterial Transformation

The above ligated product was transformed into E. coli. DH5 α competent cells. DH5 α cells were thawed for 5 minutes on ice, ligated product was added to thawed cells and kept on ice further for 20 minutes followed by a heat shock at 42°C for 90 sec. After incubation on ice for 2 minutes, 1 ml of LB media was added to the cells and incubated for 1-2 hours at 37°C with shaking. The cells were centrifuged at 6000 rpm for 2 minutes. 900 μ l of LB media was discarded, and the pelleted cells were resuspended in 100 μ l LB media. 100 μ l DH5 α cell suspension was then spread on LB agar plate containing antibiotic (ampicillin or kanamycin) and incubated at 37°C overnight. The colonies were screened for the presence of insert by colony PCR. Plasmid DNA was isolated from the positive transformed colonies using a Thermo Scientific miniprep plasmid isolation kit as per the manufacturer's instructions. The obtained plasmids containing the inserts were confirmed by sequencing.

pEGFP-N1 NS2BNS3pro, the above pRSET-A NS2BNS3pro was used as a template with forward 5' TATG<u>CTCGAG</u>ATGGCTGATTTATCATTGGAC 3' and reverse 5' TATC<u>GGATCC</u>GTAAACACCTCGTCCTC 3' primers. The amplified fragment (696 bp) and pEGFP-N1 vector were digested with *XhoI/BamHI* enzymes and gel purified by a gel extraction kit (Thermofisher Scientific) [84].

pEGFP-N1 NS3pro-helicase (464 a.a) construct was also developed during our previous study [147]. To develop this construct, NS3pro (185 a.a) was amplified using the NS3 forward 5' TATG<u>CTCGAG</u>ATGGGATGGTATCTATAGA3' and reverse 5' GGATGTAGGTCCATTATTGTTAGGT 3' primers. Helicase was amplified using forward F

5'TATC*GGATCC*CCCATGTAAATATACTGG 3' primers. The reaction was performed in a final volume of 25 μl containing 0.5 μl of cDNA template, 2.5 μl reaction buffer, 0.5 μl of 10mM dNTPs, 0.25U of Taq polymerase enzyme, 0.5 μl of each of 10 μM forward and reverse primers. Cycling conditions were followed with an initial denaturation step at 95°C for 4 minutes, followed by 35 cycles of 94°C for 30 seconds, 53°C for 30 seconds and 72°C for 1 minute, and a final extension at 72°C for 10 minutes. The final products were electrophoresed on 1% agarose gel and purified by gel extraction method. Further, overlapping extension PCR was carried out to generate NS3pro-helicase (464 a.a) using forward primer of NS3 protease containing *XhoI* restriction site at 5' end and reverse primer of helicase containing *BamHI* restriction site at 3' end as mentioned above. The plasmid construct, NS3pro-helicase, consists of 185 amino acids protease domain of NS3 and 283 amino acids of helicase domain. The obtained clone was ligated into the pJET 1.2 vector, transformed and further subcloned into the pEGFP-N1 vector using *XhoI/BamHI* restriction sites to obtain pEGFP-N1 NS3pro-helicase.

pEGFP-N1 NS2BNS3 (130+464=594 a.a), NS2B fragment was amplified using NS2B forward GCCCCTCAATGAAGGAATTATGG NS2B 5' and reverse TGATCTCTGTTTCTGCCA 3' primers. The reaction was performed in a final volume of 25µl containing 0.5µl of cDNA template, 2.5µl reaction buffer, 0.5µl of 10mM dNTPs mix, 0.25U of Taq polymerase enzyme, 0.5 µl of each 10 µM forward and reverse primers. The pTZ57RT-NS2BTA construct that existed in lab was used as a template. Cycling conditions were followed with an initial denaturation step at 95°C for 4 minutes, followed by 35 cycles of 94°C for 30 seconds, 53°C for 30 seconds, 72°C for 1 minute, and a final extension at 72°C for 10 minutes. The final products were electrophoresed on 1% agarose gel and purified by a gel extraction method and used as templates for overlapping extension PCR. The reaction mixture was prepared by adding the templates, NS2B and NS3pro-helicase (100 ng each), 1X buffer, 10 mM dNTP and Q5 polymerase. Two-step overlapping extension PCR was carried out to join NS2B at the 5' end of NS3pro-helicase: 94°C for 4 minutes, (94°C for 30 seconds, 55°C for 40 seconds, 72°C for 1.4 minutes) 10 cycles followed by 72°C for 15 minutes as a final extension. Later, external primers (NS2B forward & helicase reverse) were added and followed by 35 cycles of second round of PCR, 94°C for 30 seconds, 53°C for 30 seconds, 72°C for 1.4 minutes, and final extension at 72°C for 10 minutes. The obtained fusion fragment was electrophoresed on 0.8% agarose gel and purified by gel extraction method. The overlapping extension PCR amplified product of NS2BNS3 (594 a.a) was ligated to pJET 1.2 using T4 DNA ligase. The ligated product was transformed into *E. coli*. DH5α competent cells. Plasmid was isolated, and insert was confirmed by restriction digestion. To sub-clone pJET 1.2 NS2BNS3 into pEGFP-N1 vector, pJET 1.2 NS2BNS3 and pEGFP-N1 vector were subjected to *Xhol/HindIII* restriction enzyme digestion. 1.8 kbp digested product from pJET1.2 clone was obtained and further ligated to linearized pEGFP-N1 vector. The ligated recombinant was transformed into *E. coli*. DH5α competent cells. Plasmid was isolated, and insertion was confirmed by restriction digestion and further by sequencing.

NS2BNS3pro (S135A) mutant (130+185 a.a), NS3pro (S135A) was generated by site-directed mutagenesis [147]. The dengue virus NS3 protease inactive mutant was generated by amino acid substitution Ser135 in a catalytic triad with Ala using the primers Forward, 5'-TTTTAAACCCGGCACAGCTGGATCTCCC 3' and Reverse, 5'-TCACGATGGGAGATCCAGCTGTGCCGG 3' primers. Above amplified NS2B (130 a.a) and NS3pro (S135A) (185 a.a) were overlapped with overlapping extension PCR using forward 5' GCCCCTCAATGAAGGAATTATGG 3' of NS2B at 5' end and reverse 5' GGATGTAGGTCCATTATTGTTAGGT 3' primers of NS3 at 3' end as described above. The obtained fusion fragment was electrophoresed on 0.8% agarose gel and purified by gel extraction method. NS2BNS3pro (S135A) mutant was ligated to pJET 1.2 blunt end vector

using T4 ligase and clone was confirmed using *XhoI/HindIII* restriction digestion. The digested NS2BNS3pro (S135A) mutant was further subcloned to pEGFP-N1 vector as described above. NS2BNS3 (594 a.a) and NS3pro-helicase (464 a.a) are the naturally existing forms of dengue virus infections.

2.2.3 Cell Lines

For the present study, we have used HEK, Vero, K562 and HepG2 cells. The cells were cultured and maintained regularly. Routine check and sterilization practices were followed to avoid any contamination during culturing.

2.2.4 Culturing and Maintenance of Cells

Fresh 2 ml cryovial of HEK, Vero, HepG2 and K562 cells from liquid nitrogen or -80°C were thawed at 37°C in a water bath for 2-3 minutes. 1 ml of fresh Dulbecco's Modified Eagle's Medium (DMEM; Gibco) (serum-free) was added for HEK, Vero and HepG2 cells and RPMI for K562 cells. Cells were centrifuged for 3 minutes at 3000 rpm. The media was replaced and the cells were resuspended in 1 ml of fresh DMEM and RPMI media containing heatinactivated 10% (v/v) Fetal Bovine Serum (FBS) and 1% antibiotic (penicillin and streptomycin). The cells were seeded in 3 ml of DMEM and RPMI in T-25 flask and incubated at 37°C in a humidified incubator for 12-16 hours with 5% CO₂. The next day, the cells were observed to check the cell adherence of HEK, Vero and HepG2 cells under an inverted bright field microscope. The media was replaced with the fresh complete DMEM. K562 cells are non-adherent, so the media was changed during the splitting of the cells. The cells were cultured and splitted for at least 4-5 times to get the confluency up to 70-80%.

2.2.5 Dengue Virus Protease Localization Analysis

1. Cell Counting, Seeding and Transient Transfection

The above-maintained K562 cells were used for transfection. Prior to the day of transfection, $\sim 5 \times 10^5$ cells were seeded in a 6-well plate. Next day, the media was replaced with the serum-free media. Alternatively, the cells can be seeded on the day of transfection on the same day a few hours (~ 4 hours) before transfection, in serum free RPMI media.

2. Transient Transfections in K562 suspension cells

- ➤ The following plasmid constructs were used for transfections and localization studies: pEGFP-N1 vector, pEGFP-N1 NS2BNS3pro (46+185a.a), pEGFP-N1 NS2BNS3pro (S135A) mutant (130+ 185 a.a) and pEGFP-N1 NS2BNS3 (130 + 464 a.a) in K562 cells.
- Fransfection was performed using Lipofectamine 2000 reagent as per the manufacturer's protocol in a ratio of 1μg plasmid and 3μl Lipofectamine. Briefly, each plasmid construct (1.5 μg) and Lipofectamine (4.5 μl) were both diluted in serum-free OptiMEM media in two separate 1.5 ml tubes and incubated separately for 2-3 minutes.
- The diluted plasmid was mixed into diluted Lipofectamine and further incubated for 20 minutes. Plasmid-Lipofectamine complex was added to the cells and allowed to grow at 37°C incubator with 5% CO₂.
- ➤ After 28 hours, the cells were analyzed for GFP expression using fluorescence microscopy.
- Cells were harvested and washed with 1X PBS at 3000rpm for 5 minutes.
- ➤ Cells were fixed using 4% paraformaldehyde for 20 minutes.
- ➤ Then the cells were permeabilized with 0.25% Triton-X 100 buffer (0.25% in1X PBS) for 5 minutes.
- Cells were washed with 1X PBS until the Triton-X 100 buffer was removed completely.

- ➤ Cells were stained using nuclear staining Hoechst 33342 stain (Molecular probes) for 3 minutes in the dark at room temperature (RT) and the cells were washed again with 1X PBS.
- ➤ Cells were resuspended in 1X PBS and Glycerol in ratio (1:1) and mounted onto glass slide with a coverslip.
- Finally, the cells were analyzed using a laser scanning confocal microscope (Carl Zeiss) at 20X and 100X magnifications. The images were merged in order to observe the colocalizations.
- The localization color (green/blue) intensity profiles were prepared using the NIS Elements AR software program to analyze the GFP (green peak) in the nucleus along with the Hoechst stain (blue). The fluorescence percentage was calculated using (Mean intensity of each channel/total intensity in nucleus X100). *p* values indicated p<0.0001, **** = significant, ns = non-significant.

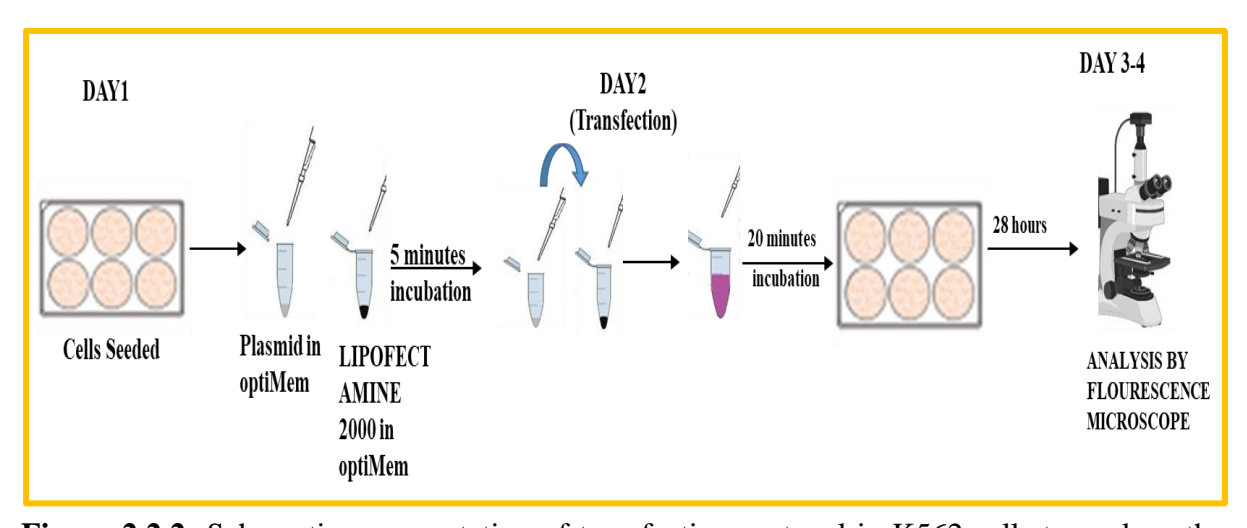


Figure 2.2.2: Schematic representation of transfection protocol in K562 cells to analyze the GFP expression.

2.2.6 Co-transfection and dual localization of dengue virus protease

1. Preparation of the cells

For this experiment, we have used HEK cells from the above-cultured cells. One T-25 flask of adherent HEK cells cultured at 37° C in a CO₂ incubator, was trypsinised for 3 minutes. DMEM containing 10% FBS was added to inactivate the trypsin and harvested the cells by centrifugation at 2500 rpm for 3 minutes. The pelleted cells were washed twice with 500 μ l 1XPBS/DMEM (without serum) in a ratio of 1:1, centrifuged at 2500 rpm for 3 minutes. After washing, cells were resuspended in the complete DMEM. Cover slips were placed in 12-well plates and the cells were counted using a haemocytometer and 8 x 10^4 to 1 x 10^5 cells per well were seeded. The seeded cells were incubated to grow for 12-16 hours in a humidified incubator at 37°C to obtain the confluency up to 70 -80 %.

2. Co-transfection in HEK cells

- ➤ HEK cells seeded in a 12-well plate, were viewed under a microscope to check the confluency.
- Plasmid constructs (pEGFP-N1 Vector, pEGFP-N1 NS2BNS3 and pEGFP-N1 NS3pro Helicase) were used for co-transfection. Co-transfection was performed using Lipofectamine 2000 reagent in a ratio of 1:2 (1μg to 2μl).
- Each of the above plasmid constructs were co-transfected along with the mitoRFP vector (1μg to 2μl Lipofectamine). Briefly, each plasmid construct (400ng to 600ng) and mitoRFP Vector (400-800 ng) were mixed together and diluted in serum-free OptiMEM. Similarly, 2 μl of Lipofectamine2000, was also diluted in serum-free DMEM or OptiMEM and both the above mixes were left for 2-3 minutes separately at room temperature. Then, the diluted plasmid was mixed with the diluted Lipofectamine to form the complex and incubated at room temperature again for 18-20 minutes. The complex was added on to cells gently on the cell monolayer and allowed to incubate for 4-6 hours at 37° C in CO₂ incubator for the transfection.

- After 4-6 hours, the serum-free media was replaced with fresh complete DMEM media and cells were allowed to grow for 48 hours to analyse the GFP and MitoRFP expression.
- After 48 hours, the cells were washed with 1X PBS and fixed using 4% paraformaldehyde for 10-20 minutes and permeablized with 0.25% Triton-X 100 buffer for 5 minutes, followed up with staining with Hoechst stain (nucleus) and mounting the coverslip with glycerol on to glass slide.

Phosphate Buffer Saline (10X)

Reagent	Stock concentrations (10X)	Amount (for 1L)
NaCl	1.37 M	80
NaH2PO4	100 mM	17.8
KH2PO4	18 mM	2.4
KCl	27 mM	2
H₂O	-	Up to 1 L

Note: Adjust pH to 7.4. Stock can be stored at room temperature up to 1 month. 1X PBS can be prepared from 10X stock: Dissolve 50 ml of 10X PBS to make up the volume to 500 ml (store at room temperature for a week).

Triton-X100 buffer

Reagent	Final concentration	Amount
Triton-X 100	0.25%	25 μΙ
1X PBS	-	10 ml

Note: Stocks can be stored at room temperature for 1 week and 4°C up to 1 month.

Hoechst 33342 stain

Reagent	Stock concentrations	Amount
Hoechst 33342 stain	10 mg/ml	10mg
H ₂ O	N/A	1 ml

Note: Working solution can be prepared by dissolving the stock in 1XPBS (1:1000). Stock solution can be stored at 4°C up to 8-12 months and protected from light.

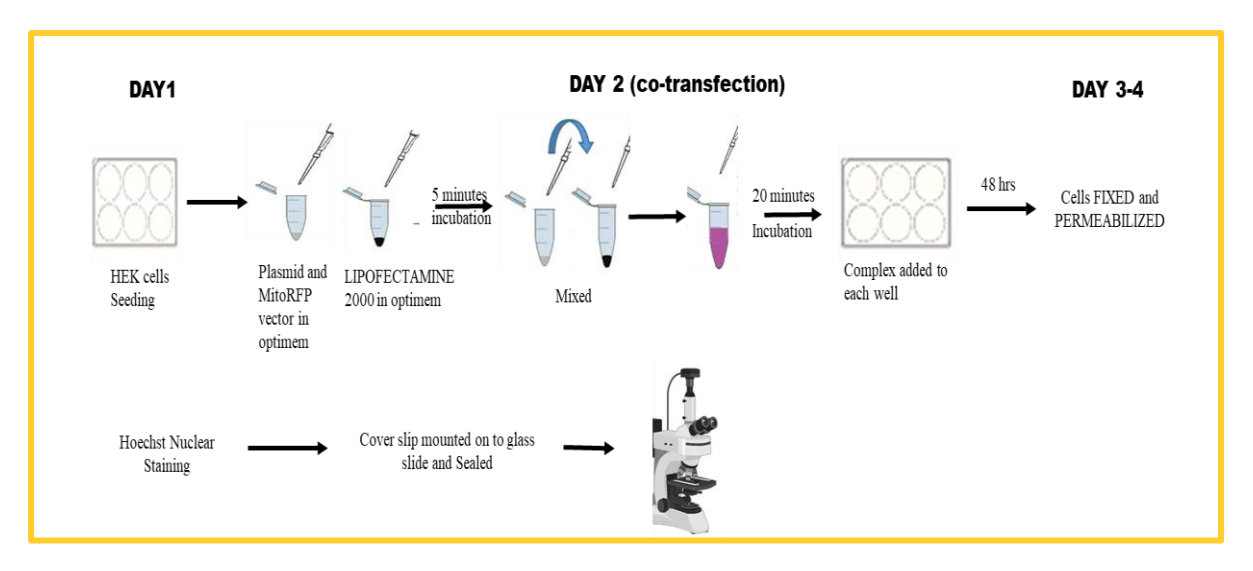


Figure 2.2.3: Schematic presentation of co-transfection and fixation protocol in HEK cells for co-localization analysis.

2.2.7 SUBCELLULAR FRACTIONATION

For the preparation of subcellular fractions, all steps are required to be performed at 4°C. Buffers should be sufficient while conducting the experiments and must be pre-cooled. 1x 10^6 HEK cells were seeded in 60 mm dishes. After 12-16 hours' cells attains ~80% confluency. Transient transfection procedure followed as mentioned above, excluding the mitoRFP plasmid construct. After 48 hours of transfection, the cells were harvested by scraping and centrifuged at 3000 rpm for 5 minutes. Cell pellets were washed with 1ml of 1XPBS by centrifuging at 3000 rpm for 5 minutes.

(i) Preparation of whole cell lysate

- 1. For whole cell lysate, the cell pellet was resuspended in 100-120 µl RIPA buffer, incubated on ice for 30 minutes and vortexed 2-3 times in intervals for 15 minutes.
- 2. The solubilized lysate was centrifuged at 20000x g for 15 minutes and the supernatant was collected as whole cell lysate.

(ii) Preparation of Cytoplasmic Fraction /mitochondria

- 1. For preparing the cytoplasmic fraction, harvested cells were washed with 1ml of ice-cold 1XPBS.
- 2. Cells were incubated for 5 minutes or mildly homogenized in hypotonic buffer and further incubated for 10 minutes. The homogenized lysate was centrifuged at $2000-3000x\ g$ at 4° C for 10 minutes. The supernatant was collected as cytoplasmic fraction and the pellet was used for nuclear extraction.

Hypotonic Buffer

Reagent	Stock concentrations	Final concentrations	Amount
HEPES (pH 7.9)	1M	20 mM	1 ml
KCl	1M	10 mM	500 μl
EDTA	100mM	1 mM,	500 μl
Glycerol	100%	10%	5 ml
Triton-X100	100%	0.5%	250 μl
H2O	N/A	-	40.50 ml

Note: EDTA can be stored at -20°C up to 1-3 months. Stocks can be stored at 4°C up to 1 month.

(iii) Preparation of Nuclear Extract

- 1. For preparing the nuclear extract, the nuclear pellet obtained from above fractionation was further washed twice with 1ml 1XPBS and resuspended in 100 μ l RIPA buffer.
- 2. The resuspended pellet was incubated for 30 minutes on ice and vortexed at 5-minute intervals.
- 3. The completely dissolved pellet was allowed for centrifugation at $20,000 \times g$ for 15 minutes and the supernatant was collected as a nuclear fraction.

For nuclear fraction, the hypertonic buffer can be used. The lysates (whole cell lysates, cytoplasmic and nuclear fractions) were quantified using Bradford reagent and resolved on 10% SDS PAGE and immunoblotted with NS2BNS3pro antibody (1:1000), anti-GFP antibody (1:1000) and actin (1:2500), or can be stored in -80°C until use.

Hypertonic Buffer

Reagent	Stock concentrations	Final concentrations	Amount
HEPES (pH 7.9)	1M	20 mM	1ml
KCI	1M	10 mM	500 μl
NaCl	1M	240 mM	12 ml
EDTA	100 mM	1 mM,	500 μl
Glycerol	100%	20%	10 ml
Triton-X100	100%	1%	0.5 ml
H2O	N/A	-	25.50 ml
Stocks can be stored at 4°C up to 1 month.			

RIPA Buffer (1X) Ready-to-use buffer containing 150 mM NaCl, 1.0% IGEPAL® CA- 630, 0.5% sodium deoxycholate, 0.1% SDS, 50 mM Tris. pH 8.0 can be stored at 4°C up to 3-4 months.

Protease Inhibitor Cocktail (10X)

Reagent	Stock Concentrations	Amount for 1 ml
Protease Inhibitor Cocktail	100X	100 μl
Н2О	-	900 μl

Note: Aliquots of 10X Stock can be stored at -20°C up to 3-4 months or at 4°C for 1 month. Donot repeat freeze thaw.10X stock can be directly used to make 1X (final concentration) according to the volume of RIPA buffer required for the extraction procedure.

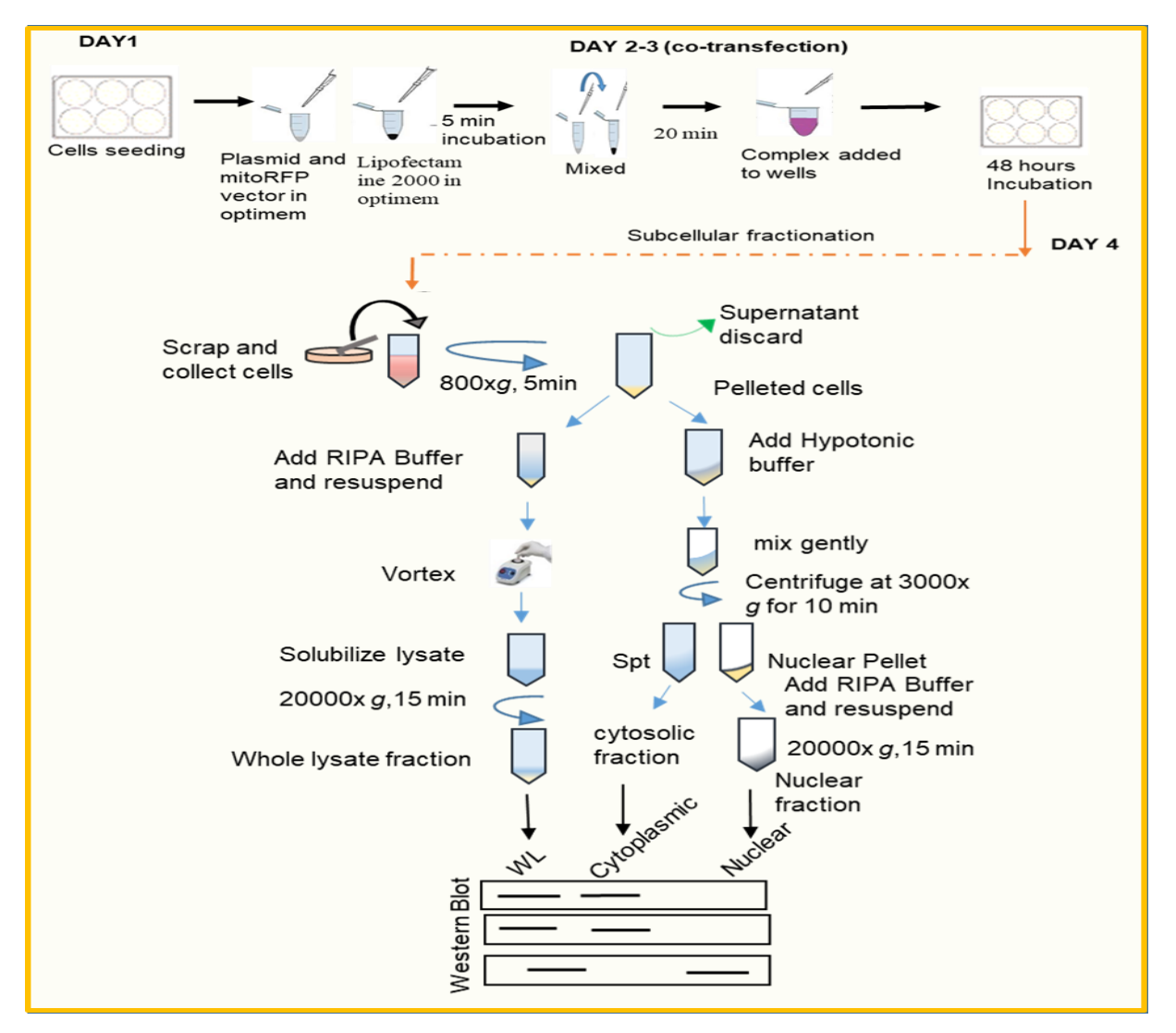


Figure 2.2.4: Schematic protocol briefing the procedure of transfection followed by subcellular fractionation.

2.2.5 Dengue Protease Localization in Nucleus of virus infected K562 cells

K562 cells were seeded in a 12-well plate at a density of 1 x 10⁵ cells per well. Cells were infected with viral supernatant at 0.09 multiplicity of infection (MoI). After 2-3 hours of viral adsorption, the media was replaced with RPMI containing 4% FBS and further incubated for 72 hrs. The cells were fixed using 4% paraformaldehyde and permeabilized using 0.25% Triton-X 100. The cells were allowed for blocking with BSA for 1 hour 30 minutes and incubated overnight with primary antibody (NS2BNS3pro raised in-house) in 1:1000 followed

up by fluorescent conjugated secondary antibody Alexa flour 488. Cells washed by 1X PBST and stained with Hoechst stain (1:1000). Cells were analyzed using immunofluorescence microscope and analyzed at 60X magnification. The viral supernatants collected, aliquoted for quantification by focus forming assay or stored at -80°C for further use (Figure 2.2.5).

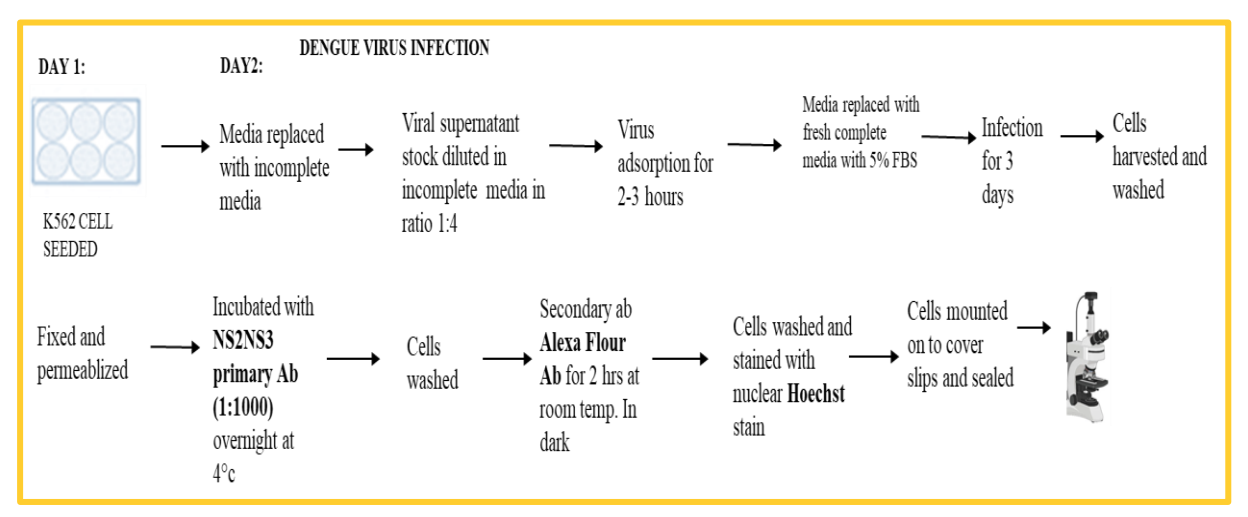


Figure 2.2.5: Represents the protocol describing the infection in K562 cells and detecting the virus infection by indirect immunofluorescence assay.

2.3 RESULTS

2.3.1 Identification of Nuclear Localization Signals (NLS) and development of recombinant constructs

Using *in silico* method, NLS sequences were identified in both NS2BNS3 (594 a.a) and NS3pro-helicase (464 a.a). In NS2B (130 a.a), three basic amino acid residues ¹⁴⁷¹KKKQR¹⁴⁷⁵ at position 1471-1475 were identified which are similar to classical monopartite NLS stretch that consists of basic amino acid residues with motif K (K/R) X (K/R). In the NS3 sequence, two stretches of bipartite signal (2 to 3 positively charged amino acid followed by 9-12 linker sequence containing proline residue) were identified at positions (a.a 1656-1716 and 1839-1856) with a score of 4-4.1 (Figure 2.3.1) [148]. The mitochondrial targeting sequence (MTS) was identified in NS3 during our earlier study [147].



Figure 2.3.1: Amino acid sequences of existing forms of protease **(A)** NS2BNS3 (NS2B-130+NS3-464 = 594 a.a), **(B)** NS3pro-helicase (464 a.a). Amino acid sequence showing the nuclear localization sequence (NLS) in green and mitochondrial targeting sequence (MTS) in red. Full length NS2B sequence in (blue) and NS3 sequence in (black).

Based on the *in silico* analyses, the recombinant constructs NS2BNS3pro (46 + 185 a.a), NS2BNS3pro (S135A) mutant (130 + 185 a.a), NS2BNS3 (594 a.a) and NS3pro-helicase (464 a.a) were generated in pEGFP-N1vector (Figure 2.3.2).

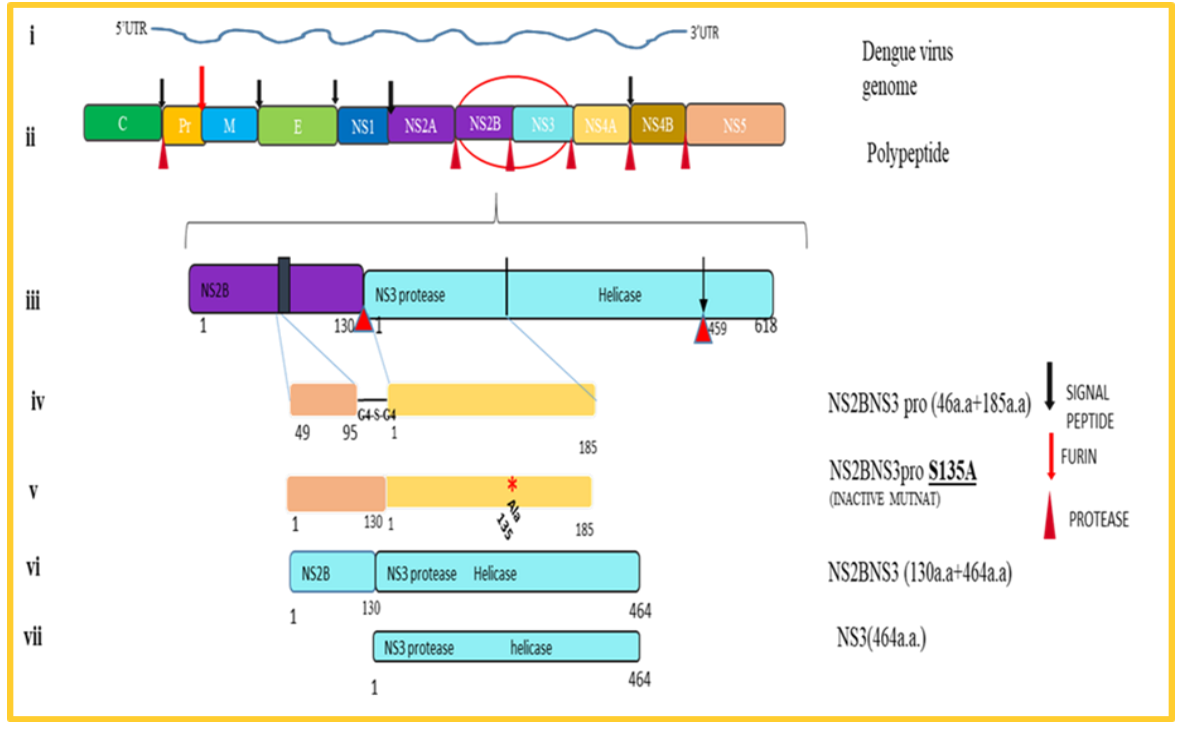
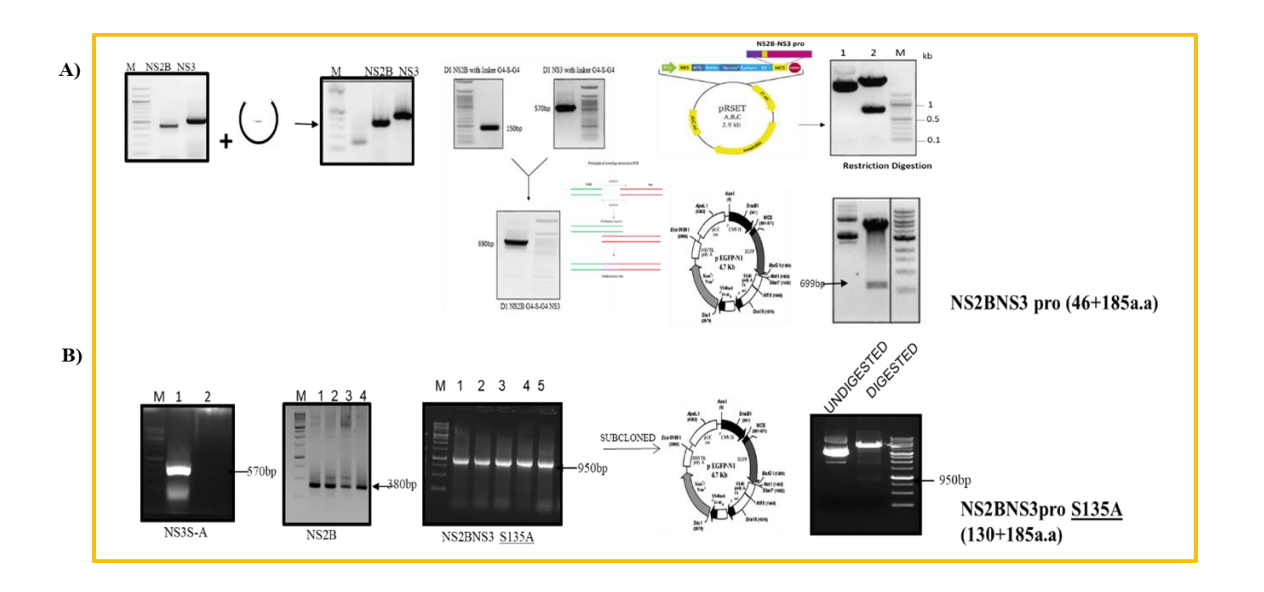


Figure 2.3.2: Diagrammatic presentation of recombinant constructs generated in the present study. (i) Dengue virus genome (RNA) (ii) Dengue virus mature polypeptide showing

structural proteins (capsid, pre-membrane and envelope) and non-structural proteins (NS1 – NS5) (iii) Dengue virus full length protease with NS2B and NS3 fragments. (iv) NS2B (46 a.a) Glycine linked (G4-S-G4) NS3 protease (185 a.a) (v) Mutant form of NS2BNS3pro (S135A) (NS2B -130 a.a and NS3pro-185 a.a) (vi) NS2BNS3 (130 + 464 a.a) (vii) NS3 pro-helicase (464 a.a).

The construction of NS2NS3pro (46+185a.a) as mentioned in materials and methods (Figure 2.3.3 A). The nucleotide sequences corresponding to 46 amino acid hydrophilic domains of NS2B and N-terminal 185 amino acids of NS3 were amplified (Figure 2.3.3 A). Both the domains were fused by overlapping extension PCR. A 696 bp fragment was obtained for the recombinant construct of NS2NS3B3pro. Further, the pRSET-A expression vector with N-terminal 6X His-tag containing the above recombinant segment of NS2BNS3 pro was also generated used (Figure 2.3.3 A). We have also generated the mutant form of the above NS2BNS3pro (S135A). This form was developed to study the functional analysis. The clone was generated by mutating the Serine-135 to Alanine thereby inactivating the functionally active site of protease (Figure 2.3.3 B). Further, we generated the NS3pro-helicase and NS2BNS3, which are naturally occurring forms of protease existing during virus infection. Both the clones were developed by overlapping extension PCR as detailed in materials and methods 1.3kbp and 1.8kbp recombinant clones were generated and confirmed by sequencing (Figure 2.3.3 C&D) [148].



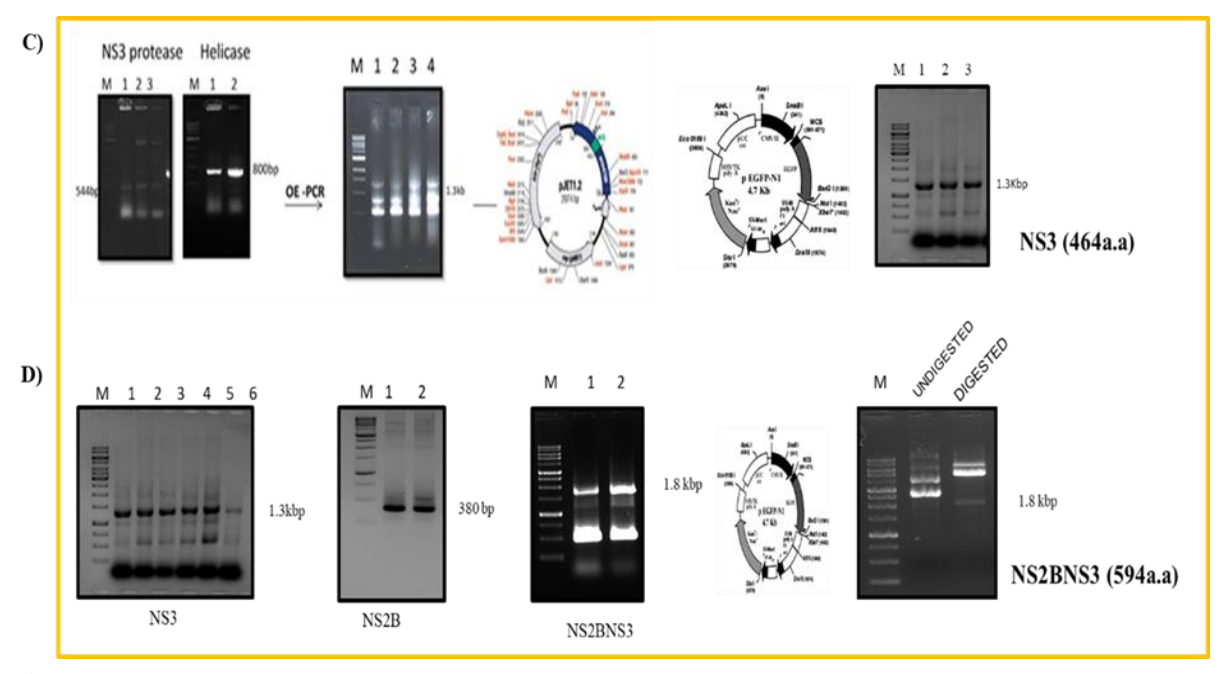
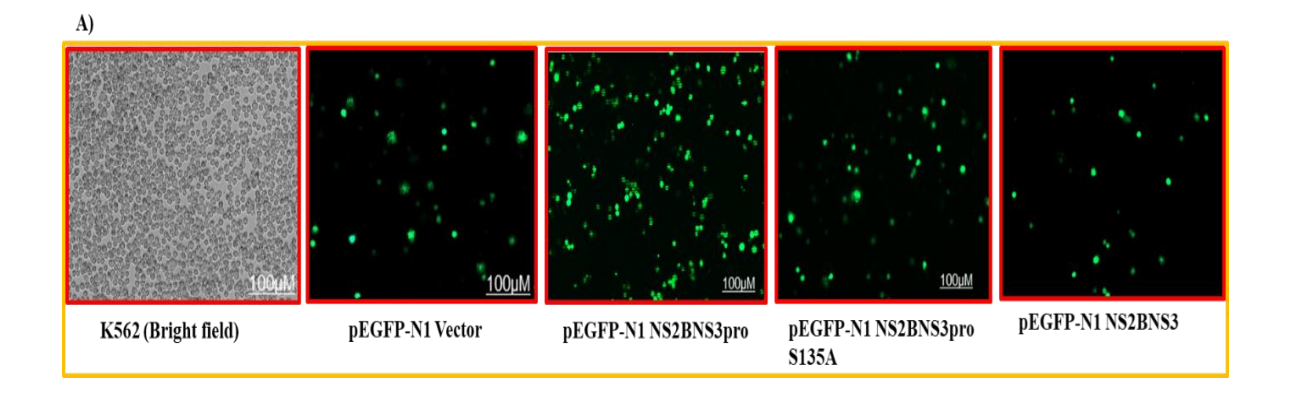


Figure 2.3.3: Representative images showing the cloning strategy of each construct in pEGFP-N1 vector. **(A)** pEGFP-N1 NS2BNS3pro (46+185 a.a), **(B)** pEGFP-N1 NS2BNS3pro (S135A) mutant (130+185 a.a), **(C)** pEGFP-N1 NS3 (464 a.a) **(D)** pEGFP-N1 NS2BNS3 (594 a.a).

2.3.2 Protease Localization Studies

We have performed transfections in K562 cells and analyzed the cells at 10X and 20X magnification for the transfection efficiency and the data suggested that 50-60% of the cells were positively transfected (Figure 2.3.4 A and B).



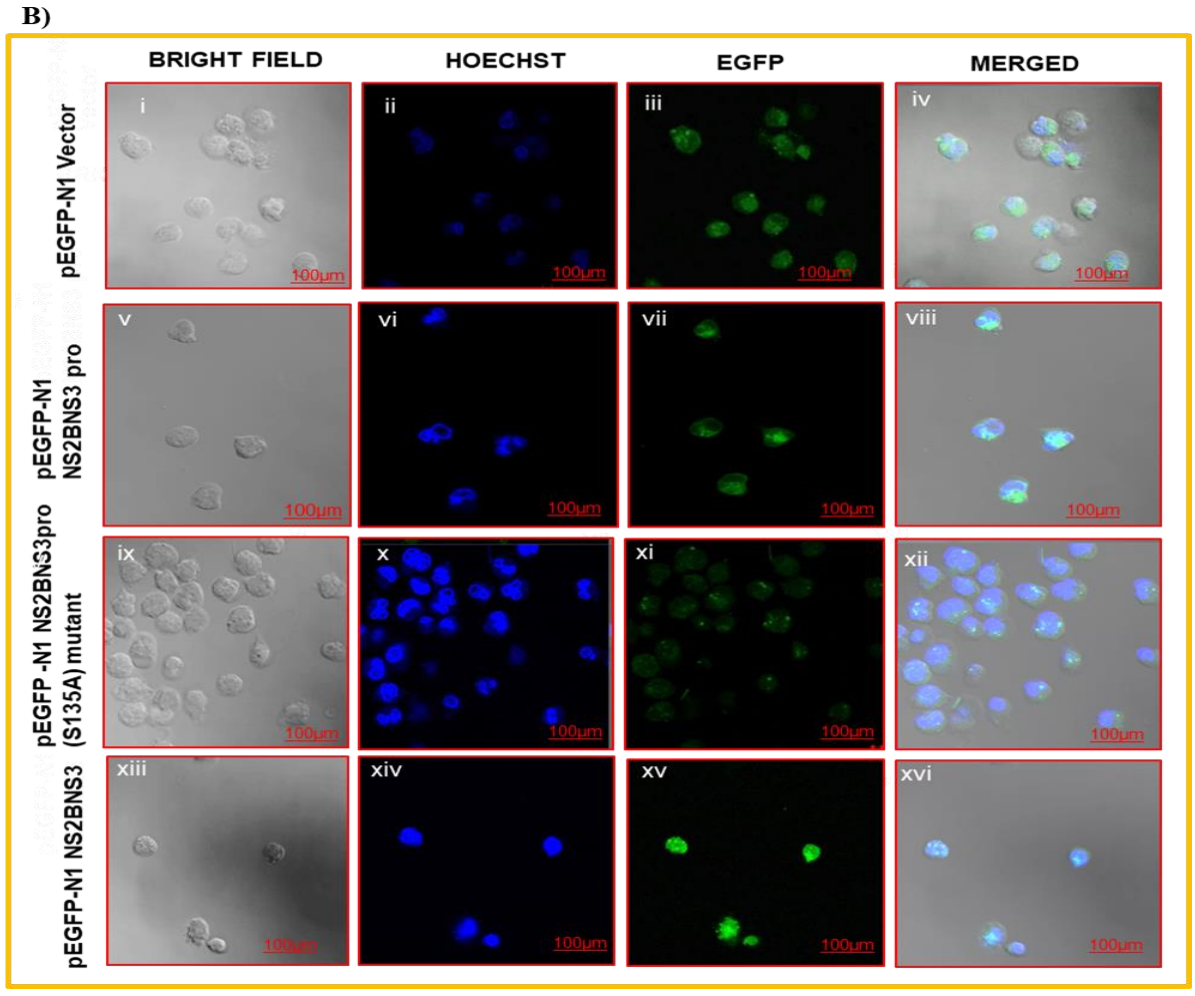
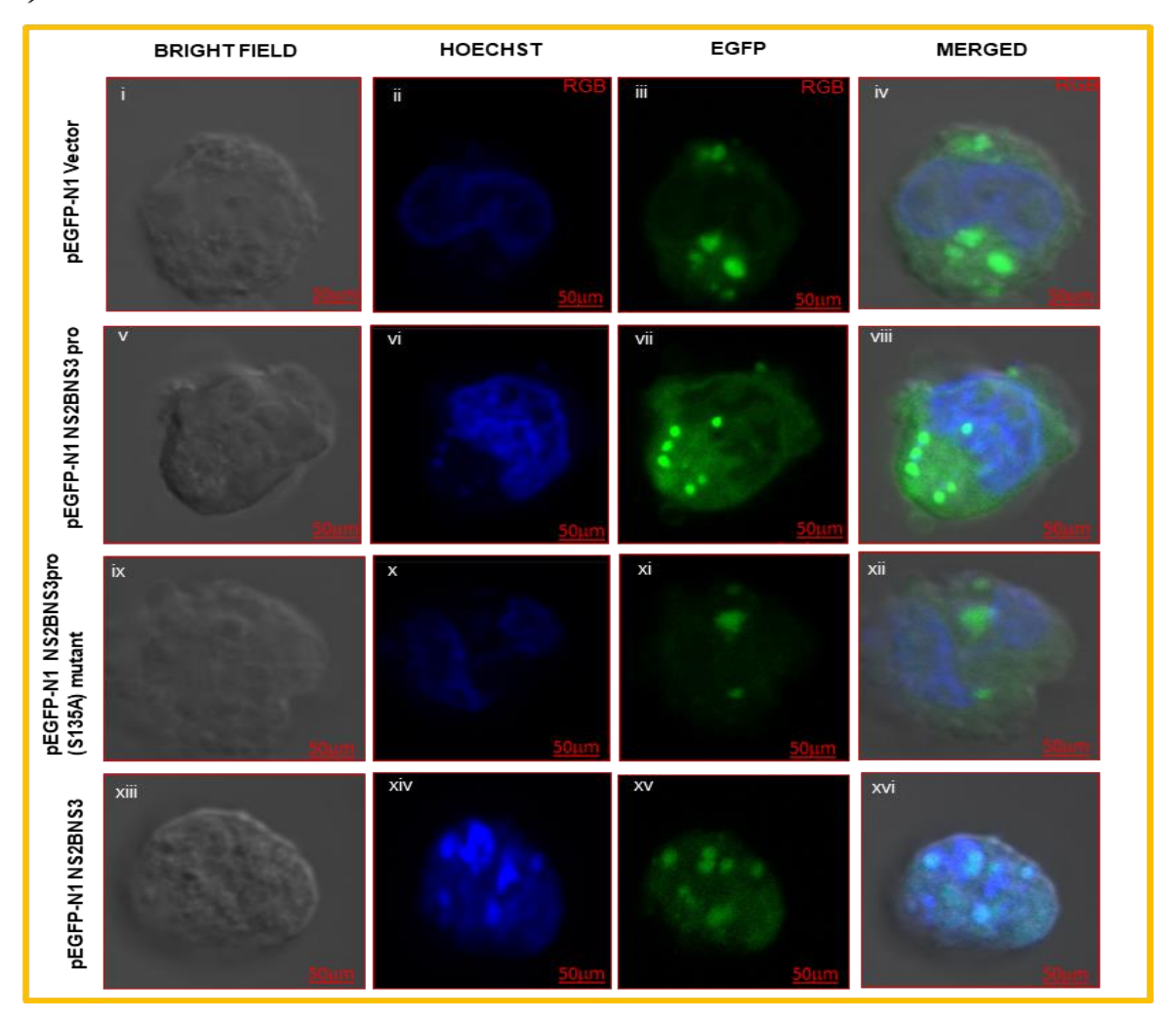


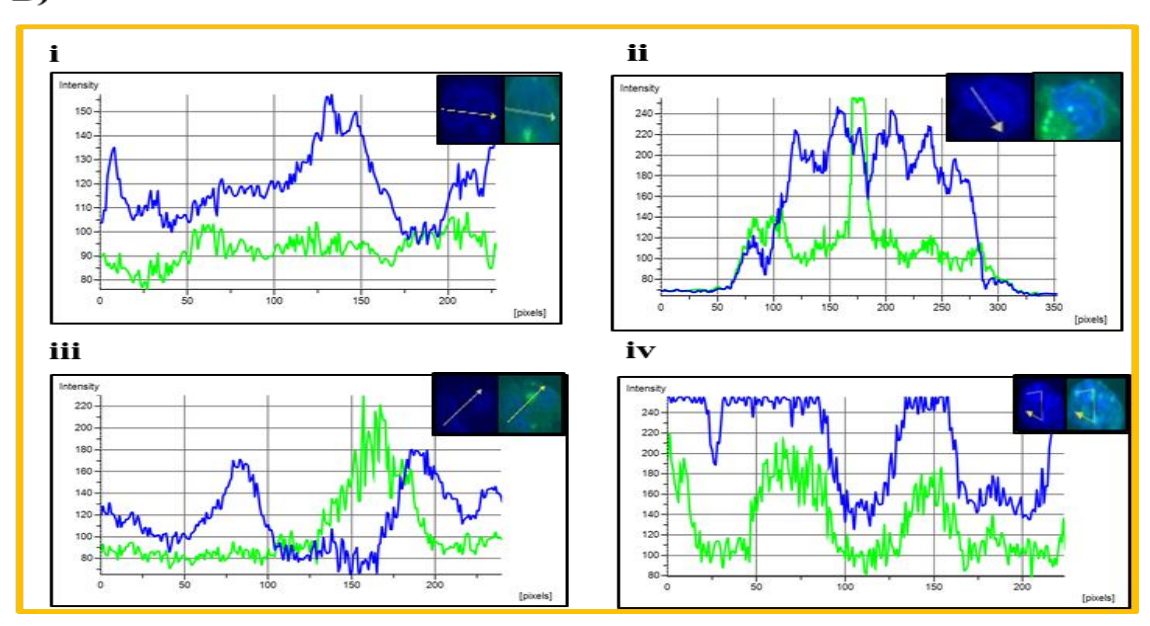
Figure 2.3.4: Representative images of transfected K562 cells analyzed using the confocal microscope. (**A**) 10X and (**B**) 20X-100μm, analyzing the transfection efficiency of the GFP-tagged recombinant constructs.

Further, the data indicated that the expressed proteins (GFP-tagged) of all three constructs [(NS2BNS3pro, NS2BNS3pro (S135A) mutant and NS2BNS3)] localized to the nucleus compared to vector alone as the GFP was found to merge with the Hoechst stain (nucleus) (Figure 2.3.5 A & B). In pEGFP-N1 vector, the intensity of the green peak is low and does not merge with blue peak, but in case of pEGFP-N1 NS2BNS3pro, pEGFP-N1 NS2BNS3pro (S135A) mutant and pEGFP-N1 NS2BNS3 shows merged green peaks with blue peaks of varying intensities indicating the GFP expression in nucleus (Figure 2.3.5 B (i-iv)). The bar graphs further support the above observation with the high GFP/blue expression ratios which represent the percentage mean arbitrary intensity in the nucleus (Figure 2.3.5.C) [148].

A)



B)



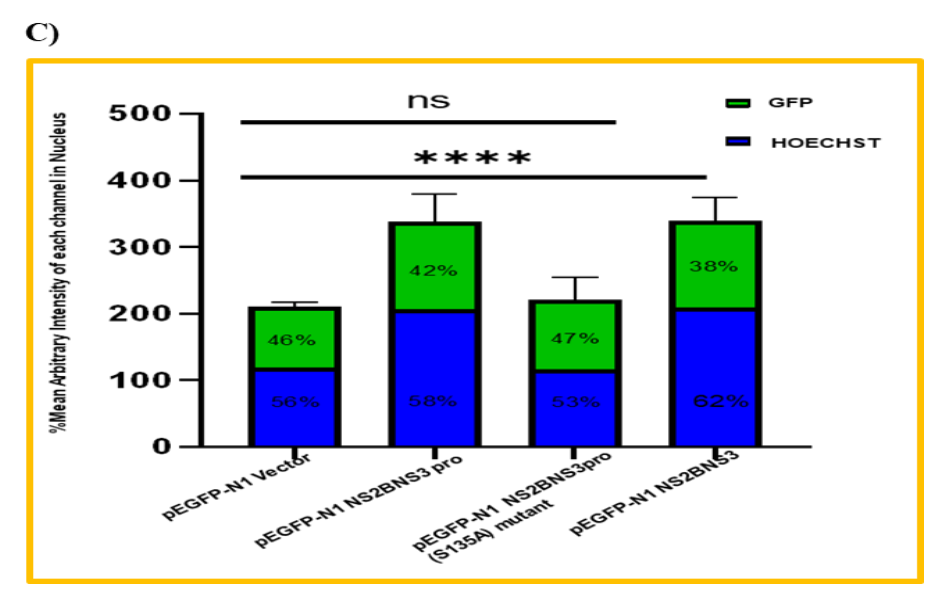
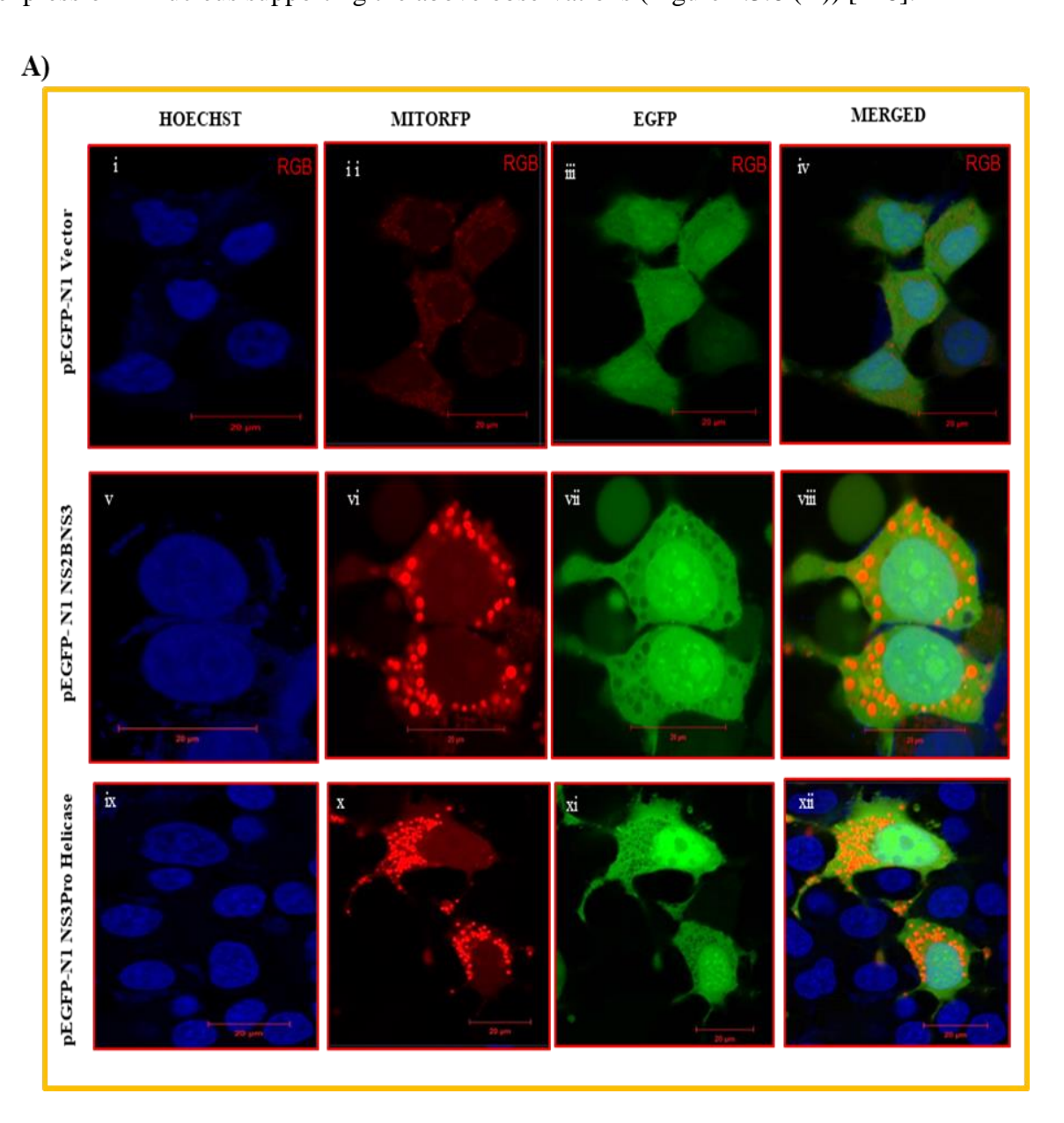
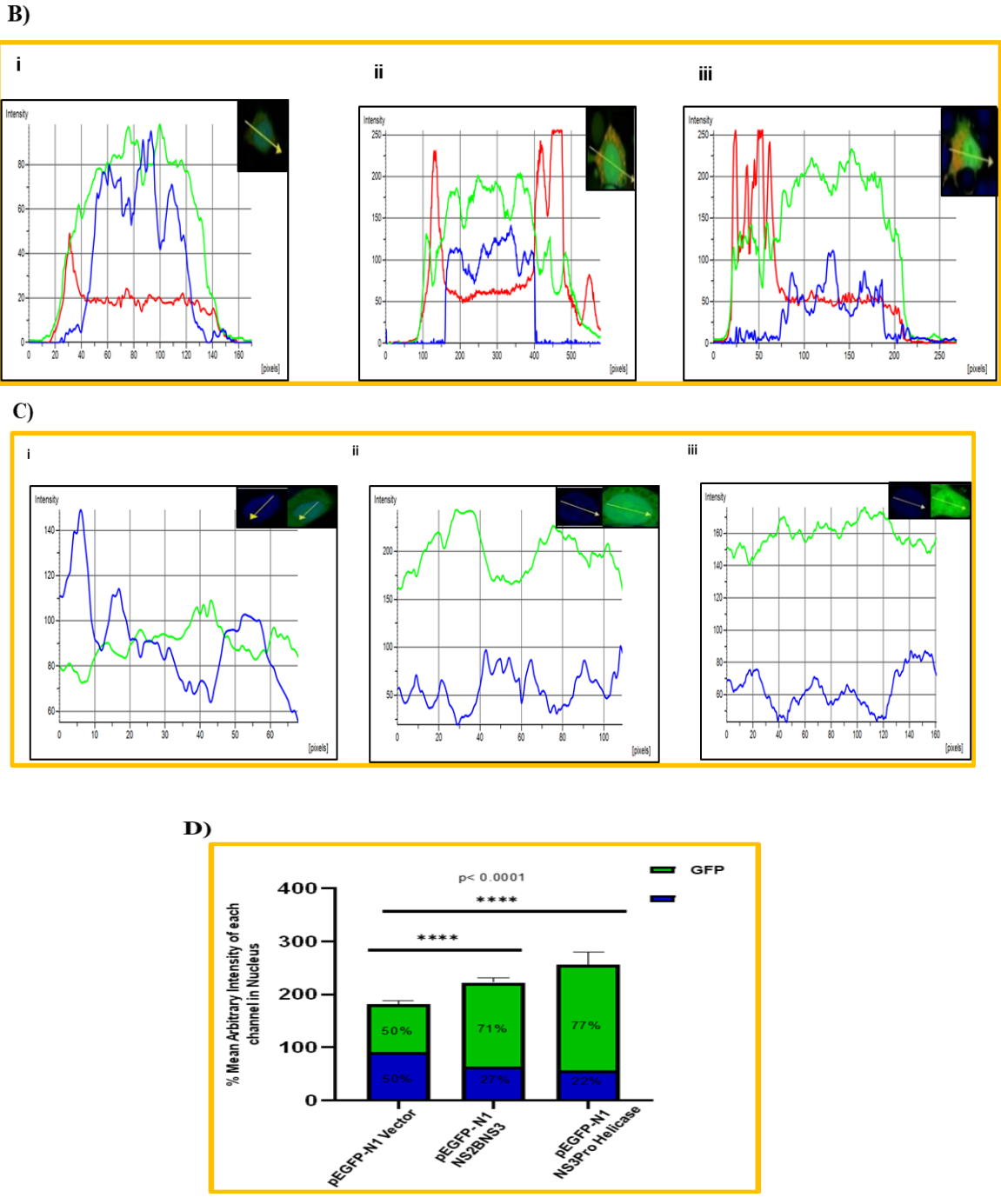


Figure 2.3.5: Localization of expressed dengue virus protease in K562 cells. (A) pEGFP-N1 vector (i-iv), pEGFP-N1 NS2BNS3pro (v-viii), pEGFP-N1 NS2BNS3pro (S135A) mutant (ix-xii), pEGFP-N1 NS2BNS3 (xiii-xvi) were transfected transiently and observed after 28 hours post-transfection. The images represent the bright field (Grey), Hoechst33342 (nuclear staining blue), GFP (green) and merged at 100X (scale bar = 50 μm) magnification using Carl Zeiss confocal microscopy. (B) (i) Fluorescence intensity profiles using NIS Elements AR software of pEGFP-N1 vector showing GFP expression (green) in cytoplasm. (ii-iv) pEGFP-N1 NS2BNS3pro, pEGFP-N1 NS2BNS3pro (S135A) mutant and pEGFP-N1 NS2BNS3 show the expression in nucleus with different intensities. (C) The bar graphs represent the percentage arbitrary mean intensity of each channel (Green and Blue) in nucleus of transfected cells presented as mean values (±) SD plotted in graph pad prism 9. The percentage was calculated using (Mean intensity of each channel/total intensity in nucleus X100). *p*- values indicated <0.0001, **** = significant, ns = non-significant.

The NS2BNS3 also possesses the MTS along with NLS, hence we intended to analyze the possibility of its localization to the mitochondria also. In this direction, the NS2BNS3 was transfected along with MitoRFP, stained with Hoechst stain and analyzed for the localizations. The data suggested GFP and the MitoRFP expression are not merged, suggesting no localization of NS2BNS3 to the mitochondria (Figure 2.3.6 A (v-viii)). This observation is further supported by the graphical analysis showing that the red peaks are completely separated from the green peaks (Figure 2.3.6 B (ii)). It was further confirmed that NS2BNS3 localized in nucleus as indicated with a high intensity peak of GFP (green peak) in the nuclear region (Figure 2.3.6. C (ii)). But, NS3 alone was reported to be localized to the mitochondrial matrix

which shows both the MTS and NLS. In order to properly understand the localization of NS3 also, we carried the transfections along with MitoRFP, stained with Hoechst stain and analyzed the localizations in mitochondria and nucleus (Figure 2.3.6 A (ix-xii)). The results show that NS3pro-helicase enters both mitochondria and nucleus as indicated by the intensity profiles where the GFP expression (green) is merging with red (mitochondria) and high GFP intensity in blue peak region (nucleus) (Figure 2.3.6 B (iii) & C (iii)). The bar graphs which represent the percentage mean arbitrary intensity of each channel in the nucleus indicated the GFP expression in nucleus supporting the above observations (Figure 2.3.6 (D)) [148].





2.3.6: Localization of NS2BNS3 and NS3pro-helicase. (A) Confocal images at 60X (scale bar=20µm) showed the localization of pEGFP-N1 vector (i-iv), pEGFP-N1 NS2BNS3 (v-viii), and pEGFP-N1 NS3pro-helicase (ix-xii), with both localization markers i.e. MitoRFP and Hoechst. (B) Fluorescence intensity profiles were generated using NIS Elements AR software of (i) pEGFP-N1 vector (ii) pEGFP-N1 NS2BNS3 (iii) pEGFP-N1 NS3pro-helicase. (C) (i-iii) Represents the intensity profiles of GFP (green) in nucleus (blue). (D) The bar graph representing the arbitrary mean intensity of each channel (green and blue) in nucleus of transfected cells as calculated in Figure 2.3.5 C.

With the cell lysates of the above experiments, we have carried out the western blotting analysis (anti-NS2BNS3pro antibody) to verify the presence of protease forms that localize to the nucleus or mitochondria or both. The immunoblotting results were found to be consistent with the above localization experiments suggesting that the NS3pro-helicase (75 kDa) localized to both cytoplasm (mitochondria) and nucleus (Figure 2.3.7 (ii)), whereas NS2BNS3 (92 kDa) localized only to the nucleus (Figure 2.3.7 (i)). We also observed a 70 kDa band in the nucleus (Figure 2.3.7 (i)), possibly due to an internal self-cleavage site in NS2BNS3. The absence of actin (Figure 2.3.7 (iii)) and less GFP (Figure 2.3.7 (iv)) in nuclear fraction support the fractionations.

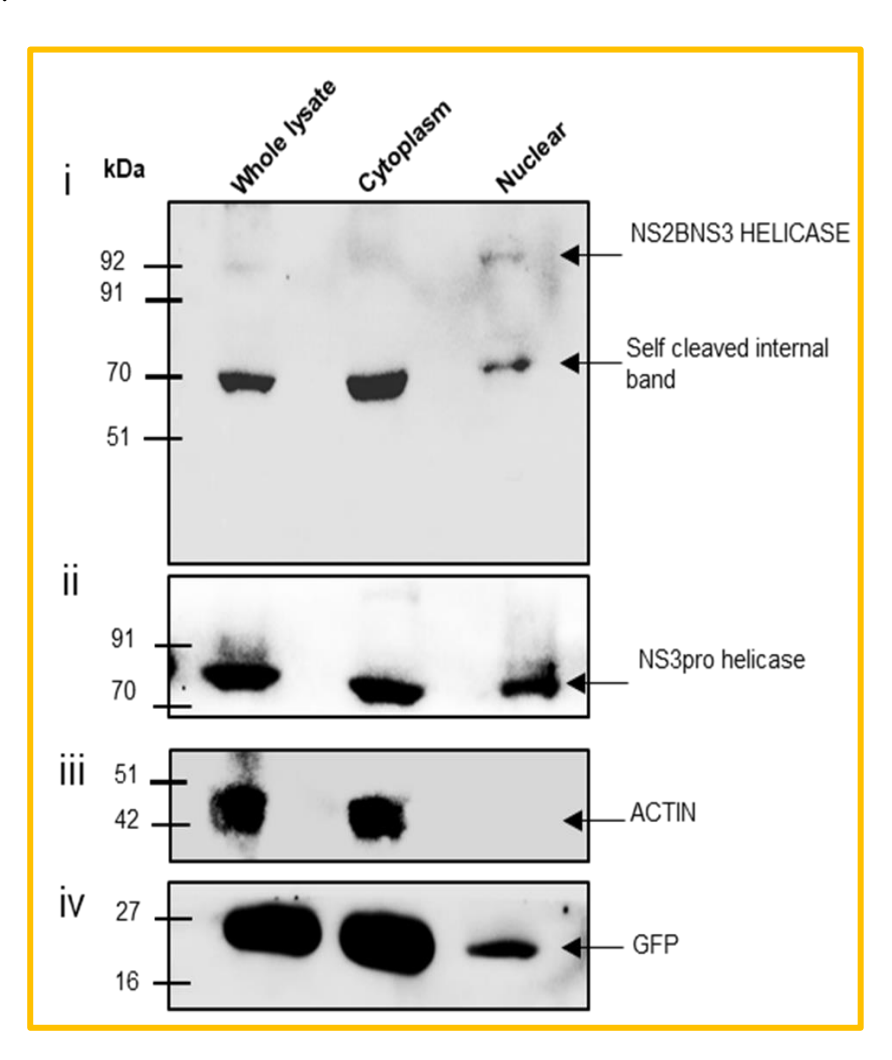


Figure 2.3.7: Western blot analysis of pEGFP-N1 NS2BNS3 and NS3pro-helicase subcellular fractions of transfected HEK cell lysates probed with NS2BNS3pro antibody (1:1000), Actin (1:2500) and GFP vector (1:1000).

With these experiments we observed that the NS2BNS3 possesses both the NLS and the MTS signals but the MTS is masked due to the presence of NS2B at N-terminal region of NS3 that might hinder the localization of NS2BNS3 to the mitochondria (Figure 2.3.8) [148].

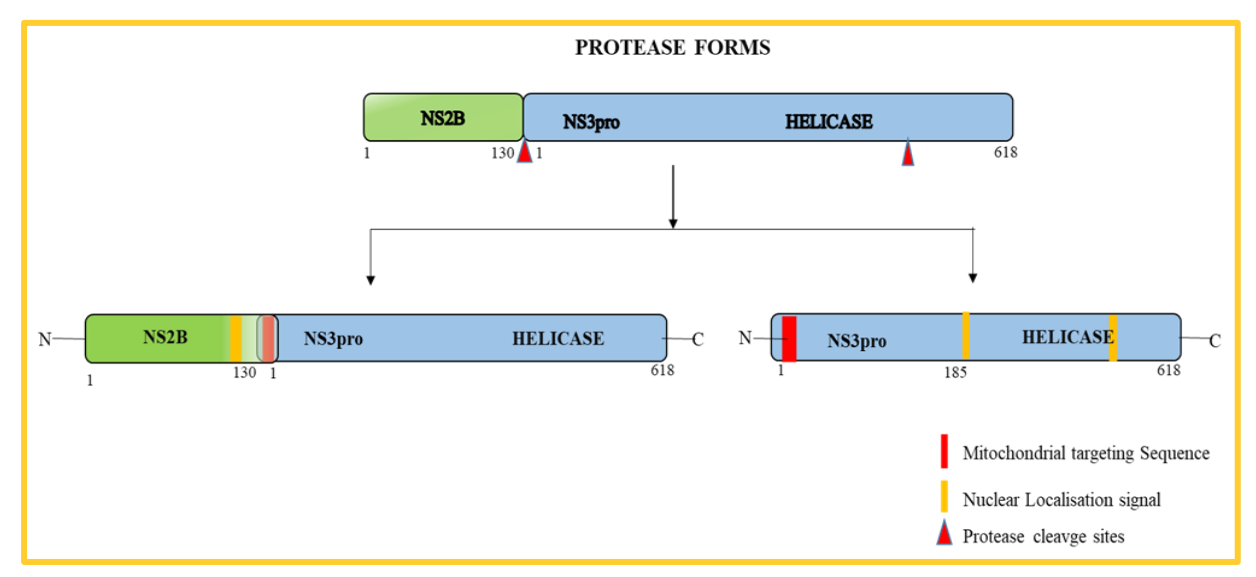


Figure 2.3.8: Schematic diagram representing the forms of dengue virus protease i.e. NS2BNS3 and NS3. NS2BNS3 and NS3 contain both NLS and MTS signal but, in NS2BNS3, the MTS signal is masked by the NS2B at the N-terminal region of NS3 [148].

Further, we have confirmed the localization during virus infection. We observed consistent results by immunofluorescence analysis when detected with NS2BNS3 antibody. It was observed the NS2BNS3 localized in the nuclear region as compared to uninfected (control) cells as observed in merged images at 60X magnification (Figure 2.3.9).

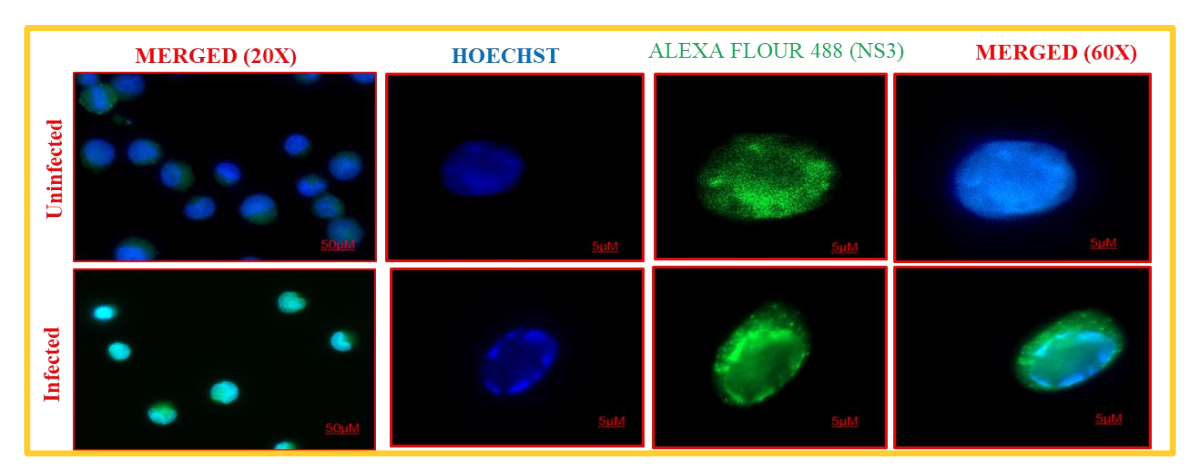
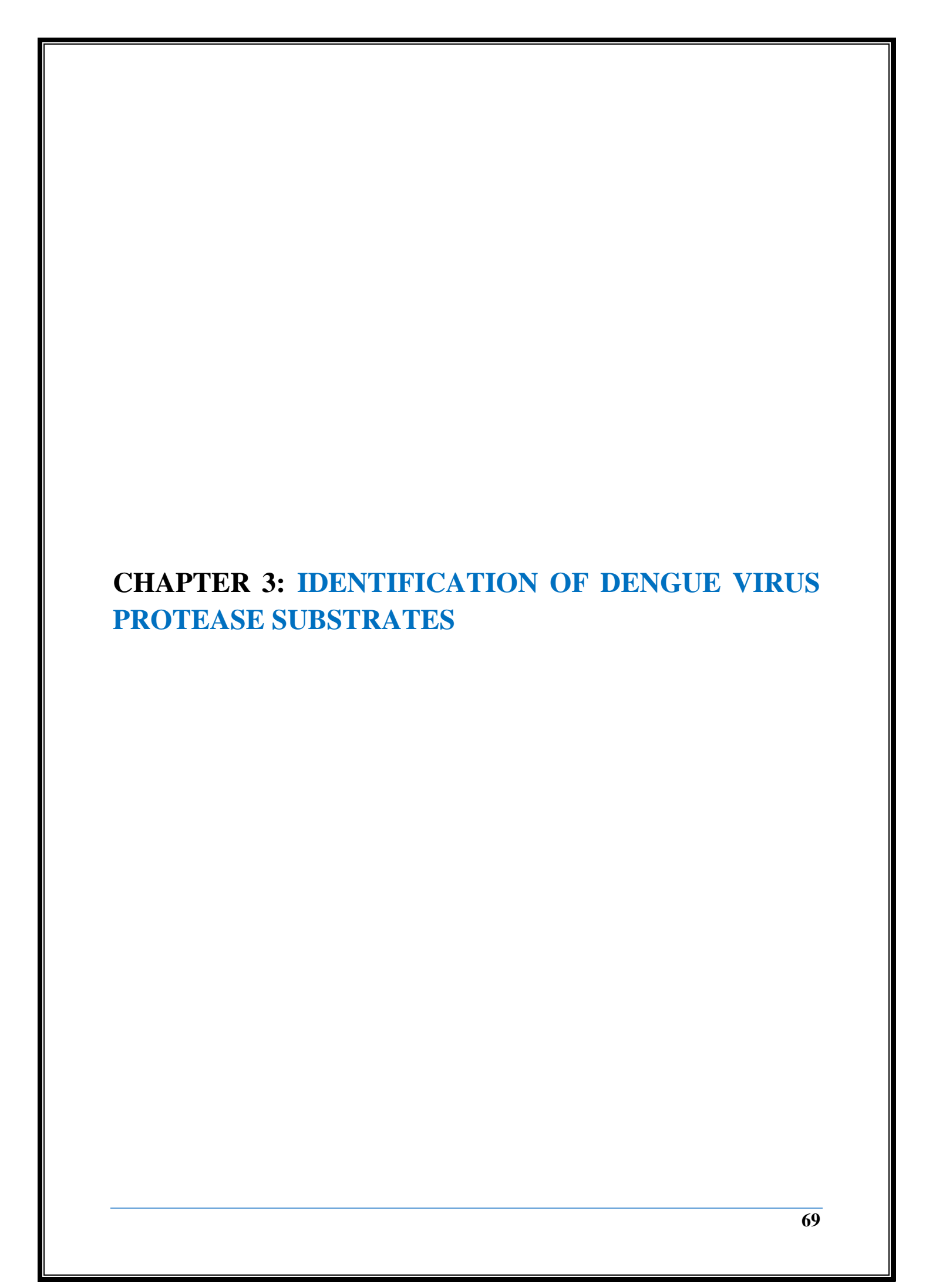


Figure 2.3.9: Representative image showing the nuclear localization of dengue virus protease during dengue virus infection.

2.4 DISCUSSION

Hosts are susceptible to viruses due to the presence of multiple binding receptors on their surfaces. Viruses bind to these receptors and enter the host cell, affecting the host mechanism. Immature virus particles or mature functional proteins, both target the host cellular factors for their survival. Flaviviruses replicate in cytoplasm and release viral proteins however, some proteins get relocated to the other organelles like mitochondria, Golgi-ER (Endoplasmic Reticulum), or nucleus for their survival in the host. JEV, Zika, YFV, TBEV and DENV share 65% similarity in their genome organization and share an almost similar mechanism of infection [149]. These viruses hijack the protein trafficking machinery of the host but do not completely inhibit the host's transcription and translation mechanisms. During the normal physiological role, some proteins are imported or exported, in and out of the nucleus. This import and export occur due to the presence of nuclear localization signals [150]. Some viral proteins like capsid and NS5 participate in viral assembly by translocating into the nucleus where they might play a crucial role during the formation of replication complexes [151]. Therefore, it is hypothesized that viral proteins might play some role in nuclear trafficking. Reports suggest that viral proteins target the nucleoporins and nuclear membrane proteins to make their entry into the nucleus. Among the flaviviruses, it is reported that Zika and DENV viruses affect the nuclear morphology by altering the functions or degrading some of the nuclear proteins essential for host survival [144, 152]. Viral proteases play a significant role during viral assembly. Previously mentioned studies on dengue viral protease (including our report published in the Journal of Virology, 2020 [147] are puzzling the scientific community regarding its role in disease pathogenesis. It is reported that during dengue virus infection in insect cells (mosquito cell lines), the viral protease localizes to nucleus and forms strand-like structures in the nucleus by altering the integrity of the nucleus. Further, the same group, reported that the dengue virus protease protein enters in nucleus during virus infection [152, 153].

Viral protease also interacts with mitochondria for cellular processes, although it is not yet clear which forms of viral protease are localized into the nucleus and mitochondria during infection. In our previous study, we reported the presence of a MTS in NS3protease that allowed its translocation in the mitochondrial matrix [147]. The self-cleavage sites in the protease, in silico analysis of the present study suggesting the presence of MTS and NLS sequences and the existing literature made us to speculate the existence of different forms of dengue virus protease and their sub-cellular localization. Thus, with this analysis, in the present study, using in silico prediction tools, NLS sequences were identified in both NS2BNS3 and NS3 which gave a hint that these proteins might target the nucleus. We found these NLS sequences in NS2B, NS3protease and helicase domains of NS3. We observed a single monopartite NLS sequence in NS2B in its C-terminal end while two bipartite NLS sequences in NS3 protease C-terminal and helicase domain of NS3 (Figure 2.3.2). To confirm this in silico prediction, we have developed the recombinant constructs of NS2NS3 and NS3. With these recombinant constructs, we have performed the localization studies and observed that viral protease exists in two forms (NS2BNS3 and NS3) that may occur in two different organelles simultaneously or at different times during the virus infection. The findings of our present study suggest the localization of dengue virus protease in two subcellular organelles of a cell i.e., nucleus and mitochondria (Figure 2.3.5 and 2.3.6). This study also suggests that in addition to the NLS sequences, MTS signals also present in both NS3 and NS2BNS3. In addition to the above confocal microscope based studies, we have carried the subcellular fractionation experiments that showed consistent results of the viral protease localization analysis in nucleus and mitochondria. But we observed that NS2NS3 enters only into nucleus while NS3 enters in both nucleus and mitochondria. In case of NS2BNS3 it appears that the MTS signal is masked by the NS2B which is present at the N-terminal end of NS3 in mitochondria, hence NS2BNS3 is not localized to the mitochondria (Figure 2.3.6, 2.3.7 and 2.3.8) [148]. With these findings, we conclude that there is no such an instant indicating the dual localization of a single protein coded by a virus genome.



3.1 INTRODUCTION

Viral proteins interact with many cellular proteins in order to carry out their successful replicative cycle. As the virus enters the host cells, some host proteases or signal peptide aid their replication by cleaving their mature polypeptide [154]. Both the structural and nonstructural viral proteins are involved directly or indirectly in virus—host interactions. It has been observed that both the host and viral factors are involved in host cellular tropism. However, very few host factors have been characterized that might play a role during virus infection. It has been reported that viral proteins like Capsid, Envelope, NS1, NS2B, NS3, NS4B and NS5 interact with host cellular proteins (humans and mosquitoes) for efficient viral entry [155]. Functionally, these proteins are associated with pathogenicity and immune responses. It has been reported that NS2A, NS4A&B and NS5 have been involved in inhibiting interferon stimulating viral mediated defense system of the hosts [156, 157]. NS1, a secretory protein, has a significant role in immune escape via the complement fixation pathway [158]. Dengue capsid protein shows interaction with host cellular proteins like DEAD (Asp-Glu-Ala-Asp) BOX helicase 3, human Death-domain Associated X-Linked protein (DAXX) and cytosolic ATPdependent RNA helicase that is involved in the apoptosis of liver cells and antiviral immune responses [159]. NS5 binds directly or indirectly to interferon signaling pathway transcription factor, Signal Transducer and Activator of Transcription 2 (STAT2), leading to STAT2 degradation during infection [160]. DENV proteases play a pivotal role in the host system by targeting its substrates. NS3 shares similarities among flaviviruses and it has been reported to interact with many host proteins which are common for other flavivirus including dengue virus. It has been reported that NS3 interacts with mosquito proteins such as titin (an ortholog of human obscurin) and nucleosome assembly protein 1 (NAP-1), an ortholog of human Nucleosome Assembly Protein-1 like 1(NAP1-L1) [158]. Both these proteins also showed interaction with NS3 of HCV. Dengue virus protease interacts with nuclear transcription factors which are crucial for regulated gene expression.

Since many researchers are exploring the cause of viral protease localization into the nucleus, the nucleus has been the targeted host organelle for identifying viral protease substrates. In addition to this, dengue protease targets other cellular organelles like mitochondria for their replication. Earlier reports showed that the dengue virus causes the elongation of mitochondria by altering the fusion and fission process. It is reported that NS2BNS3pro cleaves the mitofusins (MFN1 and MFN2), and modulates the mitochondrial dynamics by inducing apoptosis [74]. These morphological modulations led to dysregulated mitochondria, causing cell death and disease pathogenesis. Another host protein MITA, involved in interferon production and antiviral signaling during virus infection, has been reported to be cleaved by NS2BNS3 protease, subverting the host's immune response [73]. Further, in our previous study, it was reported that NS3 protease localizes to mitochondrial matrix and cleaves the GrpEL1 protein [147].

It is reported that dengue virus infection in megakaryocytes causes a reduction in cell number with depleting mature megakaryocytes suggesting the effect of infection in bone marrow homeostasis [161]. Further, it has been reported that the dengue virus inhibits the expression of master transcription factors GATA binding factors 1 and 2 (GATA1, GATA2) and nuclear factor erythroid 2 (NF-E2) which are involved in megakaryocytic developmental processes [162]. Moreover, the reports show that dengue virus infection *in vitro*, *ex vivo*, and *in vivo* models have been studied but the cause of low platelet number leading to 'thrombocytopenia' remains unclear.

Hence, to the best of our knowledge, there is no clear study explaining the mechanism involving the virus components in thrombocytopenia. In the previous chapter 2, we found that

dengue virus protease localizes in two subcellular organelles of a cell i.e., nucleus and mitochondria. In the previously published study, we observed that protease localizes to mitochondria due to the presence of a MTS signal and cleaves its substrate GrpEL1. In the previous chapter, we observed that NS2BNS3 nucleus due to the presence of NLS sequences so we made an attempt in this chapter to identify any substrate in the nucleus that might give a plausible explanation for the cause of thrombocytopenia.

3.2 MATERIALS AND METHODS

3.2.1 In vitro pulldown assay and protein identification

K562 cells were cultured in 100 mm dishes. The cells were harvested and lysed with RIPA buffer. The lysate was quantified by Bradford reagent (Bio-Rad) and 250-300μg protein (500 μl) lysate was used for pulldown. Purified pRSET-A NS2BNS3pro protein (200 μg) was allowed for binding to Ni-NTA His beads for 3 hours with gentle rocking and centrifuged for 1 minute at 4°C to remove the unbound protein. K562 cell lysate was incubated with the protein bead complex overnight with gentle rocking at 4°C. The complex was centrifuged for 1 minute and unbound proteins were collected as flow through (FT), followed by washes of 10-50mM imidazole (500 μl each). The interacting proteins were eluted from washed bead complex using imidazole (100-300mM) [148].

3.2.2 Identification of proteins obtained in the above pull-down experiment

Elutes, FT washes and the bead complex were mixed with 4X Laemmli buffer and boiled for 10 minutes, centrifuged for 1 minute and resolved on 10% SDS PAGE. A similar procedure was followed up with Ni-NTA beads bound to K562 cell extract without purified protein (control). The gel containing the bands were eluted and followed up by MALDI TOFF mass spectrometry analysis (Galaxy International /Sandor Life Sciences Pvt. Ltd.). Further, the

above-mentioned flow through, washes and elutes were resolved on 10% SDS PAGE, transferred onto PVDF membrane and probed with anti-EDRF1 antibody (1:3000). The antirabbit secondary HRP conjugated antibody was used (1:10000) and the developed image was recorded (Chemidoc, Bio-Rad) [148].

3.2.3 Identification of protease cleavage sites in EDRF1 using *in silico* methods

Full-length EDRF1 protein sequence accession no: Q3B7T1.1, was retrieved from NCBI database. Protease cleavage sites were identified by using ProP-1.0 Server-DTU Health Tech. Further, the protease and EDRF1 structures were superimposed using auto-docking tool to identify the cleavage sites for the protease catalytic triad [148].

3.2.4 Cloning of EDRF1 (798-1238 a.a) in pGEX-6P-2 (GST tagged) and pcDNA 3.1 C-Myc Vector

From K562 cell pellet, total RNA was isolated using Trizol as per manufacturer's protocol. For cDNA synthesis, total isolated RNA was mixed with oligo (dT) primers in sterile RNase-free water and reaction was followed up with mixing: total RNA (1μg), oligo(dT) random primer mix (0.5μg/μl), 10 mM dNTP, and RNase free water. The RNA was denatured for 5 minutes at 65°C. Then 10X AMV buffer, AMV Reverse Transcriptase (10U/μl), RNase inhibitor (40U) and RNase free water were added. Total RNA was reverse transcribed using the reaction cycle: 45°C for 50 minutes, 80°C for 5 minutes. The cDNA generated was used as a template for the amplification of EDRF1 with forward F- ATC*GGATCC*ATGACTGATTTGTCTACAGACTT and Reverse R- CGA*GAATTC*TCACTGAACGGCATTGCTGC primers. This amplified product was cloned in pGEX-6P-2. In order to clone EDRF1 in pcDNA 3.1 C-Myc vector also, Forward 5' TATC*GAATTC*GCCATGGCTGATTTGTCTACAGACTT 3' and reverse 5' TATG*CTCGAG*CTGAACGGCATTGCTGCT 3' primers were used for amplifications. The

primers were designed based on the EDRF1 sequence available with accession no NP_001189367.1. The PCR mix contains 10X buffer, 10mM dNTPs, forward and reverse primers (10μM each), cDNA (100 ng), Taq Polymerase (0.25U) and nuclease-free water. Cycling conditions were followed with an initial denaturation step at 94°C for 5 minutes, followed by 35 cycles of 94°C for 1 minute, 58°C for 30 seconds, 72°C for 1.5 minutes, and final extension at 72°C for 10 minutes. The amplified fragment was run on 1% agarose gel and 1.3 kbp amplified product was obtained. The amplified products were gel extracted and further cloned in to pGEX-6P-2 and pcDNA 3.1 C-Myc vectors. To clone in pGEX-6P-2 vector, the amplified product and the pGEX-6P-2 vector were digested with *EcoRI/BamHI* restriction sites, ligated and transformed into *E. coli*. DH5α competent cells. Similarly, to clone in pcDNA 3.1 C-Myc vector, the amplified product and the pcDNA 3.1 C-Myc vector were digested with restriction sites *Xhol/EcoRI*, ligated and transformed into *E. coli*. DH5α competent cells. Both the recombinant plasmids were isolated and further confirmed with restriction digestion and sequencing [148].

3.2.5 Expression and Purification of EDRF1 Protein

Competent *Escherichia coli* strain BL21 cells were transformed with the recombinant expression vector (pGEX-6P-2 EDRF1), were inoculated into LB media containing 100 ug/mL ampicillin and incubated at 37°C overnight. Fresh LB media was incubated for 2-3 hours at 37°C with the overnight culture to reach an O.D.600=0.5. Bacterial cells were induced for protein expression by the addition of isopropyl-βD-thiogalactoside (IPTG) to a final concentration of 0.1 mM at 15°C for 18-22 hours or with 0.5mM at 20°C for 14 hours. After incubation, cells were harvested at 8000 rpm for 10 minutes. Cell pellets were resuspended in GST Lysis buffer (1x PBS pH 7.4, 1mM DTT, 0.5% Triton X-100) followed by sonication and centrifuge the lysate at 10000 rpm for 45 minutes. The supernatant was incubated with

glutathione agarose resin overnight at 4°C. After adsorption, beads were collected in gravity flow columns and washed 3 times with wash buffer (1XPBS and 3mM DTT). Either GST or GST- EDRF1 were eluted by competition with a free reduced glutathione elution buffer (15 mM glutathione in 100 mM Tris-HCl pH 8.0). Further, the eluted protein fractions were analyzed on 10% SDS PAGE. The eluted fractions were pooled and dialyzed against 500-fold volume of 1X PBS.

3.2.6 *In vitro* cleavage assay of GST-EDRF1 protein with NS2BNS3 (Protease)

Cleavage assay was performed with purified GST-tagged EDRF1 protein and purified NS2BNS3. In a 50 µl reaction, purified GST-EDRF1 protein (20 µg) was incubated with varying conc of NS2BNS3pro protein (5-25 µg/ml) at 37°C for 1 hour 30 minutes and the cleaved products were analyzed on 10% SDS PAGE and further with western blotting with anti-EDRF1 antibody. Alternatively, pcDNA 3.1 C-Myc EDRF1 was over expressed in HEK cells. The cell lysate was prepared and incubated with purified NS2BNS3pro. The levels of cleaved EDRF1 were detected by western blotting using EDRF1 antibody (1:3000).

3.2.7 EDRF1 cleavage analysis with co-transfection studies

For the co-transfection experiment, HEK cells (~ 8x 10^5) were seeded in 60 mm dishes and allowed to grow up to 80% confluency. The next day, cells were viewed under a microscope to confirm the cell confluency to ~80%. The recombinant plasmids (pcDNA 3.1 C-Myc vector/pEGFP-N1 Vector) and (pcDNA 3.1 C-Myc EDRF1 and pEGFP-N1NS2BNS3pro) were co-transfected. Briefly, pcDNA 3.1 C-Myc Vector / pEGFP-N1 Vector (1 µg each) and pcDNA 3.1 C-Myc EDRF1/ pEGFP-N1 NS2BNS3pro (1 µg each) plasmids were mixed together, and Lipofectamine 2000, diluted in serum free DMEM or OptiMEM for 2-3 minutes separately. The diluted plasmids were mixed in diluted Lipofectamine to form complex and

incubated at room temperature for 18-20 minutes. Then, the complex was added onto the cell monolayer gently and allowed to incubate the cells at 37° C in a CO₂ incubator for 4-6 hours. After 4-6 hours, the serum free media was replaced with fresh complete DMEM and cells were allowed to grow for 48 hours to analyse the expression. Media was removed, 1 ml of 1X PBS was added gently and the cells were scraped by scrapper. The cells were collected in a fresh 1.5 ml Eppendorf tube and centrifuged at 3000 rpm for 5 minutes. The pelleted cells were ready for preparing the whole cell lysate using Radio Immunoprecipitation Assay Buffer (RIPA). Briefly, 200µl RIPA buffer was added to the cells along with the protease inhibitor cocktail (1X). The cells were resuspended gently with pipette to form clear solubilized lysate. The lysate was incubated on ice for 30 minutes and vortexed 2-3 times at 5 minutes intervals each. Lysate was centrifuged at 13000 rpm for 15 minutes and the supernatant was collected in fresh Eppendorf tube as whole cell lysate. The pellet was discarded. 10µl of whole cell lysate was aliquoted for quantification and quantified with Bradford reagent. The samples were denatured and resolved on 10% SDS-PAGE followed by western blotting to analyse the expression of co-transfected plasmids with anti-Myc Tag (1:1000) and GFP (1:1000) antibodies (Figure 3.2.1) [148].

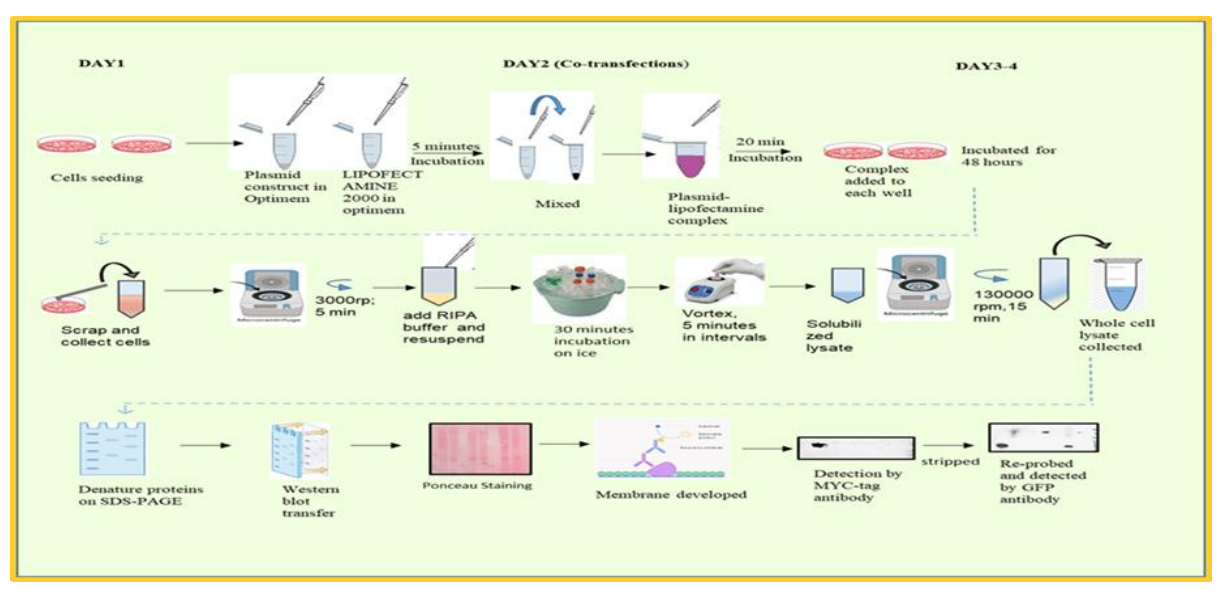


Figure 3.2.1: Schematic diagram of the protocol for co-transfection in HEK cells.

3.2.8 Analysis of EDRF1, GATA1 and Spectrin levels in transfected cell extracts

Cells were seeded at conc. of 5 x 10⁵ cells/ml in 6 well plates prior to the day of transfection in RPMI growth media with 10% FBS without antibiotic and incubated at 37°C with 5% CO₂. After 12 hours, cells were transfected with pEGFP-N1 vector, pEGFP-N1 NS2BNS3pro, pEGFP-N1 NS2BNS3pro (S135A) mutant, pEGFP-N1 NS2BNS3 (1-5 µg/µl) and allowed to grow for 28 hours. Cells were analyzed for GFP expression using a fluorescence microscope. Then the cells were harvested and cell extracts prepared, resolved on 10% SDS PAGE and probed with anti-GFP (1:1000) or anti-NS2BNS3pro (1:5000) or anti-EDRF1 (1:3000) or anti-GATA1 (1:5000) or anti-alpha1 spectrin (1:2500) antibodies (one blot with anti-GFP or anti-NS2BNS3pro or anti-EDRF1; the other blot with anti-GATA1 or anti-alpha1 spectrin). The secondary anti-rabbit HRP-conjugated antibody (1:10000) was used. Anti-actin (1:2500) was also used and probed with HRP-conjugated anti-mouse secondary antibody (1:10000). The blot was developed and imaged using Chemidoc (Bio-Rad).

3.2.9 Analysis of EDRF1, GATA1 and Spectrin levels in virus infected cell extracts

Virus infection in Vero cells was performed as described in our earlier studies [147]. For infection of K562 cells, Vero cell propagated viral supernatant was used. A day before infection four dishes of size 100mm were seeded with 10⁶ cells. On the day of infection, cells were harvested and counted using a hemocytometer. Suspension cells were seeded again in 60 mm dishes (10⁵ cells per dish) and inoculated with viral supernatant in ratio 1:4 dilutions with MoI of 0.09 in serum free RPMI media. The virus was allowed for adsorption for 2-3 hours with mild agitation in 15 minutes intervals. After the adsorption, the media was replaced with RPMI media containing 4-5 % FBS and cells were allowed to grow for up to 7 days. Uninfected K562 cells were used as control which were also allowed to grow for 7 days. Infection was confirmed by western blotting with NS2BNS3pro antibody (1:1000). The cells were harvested, cell lysates

were prepared and western blotting was carried using anti-EDRF1, anti-GATA1 and antialpha1 spectrin antibodies as described above [148].

3.2.10 EDRF1 and GrpEL1 levels in clinical samples

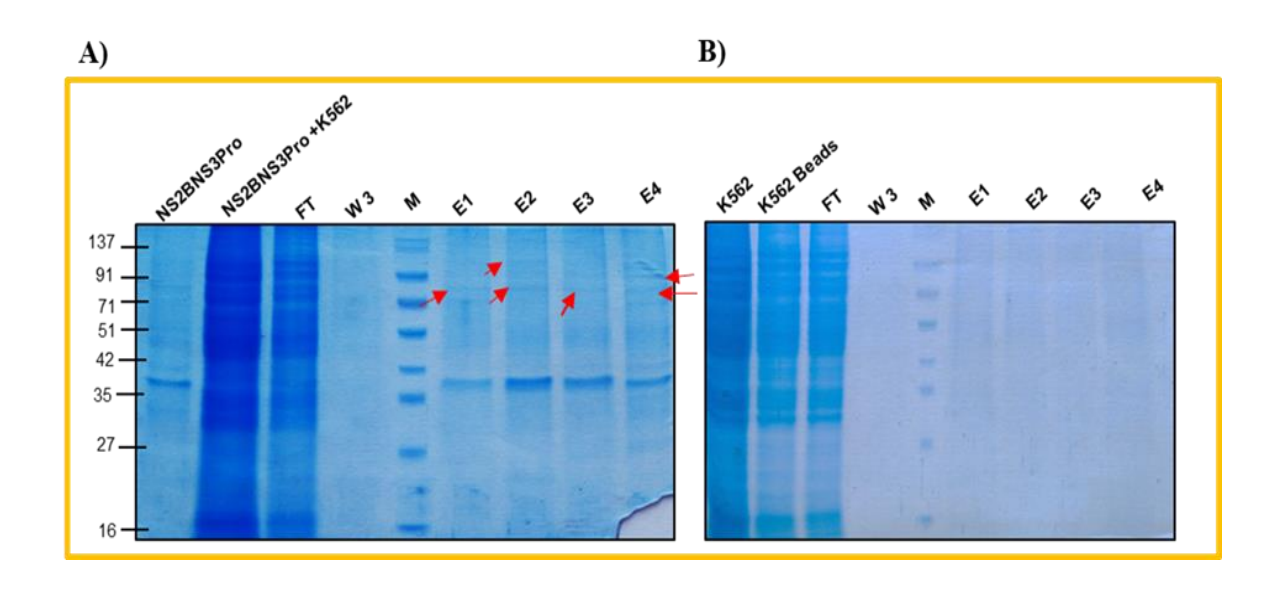
Clinical samples (n=44) were classified as DF, DHF and DSS as per WHO guidelines (Table 3.2.1). The samples were processed for albumin depletion. Briefly, in 100µl of serum sample, 1M NaCl was added to a final conc of 0.1M and incubated for 60 minutes at 4°C on rocking. Ice-cold ethanol was added to the sample to a 42% concentration and further incubated for 60 min at 4°C. The sample was centrifuged at 14000 rpm for 45 min at 4°C, and the pellet was stored. Using 0.8 M cold sodium acetate (pH 4.0), the pH of the supernatant was lowered to 5.7 and incubated for 30 min at 4°C. Again, the sample was centrifuged at 14,000 rpm for 30 min, and the supernatant containing albumin was separated. Both pellets were re-suspended and mixed in 10 mM Tris, pH 6.8 and 1 M urea. The protein concentrations of obtained albumin-depleted samples were estimated by Bradford assay. Samples (10 µg) were resolved on a 10% SDS-PAGE and immunoblotted with anti-EDRF1 antibody (1:3000) followed by stripping and probed with anti-GrpEL1 antibodies (1:2500). Anti-rabbit secondary HRP-conjugated antibodies (1:10000) were used and the blot was developed as described above [147, 148].

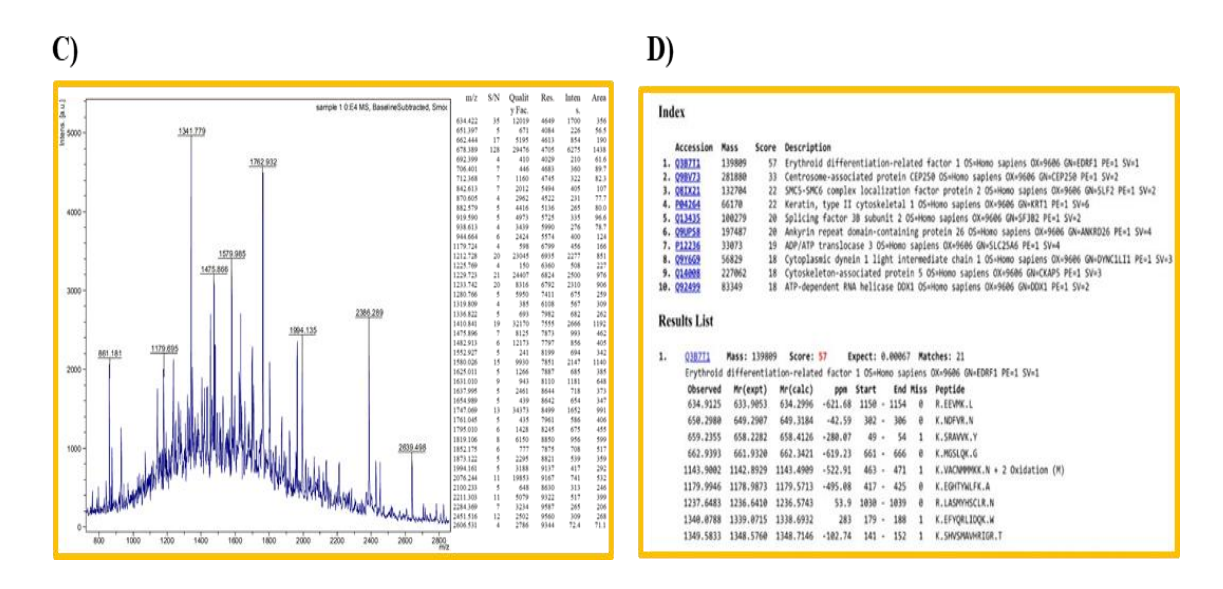
3.3 RESULTS

3.3.1 Identification of protease interacting proteins

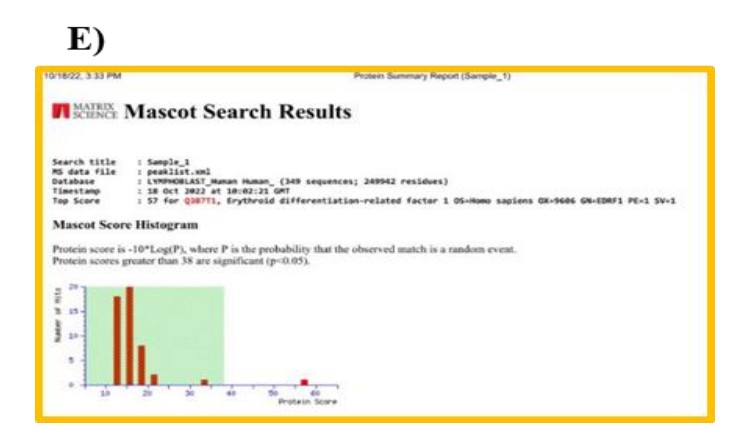
To identify the host factors interacting with NS2BNS3 protease, we performed *in vitro* Ni-NTA pulldown assay with purified NS2BNS3pro incubating with K562 whole cell lysate (Figure 3.3.1 A and B). Protein bands that appeared in elutes (E1-E4) were gel eluted and identified by MALDI-TOFF mass spectrometry. The identified bands from the above elutes

were found to be erythroid differentiation regulatory factor 1 (EDRF1) (Figure 3.3.1 C and D). Also, the Mascot search result supported the above finding that the identified protein EDRF1 has a score of 57 which is the highest among the list (Figure 3.3.1 E). Western blot analysis using anti-EDRF1 antibody showed the presence of EDRF1 in elutes and beads thus confirming EDRF1 as a protease interacting host protein (Figure 3.3.1 F&G) [148].





Continued...



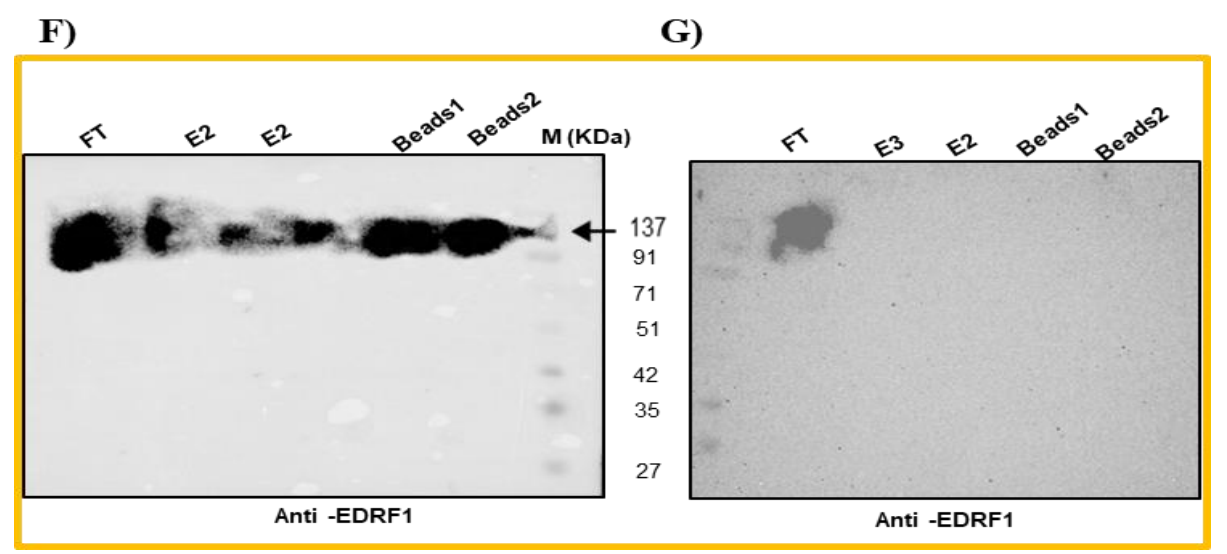


Figure 3.3.1: (A) *In vitro* pulldown assay from K562 cell lysate with pRSET-A NS2BNS3pro purified protein and (B) Negative control. The arrows indicate the bands used for identification. (C&D) Identification data of the protein bands obtained from above *in vitro* pulldown assay. (E) The graph represents the Mascot search result showing the identified protein as EDRF1 with the top score of 57. Western blotting analysis of the fractions of pulldown assay by using anti-EDRF1 antibody, (F) experimental and (G) negative control.

3.3.2 Identification of protease cleavage sites in EDRF1 using *in silico* methods

ProP-1.0 server identified a total of five cleavage sites (dibasic amino acid residues i.e. Arg/Lys in P1/P2 position) at different amino acid sequence positions of EDRF1 (50,100,152,926,987) (Figure 3.3.2 A). In order to know which of the above cleavage sites is located in/near the catalytic triad of protease, we performed an *in silico* docking method for analyzing the interactions of protease and EDRF1 by superimposed models (Figure 3.3.2 B). It was observed that the cleavage site at a.a 985-988 of EDRF1 (cyan) interacted with the catalytic triad of

protease (H-51, D-75, S-135) (green) (Figure 3.3.2 B). Thus, we have developed a recombinant pcDNA 3.1 C-Myc and pGEX-6P-2 vectors containing the c-terminal end from amino acid 798 to 1238, approximately 50 kDa of EDRF1 (encompassing a.a 985-988 cleavage site) [148].

A)

EDRF1: (Q3BT71)

>sp|Q3B7T1.1| EDRF1_HUMAN Full=Erythroid differentiation-related factor 1

MGDAKEAGAEGPPAGAAARGGLSLLSQESEESSAQGSALFLGGNEVK\$RAVVKYSSAPPRTAFARLEEKTDLKLPPANWLRESAKLG
PAGTTILGN\$KK\$KPF\$SFGMAYDFID\$VGNDVDVV\$D\$ENIKKLLKIPY\$K\$HV\$MAVHRIGRTLLLDELDIQELFMR\$SQTGDWTWLK
EFYQRLIDQKWQRKKK\$KEHWYQKAIL\$KFLYY\$INGDGAAQPV\$STAEQQE\$S\$SDQTND\$EGA\$WPAPFEMP\$\$SV\$EDP\$A\$SQG\$E
PLEP\$YIVGHVA\$APKEQNLITLFNDGEH\$QGLKNDFVRNILWTFEDIHMLVG\$NMPIFGGGRYPAV\$LRLDNNKPINVLTGIDYWLDN
LICNVPELVMCFHVNGIVQKYEMIKTEEIPNLEN\$NF\$TKVIKDIAQNIL\$FLK\$NCTKEGHTYWLFKA\$G\$DIVKLYDLTTLCEETEDKY
QNPFTMPVAILLYKVACNMMMKKNQNKKHYGTIRTLLLNCLKLLDK\$RHPQIIA\$ANYML\$ELFQLDEPKKEEN\$E\$PLNEN\$DE\$Y\$E
EEEEMPD\$DENG\$Y\$T\$\$DP\$DD\$KAVAIIK\$VGEL\$VPEKYK\$IHQIRP\$CAFPVCHDTEERCRLVL\$YVLEGLK\$VD\$SIKKE\$DLPAAD
P\$TPIPLKYEDE\$\$RGGPEGLEKQMALFLDKMG\$LQKGNY\$\$Q\$GMIPG\$WQHKMKLQLILK\$\$KAYYVL\$DAAM\$LQKYGRALRYIK
LALQ\$HDTYCCLCTNML\$EVLLFL\$QYLTLCGDIQLMLAQNANNRAAHLEEFHYQTKEDQEILH\$LHRE\$\$CQGFAWATDL\$TDLE\$Q
L\$V\$\$CKCYEAANEILQF\$DLK\$QNPEHYVQVLKRMGNIRNEIGVFYMNQAAALQ\$ERLV\$K\$V\$AAEQQLWKK\$F\$CFEKGIHNFESIE
DATNAALLLCNTGRLMRICAQAHCGAGDELKREF\$PEEGLYYNKAIDYYLKALR\$LGTRDIHPAVWD\$VNWEL\$TTYFTMATLQQDY
APL\$RKAQEQIEKEV\$EAMMK\$LKYCDVD\$V\$ARQPLCQYRAATIHHRLA\$MYH\$CLRNQVGDEHLRKQHRVLADLHY\$KAAKLFQ
LLKDAPCELLRVQLERVAFAEFQMT\$QN\$NVGKLKTL\$GALDIMVRTEHAFQLIQKELIEEFGQPK\$GDAAAAADA\$P\$LNREEVMKLL
\$SIFE\$RL\$FLLLQ\$IKLL\$\$TKKKT\$NNIEDDTILKTNKHIY\$QLLRATANKTATLLERINVIVHLLGQLAAG\$AA\$\$NAVQ

*Cleavge sites identified by the ProP1 server

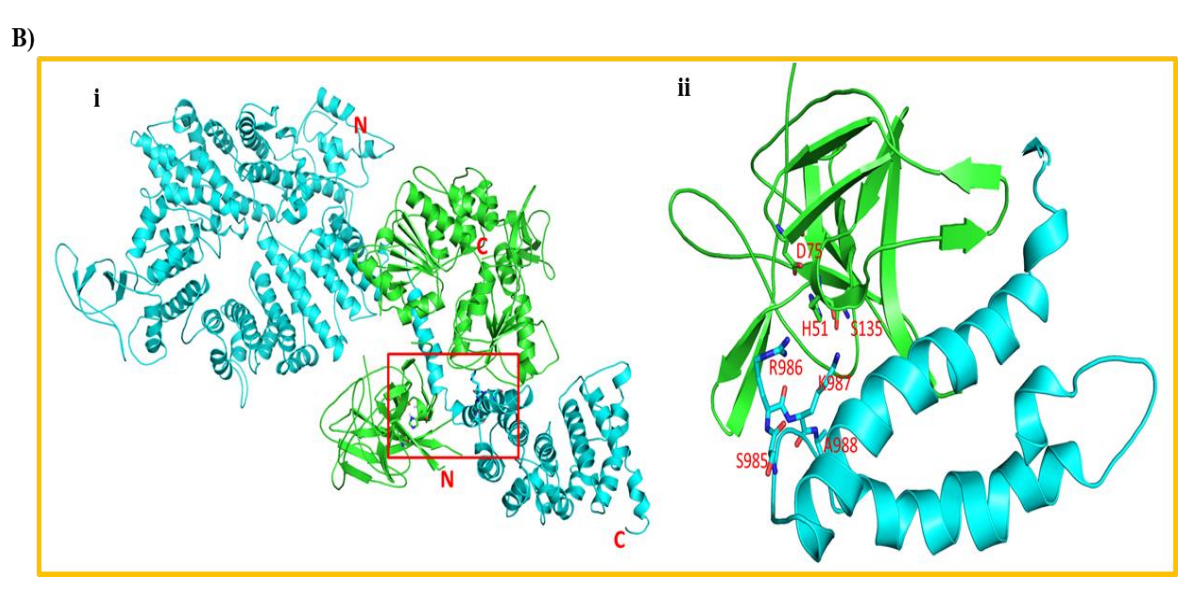


Figure 3.3.2: The full-length protein sequence of EDRF1 retrieved from NCBI database; Protein Id. Q3B7T1.1. (**A**) The amino acid shows the cleavage sites (red) identified by ProP-1.0 server. (**B**) (**i**) The *in silico* superimposed models of EDRF1 (Cyan) and NS3pro-helicase (green). (**ii**) Enlarged version of the superimposed area showing the interactions of the catalytic triad of NS3pro-helicase (H-51, D-75, S-135) and the cleavage site at a.a 985-988 (RK987A).

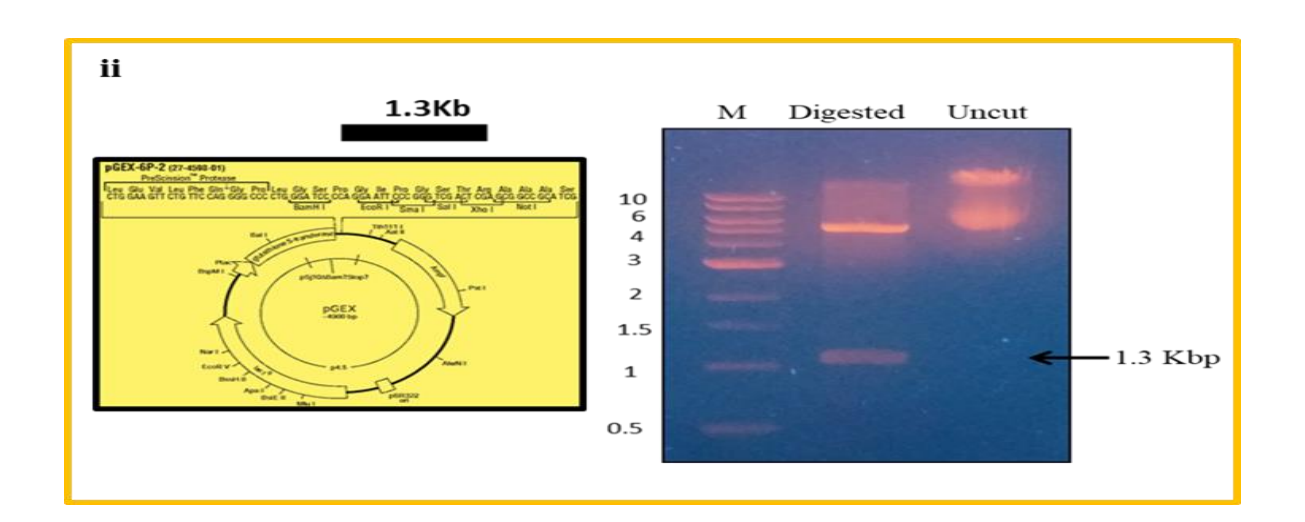
3.3.3 Cloning, Expression and Purification of EDRF1 Protein

The cloned pGEX-6P-2 vector containing the EDRF1 insert was confirmed by digestion and sequencing. 1.3 kbp fragment was obtained. EDRF1 was expressed with 0.1mM IPTG induction at 15°C and purified by free glutathione bound to glutathione resin. The GST fused protein of 70 kDa was obtained in solubilized form and was eluted with 15mM free Glutathione. Since the eluted protein contains free GST it was removed by two times dialysis and then by using 30kDa amicon concentrators (Figure 3.3.3).

A)

i

MTDLSTDLESQLSVSCKCYEAANEILQFSDLKSQNPEHYVQVL
KRMGNIRNEIGVFYMNQAAALQSERLVSKSVSAAEQQLWKKSF
SCFEKGIHNFESIEDATNAALLLCNTGRLMRICAQAHCGAGDEL
KREFSPEEGLYYNKAIDYYLKALRSLGTRDIHPAVWDSVNWEL
STTYFTMATLQQDYAPLSRKAQEQIEKEVSEAMMKSLKYCDVD
SVSARQPLCQYRAATIHHRLASMYHSCLRNQVGDEHLRKQHRV
LADLHYSKAAKLFQLLKDAPCELLRVQLERVAFAEFQMTSQNS
NVGKLKTLSGALDIMVRTEHAFQLIQKELIEEFGQPKSGDAAAA
ADASPSLNREEVMKLLSIFESRLSFLLLQSIKLLSSTKKKTSNNI
EDDTILKTNKHIYSQLLRATANKTATLLERINVIVHLLGQLAAG
SAASSNAVQStop



B)

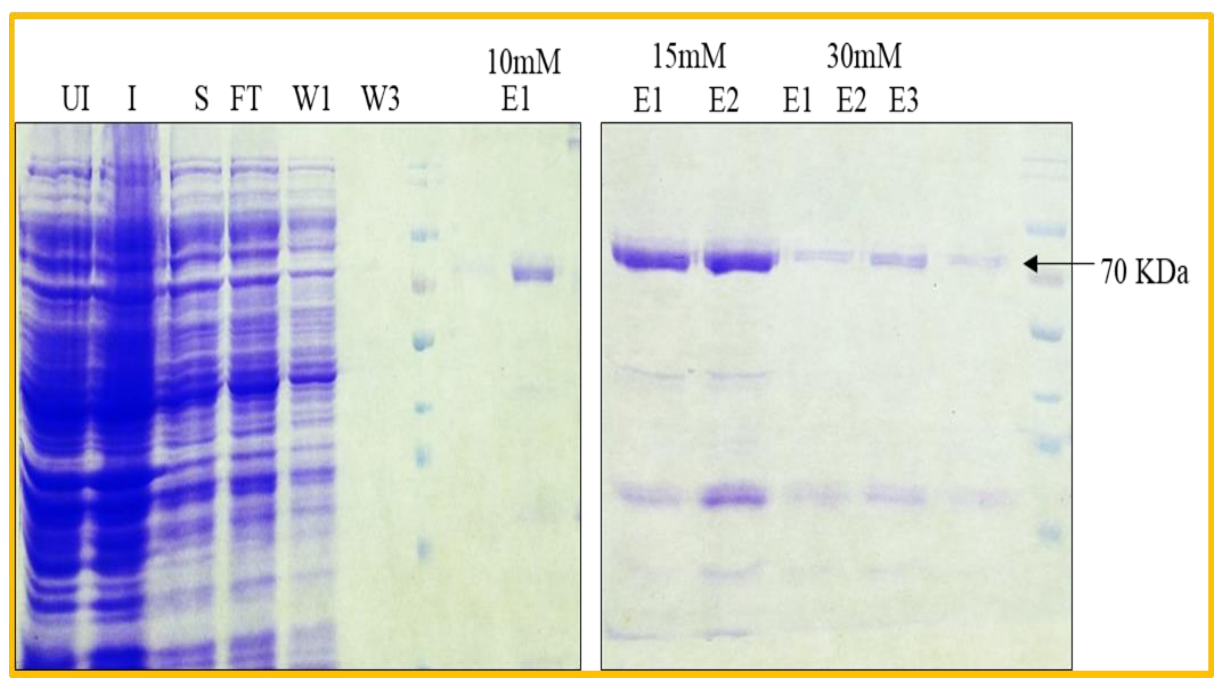


Figure 3.3.3: (**A**) (**i**) Amino acid sequence of C-terminal end of EDRF1 with the protease cleavage sites, cloned in pGEX-6P-2 vector. (**ii**) Clone was confirmed by restriction digestion. (**B**) Protein Expression and purification of EDRF1. The 70 kDa fused protein purified by 15mM and 30mM Glutathione.

3.3.4 *In vitro* cleavage assay of GST-EDRF1 protein with NS2BNS3protease

In order to analyse the EDRF1 cleavage by the protease we have performed *in vitro* cleavage assay. For this, an increasing concentration of purified NS2BNS3pro was incubated with GST tagged fusion EDRF1 protein at 37°C for 1 hour 30 minutes. With the SDS PAGE followed by western blot analysis, we observed a decrease in the levels of EDRF1 concentrations from 15 to 25 μ g (Figure 3.3.4 A and B). Similarly, we have overexpressed the EDRF1 in the HEK transfected, made the lysate of the same and found the reduced levels of overexpressed pcDNA 3.1 C-Myc EDRF1 in the presence of purified protease (Figure 3.3.4 C (i & ii)).

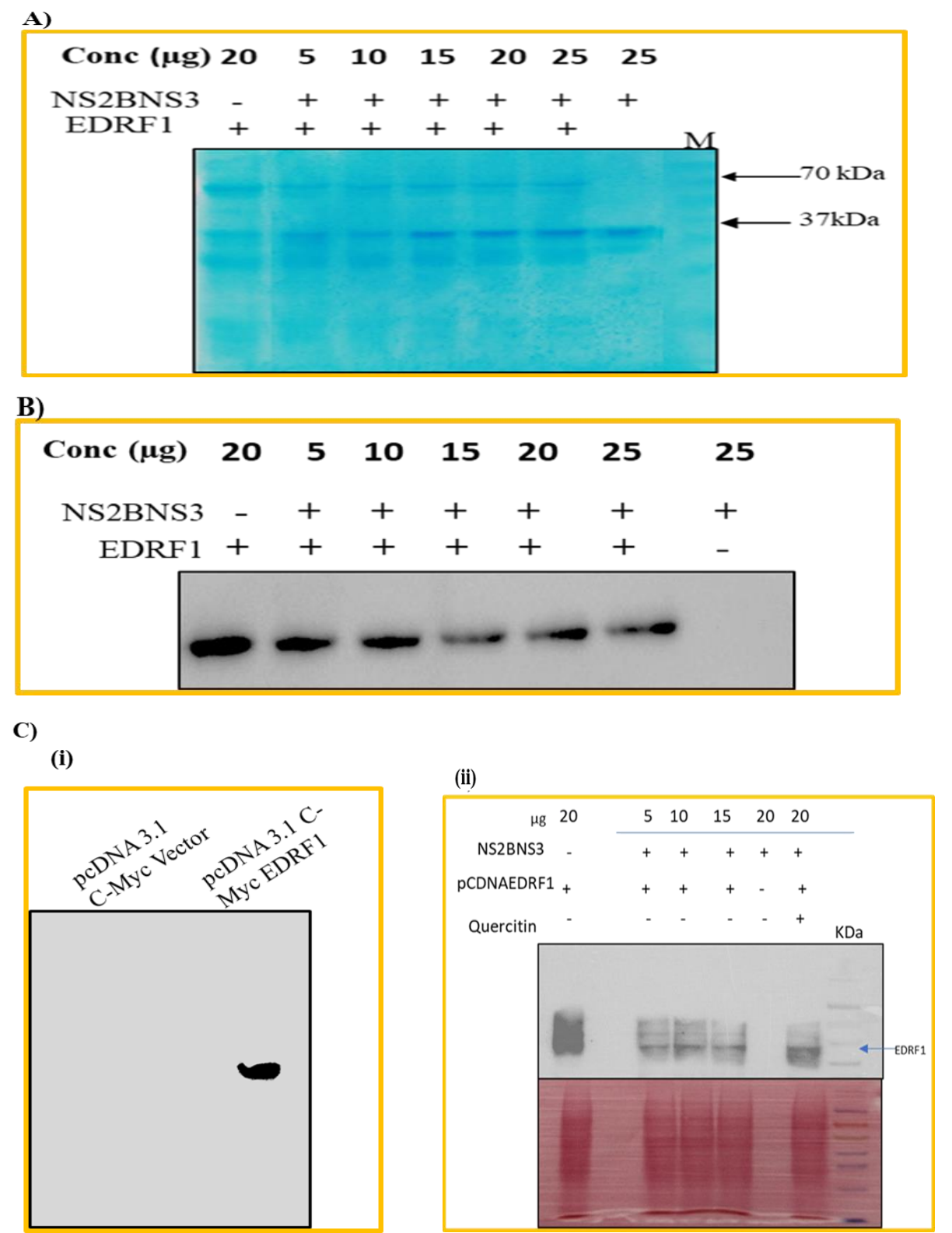


Figure 3.3.4 *In vitro* cleavage of EDRF1 in presence of protease. (**A**) Coomassie staining, *in vitro* cleavage assay (70 kDa) and protease (37 kDa), with increasing concentration of protease incubated at 37°C for 1 hour 30 minutes. (**B**) Western blot analysis to detect *in vitro* cleaved EDRF1 by anti-EDRF1 antibody (1:3000). (**C**) (**i**) Over expression of pCDNA 3.1 C-Myc EDRF1 in HEK transfected cells confirmed by western blotting. (**ii-top**) *In vitro* cleavage assay of overexpressed pcDNA 3.1 C-Myc EDRF1 protein (50 kDa) and protease (37kDa) incubated

at 37°C for 1 hour 30 minutes and detected using EDRF1 antibodies. (**ii-bottom**) Ponceau S stain of the same membrane.

3.3.5 EDRF1 cleavage in co-expressed conditions

The cell extracts co-expressed with both EDRF1 and protease were resolved on 10% SDS PAGE and transferred onto the hydrophilic polyvinylidene fluoride (PVDF) membrane. Western blot analysis was done to detect the levels of EDRF1 using anti-Myc tag antibody. The blot showed no band in co-transfected vectors as the Myc tag is only 1.2 kDa (very small to detect) (Figure 3.3.5 A lane 1). In pcDNA 3.1 C-Myc containing EDRF1 as an insert, the EDRF1 band was detected as intact showing the presence of overexpressed EDRF1 alone (Figure 3.3.5 A lane 2). As expected, no expression was observed in pcDNA 3.1 C-Myc vector (Figure 3.3.5 A lane 3). Importantly, EDRF1 was completely disappeared in presence of protease in co-transfected pcDNA3.1 C-Myc EDRF1 and pEGFP-N1 NS2BNS3pro, suggesting EDRF1 as a substrate of protease (Figure 3.3.5 A lane 4). pEGFP-N1 vector alone and pEGFP-N1 NS2BNS3pro lysates were loaded as controls (Figure 3.3.5 A lanes 5 &6). To confirm the expression of NS2BNS3pro in the above experiment, we have checked the expression of protease using anti-GFP antibody after stripping the same membrane. It was observed that, in co-transfected vectors and pEGFP-N1 vector alone, GFP was expressed (Figure 3.3.5 C lanes 13 & 17). No band to be observed in pcDNA3.1 C-Myc EDRF1 and pcDNA 3.1 C-Myc vector alone (Figure 3.3.5 C lanes 14 &15). In co-transfected pcDNA 3.1 C-Myc EDRF1 and pEGFP-N1 NS2BNS3pro cell lysates, the protease was detected thus confirming the expression of NS2BNS3pro in the co-transfected conditions (Figure 3.3.5 C lane 16). pEGFP-N1 NS2BNS3pro was also found to be expressed alone as a control (Figure 3.3.5 C lane 18) [148].

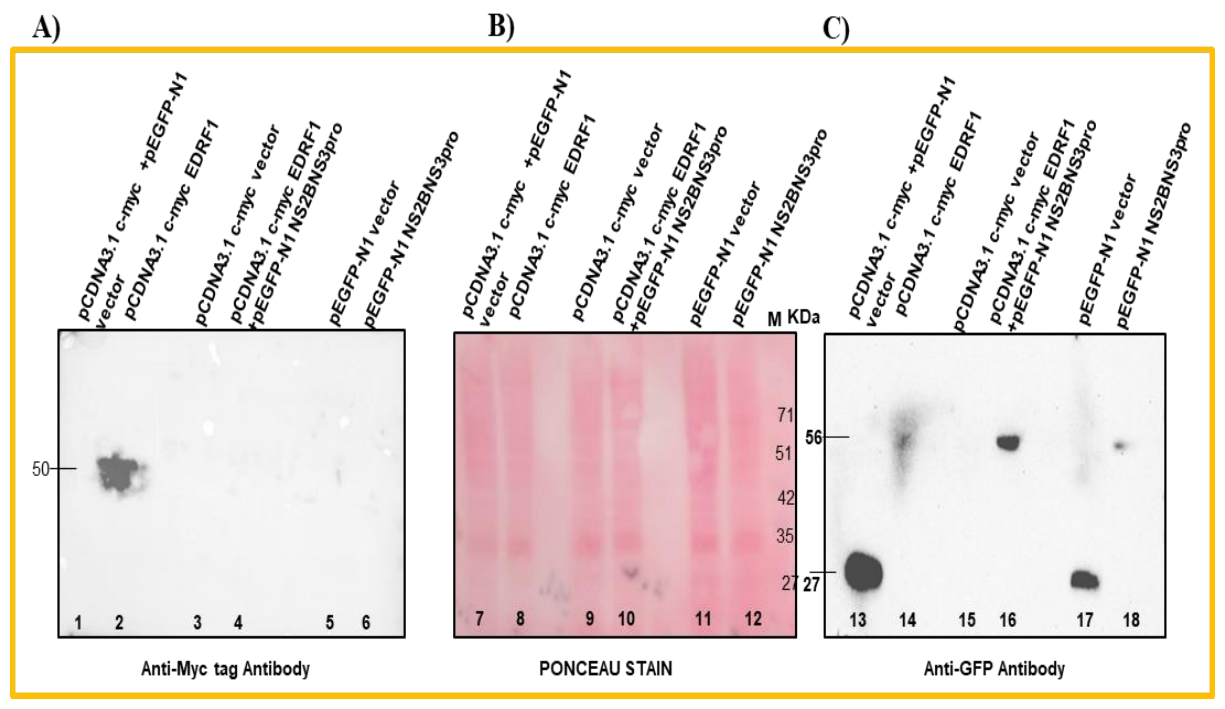
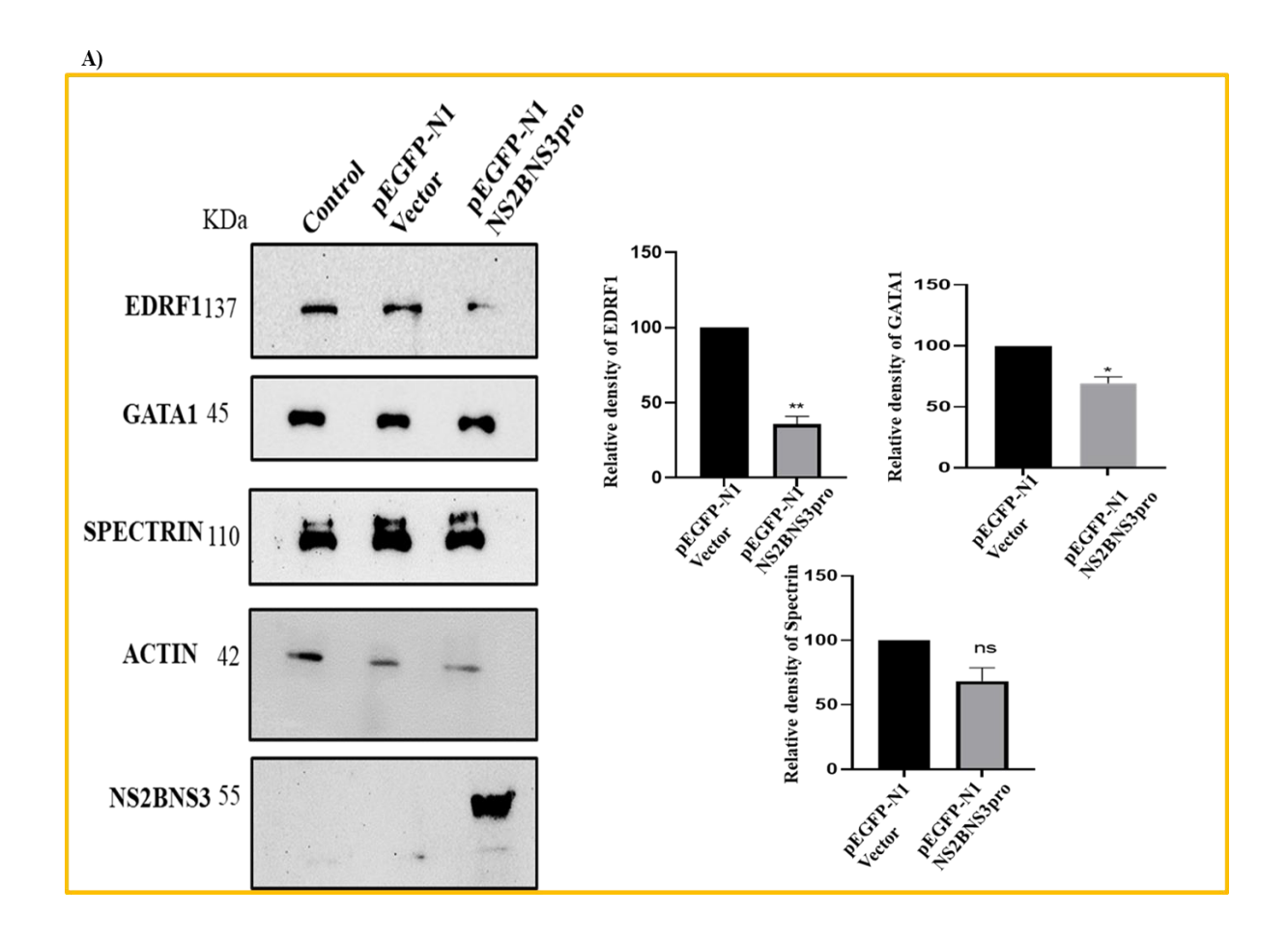


Figure 3.3.5: Western blot analysis of the cell lysates after 48 hrs of co-transfection. **(A)** HEK cells were transfected with single or co-transfected with recombinant vectors as indicated on the blots and probed with anti-Myc tag antibodies. **(B)** Ponceau S staining of the above membrane Lanes: 7-12 and M (protein marker). **(C)** The above membrane was stripped and probed with anti-GFP antibodies [148].

3.3.6 Analysis of levels of EDRF1, GATA1 and Spectrins in protease transfected and virus infected cell lysates

The GATA1 expression and activity were reported to be regulated by EDRF1 [163]. GATA1 in turn controls the synthesis of spectrin proteins which are required for pro-platelet and platelet formation [164]. EDRF1, a 138 kDa protein is reported to be expressed in megakaryocytic (K562) and erythroid cell lineages. Hence, we intended to analyze the levels of EDRF1, GATA1 and spectrins in protease transfected and virus infected K562 cells [165, 166]. For this purpose, total cell lysates of transfected/infected were resolved on 10% SDS PAGE followed by western blot analysis with anti-EDRF1 antibody as detailed in methods. It was observed that EDRF1 levels were deteriorated significantly in presence of pEGFP-N1 NS2BNS3pro as compared to the vector, concluding that EDRF1 is being cleaved by dengue virus protease (Figure 3.3.6 A, left). The bar graph representation from the three experiments support the

above data (Figure 3.3.6 A, right). The same cell lysates were used to check the endogenous levels of GATA1 and spectrins. It was observed that, compared to pEGFP-N1 vector alone, GATA1 and spectrin levels were found to be reduced (Figure 3.3.6 A, left). The bar graph representation from the three experiments supports the above data (Figure 3.3.6 A, right). To confirm the above data, we have transfected pEGFP-N1 NS2BNS3 (594 a.a) which represents one of the forms of naturally existing dengue virus protease. A mutant of NS2BNS3pro (NS2BNS3pro S135A) carrying the mutation in the catalytic triad was also included. The data suggest that the levels of EDRF1 and GATA1 were drastically reduced in presence of pEGFP-N1 NS2BNS3, compared to the mutant and the vector (Figure 3.3.6 B, left). The bar graph representation from the three experiments support the above data (Figure 3.3.6 B, right) [148].



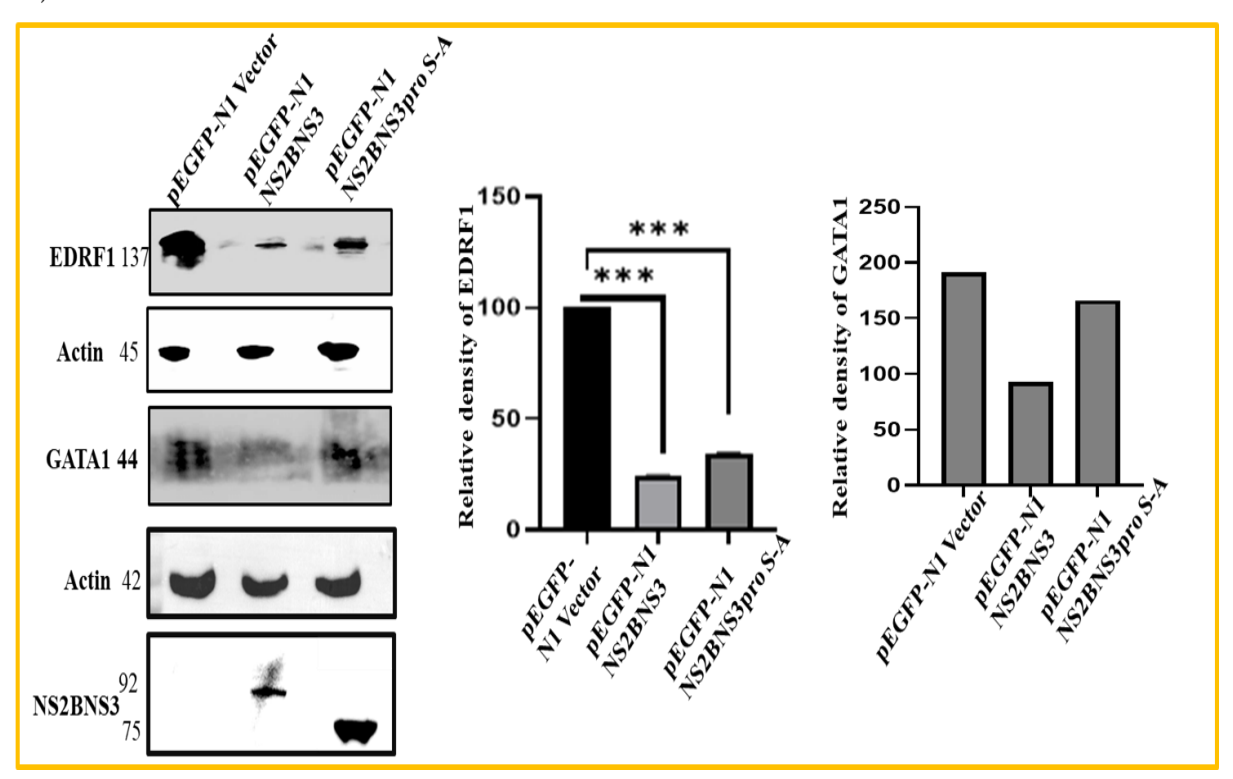
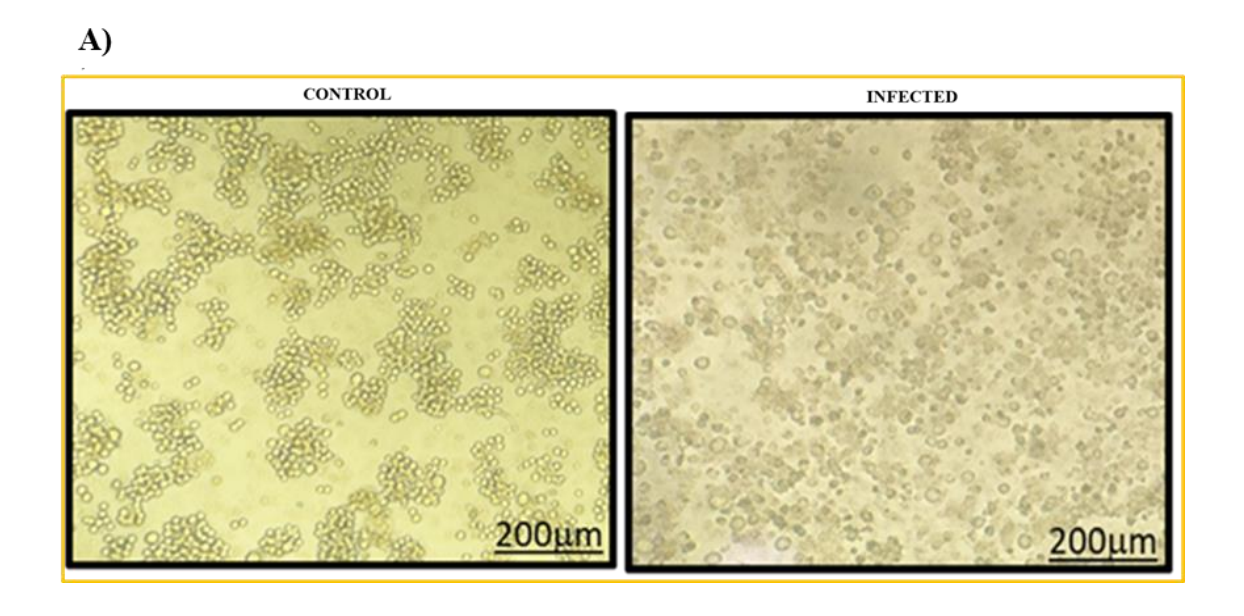


Figure 3.3.6: Analysis of levels of EDRF1, GATA1 and Spectrin levels: (A) pEGFP-N1 Vector and pEGFP-N1 NS2BNS3pro for 28 hrs of transient transfections with indicated antibodies on the left. Bar diagram represents the means of 3 independent sets of experiments for proteins indicated. (B) Western blot analysis of K562 cell lysate transiently transfected with pEGFP-N1 NS2BNS3 and pEGFP-N1 NS2BNS3pro (S135A) mutant analyzed after 28 hours of transfection with indicated antibodies. Bar diagram represents the means of three sets of independent experiments for the indicated proteins.

3.3.7 Analysis of levels of EDRF1, GATA1 and Spectrins in virus infected cell lysates

To further confirm the above result, we extended our study using the K562 virus infected cell lysates (7days post infection). Supporting the transfection analyses, the levels of EDRF1, GATA1 and spectrin proteins were compromised significantly, clearly depicting the role of protease in EDRF1 cleavage (Figure 3.3.7 A & B). It was observed that the reduction of EDRF1 levels is clear in virus infected cell lysates compared to the above transfection studies [148].



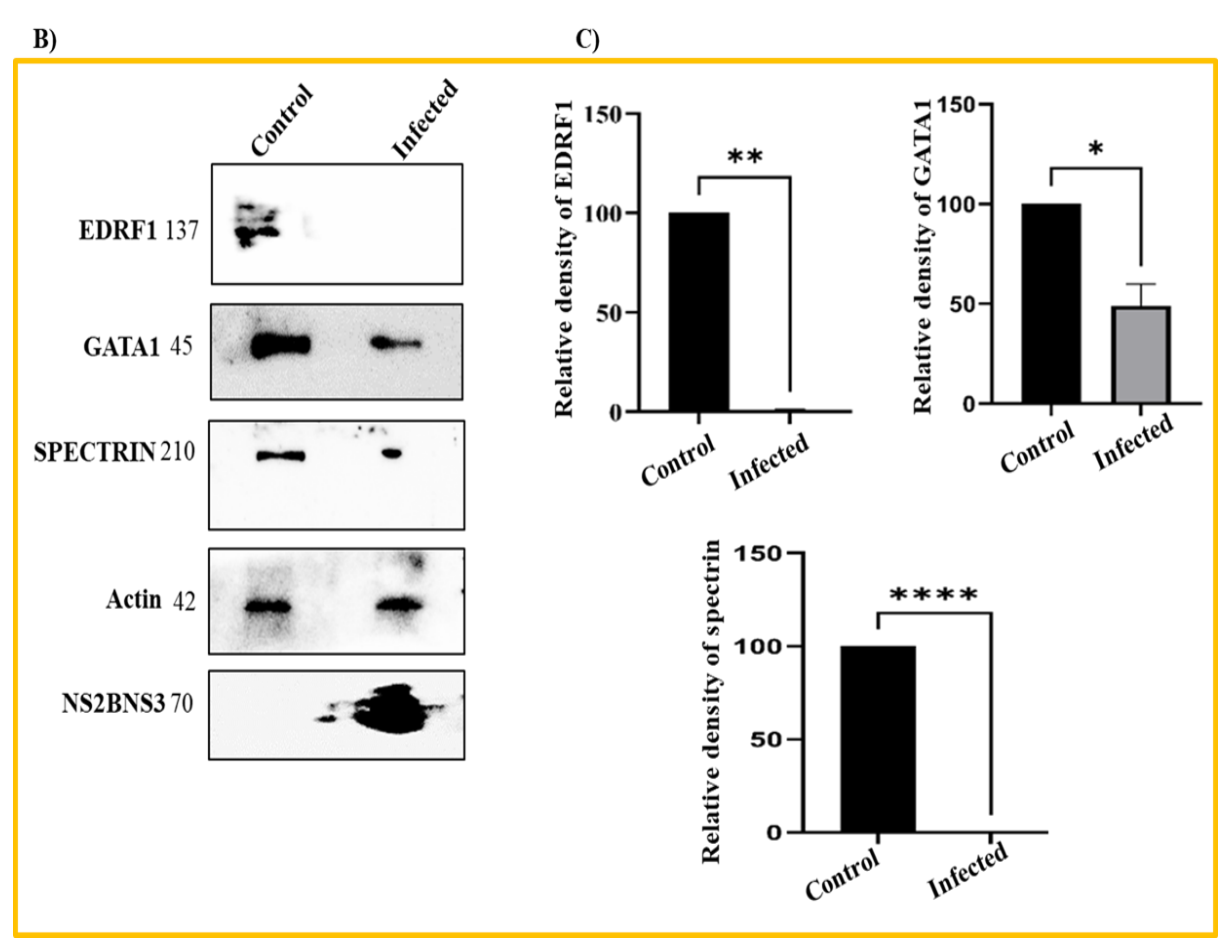


Figure 3.3.7 (A) Figure showing the K562 cells after 7 days of infection (control and Infected). **(B)** Western blot analysis of DENV infected and uninfected in K562 cell lysates after 7 days with indicated antibodies. **(C)** Bar diagram of respective proteins of 3 sets of independent experiments.

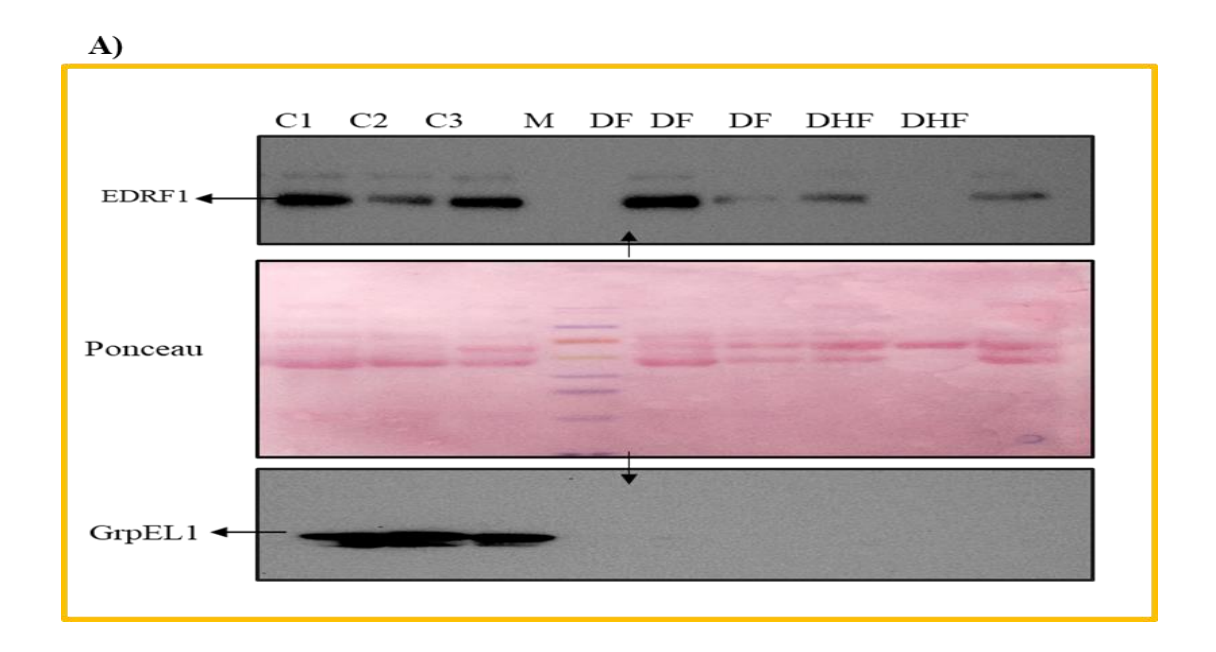
3.3.8 Analysis of EDRF1 and GrpEL1 levels in clinical samples

Total forty-four albumin out clinical samples with different grades of infections i.e., DF, DHF and DSS were included for the analysis (Table 3.3.1). Other febrile infected samples were used as controls. 10% SDS PAGE followed by western blotting was done to analyse the levels of EDRF1. It was observed that EDRF1 levels were reduced in DF, DHF and DSS samples and a significant difference was observed in DHF and DSS samples (Figure 3.3.8 A (upper panel) and B) and (Figure 3.3.9 A and B). GrpEL1 was also included in this study as this protein was identified as a substrate of NS3 in our earlier studies. The GrpEL1 levels were also found to be reduced (consistent with our earlier report) in the samples in which the EDRF1 levels were reduced i.e., in case of DF and DHF (Figure 3.3.8 A (lower panel)) and B [148].

Table 3.3.1: Clinical characteristics of dengue virus infected patient samples used in the study.

A.) Clinical features	B.) Dengue fever (n=24)	C.) Dengue Hemorrhagic Fever (n=17)	D.) Dengue Shock Syndrome (n=4)
GENDER (MALE/FEMALE)	11/13	9/8	3/1
AGE	<1Year to 14 years	<1 year to 15years	<1 year to 12 years
NS1 POSITIVE	15	15	4
lgM/lgG	10	8	1
Thrombocytopenia	19	14	4
Platelet count	(>6000 to <1,50,000)*	(>2000 to <2,30,000)*	(>5000 to <1,50,000)*

Platelet counts were analyzed that are present in the clinical data sheets. * Represents the range of platelet counts.



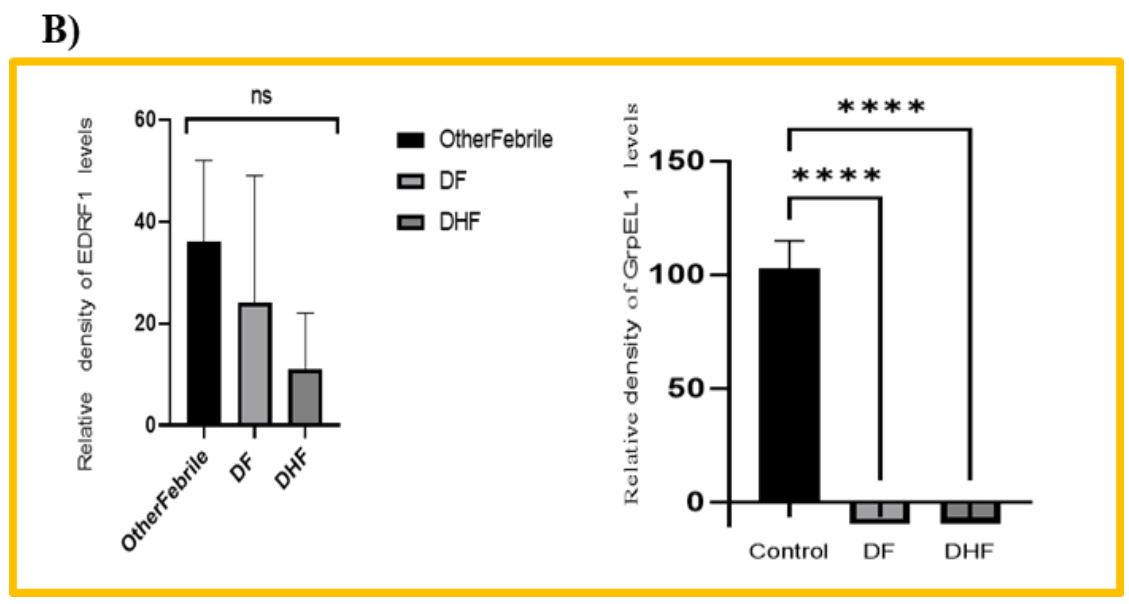


Figure 3.3.8: Western blotting of albumin out other febrile (C1, C2, C3) and dengue infected serum samples (DF and DHF). **(A)** The samples were separated on 10% SDS PAGE and western blotting was done with anti-EDRF1 (top) and anti-GrpEL1 (bottom) antibodies and Ponceau stained membrane (Middle). **(B)** Bar diagram represent the relative densities of EDRF1 and GrpEL1 proteins in clinical samples.

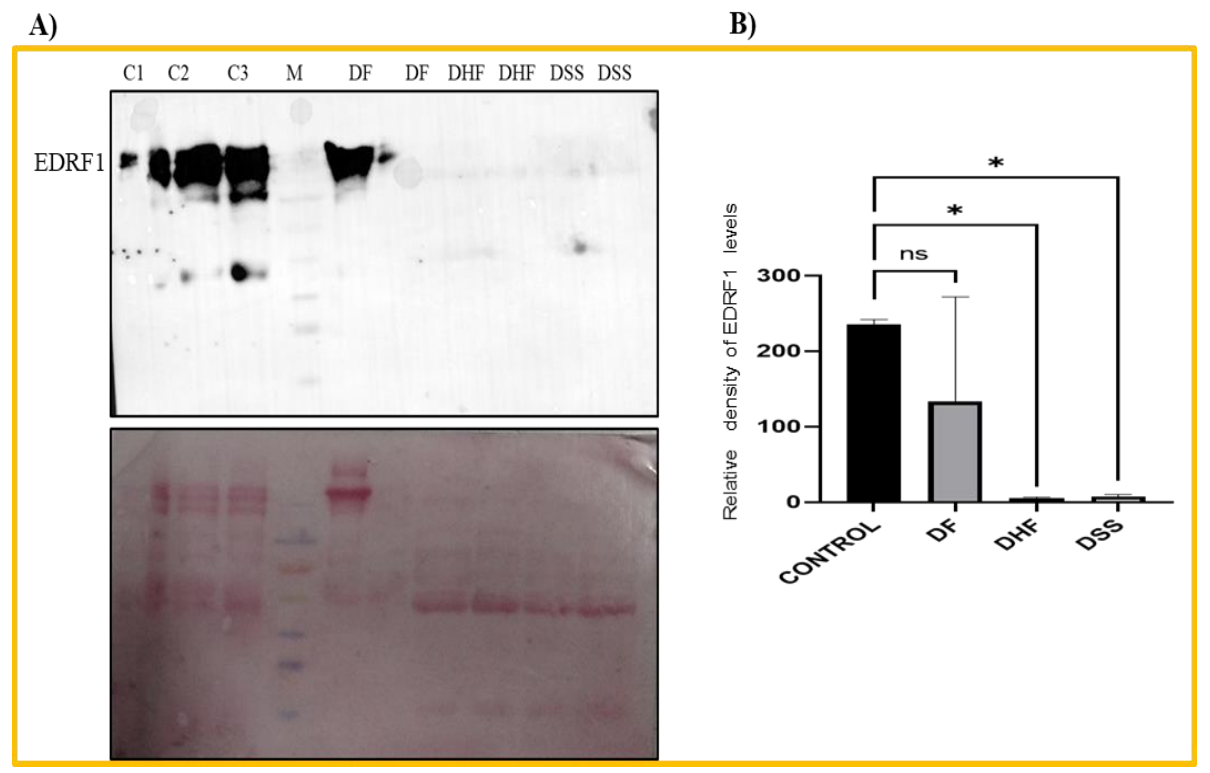


Figure 3.3.9: (A) Albumin out other febrile (control) and dengue infected serum samples (DF, DHF and DSS) were separated on SDS PAGE and western blotting was done to analyze the EDRF1 levels. Bottom panel represents the Ponceau S stained membrane. **(B)** Bar diagram represents the relative density of EDRF1 protein in clinical samples. (*) signifies p-values < 0.05 and ns- non-significant.

3.4 DISCUSSION

Literature suggests the virus coded proteins localize to the subcellular organelles with a specific assignment that favors the virus life cycle. In this direction, the localized proteins interact with the host proteins and divert their normal functions as a result the regular activities of the cells get disturbed. In the previous chapter we show that NS2BNS3 localizes to the nucleus and NS3localizes to both nucleus and mitochondria. Hence, to identify the interacting proteins/substrates of NS2BNS3/NS3, if any, from the nucleus we have carried the pulldown experiment consisting of total cell extracts with purified NS2BNS3pro. The co-eluted protein bands were identified by mass spectrometry analysis and were found to be erythroid differentiation factor 1 (EDRF1) (Figure 3.3.1 A-E). Western blotting analysis of the elutes of the above experiment using anti-EDRF1 antibodies confirms the interaction of NS2BNS3 with EDRF1 (Figure 3.3.1 F and G). In continuation, the amino acid sequence of ERDF1 was searched for the cleavage sites and found five sites at amino acid sequence numbers 50, 100, 152, 926, 987 (Figure 3.3.2 A). Structural superimposition of EDRF1 and protease suggested that the cleavage site (RK/A) (985-988) is located in close proximity of the catalytic triad of protease (Figure 3.3.2 B). To confirm EDRF1 cleavage by the protease, in vitro cleavage analysis was carried out using the purified NS2BNS3pro, with both the purified EDRF1 and overexpressed EDRF1 (cell lysates) which suggest that the increased concentrations of NS2BNS3 lead to the decreased levels of EDRF1 (Figure 3.3.4). In order to cross verify the above observation, the co-transfection experiments carried with the EDRF1 and the NS2BNS3pro constructs. The data suggested the complete disappearance of EDRF1 but not in controls (Figure 3.3.5 A lane 4). This observation suggested that EDRF1 as a novel substrate of dengue virus protease, which reportedly regulates the expression and activity of GATA1. Importantly, GATA1 is known to be involved in erythrocyte and megakaryocytic precursor development, disruption of any of the above-mentioned two functions of GATA1 leads to thrombocytopenia and anemia [167, 168]. GATA1 is also known to be involved in spectrin mRNA synthesis and the spectrin proteins are reportedly needed for pro-platelet and platelet formation. Reports indicate that EDRF1 plays a key regulatory role in GATA1 mRNA expression and DNA binding activity. EDRF1 has been reported to play a major role in transcriptional regulation and expression of GATA1 and globin gene expression, a key factor in megakaryopoiesis [168, 169]. Several lines of research indicated that alpha and beta spectrins are essential proteins involved in cytoskeleton formation, particularly in erythrocytes, in association with actin. An interesting function of spectrin proteins, as far as the present study concerned is their involvement in the pro-platelet and platelet formation [169, 170].

Based on these reports we framed the hypothesis that EDRF1, GATA1 and spectrins might be affected during the dengue virus infection which might contribute for the 'thrombocytopenia' in the patients (Figure 3.4).

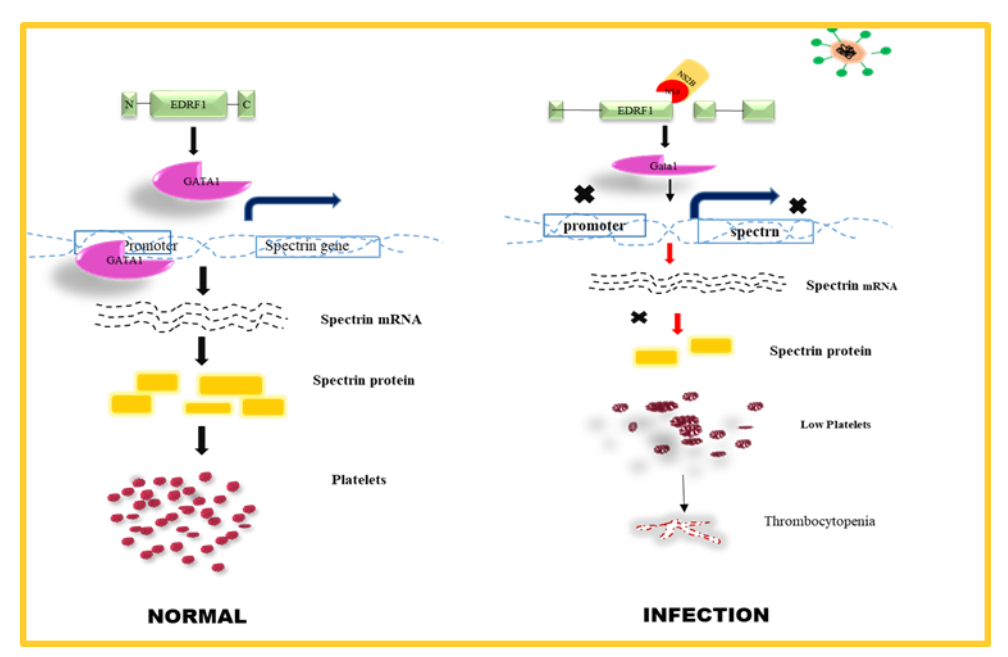
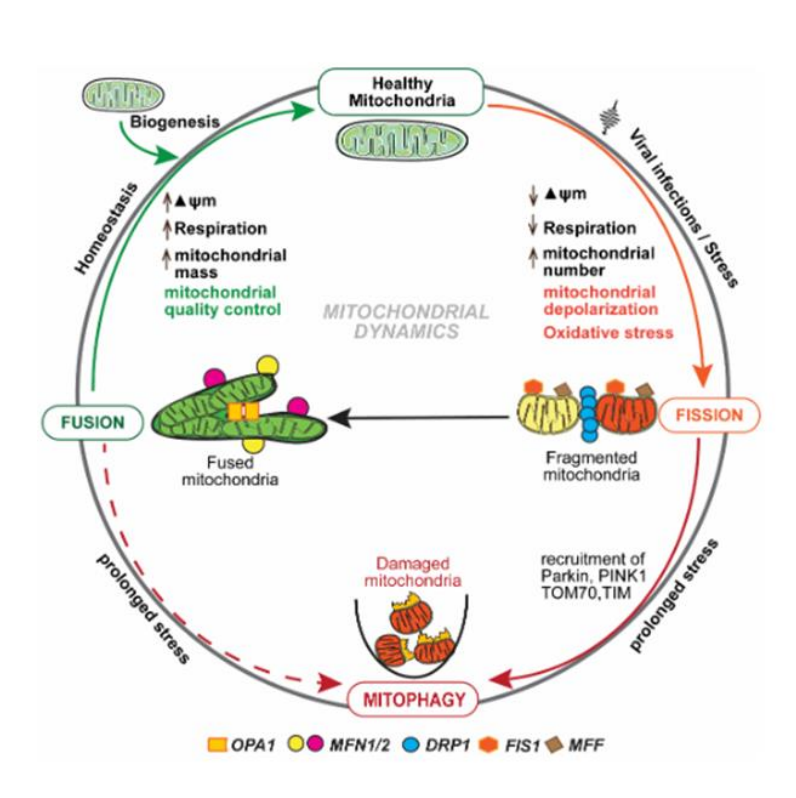


Figure 3.4 Schematic model of the hypothesis showing the cleavage of EDRF1 by dengue virus protease (Right panel) compared to the normal (Left panel) leading to thrombocytopenia [148].

In order to validate the set hypothesis, the NS2BNS3 transfection experiments carried in K562 (megakaryocyte derived) cells suggested the reduced levels of EDRF1, GATA1 and spectrin proteins in the expressed conditions of protease (Figure 3.3.6). Similar analysis carried using the cell extracts of the dengue virus infected cells supported the above observations (Figure 3.3.7). Both the above two conditions strongly suggest the cleavage of EDRF1 and as a result the down regulation of GATA1 and spectrin proteins. Further, the EDRF1 and the GrpEL1 levels were analyzed in the dengue virus infected clinical samples. GrpEL1 was also chosen, as it was shown to be the substrate of NS3 in our earlier studies. The levels of both the above proteins significantly reduced in dengue virus infected samples which are drastic in case of the severe disease (DHF and DSS), indicating the cleavage of ERDF1 (Figure 3.3.8). The effect on the EDRF1 levels is more and more clear from *in vitro ex vivo* to *in vivo* (clinical samples) conditions (Figures 3.3.4, 3.3.5, 3.3.6, 3.3.7, 3.3.8 and 3.3.9). Hence it is concluded that the cleavage of EDRF1 observed in the present study led to decreased levels of GATA1 and subsequently to fewer spectrins and finally to the reduced number of platelets i.e., thrombocytopenia. The earlier proposed mechanisms of thrombocytopenia in dengue virus infections and present observations are possibly parts of a cascade of events of a single mechanism. However, further research is required to indicate whether they are interlinked or different and which is predominant, if different. Non-functional platelets without the number change (thrombopathy) is another possible disorder to be considered in dengue virus infected patients. But, as the current literature including the present study supports the reduction in platelet number, the 'thrombopathy' may need to be further assessed.

CHAPTER 4: EFFECT OF DENGUE VIRUS PROTEASE ON CELL HOMEOSTASIS



4.1 INTRODUCTION

Cell homeostasis is a self-regulatory biological process to maintain a stable internal environment for cell survival. Living organisms require a continuous supply of energy to maintain cellular functions which is generated by cellular mitochondria. Thus, an equilibrium is required between energy generation and energy consumption to maintain cellular homeostasis. In order to understand the balance between energy generation and energy consumption, the metabolic differences between growing cells and differentiated/quiescent cells are determined. For sustained growth and proliferation, cells divide, synthesize and perform anabolic processes i.e. generating the important macromolecules like proteins, carbohydrates, lipids and nucleic acids that are essentially required for producing more cells [171]. On the other hand, cells which are differentiated and non-dividing, their metabolism is maintained by catabolic processes that release energy to maintain cellular functions. Thus, eukaryotic cells have maintained a balanced environment for their continuous growth and cell proliferation capacity [172]. To maintain energetic and cellular stability, cells must be responsive to their extracellular environment. Cells sense the secreted proteins (like growth factors, cytokines, hormones), by binding to cell receptors on the cell membrane. This allows the initiation of signaling cascade events that help in regulating cellular metabolism [172]. Moreover, many recent findings have reported that cells are in a continuous state of modifications such as post-translational modifications, acetylation, methylation and glycosylation, that are required for regulating the cells metabolic activities [173].

Nucleus and mitochondria are the key organelles for regulating the cellular homeostasis. With the signaling events, the flow of energy is maintained for transcriptional and translation processes. While the nucleus controls the fate of a cell, mitochondria fuel the cells for performing metabolic activities and have multi-faceted functions for maintaining cellular metabolism. Mitochondria respond to multiple stress conditions such as nutrient deficiency, oxidative stress i.e. generation of reactive oxygen species (ROS), chromosomal instability (DNA breakage) and ER stress response [174]. In addition to perform bioenergetic and ATP production, mitochondria synthesizes metabolic precursors for macromolecules such as lipids, proteins, DNA and RNA. In response to stress, mitochondria produce reactive oxygen species (ROS) and unwanted cellular factors, and also possess mechanisms to remove them. Extensive research has been done to show that mitochondria as the key organelles for cell survival. Many studies highlighted to show that stress to mitochondria or dysfunctioning in any of its regulatory processes led to disease pathogenesis such as neurological disorders, cancer, inflammation, organ failure, and cardiac dysfunction.

Many studies reported mitochondrial dysfunction during viral infections also [175]. During viral infection, mitochondria play a major role in regulating its self-metabolic activities. To propagate in host cells, viruses hijack the cellular components and also target the host mitochondria directly or indirectly for their survival. Viruses like HSV target mitochondrial DNA while HIV targets the mitochondrial proteins thereby disturbing mitochondrial functions [176]. Some viruses localize to the mitochondria or bind to the outer membrane leading to changes in mitochondrial morphology and its function. There are two processes involved in maintaining the mitochondrial morphology i.e. fission and fusion. Fission causes mitochondrial fragmentation, and is triggered when cells are under stress conditions (disease or any viral attack) to remove the damaged mitochondria while the fusion process serves to prevent the mitochondria from any damage (mitophagy) to maintain its activities. Thus, both the processes are crucial for maintaining the mitochondrial morphology. Mitofusins (MFN1 and MFN2) are involved in the fusion process, on the contrary, Drp-1 and S-OPA 1 are involved in the fission process [177, 178]. It is well documented that both DNA and RNA viral proteins impair the mitochondrial morphology and alter its functions by targeting its fission or fusion processes.

DNA viruses like the human cytomegalovirus, human herpes virus, human papillomavirus, and herpes simplex virus have been reported to alter the mitochondrial morphology causing mitochondrial fragmentation, mitochondrial membrane potential and ROS stimulation. Proteins of RNA viruses like such as NS3-4A of flaviviruses, a serine protease of Hepatitis C virus target its mitochondrial antiviral signaling protein [179]. Similarly, in case of dengue virus, it has been reported that NS2BNS3 protease cleaves the mitofusins altering the fusion process. Further, it has been reported that dengue virus affects the mitochondria by modulating its membrane potential, ATP production, mitochondrial matrix proteins and electron transport chain complexes. Also, the viral proteins disturb the protein folding causing alternations in cellular homeostasis [178, 179]. It has been observed that the NS2BNS3 and NS3 localize to the nucleus and EDRF1, a nuclear transcription factor was identified as a novel substrate of NS3BNS3 (Chapter 2 and 3). In our previous studies, also as described in previous chapters, dengue virus NS3 protease is shown to import to the mitochondrial matrix due to the presence of the MTS signal. This importation of protease leads to the cleavage of GrpEL1 protein, a cochaperone of mtHSP70 which is involved in protein folding and redox homeostasis [147]. However, in the same study, we could not explain the functional consequences of protease cleaving the GrpEL1 protein. Therefore, in the present study, we expanded to analyze the mitochondrial function analysis during the dengue virus infection. Hence we expect that cleavage of mitochondrial GrpEL1 and nuclear EDRF1 account for disturbed cell homeostasis and hence 'thrombocytopenia' in megakaryocyte derived cells.

4.2 MATERIALS AND METHODS

4.2.1 Cell lines

To analyze the functions of mitochondria, HepG2 cells were maintained in DMEM media containing 10% FBS and 1% (V/V) antibiotic. Cells were cultured in T-25 flasks at 37°C and 5% CO₂ under humid conditions.

4.2.2 Transient transfection in HepG2 cells

A day before transfection, the above cultured HepG2 cells nearly 5 x 10^5 cells per dish were seeded (35 mm dishes). The cells were allowed to grow for 16 -18 hours to obtain confluency up to 80%. Then, the cells were observed under a bright field inverted microscope to check confluency and cell morphology. Transient transfection was performed in HepG2 cells as described earlier plasmid constructs pEGFP-N1 vector and pEGFP-N1 NS3pro-helicase as per manufacturer's protocol using Lipofectamine reagent 2000. After 28 hours post transfection, we proceeded with mitostress assay.

4.2.3 Mitostress Assay

Mitostress assay was performed using Agilent Seahorse XFp mini analyzer. 28 hours post transfection, cells were analyzed for GFP expression using fluorescence microscope and further proceeded for the mitostress assay (Figure 4.2.1) [180,181]:

- 1. The above transfected cells were trypsinized, harvested and washed once with serum free medium. The cells were counted using a hemocytometer. 7000-8000 cells per well were seeded in Agilent Seahorse XFp mini culture plates (8-wells) up to 70% confluency and allowed to grow at 37°C in 5% CO₂ incubator, as per the manufacturer's protocol.
- 2. One day before performing the assay, the sensory cartridge provided along with mitostress kit, was hydrated with milli-Q water and incubated at 37°C incubator without CO₂. 5ml of XFP Calibrant solution was also incubated overnight at 37°C incubator without CO₂.

- 3. On the day of assay, overnight hydrated sensory cartridge with milli-Q water is replaced with the XFp Calibrant solution equilibrated for 2 hours as described in manufacturer's protocol. Simultaneously, XFP cell culture base media pH 7.4 is prepared by adding D-glucose, L-Glutamine and Pyruvate solution and filter sterilized.
- 4. XFp mini culture plates containing media are replaced and cells were washed with XFP based media prepared in above mentioned step and incubated at 37°C without CO₂ for 60 minutes.
- 5. After incubating the sensory cartridge, three drugs [Oligomycin (1.5 μ M), FCCP (0.5 μ M), Rotenone/Antimycin (0.5 μ M)] provided in kit were prepared as per protocol and loaded on to sensory cartridge. XFp cell mitostress assay was performed using Seahorse XFp Analyzer with the in-built software program.

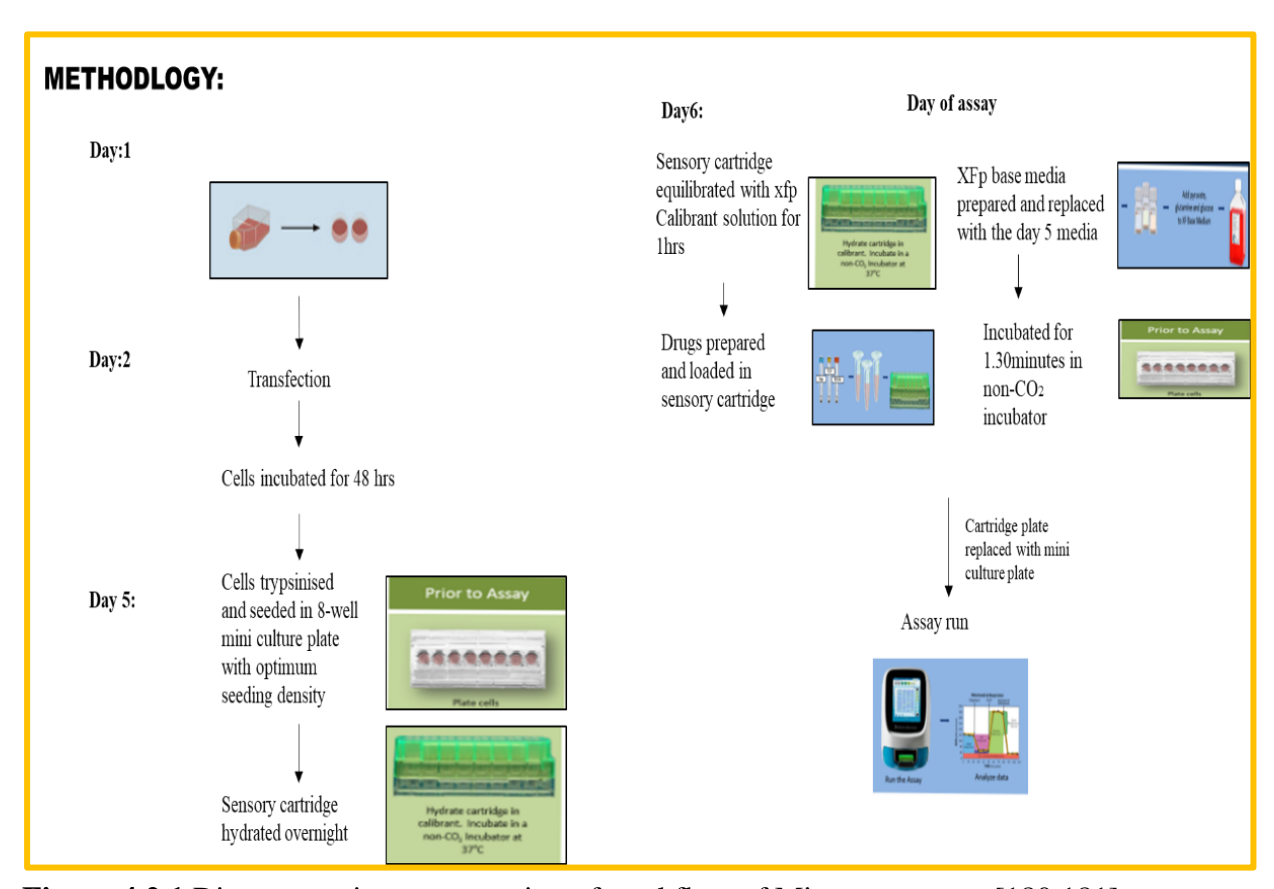


Figure 4.2.1 Diagrammatic representation of workflow of Mitostress assay [180,181].

4.2.2 Cell number analysis during dengue virus infection

K562 cells were chosen for this study, as these cells are megakaryocytic derived and hence expected to give the clue on 'thrombocytopenia'. 2 sets of 60mm dishes with 1×10^5 cells (K562 cells) per dish were infected with viral supernatant for 0, 3, 5 and 7 days, harvested and counted manually with trypan blue dye (Sigma) using a hemocytometer. Uninfected cells were also included. The virus infection was confirmed by RT-PCR of 5' UTR on 5th day. The experiments were performed for three times, the total cell count after each day of infection was taken and an average of two experiments were considered using Microsoft Excel software (Figure 4.2.2).

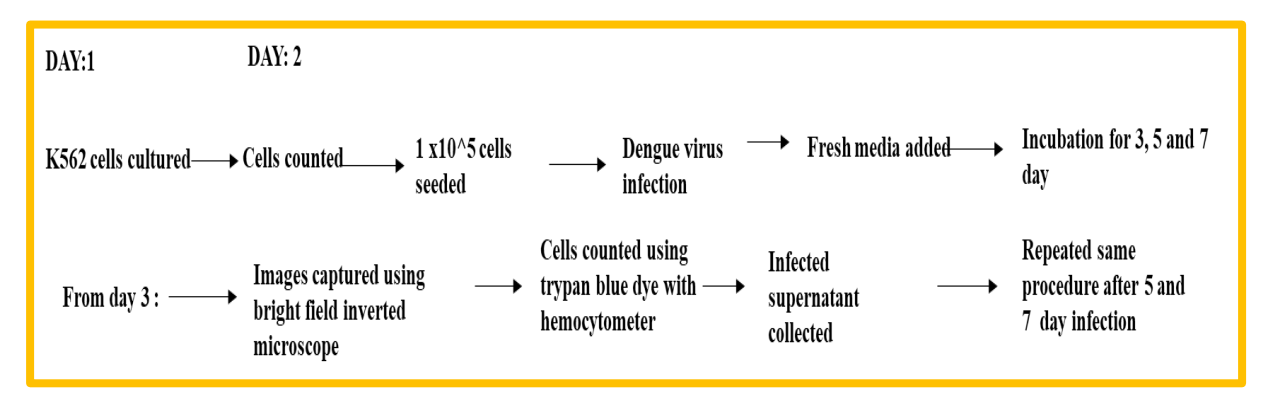


Figure 4.2.2: The schematic workflow protocol for the total cell count of the infected and uninfected K562 cells.

4.3. RESULTS

4.3.1 Effect of protease on mitochondrial functions

NS3 was shown to target the mitochondrial matrix and cleave GrpEL1, a co-chaperone of mitochondrial Hsp-70 (mtHsp-70) in our previous study [147]. In the present study also it was observed that NS3 localizes to mitochondria as well as into the nucleus (Figure 2.3.6 A (ix-xii)). In this direction, to analyze the functional activities of mitochondria we have used HepG2 cell lines (hepatocytes) that have moderate energetic demand and are frequently used for several mitochondrial studies [182]. They are also reportedly permissible for dengue virus infections [183]. Thus, in this study we have performed cell mitostress assays for pEGFP-N1

vector and pEGFP-N1 NS3pro-helicase transfected into HepG2 cells and six parameters were measured and the data is as described below:

Basal respiration: Oxygen consumption rate (OCR) is a measure of the total cellular respiration in cells that meet the cellular ATP demand of the cell under baseline conditions. Basal levels of OCR in NS3pro-helicase transfected cells were found to be decreased compared to vector transfected cells which suggested low mitochondrial respiration in transfected cells (Figure 4.3.1 C i).

ATP production coupled respiration: On the addition of oligomycin, F0/F1 ATPase (complex V) shuts off, which relates to the activity of mitochondria generating the ATP linked to basal respiration. It was observed that in the presence of oligomycin, the ATP production was compromised in NS3pro-helicase transfected cells when compared to the vector (Figure 4.3.1 C ii). A decrease in ATP production coupled respiration results in low ATP demand indicating damage to the electron transport chain (ETC).

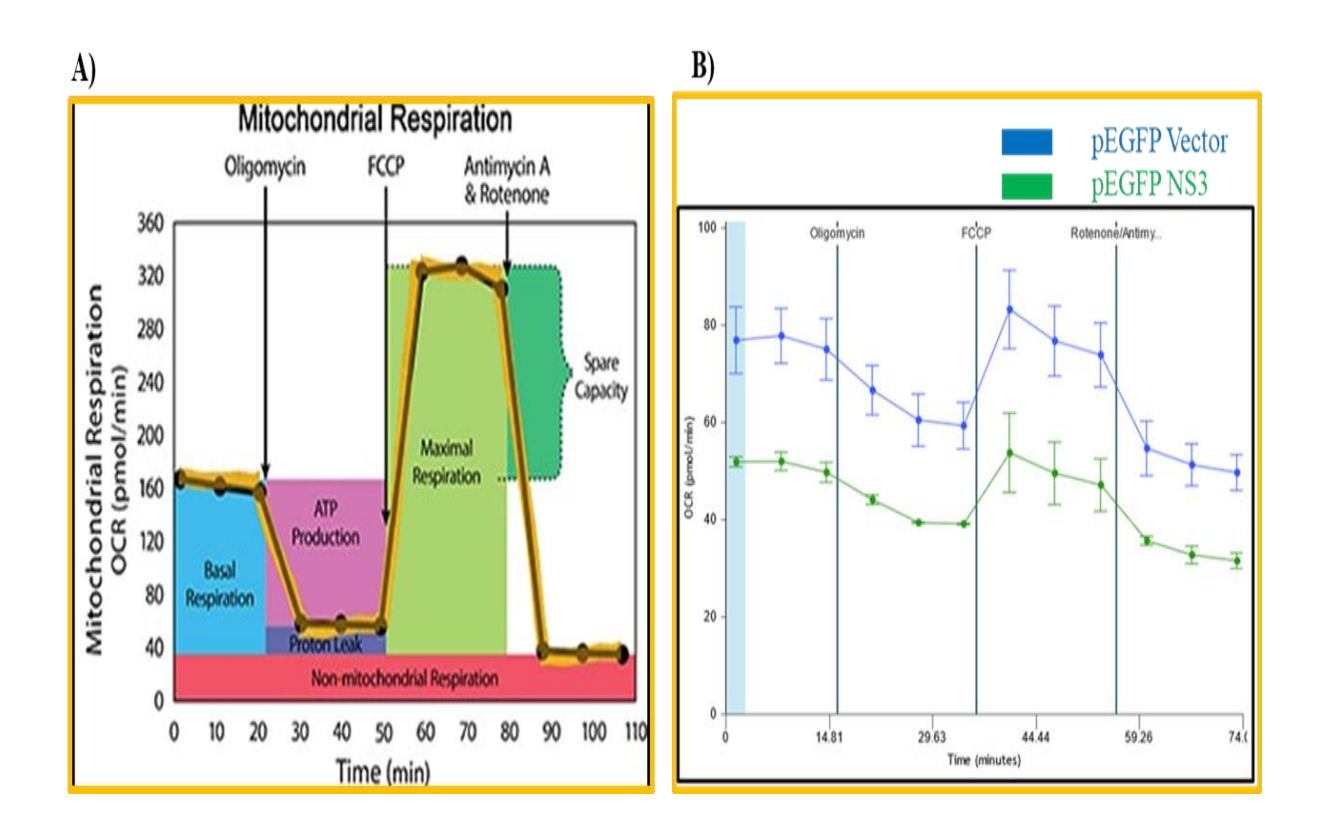
Maximal respiration: On the addition of Carbonyl cyanide p-(trifluoromethoxy) phenylhydrazone (FCCP) (uncoupler), the movement of protons (H+ ions) will be allowed. This phenomenon leads to a sudden increase in maximal respiration indicating high substrate availability and good integrity of the ETC as observed in vector transfected cells. However, there was no increment in maximal respiration in NS3-pro helicase transfected HepG2 cells indicating the defective mitochondrial ETC (Figure 4.3.1 C iii).

Spare Respiratory Capacity: It is a measure of the difference between maximal respiration and basal respiration and represents the cell fitness and the cell response due to high energy demand. In NS3pro-helicase transfected cells, maximal respiration was found to be low

compared to vector, thus there was low spare respiratory capacity compared to the vector. Low respiratory capacity indicates low fitness of the cell (Figure 4.3.1 C iv).

Proton Leak: Basal respiration that is not linked to ATP production indicates the proton leak. There was no significant change in proton leak due to low energy demand or low substrate availability in transfected cells (Figure 4.3.1 C v).

Non-mitochondrial oxygen consumption: The addition of antimycin and rotenone inhibits complex III leading to low cellular respiration. Non-mitochondrial oxygen consumption is the measure of the cells recovering their energy demand through other cellular processes. In the NS3pro-helicase transfected cells, there was no increase in non-mitochondrial oxygen consumption rate as compared to the vector indicating the damage to mitochondria (Figure 4.3.1 C vi).



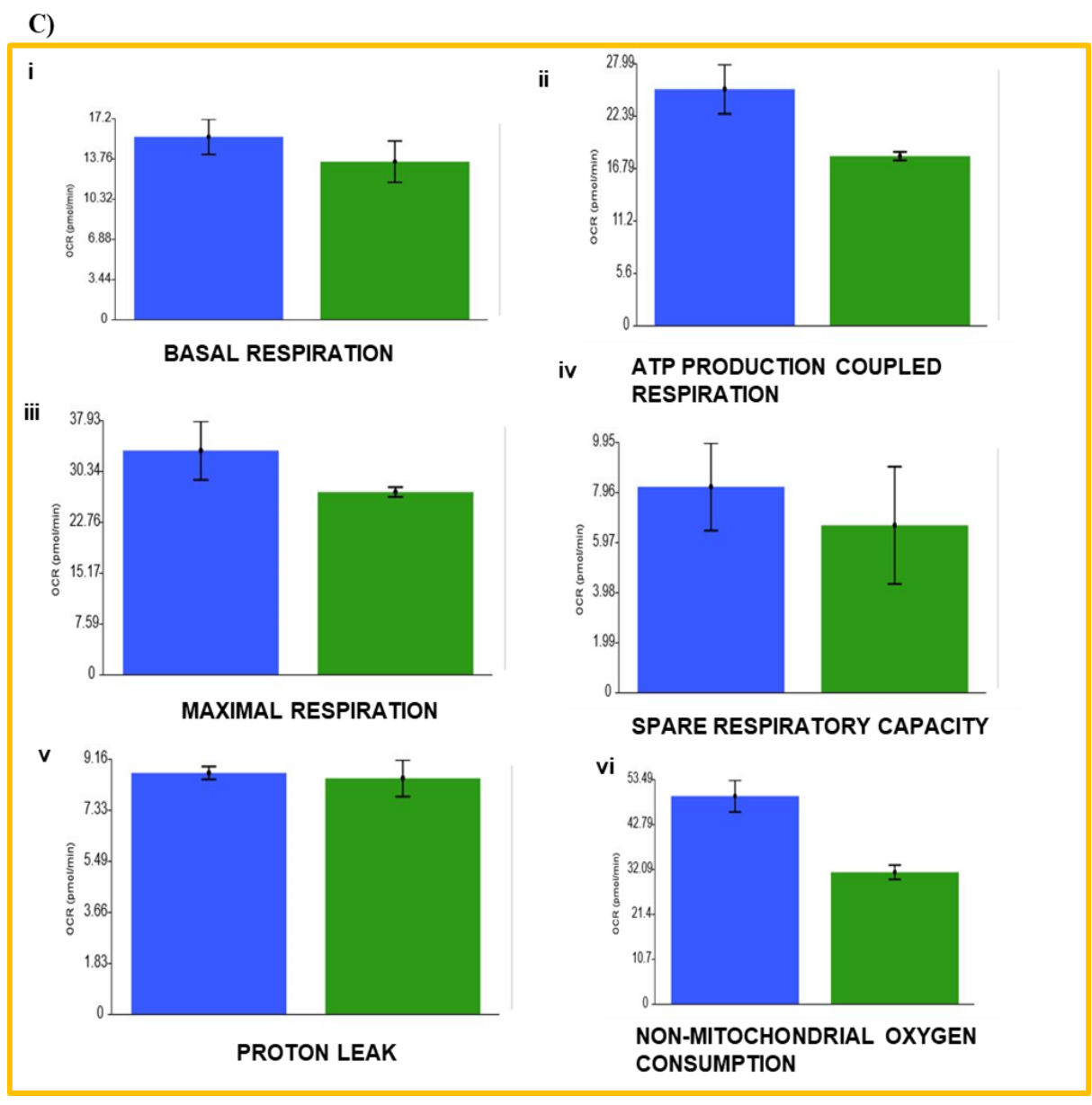


Figure 4.3.1: Mitochondrial function analysis in protease transfected cells. (A) Represents the reference model for the analysis of mitochondrial bioenergetics in mitostress assay. (B) Agilent Seahorse XFp cell mitostress assay showing bioenergetics of mitochondria in cells transfected with pEGFP-N1 vector and pEGFP-N1 NS3pro-helicase with respect to oxygen consumption rate vs time. (C) The graphs represent the oxygen consumption rate vs time during injection of the three drugs (Oligomycin, FCCP and Rotenone/Antimycin). (i) Basal respiration (ii) ATP production coupled respiration (iii) Maximal respiration (iv) Spare respiratory capacity (v) Proton leak (vi) Non-mitochondrial oxygen consumption. The parameters measured are shown in representative bar graphs with error bars of at least two experiments (n=3 i.e. triplicates in each experiment) [148].

4.3.2 Reduction in cell number during dengue virus infection in K562 cells

In order to analyse the effect of virus infection on K562 cells (megakaryocyte derived cell line), we performed a cell counting method to analyse the cell number during virus infection. For this purpose, K562 cells with dengue infected or uninfected were analyzed day wise (0, 3, 5 and 7) for morphological changes. 4th day post infection onwards, visible cell morphological changes (deformed shape, reduced size and tiny appearance) occurred. Total cell count starts decreasing after day 3. The rounded cell morphology of K562 cells was changed, a visible reduction in cell size on 7th day was observed and the changes were imaged under an inverted bright field microscope (magnification at 10X) (Figure 4.3.2 A and B). The virus infection was confirmed by RT-PCR on the 5th day (Figure 4.3.2 (C)) [148].

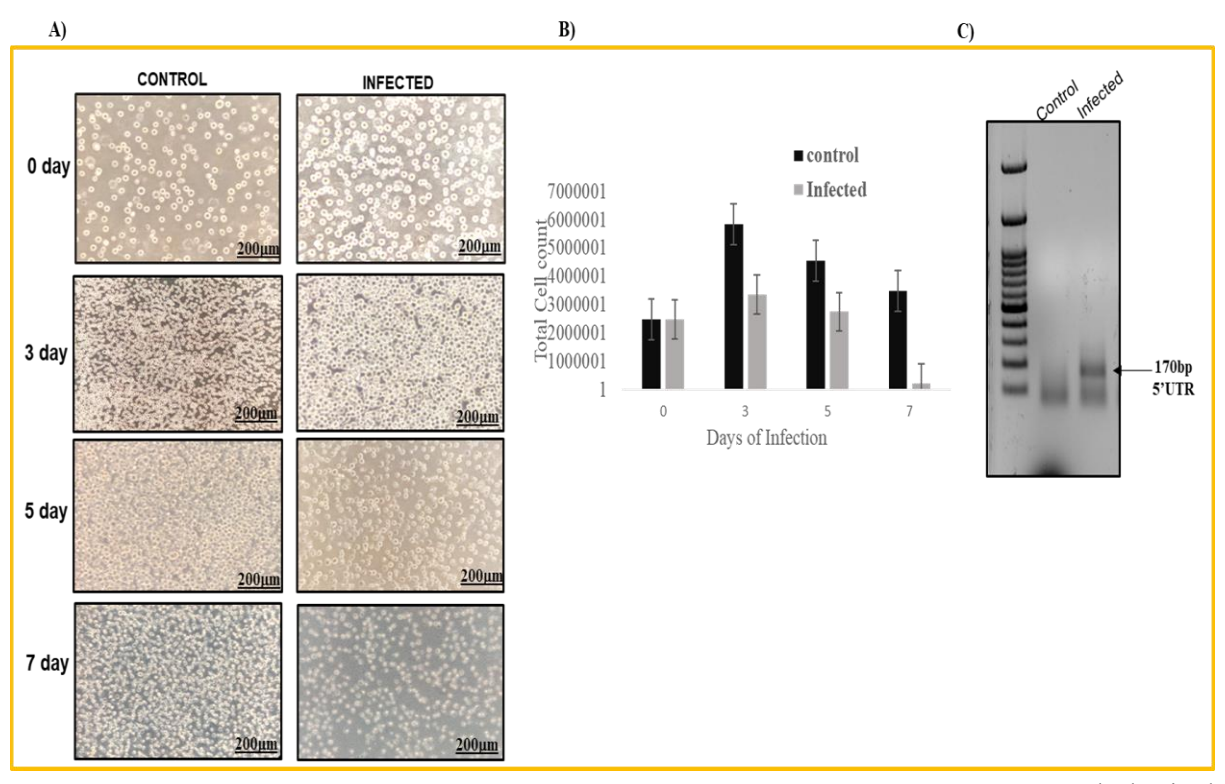


Figure 4.3.2: Analysis of cell number during dengue virus infection. (A) Morphological analysis at 10X (scale bar= $200\mu m$) of infected and uninfected K562 cells observed at different days post infection from 0 to 7^{th} day. (B) Bar graph showing the total cell count of uninfected and infected K562 cells. The error bars represent the average total cell count of at least two independent experiments. (C) RT-PCR analysis of amplified fragment of 5'UTR (170 bp) during dengue infection on the 5^{th} day [148].

4.4 DISCUSSION

All the cellular processes are driven by the normal nuclear organization, its functions and ATP generated through mitochondria. Virus itself or viral proteins overtake the host mitochondrial protein functions and consume host cell's energy for their propagation and replication. Hence, the role of mitochondria as a key organelle is inevitable. Viral proteins invade the host by inhibiting the host interferon production pathway. Dengue virus protease cleaves the interferon adaptor protein MITA/STING to modulate the immune response [73]. Viruses alter the mitochondrial dynamics but the clear mechanism is still limited. During dengue virus infection, the virus targets the mitochondria by various strategies. Previous studies reported that dengue virus infection in HepG2 cells results in metabolic stress, alters the ATP content and imbalances the mitochondrial homeostasis [184]. Another recently published study reported that defective mitochondrial quality leads to injury and necrosis in dengue infected cells resulting in severe pathogenesis [184, 185]. In the previous chapters, we have highlighted the localization of viral protease in the nucleus and mitochondria. In our earlier published study, it is reported that viral protease cleaves the GrpEL1 protein, a co-chaperon of mtHSP70. Hence, we have analyzed the activities of mitochondria (basal respiration, ATP production-coupled respiration, maximal respiration, spare respiratory capacity, proton leak, and nonmitochondrial oxygen consumption) in the cells transfected with NS3. These activities were found to be reduced (except proton leak) significantly compared to the controls. This observation supported the hypothesis that the mitochondrial dysfunction/defectiveness is due to the effect of the dengue virus-coded protease. The above findings related to mitochondria were supported by the earlier studies carried out by virus infections. As the mitochondria coordinate the fission and fusion process the oxygen consumption during both process varies and thus respond to mitochondrial dynamics. It is reported that dengue virus protease cleaves the mitofusins (MFN1 and MFN2) leading to fragmented mitochondria. This fragmentation results in low oxygen consumption in cells, low respiration, decreased membrane potential, low ATP production and increased number of damaged mitochondria. Thus, it must be highlighted due to the presence of protease that causes mitochondrial fragmentation and dysfunctioning of the mitochondria resulting in altered morphology and mitochondrial dynamics and hence the above mitochondrial activities. Mitochondrial dysfunctions are also reported to be lead to impaired platelet formation. It is reported that hematopoietic precursor cells or megakaryocytic cells follow a strenuous metabolic pathway to generate platelets [184, 185]. In addition, EDRF1, a nuclear transcription factor, was found to be cleaved as shown in earlier chapter [163, 165, 148]. EDRF1 is reported to be a crucial factor in platelet formation [166, 169]. Hence, we proceeded with the analysis of cell numbers under dengue virus infections using the megakaryocyte-derived K562 cells. The results showed a reduction in the number which is more prominent as the number of days progressed (Figure 4.3.2). Platelets are the cell types that are required in a huge number in the blood at a given point of time. In order to produce a large number of cells, the platelet lineage cells have to undergo vigorous growth and differentiation which require a high input of ATP. But the mitochondrial damage occurred during dengue virus infections (due to protease as described above), and the cells are incapable of dividing fast to yield enough platelet number because of less ATP generation by mitochondria. Hence, it is concluded that cleavage of the EDRF1, a nuclear transcription factor, by NS2BNS3 of dengue virus, and the NS3-mediated mitochondrial dysfunction contribute to the reduced number of platelet formation (thrombocytopenia) during dengue virus infection [148]. However, the depth of EDRF1 cleavage by dengue virus protease needs to be further analyzed.

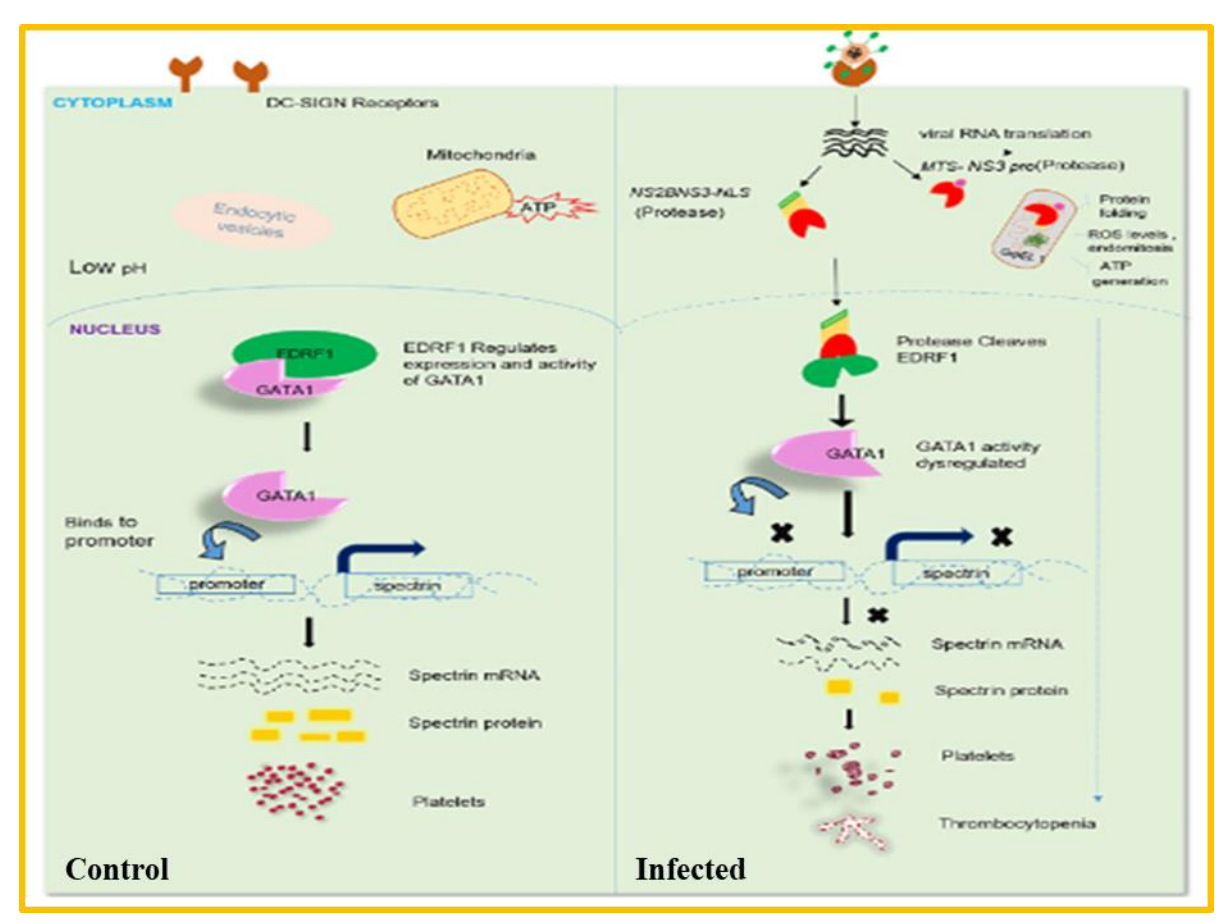
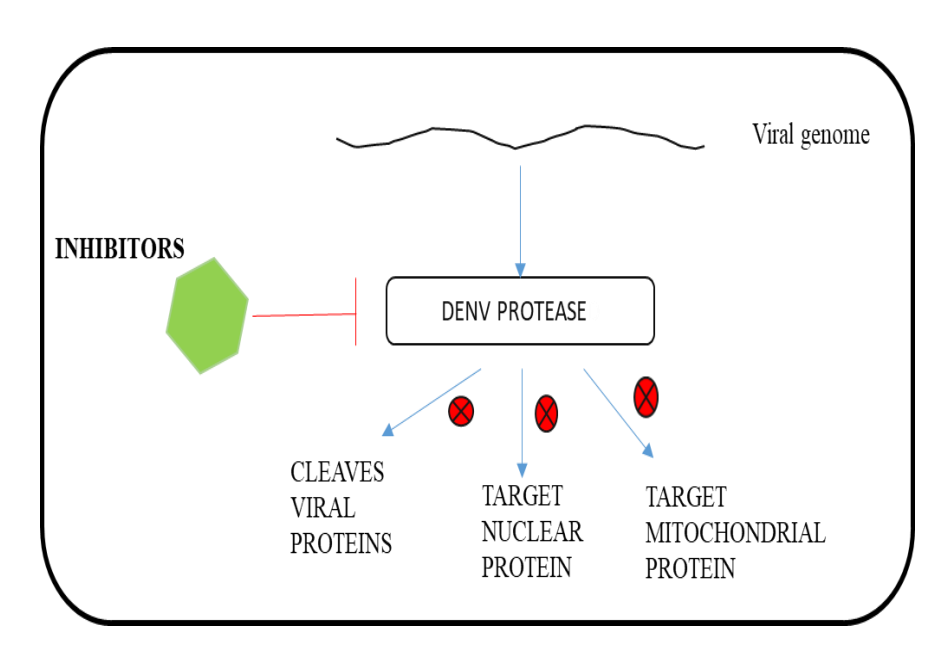


Figure 4.4: Schematic model showing the localization of dengue virus protease in subcellular organelles and consequential homeostasis. NS2BNS3 with NLS enters the nucleus and NS3 with MTS and NLS enters the mitochondria and nucleus (right panel). NS3 causes mitochondrial dysfunctioning and NS2BNS3 cleaves EDRF1 in nucleus, both accounts for the low platelet count leading to thrombocytopenia [148].

CHAPTER 5: IDENTIFICATION AND EVALUATION OF ANTI-PROTEASE MOLECULES



5.1 INTRODUCTION

Infectious diseases of viruses are the major concern of high mortality rates worldwide. The world is being exposed to many viruses like SARS-CoV 2, Influenza, RSV, HIV, HCV, Hepatitis, Chikungunya, Enterovirus, ZIKA, JEV, YFV, Ebola and Dengue viruses [186]. Among them, dengue contributes to high mortality across all age groups. Although a lot of research has been explored and documented related to the development of antivirals and vaccines, there is no specific treatment approved till now. Dengvaxia, a tetravalent dengue vaccine, has been approved but it is being restricted to specific individuals in some countries due to limitations in its efficacy against all serotypes. Currently, due to widespread epidemics and the severity of dengue, the discovery of specific antiviral drugs is an urgent need. There are many reports about the inhibition by different drug molecules during different stages of infections. These molecules target the virus proteins like NS5, Envelope, NS4B, and capsid [187, 188]. However, targeting the enzymatic proteins like NS3 and NS5 is particularly crucial because of their multifunctional roles in the virus life cycle. Viral proteases have been studied as the most successful antiviral targets as evidenced in case of HIV and HCV protease inhibitors [189, 190].

For studying the dengue viral protease inhibitors, *in vitro* and *in vivo* strategies have been implemented so far. *In silico* and high-throughput screening (HTS) methods have been used for identifying the key inhibitory molecules [191]. Peptide and non-peptide inhibitors are being screened as anti-viral molecules. Non-peptide inhibitors are screened by both *in silico* docking approach or HTS methods. Fluorogenic peptide substrates are majorly used for screening assay [191, 192]. Protease inhibitors are known to bind in a competitive manner or they break the interactions between the NS2B and NS3. Several newly synthesized compounds have been studied for their anti-viral activity but very few have reached up to clinical trials. Thus,

potential DENV protease inhibitors are required for controlling its pathogenesis. Based on previous literature studies, the development of dengue virus protease inhibitors gave several new leads of peptidic, peptidomimetics and small molecular compounds. However, due to their unsuitable pharmacokinetic and pharmacodynamic properties as well as their binding nature to non-specific targets and insufficient efficacy, none of them have reached clinical trials. Dengue virus protease inhibitors are expected to inhibit all the serotypes. A study reported the inhibition of all serotypes by a small peptide inhibitor called MB21, reported as a pan dengue inhibitor [108].

From ancient times, plant products have been the natural cure for any disease. To date, plant based products have been considered naturally effective and safe. Thus, many researchers have attempted to develop plant based or their derivatives as antivirals. Plant compounds or their derivatives have been used for their medicinal properties, bioavailability and less cytotoxicity. According to previously published literature in developing antivirals, Nordihydroguaiaretic acid (NDGA) and its derivatives have been used as an effective antiviral for HIV [193, 194]. Quercetin is a plant flavonoid reported to inhibit the dengue viral protease activity. Another study reported that Flavonoid from Carica papaya inhibits NS2BNS3 protease and prevents dengue viral assembly [195, 196]. NDGA, a plant derived synthetic molecule, is well-known for its strong antioxidant and antiviral properties. It is a phenolic compound present in leaves and twigs of the shrub Larrea tidentata. and is also the primary metabolite. NDGA has been reported to be involved in the inhibition of protein kinase C, regulates the cellular calcium levels, apoptosis and breakdown of Alzheimer's β-amyloid fibrils in vitro [197, 198]. It is also being explored in the treatment of several other diseases like diabetes, arthritis, pain, inflammation, rheumatism, kidney and gallbladder stones [199, 200]. NDGA and its derivatives (tetra-o-methyl NDGA, M₄N and terta-o-glycyl NDGA, G₄N) which block their transcription mechanism have been reported as potent anti-viral inhibitors against the viruses like HIV, HCV, HPV, HSV, Influenza, SARS-CoV2 and other DNA viruses [199-201]. NDGA, hypolipidemic agent has been reported to inhibit dengue virus replication and virion assembly [202]. Although there are many apprehensions related to the development of antiviral drugs, there are many dengue virus protease inhibitors that have been explored for their anti-viral properties [85, 86].

In the previous chapters 2, 3 and 4, we analyzed the subcellular localization of protease, its substrates and the effect of protease on host mitochondrial functions. We observed that the protease targets the host proteins significantly. Thus in this direction, we made an attempt to inhibit the activity of viral protease and hence ceasing its effect on host. For this purpose, we have used the NDGA derivatives and analyzed their anti-protease activities.

5.2 MATERIALS AND METHODS

5.2.1 Design and synthesis of compounds

NDGA and its derivatives were synthesized in the laboratory of Dr. Y.S. Ravi Kumar, Institute of Biotechnology, Ramaiah College of Higher Education, Bangalore, India.

Brief method of Tetra-O-thiophenylated NDGA (T₄N) synthesis

In order to synthesize the molecule T_4N , 30 mg of NDGA was dissolved in 2ml of 0.2 M NaOH was transferred into the reaction flask and 46 μ l (0.2 M) of 2-Thiophenecarbonyl chloride was added to the stirring mixture. 2 ml of 0.2 M NaOH was added using syringe in drops and the mixture was stirred for 1hour resulting in yellow solid. This solid was washed with an excess of distilled water and extracted with ethyl acetate (70 ml \times 3). The combined organic extract was evaporated to give yellowish solid which was recrystallized from ethyl acetate/petroleum ether. Purified using column chromatography, increased concentration of methanol in chloroform was used as solvent. Purified compound was characterized using NMR, IR and

mass spectroscopic analysis. The equation for the synthesis of T₄N from NDGA is given below (Figure 5.2.1).

Figure 5.2.1: Schematic representation of the equation for the synthesis of T₄N

Brief method for Tetra-O-benzoylated NDGA (B4N) synthesis

In order to synthesize B_4N , 30 mg of NDGA was dissolved in 2ml of 0.2 M NaOH was transferred into the reaction flask and 46 μ l (0.2 M) of Phenyl carbonyl chloride was added to the stirring mixture. 2 ml of 0.2 M NaOH was added via syringe in drops and the mixture stirred for 1h. resulting yellow solid which was washed with excess of distilled water and extracted with ethyl acetate (70 ml \times 3). The combined organic extract was evaporated to give yellowish solid which was recrystallized from ethyl acetate/petroleum ether. Purified using column chromatography, increased concentration of methanol in chloroform was used as solvent. Purified compound was characterized using NMR, IR and Mass spectroscopic analysis. The equation for the synthesis of B_4N from NDGA is given below (Figure 5.2.2).

Figure 5.2.2: Schematic representation of the equation for the synthesis of B₄N

Other compounds (F₄N, PA₄N, MOB₄N, HC₄N) were also synthesized by the following methodology for replacing the hydroxyl groups of NDGA.

5.2.2 Expression and purification of NS2BNS3 protease

pRSET A-NS2BNS3pro (46 a.a + 180 a.a) was transformed into BL21 E. coli cells. 5-6 colonies were grown in 10 ml of Luria Broth (LB) medium for overnight at 37°C. 500 ml of secondary culture was made using the above primary culture and kept under shaking until OD 600 reaches 0.6. Protein expression was induced by the addition of IPTG at 0.6 mM concentration, and the cells were incubated for 18 hours at 18°C. The cells were collected by centrifugation at 8000 rpm for 10 min at 4°C, and the pellets were resuspended in lysis buffer (50 mM Tris HCl, pH 8.0, 150 mM NaCl, 5% glycerol, 2 mM Beta-mercaptoethanol, and 10 mM imidazole) and sonicated. The sonicated lysate was centrifuged at 10000 rpm for 45 minutes. Ni-NTA His tagged beads were equilibrated with lysis buffer. The clear supernatant obtained after centrifugation was collected and incubated with equilibrated Ni-NTA beads for 2-3 hours at 4°C on the rocker for binding. The gravity column was washed with wash buffers containing 20-80 mM imidazole. Protein fractions were eluted with elution buffer containing 250 mM imidazole. 10-20 µl of each fractions were analyzed on 10% SDS PAGE. The elutions containing enriched NS2BNS3 were pooled and dialyzed over a 10 kDa cut off membrane against 200-fold volume of buffer (50 mM Tris pH 8, 100 mM NaCl and 5% glycerol) overnight. Dialyzed protein was collected, quantified by Bradford assay and stored in 50 mM Tris pH 8.0 and 10% glycerol at -80°C [84].

5.2.3 Maximum Non-toxic dose test (MNTD) for cytotoxicity assay

Cytotoxicity of compounds [Quercetin (positive control), NDGA and its derivatives T₄N, B₄N, F₄N, PA₄N, MOB₄N, HC₄N and Gallic Acid (GA)] were assessed by MTT (3-(4, 5-

Dimethylthiazol-2-yl)-2, 5-Diphenyltetrazolium Bromide) assay. Vero cells were seeded in a 96-well plate at a density of 1x10^4 cells per well and incubated overnight at 37°C. After 12-16 hours post seeding, cells were treated with increasing concentrations of the above compounds (10 μM to 3mM) dissolved in DMSO and DMSO (<1%) alone were added to the wells and incubated for 72 h. Then, the MTT reagent was added per well with final concentration of 0.5mg/ml and incubated for 4 hours at 37°C in a humidified CO₂ incubator. Finally, the formazan crystals were solubilized by the addition of DMSO (100 μl/well), and optical density (O.D) at 570 nm (basal line 600nm) was measured using a microplate reader (BMG lab tech).

5.2.4 *In vitro* Protease Assay

In vitro protease assay was used by following the existing protocols but with slight modifications [139, 147]. The activity of NS2BNS3 protease was determined by fluorescence-based protease assay. A fluorogenic peptide substrate containing the consensus cleavage site of virus protease tagged with AMC, Benzoyl-Nle-Lys-Arg-Arg-4-methyl coumarin-7-amide (Bz-Nle-KRR-AMC) was used in this study. The cleavage of the fluorescence substrate by recombinant dengue protease was monitored, and the emitted fluorescence units were recorded. The recombinant protease was pre-incubated for 15 min at 37°C in protease assay buffer (50 mM NaCl, 50 mM Tris-Cl pH 9.0, 20% Glycerol and 1 mM CHAPS). The reaction was initiated by the addition of substrate and incubated at 37°C for 1 hour 15 minutes. The fluorescence readings were recorded using an excitation filter with 380 nm and emission filter 460 nm in a microplate reader. The fluorescence readings were taken as the measure of the protease activity. The enzyme kinetics were calculated from non-linear regression by plotting relative fluorescence vs substrate concentrations from 5 μM to 80 μM following Michaelis Menton kinetics by GraphPad Prism 5.0 software [108].

5.2.5 Inhibitory activity of compounds

The enzymatic inhibition was performed with a fluorogenic substrate, Bz-Nle-Lys-Arg-Arg-AMC (Bachem) in a 96-well plate. 100 nM recombinant NS2BNS3 protease was pre-incubated for 15 min at 37°C in protease assay buffer with different dilutions of inhibitors (Quercetin, T₄N, B₄N, F₄N, PA₄N, MOB₄N, HC₄N and GA). Finally, 20 µM substrate was added to the above reaction and incubated at 37°C for 1 hour. The substrate hydrolysis was monitored as relative fluorescence units at an excitation wavelength of 380 nm and emission wavelength of 460 nm in a multimode microplate reader. The % inhibitory activity of compounds was measured by normalizing the values with control (no inhibitor) as 100% activity and IC₅₀ was determined using GraphPad prism 9.

5.2.6 Selectivity Index of the NDGA derivatives

The selectivity index of the above compounds was calculated using the following equation. Selectivity Index (SI) = Ratio of CC_{50} (50% cytotoxic concentration) to IC_{50} (50% inhibitory concentration).

5.2.7 Effect of Quercetin on protease localization

To analyze the inhibitory activity of Quercetin on the protease localization, we have performed the expression of NS2BNS3pro in K562 cells in presence of Quercetin. pEGFP-N1 vector and pEGFPN1-NS2BNS3 pro were transfected using Lipofectamine as per manufacturer's protocol and after 5 hours of transfection, Quercetin was added (10 μ M) in the complete RPMI media. After transfection, cells were fixed using 4% paraformaldehyde and permeabilized using 0.25% Triton-X100 buffer. The fixed and permeabilized cells were washed 3-4 times with 1X PBS. Cells stained by Hoechst stain and washed once with 1XPBS. The cells were resuspended in glycerol and 1X PBS in ratio (1:1) and mounted onto glass slide with a coverslip and sealed.

5.2.8 Immunofluorescence assay to evaluate the anti-protease activity of compounds

A day before infection, Vero cells were seeded in a 12-well plate at a density 1 x 10⁵ cells per well. Cells were infected with viral supernatant of 0.09 Multiplicity of Infection (MoI). After 2-3 hours of viral adsorption, the cells were treated with drugs with a conc of 15 μ M each (T_4N , F₄N, PA₄N, MOB₄N and HC₄N) and Quercetin and B₄N (40 μM), in DMEM containing 2% FBS and further incubated for 72 hours. The cells were fixed using paraformaldehyde and permeabilized using 0.25% Triton-X100. Cells were allowed for blocking with blocking buffer (3% BSA in 1X PBST) for 1 hour 30 minutes and incubated overnight with primary antibody (NS2BNS3 raised in-house) in 1:1000 followed up by washing the cells for 4 times with 1X PBST, 10 minutes each. Cells were incubated with fluorescent conjugated secondary antibody Alexa flour 488 (1:1000) for 2 hours at room temperature in dark. Then, cells were washed by 1X PBST for 5 times 10 minutes each and stained with Hoechst stain (1:1000) followed by mounting the coverslips on the glass slide and sealed. Cells were analyzed using immunofluorescence microscope (Figure 5.2.3). Three independent experiments were performed and the cells were analyzed for detecting the fluorescence (viral protease). Image analysis was performed using Image J software and the graph was plotted as mean fluorescence intensities of the individual cell (n=50). The viral supernatants were collected, aliquoted for quantification by focus forming assay and /or stored at -80°C for further use.

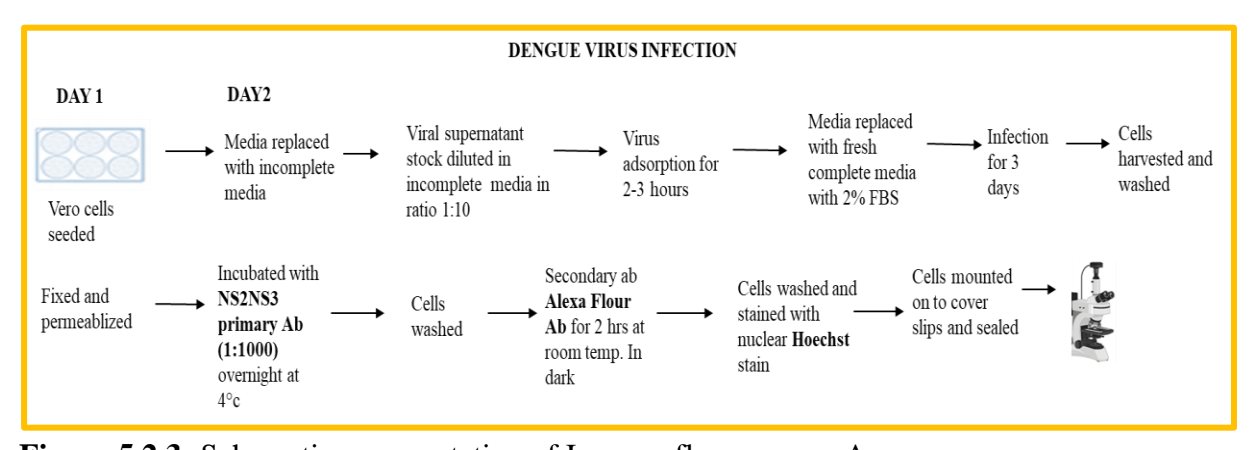


Figure 5.2.3: Schematic representation of Immunofluorescence Assay.

5.2.9 Viral RNA isolation and semi-quantitative PCR

Viral supernatants of the above experiment were thawed on ice. 140 µl of viral supernatant aliquoted and viral RNA isolation was performed using QiAamp Viral RNA isolation kit (Cat. No. 52904) as per manufacture's instruction. RNA was eluted in 40 µl of elution buffer or nuclease-free water. The eluted RNA was aliquoted and quantified using nanodrop instrument. From the quantified RNA, 1 µg of RNA from each sample was used for the first strand cDNA synthesis. For the cDNA synthesis, 10 µl of PCR reaction mix was prepared with 10X AMV buffer (1 μl), 10mM dNTPs (1 μl), 60 μM Random primer mix (1 μl), 10 U/μl AMV Reverse transcriptase (0.1 µl), 40U/µl RNase inhibitor (0.5 µl), RNA template (1 µg) and volume make up with nuclease free water. The reaction cycle of 42°C for 60 minutes and 85°C for 5 minutes was carried out for cDNA synthesis. Second round of PCR cycles for amplification of 170bp fragment were followed. For this, 10 µl PCR mix was prepared with 10X Standard Taq buffer (1 μl), 10 mM dNTPs (0.2 μl), 10 μM Forward and Reverse primers each (0.15 μl), cDNA (3 μ l), 1.25 U/ μ l Taq polymerase enzyme (0.25 μ l). The amplification condition was followed as initial denaturation step 94°C for 5 minutes, followed with 38 cycles of 94°C for 30 seconds, 60°C for 30 seconds and extension at 72°C for 10 seconds. The final extension was at 72°C for 3 minutes and 4°C on hold. The amplified product was run on 1.2% agarose gel electrophoresis with 100 bp ladder to analyse the 170 bp amplified fragment.

5.2.10 Focus Forming Assay

Vero cells were seeded in a 96-well micro titer plate at a density of 5 x 10⁴ cells per well to grow as a monolayer. After 14 -16 hours, cells were infected with serially diluted (10-fold) viral supernatant (10⁻¹ to 10⁻³) in duplicates. After 2-3 h of virus adsorption, cells were washed once with 1XPBS and incubated with 2% carboxy methyl cellulose (CMC) in DMEM (2% FBS) for 72 hours. The infected cells were washed gently with 1X PBS, fixed with 4%

paraformaldehyde for 20 minutes, and permeabilized with 0.25% Triton X-100. Cells were incubated with dengue virus anti-NS2BNS3pro antibody (1:1000) at 4°C overnight, washed three times for 10 minutes with 1X PBST, and incubated with secondary HRP-conjugated anti-rabbit antibody (1:1000) for 2 hours at room temperature. Finally, culture plates were washed with 1X PBST, and were visualized after exposure to H₂O₂-diaminobenzidine (DAB). The foci were visualized and counted under a light microscope and expressed as focus-forming units per milliliter. Two independent experiments were performed in duplicates.

5.2.11 Retrieval of host protein (EDRF1)

K562 cells were infected with viral supernatants in ratio (1:4) with MoI of 0.09 in the presence and absence of anti-protease molecules (T₄N, B₄N, F₄N, PA₄N, MOB₄N and HC₄N). The infected cells were incubated for 5 days. Cells were harvested, and centrifuged at 6000 rpm for 5 minutes. Then the cells were washed with 1X PBS and centrifuged again at 6000 rpm for 5 minutes. The washed pellet was lysed using RIPA buffer and incubated for 30 minutes on ice. The solubilized cell lysate was centrifuged at 14000 rpm for 15 minutes and the clear whole cell lysate supernatant was collected in fresh 1.5 ml Eppendorf tube. The lysates were run on 10% SDS PAGE and proteins were transferred onto PVDF membrane. The membrane was stained by Ponceau S stain to check the protein transfer. Then the membrane was treated with anti-EDRF1 antibody (1:3000) overnight, followed by washing with 1X PBST and further incubating with anti-rabbit IgG-HRP conjugated secondary antibody (1:10000) for 2 hours at room temperature. The membrane washed with 1X PBST, 3 times for 10 minutes each and developed using western blot HRP substrate.

5.2.12 Retrieval of cell number by the drug molecules

K562 cells were cultured in 2-4 T-25 flasks. 5 x 10⁵ cells per well were seeded in two 6-well plates. Infection was given in ratio of (1:4) virus supernatant and medium. After 2-3 hours of

virus adsorption, the media was replaced with fresh complete RPMI media (with 4% FBS) containing the drug molecules and incubated cells for 3, 5, and 7 days. The cells were counted using haemocytometer after 3, 5 and 7 day of infection. The total cell number counted was plotted against day wise (control, infected and drug treated) using Microsoft Excel software. The viral supernatants were collected on the 3rd day and quantified using focus forming assay and were also analysed by RT-PCR using 5'UTR primers.

5.3 RESULTS

5.3.1 Synthesis of compounds

The NDGA derivatives used in the present study were synthesized and characterized in the laboratory of Dr. Y.S. Ravi Kumar, Institute of Biotechnology, Ramaiah College of Higher education, Bangalore, India. The synthesized compounds T₄N, B₄N, F₄N, PA₄N, MOB₄N, HC₄N and GA were obtained in pure form. The compounds were dissolved in DMSO as 10mM stocks and stored at room temperature. 10mM stocks were further diluted using DMSO to 1mM and used as per the experiments. DMSO vehicle control was used at less than 1%.

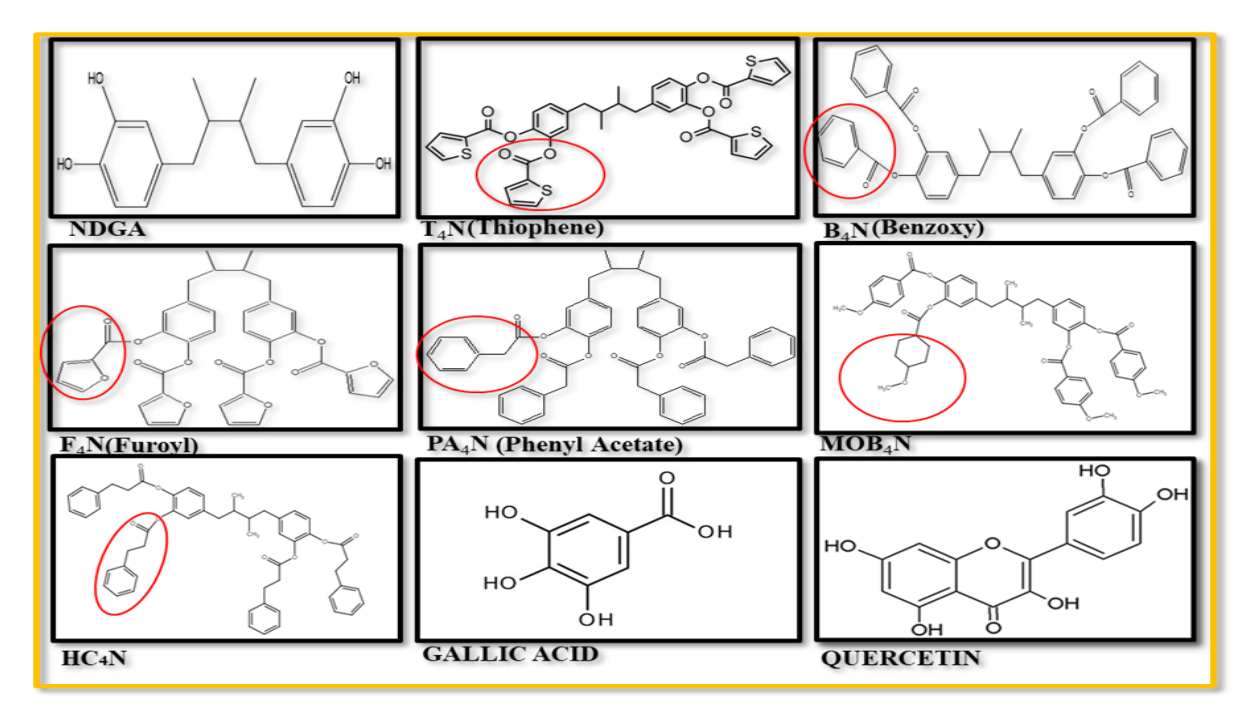


Figure 5.3.1 Structures of NDGA and its derivatives. Compounds showing the hydroxyl

groups of NDGA replaced by Thiophene (T₄N), Benzoxy (B₄N), Furoyl (F₄N), Phenyl Acetate (PA₄N), MOB₄N and HC₄N. GA (negative control) and Quercetin (positive control) structures are also shown.

5.3.2 Recombinant NS2BNS3pro purification

The NS2BNS3protease was expressed in *E. coli* BL21 bacterial cells and purified using Ni-NTA His-tag column chromatography. Expression was observed at all the concentrations (0.5-1mM) of IPTG. However, 0.6mM IPTG was used for the efficient expression and purification. Protein fraction were eluted in 250mM imidazole conc. and purified protein was observed in elutions (E1-E4) (Figure 5.3.2).

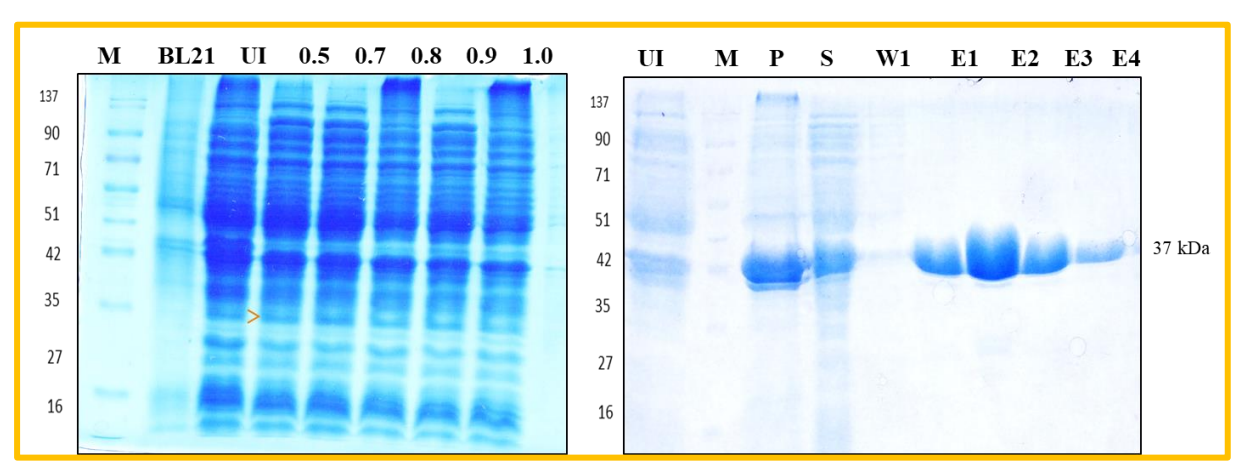


Figure 5.3.2: Expression and purification of pRSET-A NS2BNS3pro, a 37 kDa protein at 18°C with 0.6mM IPTG induction and purification by Ni-NTA affinity chromatography.

5.3.3 Cytotoxicity of compounds

As Vero cells are permissive for dengue virus propagation, we determined the cytotoxic concentrations of the above compounds in these cells. MTT (3-(4, 5-dimethylthiazol-2-yl)-2, 5-diphenyltetrazolium bromide) method was used to analyse the cytotoxic effects. Since the Quercetin is reported as anti-protease molecule [194, 195], we have used the same as positive control. The percentage viability was calculated for each compound and CC₅₀ values for T₄N (381 μ M), B₄N (2.2 mM), F₄N (3.9 mM), PA₄N (4.4 mM), MOB₄N (527 μ M), HC₄N (1.4 mM) and GA (4 mM), and Quercetin (CC₅₀=257 μ M). Comparatively less cytotoxic effects were

observed for the NDGA derivatives i.e. $381 \,\mu\text{M}$ to 1 millimolar concentration even after 72 hours of incubation. The graphs were plotted with the GraphPad prism software using non-linear regression dose-response parameters (Figure 5.3.3).

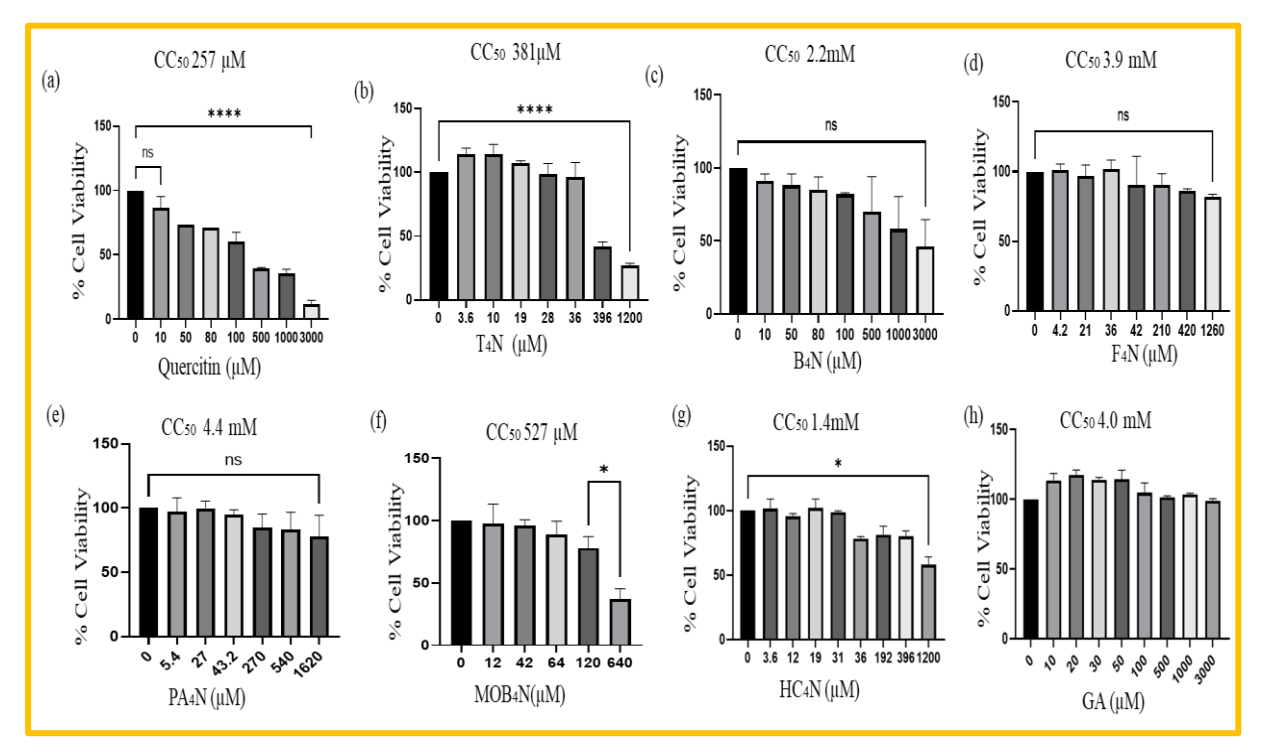


Figure 5.3.3: Bar graphs representing the cytotoxicity of compounds determined by MTT assay. % Cell viability vs increasing conc of inhibitors was determined for each compound to determine the CC_{50} values.

5.3.4 Protease activity assay

Using the synthetic fluorogenic peptide substrate (Bz-Nle-KRR-AMC), we have performed *in vitro* protease assay to analyze the functional activity of the purified protein. Enzymatic activity reaction was performed in absence (control) or presence of NS2BNS3pro purified protein. An increase in fluorescence accompanies peptide substrate cleavage, thus confirming the protease as catalytically active (Figure 5.3.4). The Km and Vmax of protease were found to be increasing (12.0 μ M and 2343 μ M/sec respectively) as compared to control (no enzyme) reaction (4.5 μ M and 839 μ M/sec) thus showing the catalytic activity of protease.

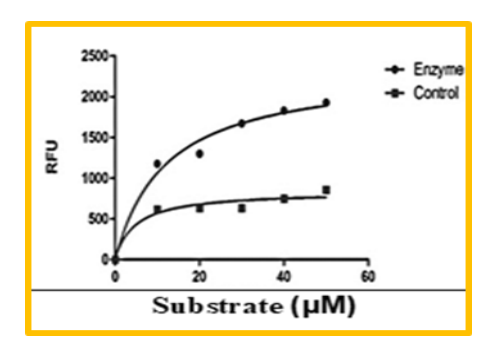


Figure 5.3.4: Represents enzymatic activity reaction in absence (control) or presence of NS2BNS3pro purified protein.

5.3.5 Inhibition activity of compounds

With the functionally active protease, we proceeded to determine the inhibitory activity of the compounds. Based on the literature studies, plant derived synthetic derivatives of NDGA (T₄N, B₄N, F₄N, PA₄N, MOB₄N and HC₄N) were used. Quercetin and GA were included as positive and negative controls. Initially, the compounds were screened for cytotoxicity. As no cytotoxicity was observed for the above selected compounds, we proceeded with the protease inhibition assay *in vitro*.

The inhibition activity of each compound was determined by the decrease in fluorescence, indicating no cleavage of the fluorogenic peptide substrate in presence of the protease inhibitor. IC₅₀ values were determined by GraphPad prism 9 using non-linear regression curve with doseresponse inhibition. Compounds showed 50% of inhibition with the IC₅₀ values T₄N (5.1 μ M), B₄N (36.30 μ M), F₄N (5.1 μ M), PA₄N (1.7 μ M), MOB₄N (2.1 μ M), HC₄N (3.6 μ M) and Quercetin (13.73 μ M). GA did not show any inhibition (Figure 5.3.5). The reactions were performed in duplicates in two sets of independent experiments.

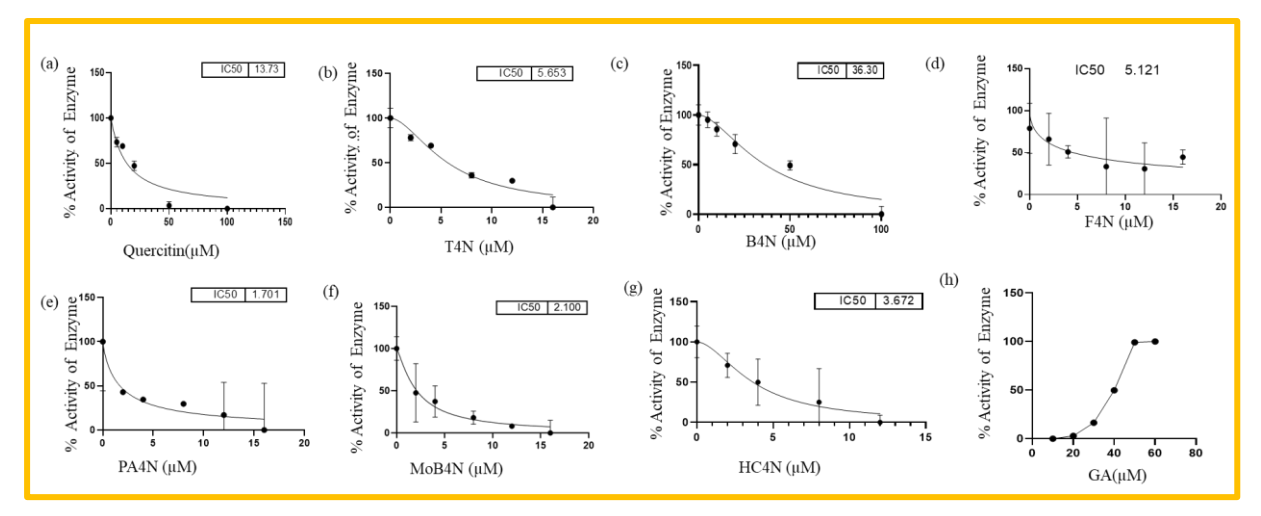


Figure 5.3.5: *In vitro* screening of anti-protease molecules and determining the IC₅₀ values of each compound. % of protease activity was determined as the function of inhibitor concentration i.e. IC₅₀ value.

5.3.6 Selectivity Index (SI) of compounds

A drug with higher SI value indicates its high effectivity, safety and efficacy during *in vivo* treatment. The ideal drug would be with high cytotoxic concentrations and low inhibitory concentrations. The SI values of Quercetin (19), NDGA (125), T₄N (68), B₄N (61), F₄N (764), PA₄N (2588), MOB₄N (250) and HC₄N (38) (Table 5.3.1). As we found the high selectivity index for the compounds which suggest their effectiveness and hence, we extended our study to analyze the anti-protease activity during virus infection in cell cultures.

COMPOUNDS	CC50 (µM)	IC50 (μM)	SI= CC50/IC50
QUERCETIN	257	13	19
NDGA	313	2.5	125
T_4N	381	5.6	68
B_4N	2200	36	61
F_4N	3900	5.1	764
PA ₄ N	4400	1.7	2588
MOB4N	527	2.1	250
HC4N	1400	3.6	38
GA	4000	-	-

Table 5.3.1: Representing the selectivity index of compounds. SELECTIVITY INDEX OF COMPOUNDS = CC_{50}/IC_{50} that shows the efficacy and potency of a drug.

5.3.7 Quercetin inhibits the protease localization

In order to analyse the inhibitory effect of Quercetin against dengue virus protease localization, we have overexpressed the protease in K562 cells in the presence of this drug. As in earlier chapter 3, we have highlighted that dengue virus protease localizes to nucleus in both transfected and infected conditions in K562 cells. To understand this, the overexpressed NS2BNS3pro in K562 cells and treated with Quercetin were analysed with fluorescence microscopy at 20X. We observed that, in the protease transfected cells, it is clearly visible that protease entered in nucleus (as observed in merged image indicated with yellow arrows). But, in Quercetin treated protease transfected cells did not show any localization and were similar to vector transfected cells (as observed in merged image indicated with white arrows). Thus, this data suggests the inhibition of protease localization in presence of Quercetin (Figure 5.3.6).

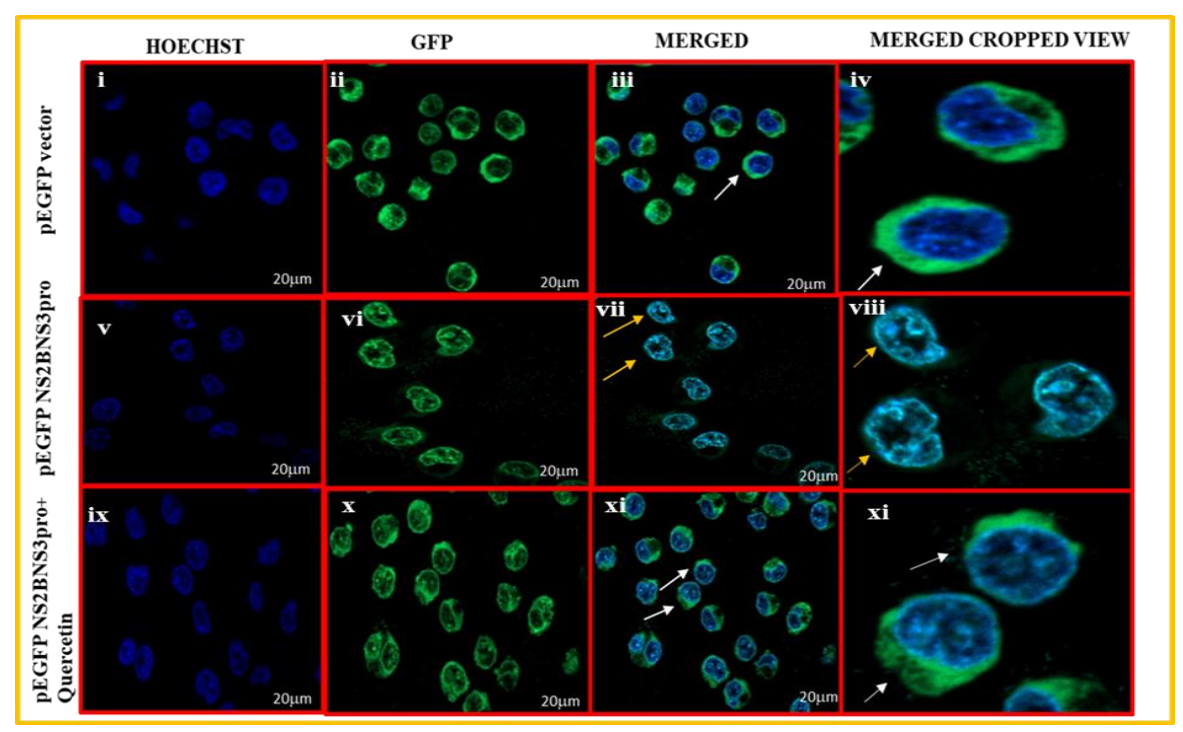
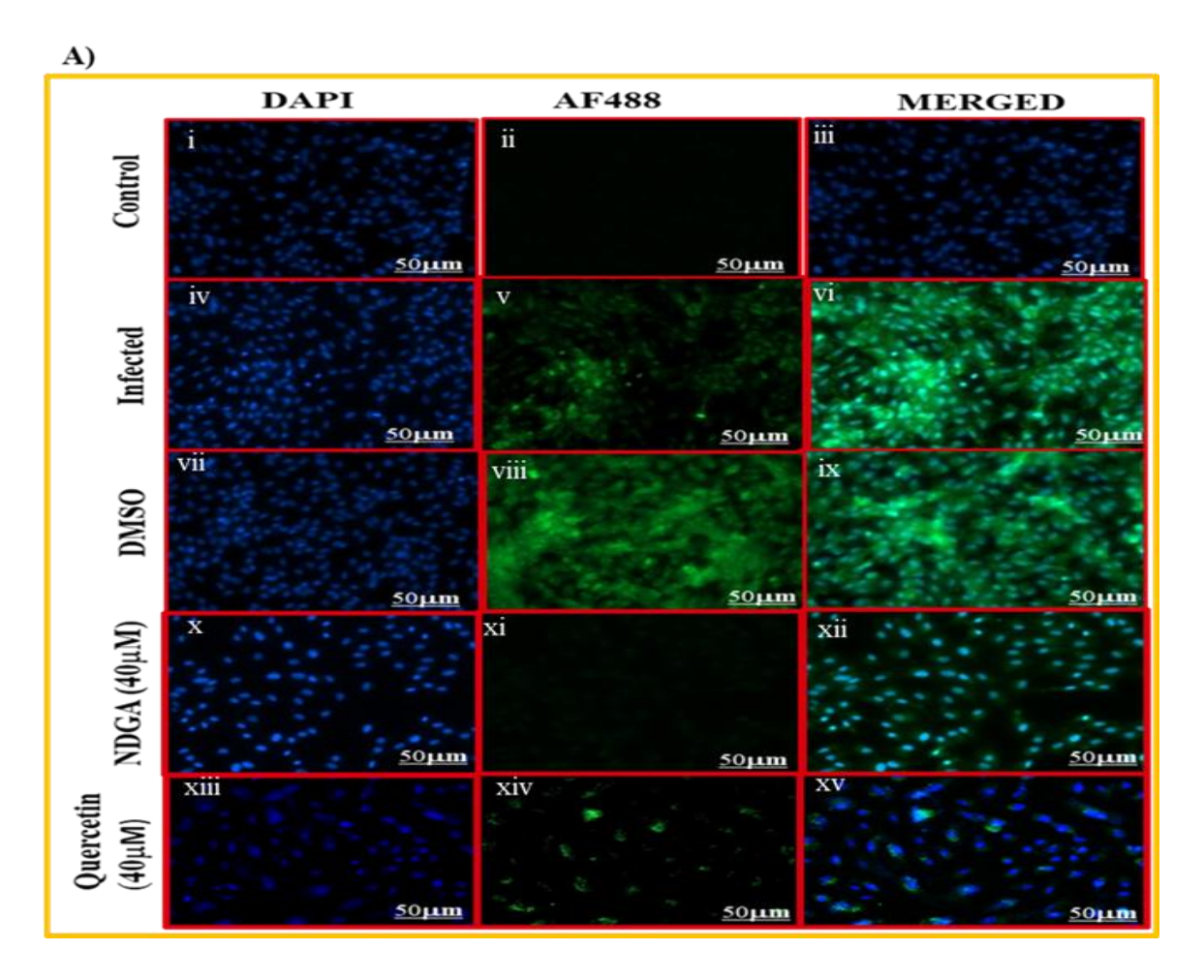


Figure 5.3.6: Localization inhibitory effect of anti-protease molecule (Quercetin) in NS2BNS3pro (46+185 a.a) expressed condition.

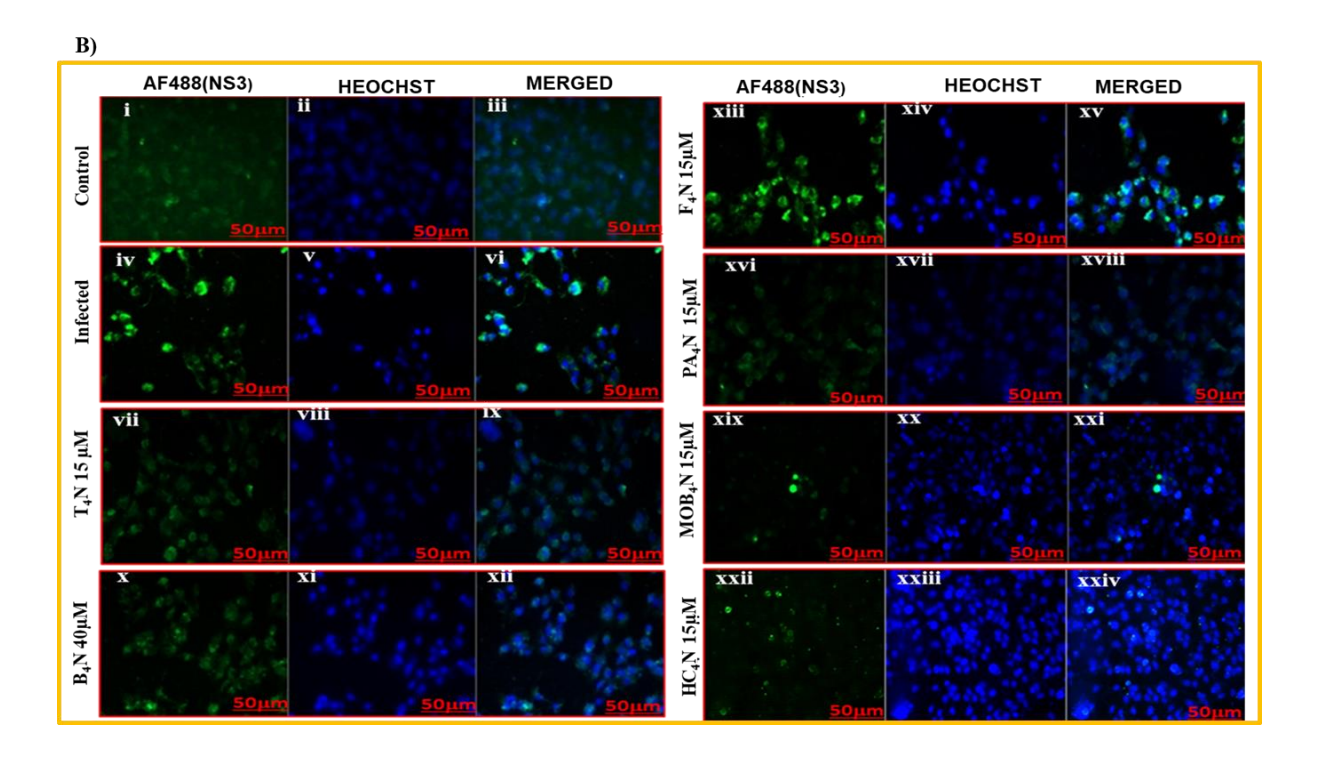
5.3.8 Evaluation of compounds for inhibition of dengue virus infection using indirect immunofluorescence assay (IFA)

We extended our study to understand the inhibition activity of above compounds by analyzing the infection inhibition in presence of the anti-protease molecules using immunofluorescence assay (IFA). For this purpose, we have first analyzed the infection inhibition (post treatment) with the NDGA and Quercetin which are known potent inhibitors but were not used because of their cytotoxicity. It was observed that both the compounds inhibited the infection significantly as observed by the reduced levels of green fluoresence and merged images (Figure 5.3.7 A (x-xii) and (xiii-xv)) compared to the infected and DMSO infected cells (Figure 5.3.7 A (iv-vi) and (vii-ix)).



Based on this observation, we have analysed the infection inhibition following the same experiment for the NDGA derivatives of the study. It was observed that T₄N, MOB₄N, PA₄N and B₄N showed inhibition as the green flourescence was reduced in drug treated cells as compared to the infected cells (Figure 5.3.7 B). Also, we observed that F₄N and HC₄N that

showed inhibition during the *in vitro* experiment did not show inhibition during infection. The above data is analysed by GraphPad prism 9 software and represented as bar diagrams (Figure 5.3.7 C).



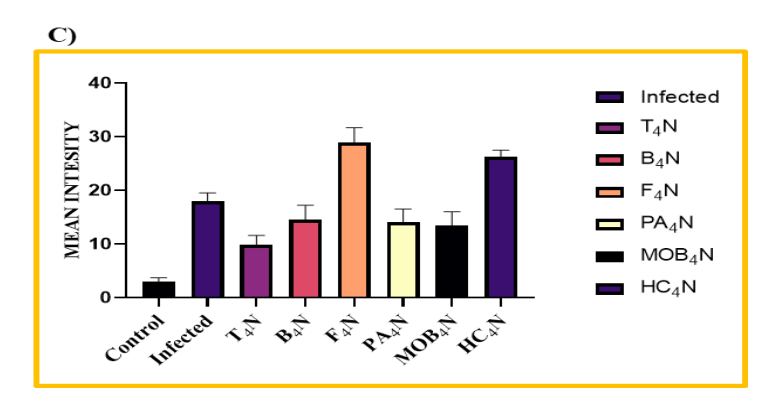
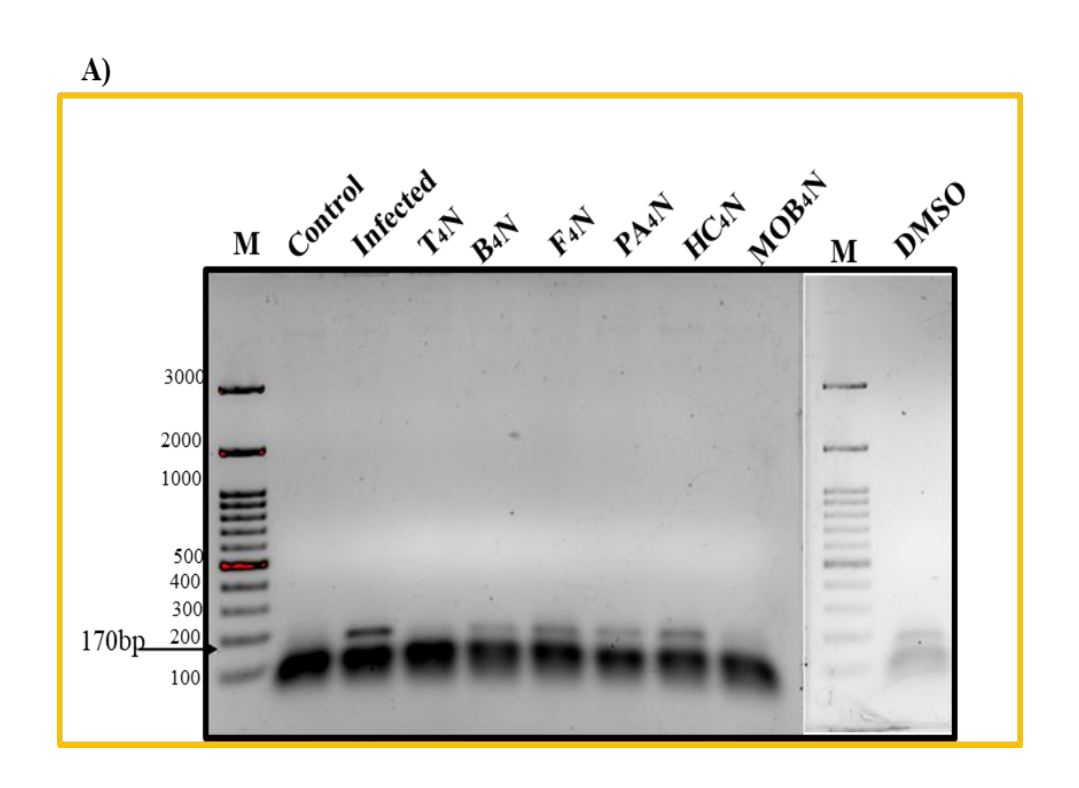
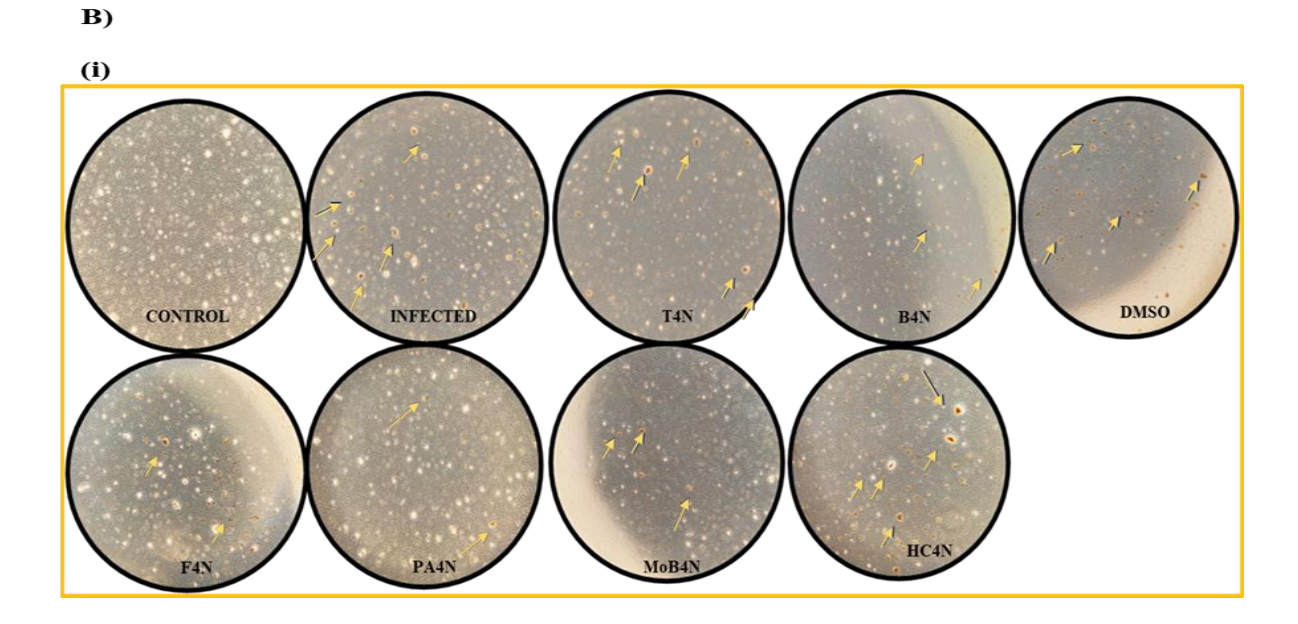


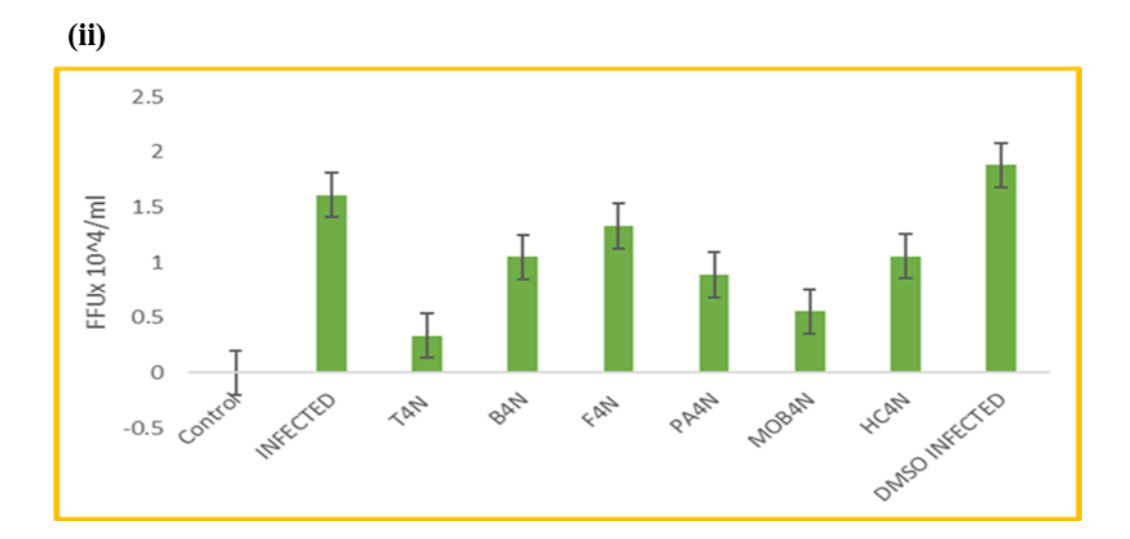
Figure 5.3.7: Effect of NDGA derivatives on dengue virus infection. (**A**) Immunofluorescence images showing the viral infection in presence and absence of NDGA (**x-xii**) and Quercetin (**xiii—iv**). (**B**) Immunofluorescence images showing the virus infected cells (**iv-vi**) and drug treated cells with T₄N, B₄N, F₄N, PA₄N, MOB₄N, HC₄N (**vii-xxiv**). (**C**) The graphical representation of the % mean intensity of total fluorescence of in presence and absence of inhibitors.

With the viral supernatants of the above IFA experiment, we performed the semi-quantitative RT-PCR with 5'UTR primers (170 bp), and the presence of amplified product confirms the infection. It was observed that T₄N, MOB₄N, and PA₄N showed no or less amplification. An

amplified band (170 bp) in infected and DMSO samples was observed. In case of F₄N, B₄N and HC₄N viral supernatants also show no inhibition as the amplified bands were observed (Figure 5.3.8 A). With the same viral supernatants, we have performed the focus forming assay and the viral titers were found to be high in Infected (16.1x10⁴), DMSO+Infected (18.8x10⁴), F₄N (13.3x10⁴), HC₄N (10.3x10⁴) as compared to the T₄N (3.3x10⁴), PA₄N (8.0x10⁴) and MoB₄N (5.5x10⁴). The presence of amplified product and high viral titers shows that F₄N and HC₄N did not show any inhibition while T₄N, PA₄N and MOB₄N showed significant inhibition. B4N showed ~50% inhibition as compared to other drugs (Figure 5.3.8 B and C).







C)					
Sample	Viral titres (FFU/ml) x10^4				
Control	N/D				
Infected	16.1				
T_4N	3.3				
B ₄ N	10.4				
F ₄ N	13.3				
PA ₄ N	8.0				
MOB ₄ N	5.5				
HC ₄ N	10.550				
DMSO Infected	18.8				

Figure 5.3.8: Effect of anti-protease molecules on dengue virus infection. **(A)** RT-PCR analysis of the viral supernatants from the IFA experiment. The presence of band with 170bp of 5'UTR indicates infection. **(B)** (i) Images of foci (yellow arrows) observed from the viral supernatants at the dilution (10⁻²) in the focus forming assay. **(ii)** Bar graph showing viral titres

(FFU/ml) in infected and uninfected cells in presence and absence of inhibitors. (C) Table representing the viral titres as indicated in the Focus forming assay.

5.3.9 Retrieval of Host protein (EDRF1) in presence of anti-protease molecules

As we observed in the previous chapter that the viral protease cleaves the host protein EDRF1 during virus infection [148], we extended our study to analyse the levels of EDRF1 during infection and in the presence of anti-protease molecules. The result suggested that the EDRF1 levels were retrieved in presence of T₄N and PA₄N as compared to the B₄N and F₄N (Figure 5.3.9 A). In the presence of the above observations, NS5 the dengue virus replicase was also not detected in presence of the inhibitors (Figure 5.3.9). Although the MOB₄N also showed inhibition in *in vitro*, virus cell culture inhibition and focus forming assays, this molecule did not used in this experiment.

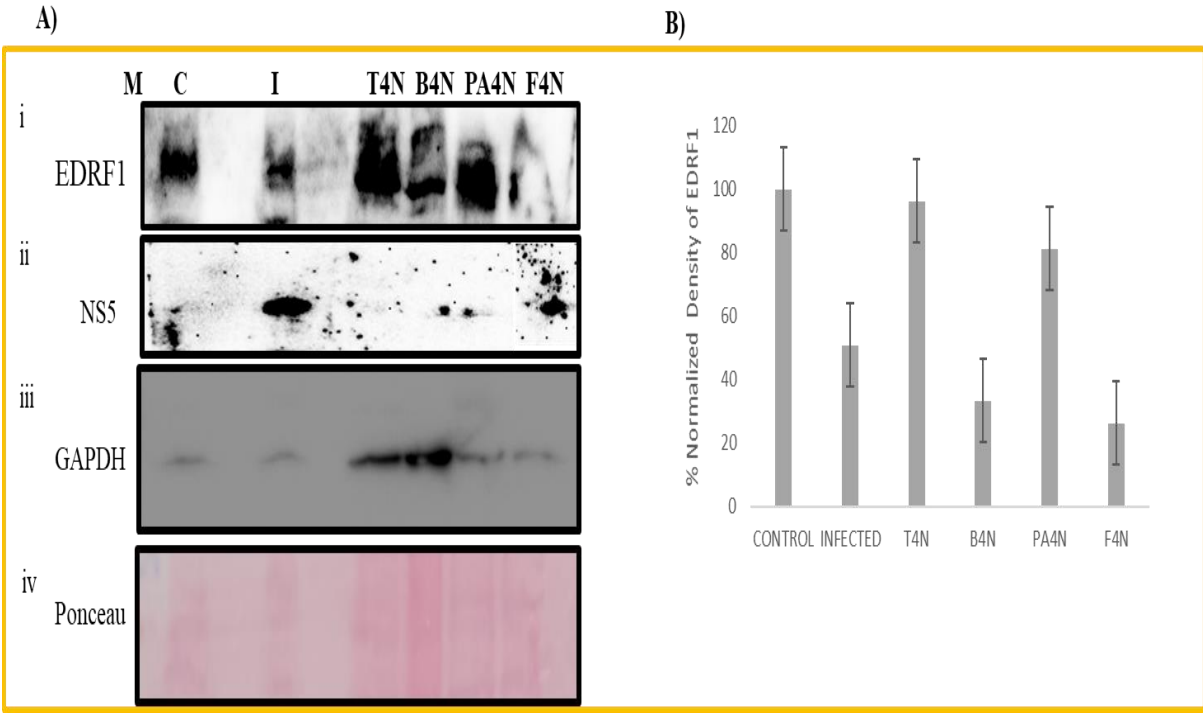
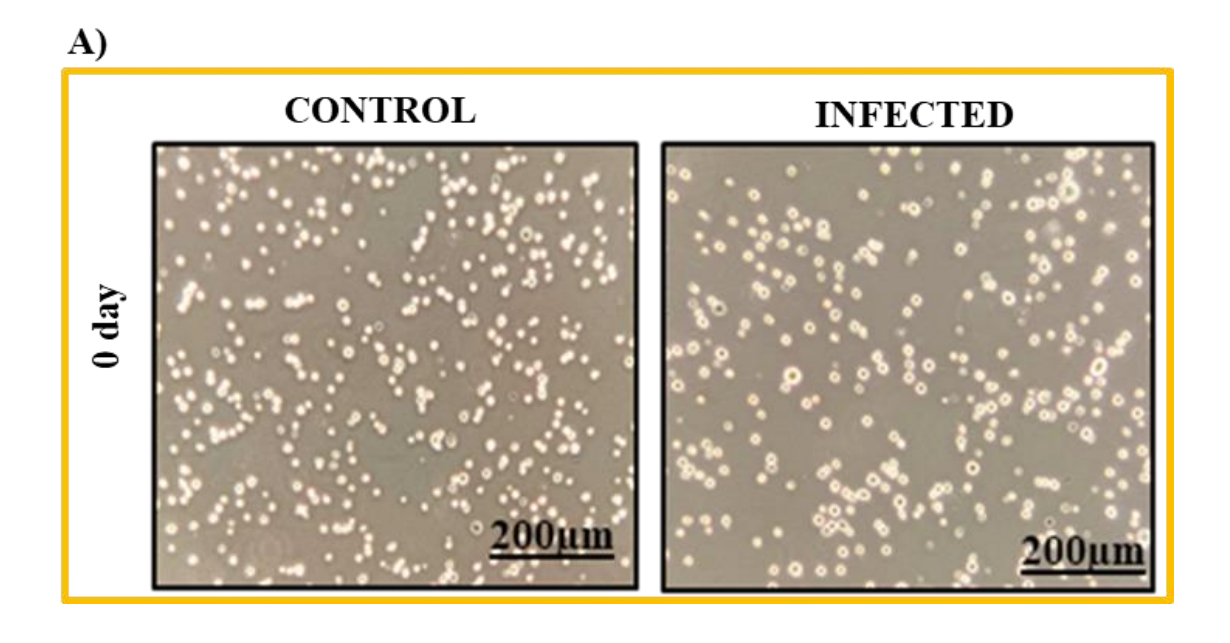


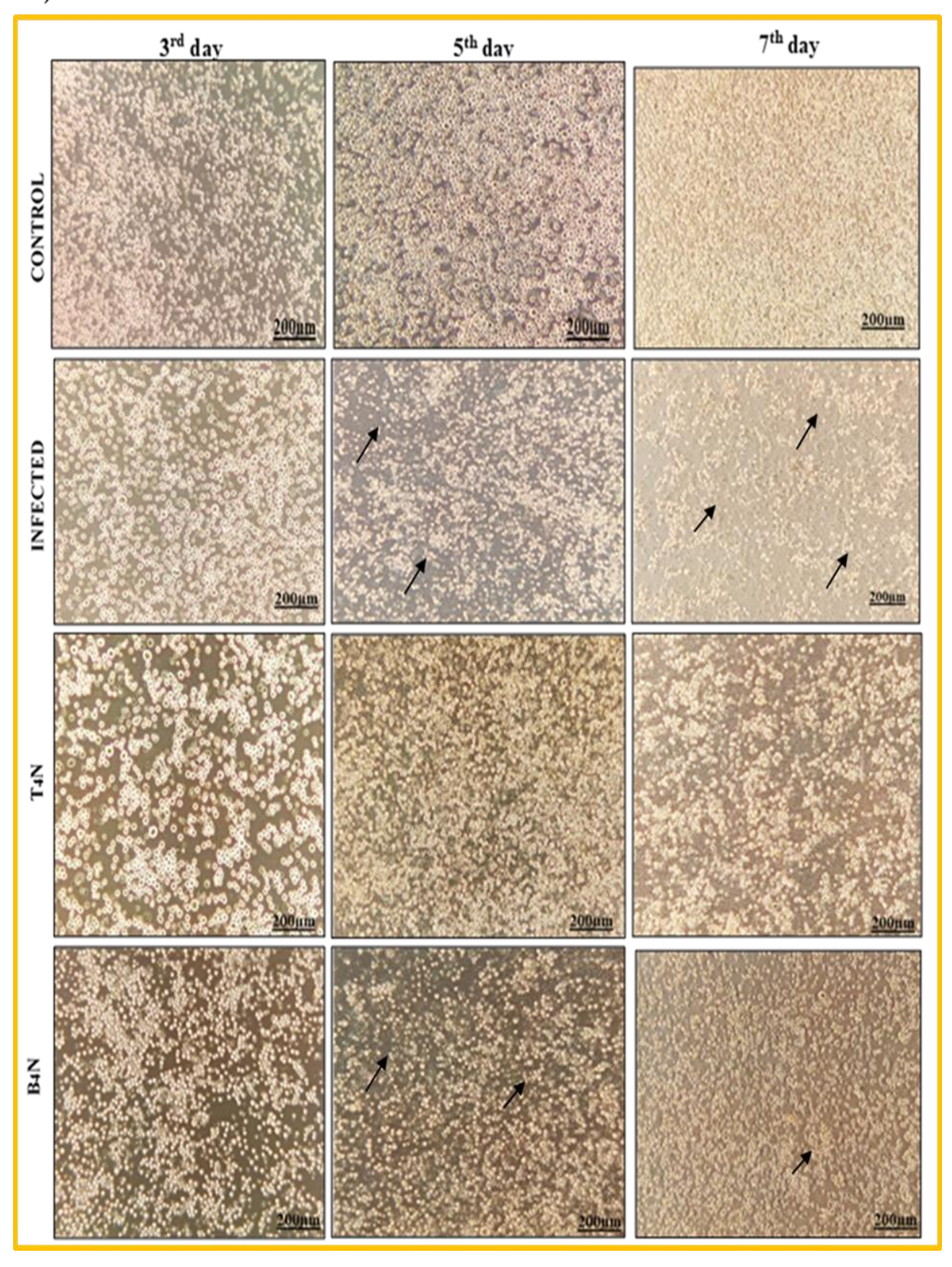
Figure 5.3.9: Retrieval of EDRF1 by NDGA derivatives. **(A) (i)** Western blot showing the expression of EDRF1 in presence and absence of protease inhibitors during virus infection. **(ii)** Blot showing NS5 expression in infected cells and no expression in presence of inhibitors. **(iii) & iv)** blots showing the internal control GAPDH and ponceau stain. **(B)** The bar graph shows the % normalized density of EDRF1 levels in presence and absence of inhibitors.

5.3.10 Retrieval of cell numbers by the protease inhibitors

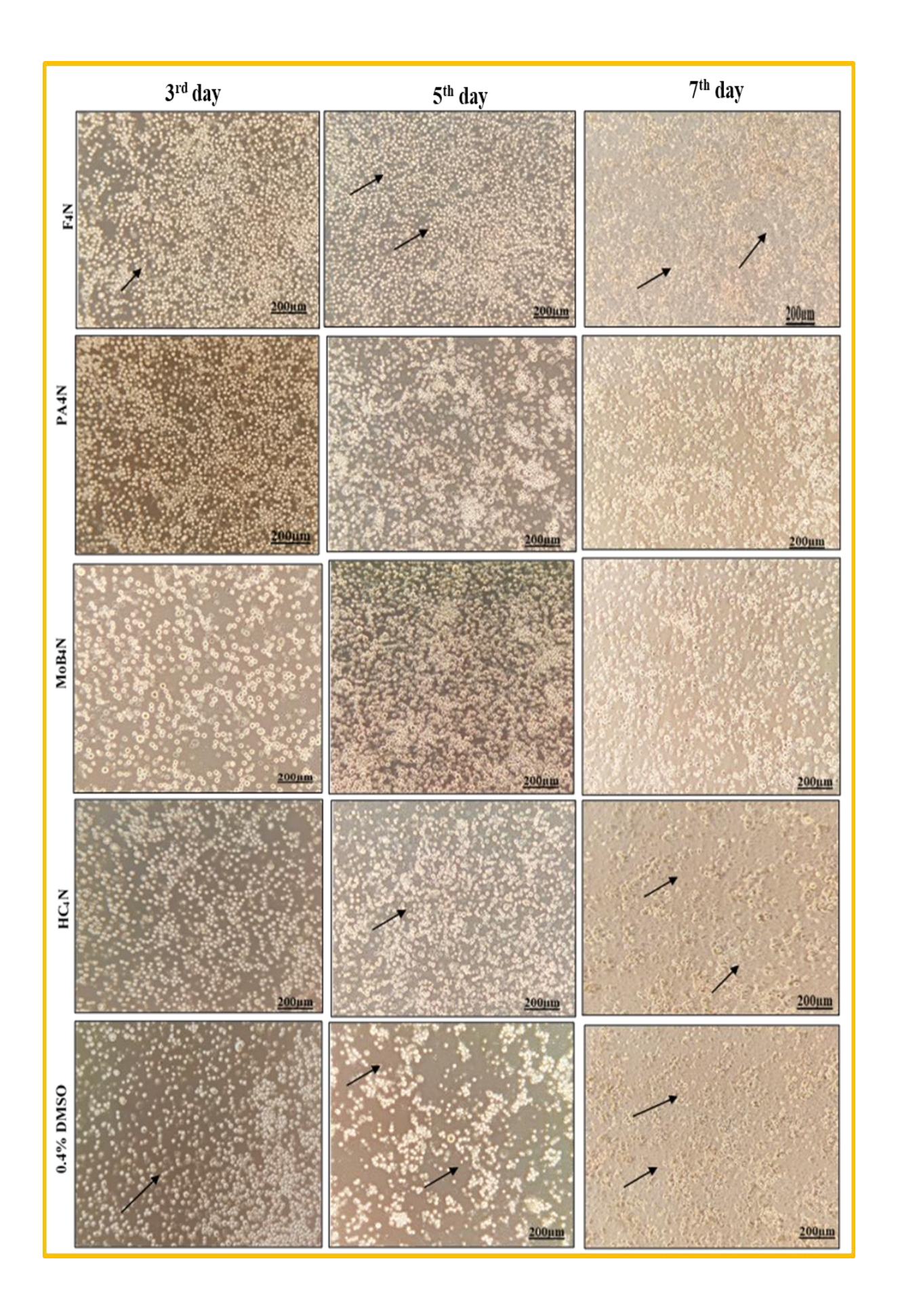
We observed that the viral protease cleaves the host protein EDRF1 and causes mitochondrial dysfunction during virus infection in earlier chapters. This was led to the reduced cell number as observed number in chapter 4 [148]. In this connection, we have carried the cell number assay in presence and absence of the NDGA derivatives. To validate these drug molecules, we performed cell counting number assay after 3, 5, and 7 days of infection in K562 cells in presence and absence of the anti-protease molecules. It was observed that after 3rd day of the infection, the cell number started decreasing, cells appeared tiny and small in morphology up till 7th day in dengue infected and DMSO infected cells. But the cell numbers and morphology were retrieved in presence of T₄N, MOB₄N and PA₄N, showing the inhibition of infection. No cell numbers were retrieved in presence of F₄N and HC₄N (Figure 5.3.10 A, B and C).



B)



Continued...



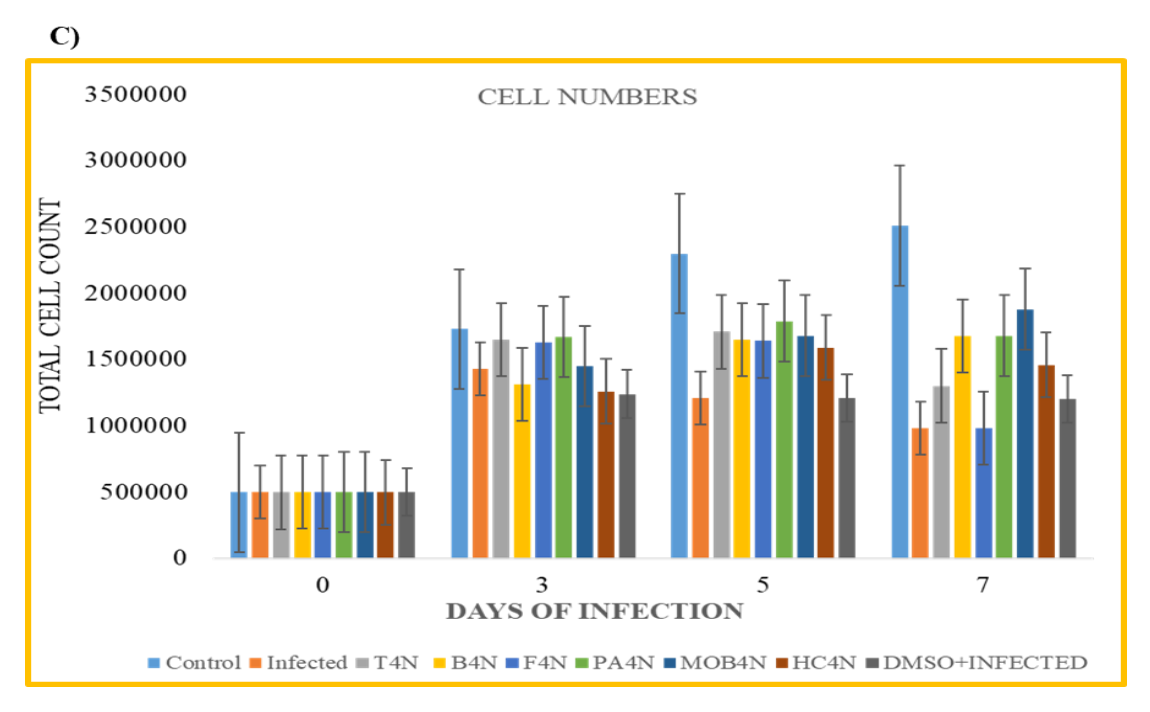


Figure 5.3.10: (**A&B**) Represent the total cell count after 3, 5 and 7 days of infection in K562 infected and drug treated cells. Black arrows show the morphological changes during the infection (**C**) Represents the bar graph of retrival of cell numbers in infected and drug treated cells after 3, 5 and 7 days of infection.

Further, we have performed the semi-quantitative RT-PCR of the above experiment, after collecting with viral supernatants of the infected and drug treated K562 cells on 3rd day. With the RT-PCR analysis we observed the amplified product in infected, F₄N, HC₄N, and DMSO infected samples. However, no band amplification was observed in T₄N and faint bands appeared in B₄N, MOB₄N and PA₄N. The results confirm the infection inhibition and retrieval of the cell numbers. Further, the same viral supernatants were also quantified using focus forming assay that showed consistent results with high viral titres in infected, F₄N, HC₄N, DMSO, B₄N while the titres were reduced in the presence T₄N, MOB₄N, PA₄N (Figure 5.3.11 A and B).

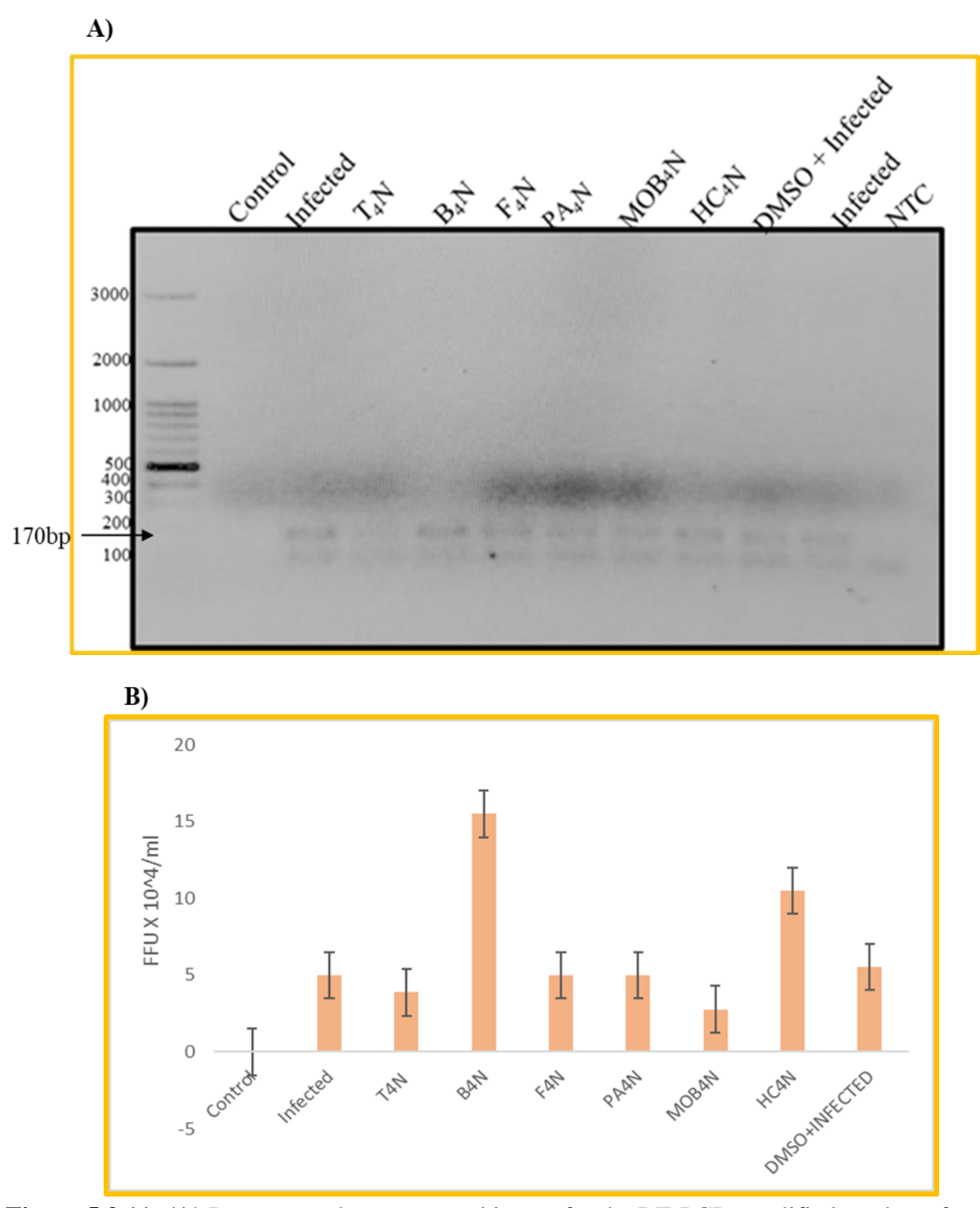


Figure 5.3.11: (**A**) Represents the agarose gel image for the RT-PCR amplified products from the supernatants of virus infected and drug treated. (**B**) Bar graph showing the viral titres in the infected and drug treated samples of the above K562 cells after 3rd day of infection.

5.4 DISCUSSION

The dengue outbreaks are occurring continuously and the lack of specific anti-viral or vaccines urges researchers to develop anti-viral molecules for controlling the disease. Failure to reach up to clinical trials and commercializing has been a major concern. Cytotoxicity and the effect of the drug on healthy cells is also the prime concern during drug discovery. In the pace of developing the anti-viral and as per the literature studies, protease is the most engrossing target for drug development. Anti-protease molecules target the protease by either inactivating the catalytic triad or interfering with the NS2BNS3 interactions. As stated above, both natural and synthetic compounds have been used for the inhibition of protease activity in vitro, ex-vivo and in vivo models. Nordihydroguaiaretic acid (NDGA), a plant derived compound has been reported for its high cytotoxic effects while being a potential anti-viral and anti-cancer compound [194]. Thus, in the present study, to avoid cytotoxic effects, we have used a few compounds which are synthetic derivatives of NDGA (T₄N, B₄N, PA₄N, F₄N, MOB₄N and HC₄N), that exhibited less or no toxicity on mammalian cells up to millimolar concentrations (Figure 5.3.5). We have evaluated the inhibitory potential of these compounds against dengue protease in vitro by fluorometric enzyme assay. NDGA derivatives and Quercetin (positive control) showed good anti-dengue protease activity with low concentrations i.e. up to micromolar levels (Figure 5.3.6). The compounds with Selectivity Index (SI) values above 10 were considered as good inhibitors in many studies [203-205]. The selectivity of these compounds against protease activity was quite high with good SI values >60 (except HC₄N) (Table 5.3.1). Among the compounds, T₄N, PA₄N and MOB₄N, showed significant SI values i.e. more than >60, thus indicating these molecules to be safe and effective for further studies. Quercetin being considered as positive control in this study, we have also analysed the protease localization inhibition activity of this compound. We observed the inhibition of dengue virus protease localization into the nucleus in the presence of Quercetin (Figure 5.3.6), hence we considered this compound as a suitable positive control. Further, we have analyzed the dengue virus infection inhibition activity of NDGA and Quercetin. NDGA and Quercetin were found to inhibit the virus infection given to the vero cells (Figure 5.3.7 A). Under the same conditions, we have analysed the anti-protease activity with NDGA derivatives by treating dengue virus infected cells. We observed that T₄N, PA₄N, MOB₄N showed dengue virus infection inhibition effectively as compared to B₄N, F₄N and HC₄N (Figure 5.3.7 B) Also, we observed that, although F₄N and HC₄N (with less SI value) showed negligible cytotoxicity and significant anti-protease activity in *in vitro* studies, both the compounds did not show inhibition during infection when analysed by IFA and RT-PCR (Figure 5.3.7 and 5.3.8). As observed in chapter 3, dengue virus protease cleaves EDRF1 protein, thus we extended our study to analyse the retrieval of EDRF1 in the presence of these anti-protease molecules. The results were consistent with the above analysis as we observed that EDRF1 is being retrieved in the presence of T₄N, PA₄N, and B₄N (Figure 5.3.9). As the cell number was reduced under the dengue virus infection at 3, 5 and 7 days (chapter 4), we observed that the cell numbers were retrieved in the presence of T₄N, PA₄N and MO₄BN (Figure 5.3.10). High titres of virus multiplication were observed in the infected cells compared to the drug treated cells in focus forming assay (Figure 5.3.11 B).

Thus, we conclude that the NDGA derivatives T₄N, PA₄N, MOB₄N and B₄N can be considered as potent inhibitors of dengue virus protease. Further validation of these anti-protease molecules can be done by *in vivo* models.

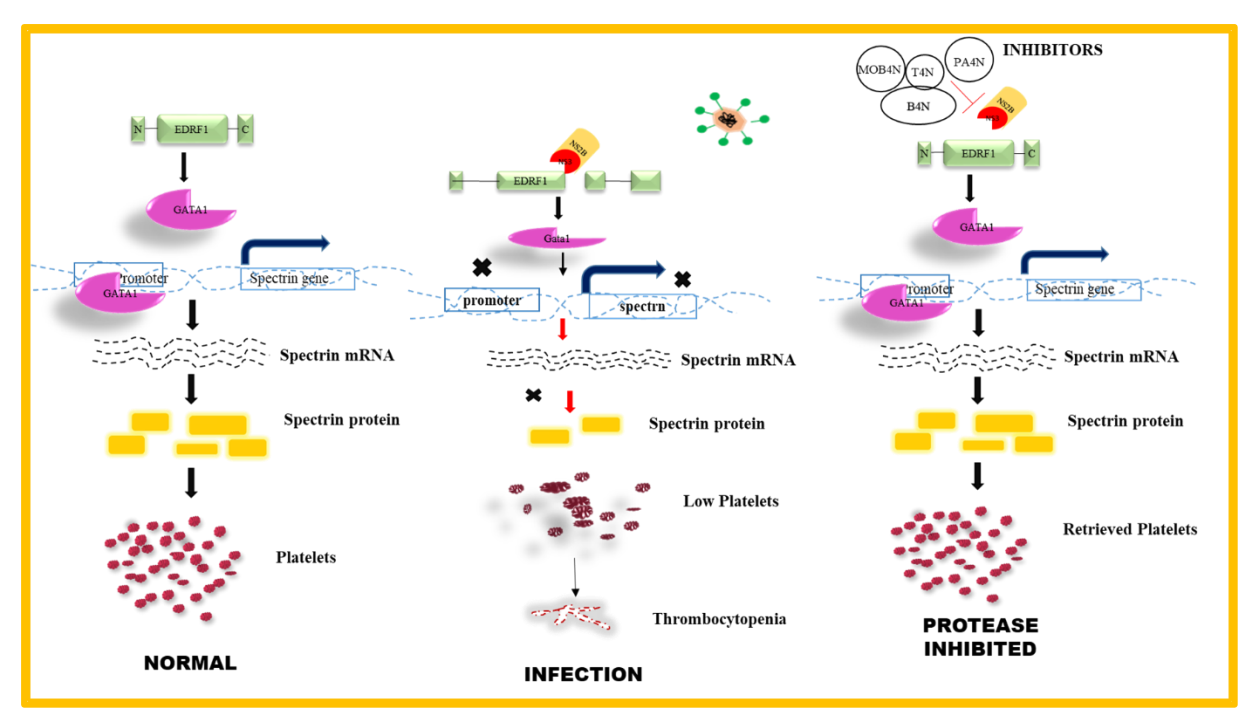


Figure 5.4: Representative model showing the action of protease inhibitors on the dengue virus infection and hence on 'thrombocytopenia.'

CONCLUSIONS OF THE STUDY

Dengue is on the top of the virus infections causing morbidity and mortality. As we all know, dengue has expanded worldwide rapidly thus there is an urgency to find solutions for controlling the disease. Till now there is no particular medication provided to the infected individuals. Researchers are working continuously to develop and bring some solutions to control the dengue virus spread. Despite many efforts, researchers are facing challenges due to the serotype differences. With literature studies, we have analyzed that there were many questions left unanswered in understanding the mechanism of dengue virus infection. Thus, in context to the literature studies, we attempted to answer a few questions by framing certain objectives. The following are the key conclusions drawn from the experimental data of the study.

Chapter 2:

- ▶ In this chapter, we have found that dengue virus protease exists in two forms i.e. NS3 and NS2BNS3 during natural infections. With the *in silico* study, we found that NLS and MTS signal sequences are present in both NS2BNS3 and NS3 but the MTS signal in NS2BNS3 form is masked by NS2B at the N-terminal region of NS3. NS2BNS3 possess two types of nuclear localization signals: one monopartite NLS in NS2B and two bi-partite NLS sequence in the N-terminal region of NS3 helicase.
- ► The localization and subcellular fractionation studies suggested that NS2BNS3 (92kDa) localizes to the nucleus only whereas NS3 (75kDa) localizes to both mitochondria and nucleus.

Chapter 3:

▶ With the *in vitro* protein interaction studies, followed by MALDI TOFF mass spectrometry analysis we have identified EDRF1, a nuclear transcription factor as NS2BNS3 interacting

protein. The interaction was further confirmed by western blotting using anti-EDRF1 antibodies.

- ► *In vitro, ex vivo*, virus culture and *in vivo* (clinical samples) experimental analyses suggest that EDRF1 is a novel substrate of dengue virus protease.
- ▶ As the EDRF1 regulates the GATA1 expression which in turn regulate the expression of spectrins, GATA1 and spectrins were also found to be reduced in *ex vivo* and virus cultures experiments.

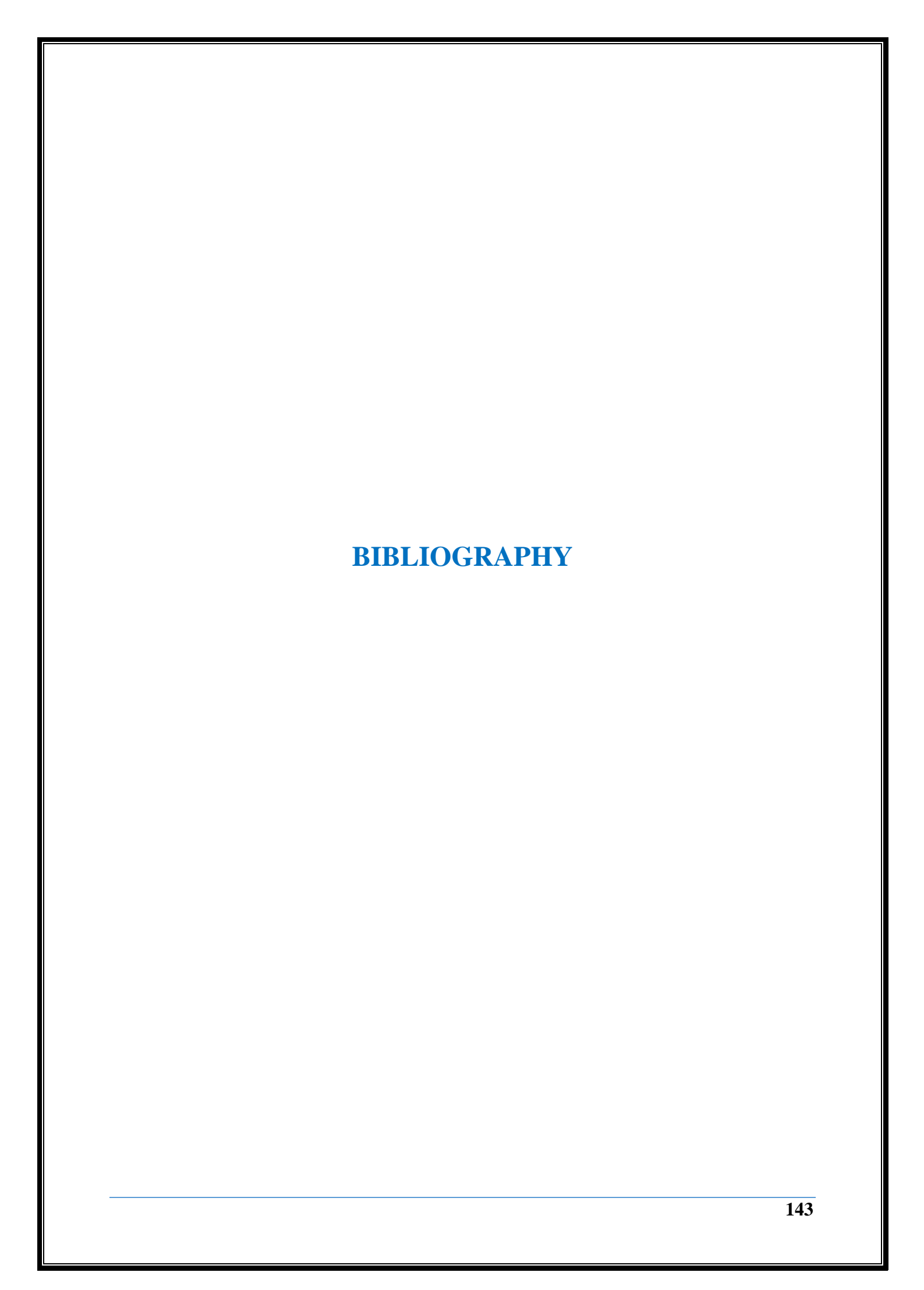
Chapter 4:

- ► Mitochondrial functions like Basal respiration, ATP production coupled respiration, maximal respiration, spare respiratory capacity and non-mitochondrial oxygen consumption were found to be reduced in NS3 transfected cells.
- ► We observed the altered cell morphology, reduced number and size during virus infection in K562 cells (megakaryocytic lineage) from 3, 5, and 7 days.

Chapter 5:

- ► We identified the NDGA synthetic derivatives as the anti-protease molecules. *In vitro* protease assay data show that T₄N, B₄N, PA₄N, F₄N, MOB₄N and HC₄N showed inhibition activity and these molecules did not show any cytotoxicity up to millimolar concentrations.
- ► Immunofluorescence assay data and semi-quantitative RT-PCR show that the dengue virus infections were inhibited significantly in the presence of T₄N, PA₄N, MOB₄N and B₄N.
- ► These lead molecules (T₄N, B₄N, PA₄N, F₄N, HC₄N and MOB₄N) were found to retrieve the infected K562 cell number during 3,5 and 7 days of infection.
- ► The above NDGA derivatives were found to be retrieved the levels of EDRF1which is a substrate of NS2BNS3.

protease molecule with least cytotoxicity and more potency for in vivo studies.					



BIBLIOGRAPHY

- French RK, Holmes EC. An Ecosystems Perspective on Virus Evolution and Emergence.
 Trends Microbiol. 2020. 28(3): 165-175.
- 2. Mirahmadizadeh A, Yaghobi R, Soleimanian S. Viral ecosystem: An epidemiological hypothesis. *Rev Med Virol*. 2019. 29(4): e2053.
- 3. Pierson TC, Diamond MS. The continued threat of emerging flaviviruses. *Nat Microbiol*. 2020. 5(6): 796-812.
- 4. Markoff LJ, Falgout B. The family Flaviviridae and its diseases. In: Porterfield JS, ed. Exotic Viral Infections. London: Chapman and Hall, 1985: 48–66.
- 5. Solomon T, Mallewa M. Dengue and other emerging flaviviruses. *J Infect*. 2001. 42(2): 104-115.
- 6. Sudipta Kumar Roy and Soumen Bhattacharjee. Dengue virus: epidemiology, biology, and disease aetiology. *Canadian Journal of Microbiology*. 2021. 67(10): 687-702.
- 7. World Health Organization. Global strategy for dengue prevention and control. 2012. https://apps.who.int/iris/bitstream/handle/10665/75303/9789241504034_eng.pdf.
- 8. Zenga Z, Zhanb J, Chenc L, Chena H, and Cheng, S. Global, regional, and national dengue burden from 1990 to 2017: A systematic analysis based on the global burden of disease study 2017. *E Clinical Medicine*. 2021. 32:100712.
- O'Driscoll M, Imai N, Ferguson N.M, Hadinegoro S.R, Satari H.I, Tam C.C, Dorigatti
 I. Spatiotemporal Variability in Dengue Transmission Intensity in Jakarta, Indonesia.

 PLoS Negl Trop Dis. 2020. 14: e0008102.
- 10. Lv M, Liu Q. The Epidemiological Characteristics and Dynamic Transmission of Dengue in China. PLoS Negl Trop Dis. 2013.10: e0005095.
- 11. Murugesan A, Manoharan M. Dengue Virus. *Emerging and Reemerging Viral Pathogens*. 2020. 281–359.

- 12. Bhatt S, Gething P, Brady O, Messina P, Farlow AW, Moyes CL, *et al.* The global distribution and burden of dengue. *Nature*. 2013. 496: 504–507.
- 13. https://www.who.int/emergencies/disease-outbreak-news/item/2023-DON448.
- 14. https://www.ecdc.europa.eu/en.
- 15. Afreen N, Naqvi IH, Broor S, Ahmed A, Parveen S. Phylogenetic and molecular clock analysis of dengue serotype 1 and 3 from New Delhi, India. *PLoS One*. 2015. 4,10(11): e0141628.
- 16. Jagtap S, Pattabiraman C, Sankaradoss A, Krishna S, Roy R. Evolutionary dynamics of dengue virus in India. *PLoS Pathog*. 2023.19(4): e1010862.
- 17. Vaddadi K, Gandikota, C Jain PK, Prasad VSV, and Venkataramana M. Co-circulation and co-infections of all dengue virus serotypes in Hyderabad, India 2014. *Epidemiol Infect*. 2017. 145(12): 2563-2574.
- 18. Maisnam D, Billoria A, Prasad V.S.V, Venkataramana, M. Association of Dengue Virus Serotypes 1&2 with Severe Dengue Having Deletions in Their 3'Untranslated Regions (3'UTRs). *Microorganisms*. 2023. 11: 666.
- 19. Dash PK, Sharma S, Srivastava A, Santhosh SR, Parida MM, Neeraja M, Subbalaxmi MV, Lakshmi V, Rao PV. Emergence of dengue virus type 4 (genotype I) in India. *Epidemiol Infect.* 2011. 139(6): 857-61.
- 20. Horstick O, Martinez E, Guzman MG, Martin JLS, & Ranzinger SR. WHO dengue case classification 2009 and its usefulness in practice: an expert consensus in the Americas. *Pathogens and global health.* 2015. 109(1): 19-25.
- 21. Martina BEE, Koraka, P, and Osterhaus, ADME. Dengue virus pathogenesis: An integrated view. *Clin Microbiol Rev.* 2015. 22(4): 564–581.
- 22. Malavige GN, Fernando S, Fernando DJ, and Seneviratne, SL. Dengue viral infections. *Postgrad Med J.* 2004. 80: 588-601.

- 23. Neeraja M, Iakshmi V, Teja VD, Lavanya V, Priyanka EN, Subhada K, Parida MM, *et al.* Unusual and rare manifestations of dengue during a dengue outbreak in a tertiary care hospital in South India. *Arch Virol.* 2014. 159(7): 1567-1573.
- 24. Loroño-Pino MA, Cropp CB, Farfán JA, Vorndam AV, Rodríguez-Angulo EM, Rosado-Paredes EP, Flores-Flores LF, et al. Common occurrence of concurrent infections by multiple dengue virus serotypes. Am J Trop Med Hyg. 1999. 61(5): 725-30.
- 25. Das S, Abreu C, Harris M, Shrader J, Sarvepalli S. Severe Thrombocytopenia Associated with Dengue Fever: An Evidence-Based Approach to Management of Thrombocytopenia. *Case Rep Hematol.* 2022. 12: 3358325.
- 26. Sridharan A, Chen Q, Tang KF, Ooi EE, Hibberd ML, Chen J. Inhibition of megakaryocyte development in the bone marrow underlies dengue virus-induced thrombocytopenia in humanized mice. *J Virol*. 2013. 87(21): 11648-11658.
- 27. de Azeredo EL, Monteiro RQ, de-Oliveira Pinto LM. Thrombocytopenia in Dengue: Interrelationship between Virus and the Imbalance between Coagulation and Fibrinolysis and Inflammatory Mediators. *Mediators Inflamm*. 2015: 313842.
- 28. Green S, Rothman A. Immunopathological mechanisms in dengue and dengue hemorrhagic fever. *Current Opinion in Infectious Diseases*. 2006. 19(5): 429–436.
- 29. Nanaware N, Banerjee A, Mullick Bagchi S, Bagchi, P, Mukherjee, A. Dengue Virus Infection: A Tale of Viral Exploitations and Host Responses. *Viruses*. 2021. 13: 1967.
- 30. Guzman MG, Halstead SB, Artsob H, Buchy P, Farrar J, Gubler DJ, Hunsperger E, *et al.*Dengue: a continuing global threat. *Nat Rev Microbiol*. 2010. 8(12 Suppl): S7-16.
- 31. Filomatori CV, Lodeiro MF, Alvarez DE, Samsa MM, Pietrasanta L, Gamarnik AV. A 5' RNA element promotes dengue virus RNA synthesis on a circular genome. *Genes Dev.* 2006. 20: 2238–2249.

- 32. Gebhard, LG, Filomatori, CV, and Gamarnik, AV. Functional RNA Elements in the Dengue Virus Genome. *Viruses*. 2011. 3(9): 1739–1756.
- 33. Byk LA, Gamarnik AV. Properties and Functions of the Dengue Virus Capsid Protein. *Annu Rev Virol*. 2016. 29, 3(1): 263-281.
- 34. Ma L, Jones CT, Groesch TD, Kuhn RJ, Post CB. Solution structure of dengue virus capsid protein reveals another fold. *PNAS*. 2004.101: 3414–3419.
- 35. Wang SH, Syu WJ, Hu ST. Identification of the homotypic interaction domain of the core protein of dengue virus type 2. *J Gen Virol*. 2004. 85: 2307–2314.
- 36. Rothan H.A, Kumar, M. Role of Endoplasmic Reticulum-Associated Proteins in Flavivirus Replication and Assembly Complexes. *Pathogens*. 2019. 8: 148.
- 37. Ambroggio EE, Costa Navarro GS, Pérez Socas LB, Bagatolli LA, Gamarnik AV. Dengue and Zika virus capsid proteins bind to membranes and self-assemble into liquid droplets with nucleic acids. *J Biol Chem.* 2021. 297(3): 101059.
- 38. Wang SH, Syu WJ, Huang KJ, Lei HY, Yao CW, *et al.* Intracellular localization and determination of a nuclear localization signal of the core protein of dengue virus. *J Gen Virol.* 2002. 83: 3093–3102.
- 39. Netsawang J, Noisakran S, Puttikhunt C, Kasinrerk W, Wongwiwat W, *et al.* Nuclear localization of dengue virus capsid protein is required for DAXX interaction and apoptosis. *Virus Res.* 2010.147: 275.
- 40. Samsa MM, Mondotte JA, Iglesias NG, Assunção-Miranda I, Barbosa-Lima G, Da Poian AT, Bozza PT, Gamarnik AV. Dengue virus capsid protein usurps lipid droplets for viral particle formation. *PLoS Pathog*. 2009. 5(10): e1000632.
- 41. Tan TY, Fibriansah G, Lok SM. Capsid protein is central to the birth of flavivirus particles. *PLoS Pathog.* 2020. 28, 16(5): e1008542.

- 42. Bray M, Lai CJ. Dengue virus pre membrane and membrane proteins elicit a protective immune response. *Virology*. 1991. 185(1): 505-508.
- 43. Stolp ZD, Smurthwaite CA, Reed C, Williams W, Dharmawan A, Djaballah H, *et al.* A Multiplexed Cell-Based Assay for the Identification of Modulators of Pre-Membrane Processing as a Target against Dengue Virus. *J Biomol Screen*. 2015. 20(5): 616-626.
- 44. Sarker A, Dhama N, Gupta RD. Dengue virus neutralizing antibody: a review of targets, cross-reactivity, and antibody-dependent enhancement. *Front Immunol.* 2023. 2(14):1200195.
- 45. Modis Y, Ogata S, Clements D, Harrison SC. Structure of the dengue virus envelope protein after membrane fusion. *Nature*. 2004. 427(6972): 313-319.
- 46. Fahimi H, Mohammadipour M, Haddad Kashani H, Parvini F, Sadeghizadeh M. Dengue viruses and promising envelope protein domain III-based vaccines. *Appl Microbiol Biotechnol*. 2018. 102: 2977–2996.
- 47. Chen HR, Lai YC, & Yeh TM. Dengue virus non-structural protein 1: a pathogenic factor, therapeutic target, and vaccine candidate. *J Biomed Sci.* 2018. 25: 58.
- 48. Avirutnan P, Zhang L, Punyadee N, Manuyakorn A, Puttikhunt C, Kasinrerk W, *et al.* Secreted NS1 of Dengue Virus Attaches to the Surface of Cells via Interactions with Heparan Sulfate and Chondroitin Sulfate E. *PLoS Pathog.* 2007. 3(11): e183.
- 49. Tan B.E.K, Beard M.R, Eyre N.S. Identification of Key Residues in Dengue Virus NS1 Protein That Are Essential for Its Secretion. *Viruses*. 2023. 15: 1102.
- 50. Tien SM, Chang PC, Lai YC, Chuang YC, Tseng CK, Kao YS, Huang HJ, *et al.* Therapeutic efficacy of humanized monoclonal antibodies targeting dengue virus nonstructural protein 1 in the mouse model. *PLoS Pathog.* 2022. 29, 18(4): e1010469.
- 51. Xie X, Gayen S, Kang C, Yuan Z, Shi PY. Membrane topology and function of dengue virus NS2A protein. *J Virol.* 2013. 87(8): 4609-4622.

- 52. Xie X, Zou J, Zhang X, Zhou Y, Routh AL, Kang C, Popov VL, *et al.* Dengue NS2A Protein Orchestrates Virus Assembly. *Cell Host Microbe*. 2019.13, 26(5): 606-622.
- 53. Li Q, Kang C. Structures and Dynamics of Dengue Virus Nonstructural Membrane Proteins. *Membranes*. 2022. 12(2): 231.
- 54. Li Y, Li Q, Wong YL, Liew LS, Kang C. Membrane topology of NS2B of dengue virus revealed by NMR spectroscopy. *Biochim Biophys Acta*. 2001. 848 (10): 2244-52.
- 55. Aguirre S, Luthra P, Sanchez-Aparicio MT, Maestre AM, Patel J, *et al.* Dengue virus NS2B protein targets cGAS for degradation and prevents mitochondrial DNA sensing during infection. *Nat Microbiol.* 2017. 27, 2: 17037.
- 56. Kim YM, Gayen S, Kang C, Joy JK, Huang Q, Chen AS, Wee J LK, Ang MJ Y, *et al.* NMR Analysis of a Novel Enzymatically Active Unlinked Dengue NS2B-NS3 Protease Complex. *J Biol Chem.* 2013. 288: 12891–12900.
- 57. Luo D, Wei N, Doan DN, Paradkar PN, Chong Y, Davidson AD, Kotaka M, Lescar J, and Vasudevan, SG. Flexibility between the protease and helicase domains of the dengue virus NS3 protein conferred by the linker region and its functional implications. *J. Biol. Chem.* 2010. 285(24): 18817–18827.
- 58. Miller S, Kastner S, Krijnse-Locker J, Bühler S, Bartenschlager R. The non-structural protein 4A of dengue virus is an integral membrane protein inducing membrane alterations in a 2K-regulated manner. *J Biol Chem.* 2007. 23, 282(12): 8873-82.
- 59. Miller S, Sparacio S, Bartenschlager R. Subcellular localization and membrane topology of the Dengue virus type 2 Non-structural protein 4B. *J Biol Chem.* 2006. 31, 281(13): 8854-8863.
- 60. Stern O, Hung Y.F, Valdau O, Yaffe, Y, Harris E, Hoffmann S, Willbold D, Sklan E.H. An N-terminal amphipathic helix in dengue virus nonstructural protein 4A mediates oligomerization and is essential for replication. *J. Virol.* 2013. 87: 4080–4085.

- 61. Płaszczyca A, Scaturro P, Neufeldt CJ, Cortese M, Cerikan B, Ferla S, Brancale A, *et al*. A novel interaction between dengue virus nonstructural protein 1 and the NS4A-2K-4B precursor is required for viral RNA replication but not for formation of the membranous replication organelle. *PLoS Pathog*. 2019. 9, 15(5): e1007736.
- 62. Cortese M, Mulder K, Chatel-Chaix L, Scaturro P, Cerikan B, Plaszczyca A, Haselmann U, *et al.* Determinants in Nonstructural Protein 4A of Dengue Virus Required for RNA Replication and Replication Organelle Biogenesis. *J Virol.* 2021. 13, 95(21): e0131021.
- 63. Nemésio H, Palomares-Jerez F, Villalaín J. NS4A and NS4B proteins from dengue virus: membranotropic regions. *Biochim Biophys Acta*. 2012. 1818(11): 2818-2830.
- 64. Li Q, Kang C. Dengue virus NS4B protein as a target for developing antivirals. Front *Cell Infect Microbiol*. 2022. 9, 12: 959727.
- 65. Naik NG, Wu HN. Mutation of Putative N-Glycosylation Sites on Dengue Virus NS4B Decreases RNA Replication. *J Virol*. 2015. 89(13): 6746-60.
- 66. Munoz-Jordan JL, Laurent-Rolle M, Ashour J, Martinez-Sobrido L, Ashok M, Lipkin WI, Garcia-Sastre A. Inhibition of alpha/beta interferon signaling by the NS4B protein of flaviviruses. *J Virol*. 2005. 79: 8004–8013.
- 67. Tian JN, Yang CC, Chuang CK, Tsai MH, Wu RH, Chen CT, Yueh A. A Dengue Virus Type 2 (DENV-2) NS4B-Interacting Host Factor, SERP1, Reduces DENV-2 Production by Suppressing Viral RNA Replication. *Viruses*. 2019. 27, 11(9): 787.
- 68. Bhatnagar P, Sreekanth GP, Murali-Krishna K, Chandele A and Sitaraman R. Dengue Virus Non-Structural Protein 5 as a Versatile, Multi-Functional Effector in Host–Pathogen Interactions. *Front Cell Infect Microbiol.* 2021.11: 574067.
- 69. El Sahili A, Lescar J. Dengue Virus Non-Structural Protein 5. Viruses. 2017. 9(4): 91.

- 70. Yap TL, Xu T, Chen YL, Malet H, Egloff MP, Canard B, Vasudevan SG, *et al.* Crystal Structure of the Dengue Virus RNA-Dependent RNA Polymerase Catalytic Domain at 1.85-Angstrom Resolution. *J Virol.* 2007. 81: 4753–4765.
- 71. Kumar A, Bühler S, Selisko B, Davidson A, Mulder K, Canard B, Miller S, Bartenschlager R. Nuclear localization of dengue virus nonstructural protein 5 does not strictly correlate with efficient viral RNA replication and inhibition of type I interferon signaling. *J Virol*. 2013. 87(8): 4545-57.
- 72. Ashour J, Laurent-Rolle M, Shi PY, Garcia-Sastre A. NS5 of dengue virus mediates STAT2 binding and degradation. *J Virol.* 2009. 83: 5408–5418.
- 73. Pryor MJ, Rawlinson SM, Butcher RE, Barton CL, Waterhouse TA, Vasudevan SG, et al. Nuclear localization of dengue virus nonstructural protein 5 through its importin α/β-recognized nuclear localization sequences is integral to viral infection. *Traffic*. 2007. 8:795–807.
- 74. Lin JC, Lin SC, Chen WY, Yen YT, Lai CW, Tao MH, LIN YL, *et al.* Dengue viral protease interaction with NF-κB inhibitor α/β results in endothelial cell apoptosis and hemorrhage development. *J Immunol.* 2014. 193(3): 1258-1267.
- 75. Yu CY, Chang TH, Liang JJ, Chiang RL, Lee YL, Liao CL, Lin YL. Dengue virus targets the adaptor protein MITA to subvert host innate immunity. *PLoS Pathog*. 2017. 8(6): e1002780.
- 76. Yu, CY, Liang, JJ, Li, JK, Lee, YL, Chang, BL, Su, CI, Huang, WJ, Lai, MM, Lin, YL. Dengue Virus Impairs Mitochondrial Fusion by Cleaving Mitofusins. *PLoS Pathog.* 2015. 11(12): e1005350.
- 77. Silva EM, Conde JN, Allonso D, Ventura GT, Coelho DR, Carneiro PH, Silva ML, *et al.*Dengue virus nonstructural 3 protein interacts directly with human glyceraldehyde-3-

- phosphate dehydrogenase (GAPDH) and reduces its glycolytic activity. *Sci Rep.* 2019. 25, 9(1): 2651.
- 78. Heaton NS, Perera R, Berger KL, Khadka S, Lacount DJ, Kuhn RJ, Randall G. Dengue virus nonstructural protein 3 redistributes fatty acid synthase to sites of viral replication and increases cellular fatty acid synthesis. *Proc Natl Acad Sci U S A*. 2010. 5, 107(40): 17345-50.
- 79. Chua JJ, Ng MM, Chow VT. The non-structural 3 (NS3) protein of dengue virus type 2 interacts with human nuclear receptor binding protein and is associated with alterations in membrane structure. *Virus Res.* 2004.15, 102(2): 151-163.
- 80. García Cordero J, León Juárez M, González-Y-Merchand JA, Cedillo Barrón L, Gutiérrez Castañeda B. Caveolin-1 in lipid rafts interacts with dengue virus NS3 during polyprotein processing and replication in HMEC-1 cells. *PLoS One*. 2014. 18, 9(3): e90704.
- 81. Klungthong C, Gibbons RV, Thaisomboonsuk B, Nisalak A, Kalayanarooj S, Thirawuth V, Nutkumhang N, *et al.* Dengue virus detection using whole blood for reverse transcriptase PCR and virus isolation. *J Clin Microbiol.* 2007. 45(8): 2480-2485.
- 82. Wu SJ, Lee EM, Putvatana R, Shurtliff RN, Porter KR, Suharyono W, Watts DM, *et al.*Detection of dengue viral RNA using a nucleic acid sequence-based amplification assay. *J Clin Microbiol.* 2001. 39(8): 2794-2798.
- 83. Dussart P, Labeau B, Lagathu G, Louis P, Nunes MR, Rodrigues SG, Storck-Herrmann C, et al. Evaluation of an enzyme immunoassay for detection of dengue virus NS1 antigen in human serum. *Clin Vaccine Immunol*. 2006. 13(11):1185-9.
- 84. Gandikota C, Gandhi L, Maisnam D, Kesavulu MM, Billoria A, Prasad VSV, and Venkataramana M. A novel anti-NS2BNS3pro antibody-based indirect ELISA test for the diagnosis of dengue virus infections. *J Med Virol*. 2021. 93(6): 3312-3321.

- 85. Malik S, Ahsan O, Mumtaz H, Tahir Khan M, Sah R, Waheed Y. Tracing down the Updates on Dengue Virus-Molecular Biology, Antivirals, and Vaccine Strategies. *Vaccines (Basel)*. 2023. 5, 11(8):1328.
- 86. Norshidah H, Vignesh R, Lai NS. Updates on Dengue Vaccine and Antiviral: Where Are We Heading? Molecules. 2021. 9, 26(22): 6768.
- 87. Capeding MR, Tran NH, Hadinegoro SRS, Ismail, HIHM, Chotpitayasunondh, T, Chua, MN, Luong, *et al.* Clinical efficacy and safety of a novel tetravalent dengue vaccine in healthy children in Asia: A phase 3, randomised, observer-masked, placebo-controlled trial. *Lancet.* 2014. 384: 1358–1365.
- 88. Sabchareon A, Wallace D, Sirivichayakul C, Limkittikul K, Chanthavanich P, Suvannadabba S Jiwariyavej V, *et al.* Protective efficacy of the recombinant, liveattenuated, CYD tetravalent dengue vaccine in Thai schoolchildren: A randomised, controlled phase 2b trial. *Lancet.* 2012. 380: 1559–1567.
- 89. Villar L, Dayan GH, Arredondo-García JL, Rivera DM, Cunha R, Deseda C, Reynales H, et al. Efficacy of a Tetravalent Dengue Vaccine in Children in Latin America. N Engl J Med. 2015. 372: 13–123.
- 90. Whitehead SS, Durbin AP, Pierce KK, Elwood D, McElvany BD, Fraser EA, *et al.* In a randomized trial, the live attenuated tetravalent dengue vaccine TV003 is well-tolerated and highly immunogenic in subjects with flavivirus exposure prior to vaccination. *PLoS Negl Trop Dis.* 2017. 11: e0005584.
- 91. Kirkpatrick BD, Durbin AP, Pierce KK, Carmolli MP, Tibery CM, Grier PL, Hynes N, *et al.* Robust and Balanced Immune Responses to All 4 Dengue Virus Serotypes Following Administration of a Single Dose of a Live Attenuated Tetravalent Dengue Vaccine to Healthy, Flavivirus-Naive Adults. *J Infect Dis.* 2015. 212: 702–710.

- 92. Sirivichayakul C, Barranco-Santana EA, Esquilin-Rivera I, Oh HML, Raanan M, Sariol CA, *et al.* Safety and Immunogenicity of a Tetravalent Dengue Vaccine Candidate in Healthy Children and Adults in Dengue-Endemic Regions: A Randomized, Placebo-Controlled Phase 2 Study. *J Infect Dis.* 2016. 213: 1562–1572.
- 93. Thomas SJ, Eckels KH, Carletti I, De La Barrera R, Dessy F, Fernandez S, Putnak R, *et al.*A phase II, randomized, safety and immunogenicity study of a re-derived, live-attenuated dengue virus vaccine in healthy adults. *Am J Trop Med Hyg.* 2013. 88: 73–88.
- 94. Bauer K, Esquilin IO, Cornier AS, Thomas SJ, Del Rio AIQ, Bertran-Pasarell J, Ramirez JOM, *et al.* A phase II, randomized, safety and immunogenicity trial of a re-derived, liveattenuated dengue virus vaccine in healthy children and adults living in puerto rico. *Am J Trop Med Hyg.* 2015. 93: 441–453.
- 95. Schmidt AC, Lin L, Martinez LJ, Ruck RC, Eckels KH, Collard A, De La Barrera R, *et al.*Phase 1 randomized study of a tetravalent dengue purified inactivated vaccine in healthy adults in the United States. *Am J Trop Med Hyg.* 2017. 96: 1325–1337.
- 96. Diaz C, Koren M, Lin L, Martinez LJ, Eckels KH, Campos M, Jarman RG, *et al.* Safety and immunogenicity of different formulations of a tetravalent dengue purified inactivated vaccine in healthy adults from Puerto Rico: Final results after 3 years of follow-up from a randomized, placebo-controlled phase I study. *Am J Trop Med Hyg.* 2020. 102: 951–954.
- 97. Coller BAG, Clements DE, Bett AJ, Sagar SL, Ter Meulen JH. The development of recombinant subunit envelope-based vaccines to protect against dengue virus induced disease. *Vaccine*. 2011. 29: 7267–7275.
- 98. Manoff SB, Sausser M, Falk Russell A, Martin J, Radley D, Hyatt D, Roberts CC, *et al.* Immunogenicity and safety of an investigational tetravalent recombinant subunit vaccine for dengue: Results of a Phase I randomized clinical trial in flavivirus-naïve adults. *Hum Vaccines Immunother*. 2019. 15: 2195–2204.

- 99. Beckett CG, Tjaden J, Burgess T, Danko JR, Tamminga C, Simmons M, Wu SJ, *et al.* Evaluation of a prototype dengue-1 DNA vaccine in a Phase 1 clinical trial. *Vaccine*. 2011. 29: 960–968.
- 100. Danko JR, Kochel T, Teneza-Mora N, Luke TC, Raviprakash K, Sun P, Simmons M, *et al.* Safety and immunogenicity of a tetravalent dengue DNA vaccine administered with a cationic lipid-based adjuvant in a phase 1 clinical trial. *Am J Trop Med Hyg.* 2018. 98: 849–856.
- 101. Kochel TJ, Raviprakash K, Hayes CG, Watts DM, Russell KL, Gozalo AS, Phillips IA, *et al.* A dengue virus serotype-1 DNA vaccine induces virus neutralizing antibodies and provides protection from viral challenge in Aotus monkeys. *Vaccine*. 2000. 18: 3166–3173.
- Panya A, Sawasdee, N, Junking M, Srisawat C, Choowongkomon K, Yenchitsomanus
 P A. Peptide Inhibitor Derived from the Conserved Ectodomain Region of DENV
 Membrane (M) Protein with Activity Against Dengue Virus Infection. *Chem Biol Drug Des.* 2015. 86: 1093–1104.
- 103. Mohd Isa D, Peng Chin S, Lim Chong W, Zain SM, Abd Rahman N, Sanghiran Lee V Dynamics and binding interactions of peptide inhibitors of dengue virus entry. *J Biol Phys*. 2019. 45: 63–76.
- 104. Yang CC, Hu HS, Lin HM, Wu PS, Wu RH, Tian JN, Wu SH, *et al.* A novel flavivirus entry inhibitor BP34610, discovered through high-throughput screening with dengue reporter viruses. *Antivir Res.* 2019. 172: 104636.
- 105. Faustino AFAA, Guerra GM, Huber RG, Hollmann A, Domingues MM, Barbosa GM, Enguita FJ, Bond PJ, Castanho MARBRB, Da Poian AT, et al. Understanding Dengue Virus Capsid Protein Disordered N-Terminus and pep14-23-Based Inhibition ACS. Chem Biol. 2015. 10: 517–526.

- 106. Smith JL, Sheridan K, Parkins CJ, Frueh L, Jemison AL, Strode K, Dow G, Nilsen A, Hirsch AJ Characterization and structure-activity relationship analysis of a class of antiviral compounds that directly bind dengue virus capsid protein and are incorporated into virions.

 Antivir Res. 2018. 155: 12–19.
- 107. Bhakat S, Delang L, Kaptein S, Neyts J, Leyssen P, Jayaprakash V. Reaching beyond HIV/HCV: Nelfinavir as a potential starting point for broad-spectrum protease inhibitors against dengue and chikungunya virus. *RSC Adv.* 2015. 5: 105.
- 108. Raut R, Beesetti H, Tyagi P, Khanna I, Jain SK, Jeankumar VU, Yogeeswari P, *et al.*A small molecule inhibitor of dengue virus type 2 protease inhibits the replication of all four dengue virus serotypes in cell culture. *Virol J.* 2015. 12: 16.
- 109. Wu DW, Mao F, Ye Y, Li J, Xu CL, Luo XM, Chen J, Shen X. Policresulen, a novel NS2B/NS3 protease inhibitor effectively inhibits the replication of DENV2 virus in BHK-21 cells. *Acta Pharmacol Sin.* 2015. 36: 1126–1136.
- 110. Weigel LF, Nitsche C, Graf D, Bartenschlager R, Klein CD. Phenylalanine and Phenylglycine Analogues as Arginine Mimetics in Dengue Protease Inhibitors. *J Med Chem.* 2015. 58: 7733.
- 111. Behnam, MAM Graf D, Bartenschlager R, Zlotos DP, Klein CD Discovery of Nanomolar Dengue and West Nile Virus Protease Inhibitors Containing a 4-Benzyloxyphenylglycine Residue. *J Med Chem.* 2015. 58: 9354–9370.
- 112. Li L, Basavannacharya C, Chan KWK, Shang L, Vasudevan SG, Yin, Z. Structure-guided Discovery of a Novel Non-peptide Inhibitor of Dengue Virus NS2B–NS3 *Protease Chem Biol Drug Des.* 2015. 86, 255–264.
- 113. Balasubramanian A, Manzano M, Teramoto T, Pilankatta R, Padmanabhan R. High-throughput screening for the identification of small-molecule inhibitors of the flaviviral protease. *Antivir Res.* 2016. 1346–1416.

- 114. Rothan HA Abdulrahman, AY Khazali, AS Nor Rashid, N Chong, TT Yusof, R Carnosine exhibits significant antiviral activity against Dengue and Zika virus. *J Pept Sci*. 2019. 25: e3196.
- 115. Bhowmick S, Alissa SA, Wabaidur SM, Chikhale RV, Islam MA Structure-guided screening of chemical database to identify NS3-NS2B inhibitors for effective therapeutic application in dengue infection. *J Mol Recognit*. 2020. 33: e2838.
- 116. Hamdani SS Khan, BA Hameed, S Batool F, Saleem HN, Mughal EU, Saeed M. Synthesis and evaluation of novel S-benzyl-and S-alkylphthalimide-oxadiazole-benzenesulfonamide hybrids as inhibitors of dengue virus protease. *Bioorg Chem.* 2020. 96: 103567.
- 117. Ghosh I, Talukdar P. Molecular docking and pharmacokinetics study for selected leaf phytochemicals from Carica papaya Linn against dengue virus protein, NS2B/NS3 protease. *World Sci News*. 2019. 124. 264–278.
- 118. Lim WZ, Cheng PG, Abdulrahman AY, Teoh TC. The identification of active compounds in Ganoderma lucidum var antler extract inhibiting dengue virus serine protease and its computational studies. *J Biomol Struct Dyn.* 2020. 38: 4273–4288.
- 119. Farooq MU, Munir B, Naeem S, Yameen M, Iqbal SZ, Ahmad A, Mustaan MA, *et al*. Exploration of Carica papaya bioactive compounds as potential inhibitors of dengue NS2B, NS3 and NS5 protease. *Pak J Pharm Sci.* 2020. 33: 355–360.
- 120. Balasubramanian A, Pilankatta R, Teramoto T, Sajith AM, Nwulia E, Kulkarni A, Padmanabhan R. Inhibition of dengue virus by curcuminoids. *Antivir Res.* 2019. 62: 71–78.
- 121. Sulaiman SN, Hariono M, Salleh HM, Chong S-L, Yee LS, Zahari A, Wahab HA, *et al.* Chemical Constituents From Endiandra kingiana (Lauraceae) as Potential Inhibitors for

- Dengue Type 2 NS2B/NS3 Serine Protease and its Molecular Docking. *Nat Prod Commun.* 2019. 14: 1934578X19861014.
- 122. Salleh HM, Chong SL, Othman R, Hazni H, Ahmad K, Mohd Yusof MYZ, Fauzi NW, *et al.* Dengue protease inhibition activity of selected Malaysian medicinal herbs. *Trop Biomed*. 2019. 36: 357–366.
- 123. Yao X, Ling Y, Guo S, He S, Wang J, Zhang Q, Wu W, *et al.* Inhibition of dengue viral infection by diasarone-I is associated with 2'O methyltransferase of NS5. *Eur J Pharmacol*. 2018. 821: 11–20.
- 124. Saleem HN, Batool F, Mansoor HJ, Shahzad-ul-Hussan S, Saeed M. Inhibition of Dengue Virus Protease by Eugeniin, Isobiflorin, and Biflorin. Isolated from the Flower Buds of Syzygium aromaticum (Cloves). *ACS Omega*. 2019. 4: 1525–1533.
- 125. Shin HJ, Kim M-H, Lee J-Y, Hwang I, Yoon GY, Kim HS, Kwon Y-C Ahn, D-G Kim, K-D Kim, *et al.* Structure-Based Virtual Screening: Identification of a Novel NS2B-NS3 Protease Inhibitor with Potent Antiviral Activity against Zika and Dengue Viruses. *Microorganisms*. 2021. 9: 545.
- 126. Nobori H, Toba S, Yoshida R, Hall WW, Orba Y, Sawa H, Sato A. Identification of Compound-B, a novel anti-dengue virus agent targeting the non-structural protein 4A. *Antiviral Res* 2018 155: 60–66.
- 127. Van Cleef KWR, Overheul GJ, Thomassen MC, Marjakangas JM, Van Rij RP. Escape mutations in NS4B render dengue virus insensitive to the antiviral activity of the paracetamol metabolite AM404. *Antimicrob Agents Chemother*. 2016. 60: 2554–2557.
- 128. Moquin SA Simon, O Karuna, R, Lakshminarayana SB, Yokokawa F, Wang F, Saravanan C, Zhang J, Day CW, Chan K, *et al.* NITD-688 a pan-serotype inhibitor of the dengue virus NS4B protein, shows favorable pharmacokinetics and efficacy in preclinical animal models. *Sci Transl Med.* 2021. 13: eabb2181.

- 129. Lee JC, Tseng CK, Wu YH, Kaushik-Basu N, Lin CK, Chen WC, Wu HN. Characterization of the activity of 2'-C-methylcytidine against dengue virus replication.

 Antivir Res. 2015. 116: 19.
- 130. Vernekar SKV, Qiu L, Zhang J, Kankanala J, Li H, Geraghty RJ, Wang Z. 5'-silylated 3'-1,23-triazolyl thymidine analogues as inhibitors of West Nile Virus and Dengue virus. *J Med Chem.* 2015. 58: 4016–4028.
- 131. Bullard KM, Gullberg RC, Soltani E, Steel JJ, Geiss BJ, Keenan SM. Murine efficacy and pharmacokinetic evaluation of the flaviviral NS5 capping enzyme 2-thioxothiazolidin-4-one inhibitor BG-323. *PLoS ONE*. 2015. 10: e0130083.
- 132. Uday RVS, Misra R, Harika A, Dolui S, Saha A, Pal U, *et al.* Dabrafenib, idelalisib and nintedanib act as significant allosteric modulator for dengue NS3 protease. 2021. *PLoS ONE*. 16(9): e0257206.
- 133. Lin KH, Ali A, Rusere L, Soumana DI, Kurt Yilmaz N, Schiffer CA. Dengue Virus NS2B/NS3 Protease Inhibitors Exploiting the Prime Side. *J Virol*. 2017. 28, 91(10): e00045-17.
- 134. Nitsche C, Holloway S, Schirmeister T, and Christian D. Klein. Biochemistry and Medicinal Chemistry of the Dengue Virus Protease *Chemical Reviews*. 2014. *114* (22): 11348-11381.
- 135. Chiang PY, and Wu HN. The role of surface basic amino acids of dengue virus NS3 helicase in viral RNA replication and enzyme activities. *FEBS Lett.* 2016. 590(14), 2307-2320.
- 136. Du Pont KE, Davidson RB, McCullagh M, Geiss BJ. Motif V regulates energy transduction between the flavivirus NS3 ATPase and RNA-binding cleft. *J Biol Chem*. 2020. 7, 295(6): 1551-1564.

- 137. Chiang PY, and Wu HN. The role of surface basic amino acids of dengue virus NS3 helicase in viral RNA replication and enzyme activities. *FEBS Lett.* 2016. 590(14): 2307-2320.
- 138. Li J, Lim SP, Beer D, Patel V, Wen D, Tumanut C, Tully, DC, Williams JA, Jiricek J, et al. 2005. Functional profiling of recombinant NS3 proteases from all four serotypes of dengue virus using tetra peptide and octapeptide substrate libraries. *J Biol Chem.* 280(31): 28766-28774.
- 139. Shiryaev SA, Kozlov IA, Ratnikov BI, Smith JW, Lebl M, and Strongin, AY. Cleavage preference distinguishes the two-component NS2B–NS3 serine proteinases of Dengue and West Nile viruses. *Biochem J.* 2007. 401(3): 743–752.
- 140. Lin KH, Nalivaika EA, Prachanronarong KL, Yilmaz NK, and Schiffer CA. Dengue Protease Substrate Recognition: Binding of the Prime Side. *ACS Infect Dis.* 2016. 2(10): 734-743.
- 141. Constant DA, Mateo A, Nagamine CM, and Kirkegaard K. Targeting intramolecular proteinase NS2B/3 cleavages for trans-dominant inhibition of dengue. *Proc Natl Acad Sci U S A*. 2018. 115(40): 10136-10141.
- 142. Lennemann, NJ, Coyne CB. Dengue and Zika viruses subvert reticulophagy by NS2B3-mediated cleavage of FAM134B. *Autophagy*. 2017. 13(2): 322-332.
- 143. De Jesús-González LA, Cervantes-Salazar M, Reyes-Ruiz, JM, Osuna-Ramos, JF, Farfán-Morales CN, Palacios-Rápalo, SN, et al. The Nuclear Pore Complex: A Target for NS3 Protease of Dengue and Zika Viruses. Viruses. 2020. 12(6): 583.
- 144. Noisakran S, Onlamoon N, Songprakhon P, Hsiao HM, Chokephaibulkit K, Perng GC. Cells in dengue virus infection in vivo. *Adv Virol.* 2010.164878.

- 145. Diamond MS, Edgil D1, Roberts TG, Lu B, and Harris E. Infection of human cells by dengue virus is modulated by different cell types and viral strains. *J Virol*. 2000. 74(17): 7814-7823.
- 146. Balsitis SJ, Coloma J, Castro G, Alava A, Flores D, McKerrow JH, Beatty PR, *et al*. Tropism of dengue virus in mice and humans defined by viral nonstructural protein 3-specific immunostaining. *Am J Trop Med Hyg.* 2009. 80(3): 416-424.
- 147. Gandikota C, Mohammed F, Gandhi L, Maisnam D, Mattam U, Rathore D, *et al.*Mitochondrial Import of Dengue Virus NS3 Protease and Cleavage of GrpEL1, a

 Cochaperone of Mitochondrial Hsp70. *J. Virol.* 2020. 94(17): e01178-20.
- 148. Gandhi L, Maisnam D, Rathore, D, Chauhan P, Bonagiri A. and Venkataramana M, Differential localization of dengue virus protease affects cell homeostasis and triggers to thrombocytopenia. *iScience*. 2023. 26(7): 10702.
- 149. Wahaab A, Mustafa BE, Hameed M, Stevenson NJ, Anwar MN, Liu K, *et al.* Potential Role of Flavivirus NS2B-NS3 Proteases in Viral Pathogenesis and Anti-flavivirus Drug Discovery Employing Animal Cells and Models: A Review. *Viruses.* 2021. 14(1): 44.
- 150. Lu J, Wu T, Zhang B, Liu S, Song W, Qiao J, and Ruan H. Types of nuclear localization signals and mechanisms of protein import into the nucleus. *Cell Commun Signal*. 2021. 19: 60.
- 151. Uchil PD, Kumar AV, Satchidanandam V. Nuclear localization of flavivirus RNA synthesis in infected cells. *J Virol*. 2006. 80(11): 5451-5464.
- 152. Reyes-Ruiz JM, Osuna-Ramos JF, Cervantes-Salazar M, Lagunes Guillen AE, Chávez-Munguía B, Salas-Benito JS, *et al.* Strand-like structures and the nonstructural proteins 5, 3 and 1 are present in the nucleus of mosquito cells infected with dengue virus. *Virology*. 2018. 515: 74-80.

- 153. Morales CN, Gutiérrez EAL, and Del ÁRM. Nuclear localization of non-structural protein 3 (NS3) during dengue virus infection. *Arch. Virol.* 2021. 166(5): 1439-1446.
- 154. Perera R, Kuhn RJ. Structural proteomics of dengue virus. *Curr Opin Microbiol*. 11(4): 369-377.
- 155. Acosta EG, Castilla V, Damonte EB. Alternative infectious entry pathways for dengue virus serotypes into mammalian cells. *Cell Microbiol*. 2009. 11(10):1533-1549.
- 156. Mairiang D, Zhang H, Sodja A, Murali T, Suriyaphol P, Malasit P, Limjindaporn T, Finley RL Jr. Identification of new protein interactions between dengue fever virus and its hosts, human and mosquito. *PLoS One*. 2013. 8(1): e53535.
- 157. Doolittle JM, Gomez SM. Mapping Protein Interactions between Dengue Virus and Its Human and Insect Hosts. *PLoS Negl Trop Dis.* 2011. 5(2): e954.
- 158. Alcalá AC, Palomares LA, Ludert JE. Secretion of Nonstructural Protein 1 of Dengue Virus from Infected Mosquito Cells: Facts and Speculations. *J Virol*. 2018. 29, 92(14): e00275-18.
- 159. Kumar R, Singh N, Abdin MZ, Patel AH and Medigeshi GR. Dengue Virus Capsid Interacts with DDX3X–A Potential Mechanism for Suppression of Antiviral Functions in Dengue Infection. *Front Cell Infect Microbiol*. 2018. 7: 542.
- 160. Morrison J, García-Sastre A. STAT2 signaling and dengue virus infection. *JAKSTAT*. 2014. 1, 3(1): e27715.
- 161. Vogt MB, Lahon A, Arya RP, Clinton JLS, Hesse, RR. Dengue viruses infect human megakaryocytes, with probable clinical consequences. *PLoS Negl Trop Dis*. 2019. 13(11): 1–23.
- 162. Lahon ARP, and Banerjea, AC. Dengue Virus Dysregulates Master Transcription Factors and PI3K/AKT/mTOR Signaling Pathway in Megakaryocytes. 2021. Front Cell Infect Microbiol 26(11): 715208.

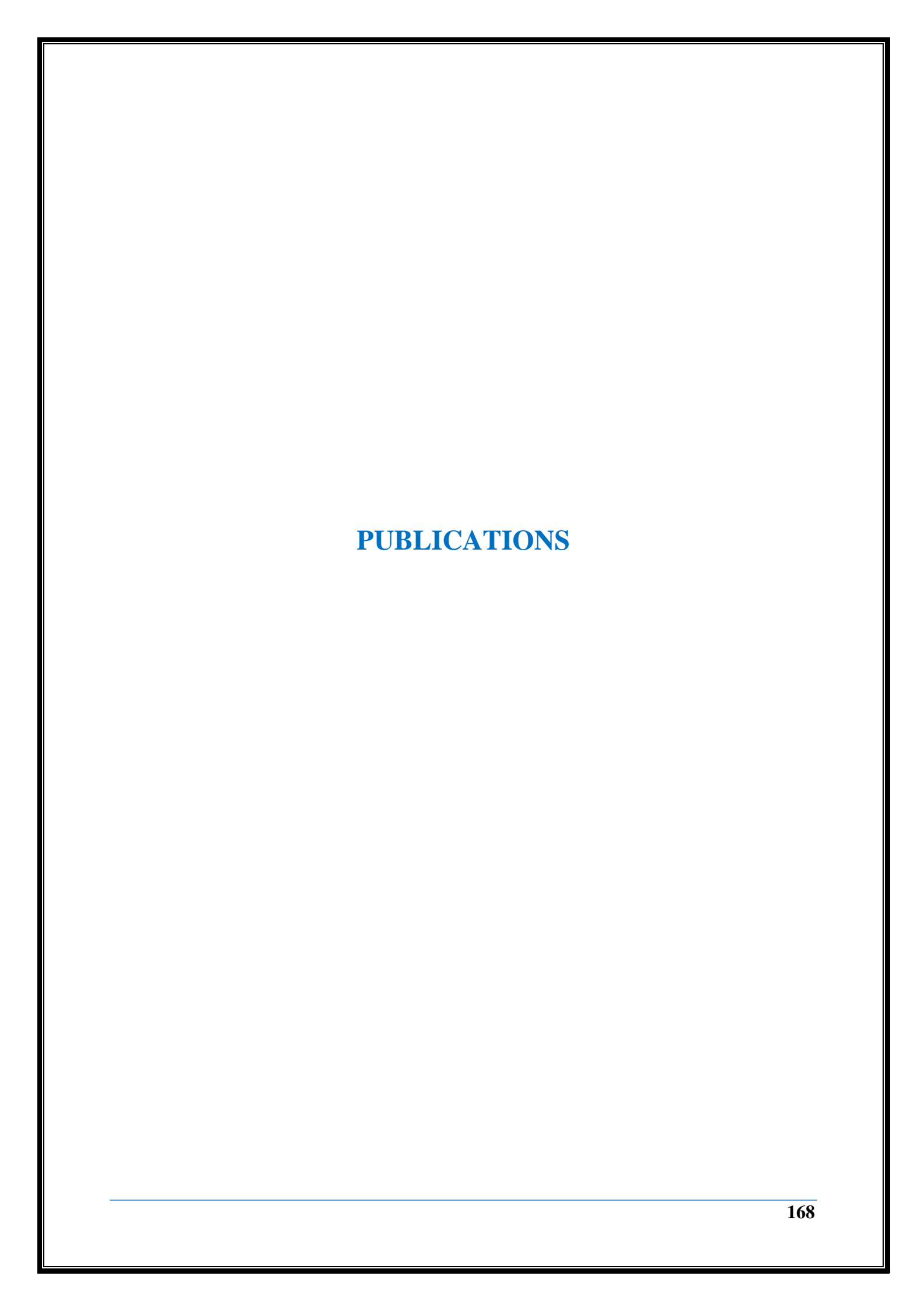
- 163. Wang D, Ma S, Wang S, and Shen B. Antisense EDRF1 gene inhibited transcription factor DNA-binding activity in K562 cells. *Sci China C Life Sci*. 2002. 45(3): 89-97.
- 164. Goldfarb, AN. Transcriptional control of megakaryocyte development. *Oncogene*. 2007. 26(47): 6795-6802.
- 165. Xin W, Duncheng W, Xing C, Meiru HU, Jianan W, Yan LI, Ning G, Beifen S. cDNA cloning and function analysis of two novel erythroid differentiation related genes. *Sci China C Life Sci.* 2001. 44 (1): 99-105.
- 166. Duncheng W, Yan LI, and Beifen S. Initial function analysis of a novel erythroid differentiation related gene EDRF1. *Sci in China*. 2001. 44(5): 489-496.
- 167. Kuhl C, Atzberger A, Iborra F, Nieswandt B Porcher C, and Vyas P. GATA-1-mediated megakaryocyte differentiation and growth control can be uncoupled and mapped to different domains in GATA1. *Mol Cell Biol.* 2005. 25(19): 8592-8606.
- 168. Boulanger L, Sabatino DE, Wong EY, Cline AP, Garrett LJ, Garbarz M, Dhermy D, *et al.* Erythroid expression of the human alpha-spectrin gene promoter is mediated by GATA-1- and NF-E2-binding proteins. *J. Biol. Chem.* 2002. 277(44): 41563-41570.
- 169. Patel HS, Wang H, Begonja AJ, Thon JN, Alden EC, Wandersee NJ, *et al.* The spectrin-based membrane skeleton stabilizes mouse megakaryocyte membrane systems and is essential for proplatelet and platelet formation. *Blood.* 2011. 118(6): 1641–1652.
- 170. Ghalloussi D, Dhenge A, and Bergmeier W. New insights into cytoskeletal remodeling during platelet production. *J. Thromb. Haemost.* 2017. 17: 1430–1439.
- 171. Gomes AP, Blenis J. A nexus for cellular homeostasis: the interplay between metabolic and signal transduction pathways. *Curr Opin Biotechnol*. 2015. 34:110-117.
- 172. Wilson DF and Matschinsky FM. Metabolic Homeostasis in Life as We Know It: Its Origin and Thermodynamic Basis. *Front Physiol.* 2021. 2: 658997.

- 173. Karve TM, Cheema AK. Small changes huge impact: the role of protein posttranslational modifications in cellular homeostasis and disease. *J Amino Acids*. 2011. 207691.
- 174. Osellame LD, Blacker TS, Duchen MR. Cellular and molecular mechanisms of mitochondrial function. *Best Pract Res Clin Endocrinol Metab*. 2012. 26(6): 711-723.
- 175. Oldstone MB, Sinha YN, Blount P, Tishon A, Rodriguez M, von Wedel R, Lampert PW. Virus-induced alterations in homeostasis: alteration in differentiated functions of infected cells in vivo. Science. 1982.10, 218(4577): 1125-1127.
- 176. Anand SK, Tikoo SK. Viruses as modulators of mitochondrial functions. *Adv Virol*. 2013. 2013: 738794.
- 177. McBride HM, Neuspiel M, Wasiak S. Mitochondria: more than just a powerhouse. *Current Biology*. 2006. 16(14): R551–R560.
- 178. Chen H, Chan DC. Emerging functions of mammalian mitochondrial fusion and fission. *Human Molecular Genetics*. 2005. 14(2): R283–R289
- 179. Saxena R, Sharma P, Kumar S, Kumar N, Agrawal N, Sharma SK, and Awasthi, A. Modulation of mitochondria by viral proteins. 2023. *Life Sci.* 313:121271.
- 180. Gu X, Ma Y, Liu Y, and Wan Q. Measurement of mitochondrial respiration in adherent cells by Seahorse XF96 Cell Mito Stress Test. *STAR Protoc*. 2020. 2(1): 100245.
- 181. https://www.agilent.com/en/product/cell-analysis/real-time-cellmetabolicanalysis/xf-software/agilent-seahorse-analytics-787485.
- 182. Hill BG, Benavides GA, Lancaster JR, Ballinger S, Dell'Italia L, Jianhua Z, and Darley-Usmar VM. Integration of cellular bioenergetics with mitochondrial quality control and autophagy. *Biol Chem.* 2012. 393(12): 1485-1512.

- 183. El-Bacha T, Midlej V, Pereira da Silva, AP, Silva da Costa, L, Benchimol, M, Galina, A, and Da Poian, AT. Mitochondrial and bioenergetic dysfunction in human hepatic cells infected with dengue 2 virus. *Biochim Biophys Acta*. 2007. 1772(10): 1158-1166.
- 184. Singh B, Avula K, Sufi SA, Parwin N, Das S, Alam MF, Samantaray S, Bankapalli L, Rani, A, Poornima, K, *et al.* Defective Mitochondrial Quality Control during Dengue Infection Contributes to Disease Pathogenesis. *J. Virol.* 2022. 96(20): e0082822.
- 185. Hottz ED, Oliveira MF, Nunes PC, Nogueira RM, Valls-de-Souza R, Da Poian AT, Weyrich AS, *et al.* Dengue induces platelet activation, mitochondrial dysfunction and cell death through mechanisms that involve DC-SIGN and caspases. *J. Thromb. Haemost.* 2013. 11(5): 951-62.
- 186. Gandhi L, Maisnam D, Rathore D, Chauhan P, Bonagiri A, Venkataramana M. Respiratory illness virus infections with special emphasis on COVID-19. *Eur J Med Res*. 2022. 8, 27(1): 236.
- 187. Murtuja S, Shilkar D, Sarkar B, Sinha BN, Jayaprakash V. A short survey of dengue protease inhibitor development in the past 6 years (2015-2020) with an emphasis on similarities between DENV and SARS-CoV-2 proteases. *Bioorg Med Chem.* 2021. 1, 49: 116415.
- 188. Knyazhanskaya E, Morais MC, Choi KH. Flavivirus enzymes and their inhibitors. *Enzymes*. 2021. 49:265-303.
- 189. Lv Z, Chu Y, Wang Y. HIV protease inhibitors: a review of molecular selectivity and toxicity. *HIV AIDS (Auckl)*. 2015. 8, 7: 95-104.
- 190. de Leuw P, Stephan C. Protease inhibitors for the treatment of hepatitis C virus infection. *GMS Infect Dis.* 2017. 28, 5: Doc08.
- 191. Chia LY, Kumar PV, Maki MAA, Ravichandran G, Thilagar S. A Review: The Antiviral Activity of Cyclic Peptides. *Int J Pept Res Ther*. 2023. 29(1): 7.

- 192. Ganji L.R, Gandhi L, Venkataramana Musturi, Meena A. Kanyalkar. Design, synthesis, and evaluation of different scaffold derivatives against NS2B-NS3 protease of dengue virus. *Med Chem Res.* 2021. 30: 285–301.
- 193. Hwu JR, Hsu MH, Huang RC. New nordihydroguaiaretic acid derivatives as anti-HIV agents. *Bioorg Med Chem Lett.* 2008. 15,18(6): 1884-1888.
- 194. Lambert JD, Zhao D, Meyers RO, Kuester RK, Timmermann BN, Dorr RT. Nordihydroguaiaretic acid: hepatotoxicity and detoxification in the mouse. *Toxicon*. 2002. 40(12): 1701-1708.
- 195. Senthilvel P, Lavanya P, Kumar KM, Swetha R, Anitha P, Bag S, *et al.* Flavonoid from Carica papaya inhibits NS2B-NS3 protease and prevents Dengue 2 viral assembly. *Bioinformation*. 2013.11, 9(18): 889-895.
- 196. de Sousa LR, Wu H, Nebo L, Fernandes JB, da Silva MF, Kiefer W, Kanitz M, Bodem J, Diederich WE, Schirmeister T, Vieira PC. Flavonoids as noncompetitive inhibitors of Dengue virus NS2B-NS3 protease: inhibition kinetics and docking studies. *Bioorg Med Chem.* 2015. 1, 23(3): 466-70.
- 197. Manda G, Rojo AI, Martínez-Klimova E, Pedraza-Chaverri J, Cuadrado A. Nordihydroguaiaretic Acid: From Herbal Medicine to Clinical Development for Cancer and Chronic Diseases. *Front Pharmacol.* 2020. 28, 11: 151.
- 198. Nusrat S, Zaidi N, Zaman M, Islam S, Ajmal M. R, Siddiqi M. K, *et al.* Repositioning nordihydroguaiaretic acid as a potent inhibitor of systemic amyloidosis and associated cellular toxicity. *Arch Biochem Biophys.* 2021. 612: 78–90.
- 199. Cui Q, Du R, Liu M, Rong L. Lignans and Their Derivatives from Plants as Antivirals. *Molecules*. 2020. 25: 183.

- 200. Villalobos-Sánchez E, García-Ruiz D, Camacho-Villegas T.A, Canales-Aguirre A.A, Gutiérrez-Ortega A, Muñoz-Medina J.E, Elizondo-Quiroga, D.E. *In Vitro* Antiviral Activity of Nordihydroguaiaretic Acid against SARS-CoV-2. *Viruses*. 2023. 15: 1155.
- 201. Chen Hongshan, Chen H, Teng L, Li JN, Park R, Mold DE, Gnabre J. "Antiviral activities of methylated nordihydroguaiaretic acids. 2. Targeting herpes simplex virus replication by the mutation insensitive transcription inhibitor tetra-O-methyl-NDGA." *Journal of medicinal chemistry*.1998. 41,16: 3001-300.
- 202. Soto-Acosta R, Bautista-Carbajal P, Cervantes-Salazar M, Angel-Ambrocio AH, Del Angel RM. DENV up-regulates the HMG-CoA reductase activity through the impairment of AMPK phosphorylation: A potential antiviral target. *Plos Pathogens*. 2017. 13(4): e1006257.
- 203. De Clercq E. Potential antivirals and antiviral strategies against SARS coronavirus infections. *Expert Rev Anti Infect Ther*. 2006. 4(2): 291-302.
- 204. Chaniad P, Techarang T, Phuwajaroanpong A, Plirat W, Na-Ek P, Konyanee A, Viriyavejakul P, Septama A.W, & Punsawad C. Preclinical evaluation of antimalarial activity of CPF-1 formulation as an alternative choice for the treatment of malaria. *BMC Complementary Med Therap.* 2023. 4, 23(1): 144.
- 205. Indrayanto G, Putra GS, & Suhud F. Validation of in-vitro bioassay methods: Application in herbal drug research. *Profiles Drug Subst Excip Relat Methodol*. 2021. 46: 273-307.



PUBLICATIONS

List of Publications:

- **1. Lekha Gandhi** and Musturi Venkataramana. Simultaneous detection of dual subcellular localized dengue virus protease by co-transfection. 2023. *STAR protocols* (Accepted).
- **2. Gandhi L,** Maisnam D, Rathore, D, Chauhan P, Bonagiri A. and Venkataramana, M., Differential localization of dengue virus protease affects cell homeostasis and triggers to thrombocytopenia. *iScience*. 2023. 26, (7):10702. https://doi.org/10.1016/j.isci.2023.107024
- **3. Gandhi L**, Maisnam, D, Rathore, Chauhan P, Bonagiri A, Venkataramana M. Respiratory illness virus infections with special emphasis on COVID-19. *Eur J Med Res*, 2022. 27:236. https://doi.org/10.1186/s40001-022-00874-x.
- **4.** Gandikota C, **Gandhi L**, Maisnam D, Kesavulu MM, Billoria A, Prasad VSV, and Venkataramana M. A novel anti-NS2BNS3pro antibody-based indirect ELISA test for the diagnosis of dengue virus infections. *J Med Virol*. 2021. 93(6):3312-3321. doi: 10.1002/jmv.26024.
- **5.** Gandikota C, Mohammed F, **Gandhi L**, Maisnam D, Mattam U, Rathore D, Chatterjee A, Mallick K, Billoria A, Prasad VSV, Sepuri NBV, Venkataramana M. Mitochondrial Import of Dengue Virus NS3 Protease and Cleavage of GrpEL1, a Cochaperone of Mitochondrial Hsp70. *J Virol.* 2020. 17,94(17): e01178-20. doi: 10.1128/JVI.01178-20.
- **6.** Ganji L.R, **Gandhi L,** Venkataramana Musturi, Meena A. Kanyalkar. Design, synthesis, and evaluation of different scaffold derivatives against NS2B-NS3 protease of dengue virus. *Med Chem Res.* 2021**30**: 285–301. https://doi.org/10.1007/s00044-020-02660-y.

In process:

1. Deepika Rathore, Preeti Chauhan, Anvesh Bonagiri, Lekha Gandhi, Deepti Maisnam,

Ramesh Kumar, Anupama T Row, M Kesavulu. Novel epitopes of SARS CoV2 spike protein

exhibit immunodominance as they elicit both innate and adaptive immune responses. (Under

communication).

2. Evaluation of NDGA synthetic derivatives as anti-protease molecules. (Manuscript under

preparation)

Patent Granted:

1. Title: Design, synthesis and evaluation of T4N and B4N, the derivatives of NDGA as

potential inhibitors of dengue virus protease.

Inventors: Ms. Chaitanya G, Ms. Lekha Gandhi, Dr. Musturi Venkataramana, Prof. Naresh

Babu Sepuri, Mr. Y.S. Ravi Kumar.

Patent No: 433631

Patent application no.: 201941014858

Patent Date Filed: 12-04-2019

2. Patent Filed: A novel anti-NS2BNS3pro antibody-based indirect ELISA test for the

diagnosis of dengue virus infections.

Inventors: Dr. Musturi Venkataramana, Ms. Chaitanya Gandikota, Ms. Lekha Gandhi, Ms.

Deepti Maisnam.

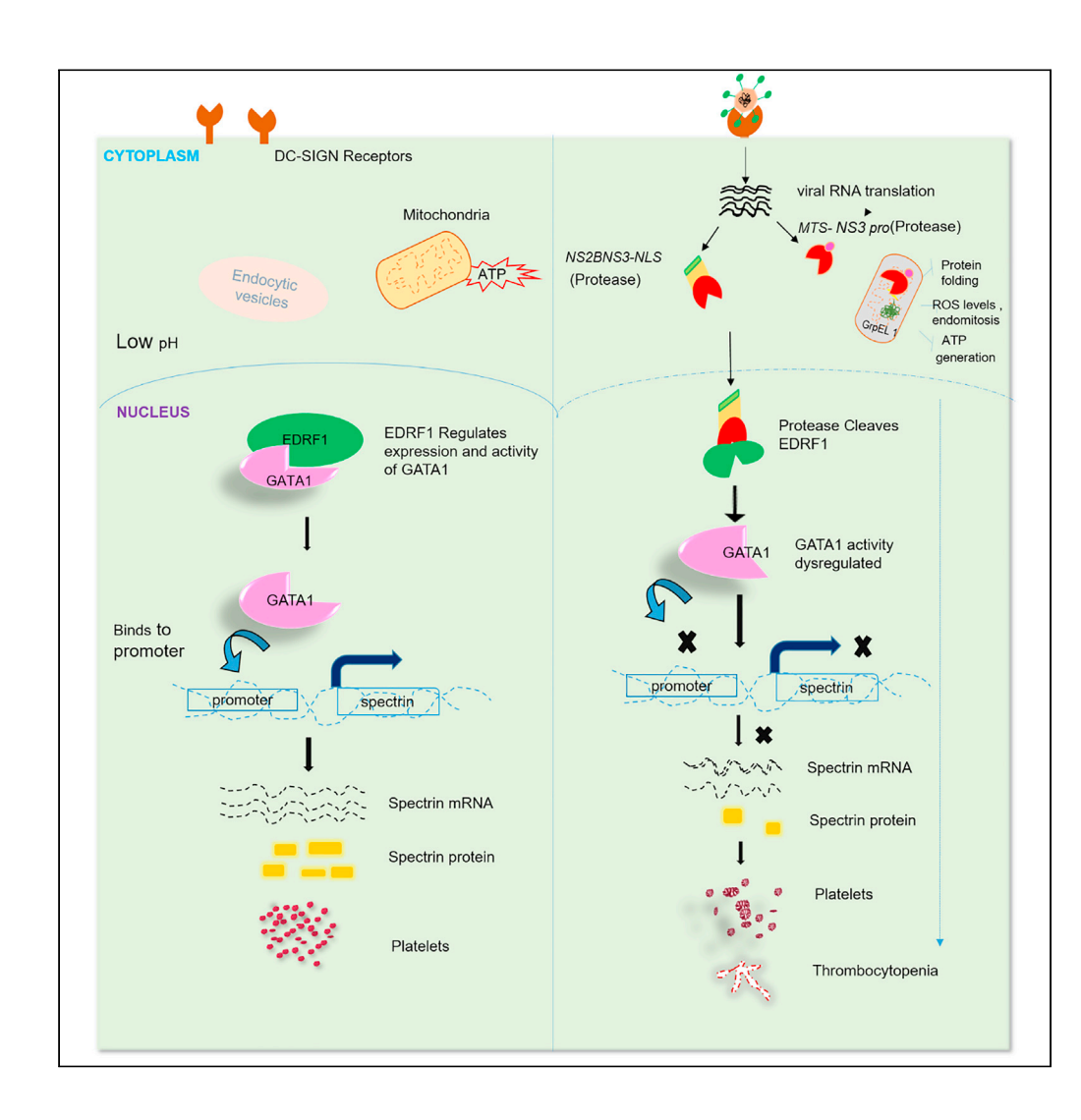
170

iScience



Article

Differential localization of dengue virus protease affects cell homeostasis and triggers to thrombocytopenia



Lekha Gandhi, Deepti Maisnam, Deepika Rathore, Preeti Chauhan, Anvesh Bonagiri, Musturi Venkataramana

mvrsl@uohyd.ernet.in

Highlights

Dengue virus protease exists in two forms i.e. non-structural protein-3 (NS3) and NS2BNS3

NS3 localizes to both mitochondria and nucleus whereas NS2BNS3 localizes to nucleus only

NS3 cleaves GrpEL1 of mitochondrial matrix, and NS2BNS3 cleaves EDRF1 of the nucleus

EDRF1 cleavage by NS2BNS3 and mitochondrial dysfunction by NS3 account for thrombocytopenia

Gandhi et al., iScience 26, 107024 July 21, 2023 © 2023 The Author(s). https://doi.org/10.1016/ j.isci.2023.107024



iScience



Article

Differential localization of dengue virus protease affects cell homeostasis and triggers to thrombocytopenia

Lekha Gandhi,¹ Deepti Maisnam,¹ Deepika Rathore,¹ Preeti Chauhan,¹ Anvesh Bonagiri,¹ and Musturi Venkataramana^{1,2,*}

SUMMARY

Thrombocytopenia is one of the symptoms of many virus infections which is the "hallmark" in the case of dengue virus. In this study, we show the differential localization of existing two forms of dengue virus protease, i.e., NS2BNS3 to the nucleus and NS3 to the nucleus and mitochondria. We also report a nuclear transcription factor, erythroid differentiation regulatory factor 1 (EDRF1), as the substrate for this protease. EDRF1 regulates the expression and activity of GATA1, which in turn controls spectrin synthesis. Both GATA1 and spectrins are required for platelet formation. On the other hand, we found that the mitochondrial activities will be damaged by NS3 localization which cleaves GrpEL1, a co-chaperone of mitochondrial Hsp70. Levels of both EDRF1 and GrpEL1 were found to deteriorate in dengue virus-infected clinical samples. Hence, we conclude that NS2BNS3-mediated EDRF1 cleavage and the NS3-led mitochondrial dysfunction account for thrombocytopenia.

INTRODUCTION

Nearly 130 countries are endemic for dengue virus infections, primarily affecting 2.5 billion inhabitants in the tropical and subtropical regions as well as 120 million travelers to these regions every year. The World Health Organization (WHO) reported an 8-fold increase in dengue cases in the past two decades with approximately 5.2 million cases in the year 2019 alone. ^{1,2} Most of the clinical literature reviews suggest that dengue infection shows asymptomatic or mild symptoms of flu like in dengue fever (DF), severe symptoms like dengue hemorrhagic fever (DHF), and dengue shock syndrome (DSS). Dengue fever manifests symptoms of headache, rashes, muscle soreness, joint pain, retro-orbital pain, and abdominal cramps. DHF is characterized by red or purple blisters on the skin, epistaxis, and gingival bleeding. Thrombocytopenia (low platelet count) and leukopenia were observed mainly during dengue fever with hemorrhagic signs. ^{3,4} In 2009, WHO guidelines defined thrombocytopenia as a major clinical symptom, with a rapid decline in platelet count (i.e., <1, 50, 000 per microliters of blood). ^{1,4}

Dengue virus (DENV) is a flavivirus of family flaviviridae. There are four distinct serotypes (DENV1-4) that have emerged from sylvatic strains in the forests of Southeast Asia. DENV is an enveloped, single-stranded positive-sense RNA virus. The RNA genome consists of approximately 10,700 nucleotides and codes nearly 3,411 amino acids (a.a) long precursor polyprotein yielding three structural proteins (Capsid (C), precursor Membrane (preM), and Envelope (E) and seven non-structural (NS) proteins (NS1, NS2A, NS2B, NS3, NS4A, NS4B, and NS5).^{5,6} Among NS proteins that play significant roles during viral replication, NS3 alone or along with NS2B possesses a crucial role and is the prime drug target for developing the anti-virals. NS2B is a 14-15 kDa amphipathic membrane protein and acts as a cofactor for NS3 protein to form an active viral protease complex.^{7,8} NS2B contains two transmembrane hydrophobic domains and a hydrophilic central domain. The hydrophilic region of 40 amino acid residues linked with G4-S-G4 linker to N-terminal of NS3 protein forming the NS2BNS3pro active protease. 8,9 NS3 is a 70 kDa, a multifunctional serine protease forming the catalytic triad with Histidine (H-51), Aspartate (D-75), and Serine (S-135). Its helicase and nucleoside triphosphatase (NTPase) activities are required for unwinding the double-stranded form of RNA. 10 The N-terminal region forms the protease domain (1–185 residues). NS3 helicase (185–618 residues) belongs to the helical superfamily 2 domain. NS2BNS3pro complex processes polyprotein into mature functional proteins which are required for virus assembly and replication. The C-terminal of NS3 forms a



¹Department of Biotechnology and Bioinformatics, School of Life Sciences, University of Hyderabad, Hyderabad, Telangana, India

²Lead contact

^{*}Correspondence: mvrsl@uohyd.ernet.in

https://doi.org/10.1016/j.isci. 2023.107024





subdomain with essential motifs, subdomain 1 and 2: recombinase A (RecA)like fold and structural motifs required for ATP hydrolysis and RNA binding activities. The other subdomain 3 is involved in forming a single-stranded DNA (ssDNA) binding tunnel during the formation of replication complex.^{6,8} Cleavage site for DENV protease possesses the dibasic amino acids (Lys-Arg, Arg-Arg, Arg-Lys, Gln-Arg) at P1/P2 followed by a small residue (Gly/Ala/Ser) at P1'. 10-12 Reports suggest that the substrate cleavage site for dengue protease is Arg/Lys-Ser-Arg-Ile/Val-Leu at P1-P4'. 13 Along with cleaving the functional polypeptides, DENV protease is known to cleave host cellular proteins FAM134B (endoplasmic receptor), $Ik\alpha/\beta$ (cellular factors), Nucleoporins (Nups), mediator of IRF3 activation (MITA), mitofusins (MFN1 and 2), thereby enhancing the viral replication and affecting host metabolism. ^{14–18} During natural infections, dengue virus primarily infects bone marrow cells, myeloid lineages, macrophages, dendritic cells, B and T cells, neuronal cells, and hepatocytes. ^{19,20} The NS protein-3 (NS3) was found to accumulate in phagocytes of spleen and lymph node, liver hepatocytes, and myeloid cells in bone marrow.²¹ Among these cells, bone marrow megakaryocytes (MKs) are highly permissible to infection. Previous reports showed that the dengue virus infection in megakaryocytes with a reduction in cell number with depleting mature megakaryocytes suggests the role of dengue virus in bone marrow homeostasis. Further, it has been reported that the dengue virus abolishes the expression of master transcription factors GATA binding factors 1 and 2 (GATA1, GATA2) and nuclear factor erythroid 2 (NF-E2) which are involved in megakaryocytic developmental processes.^{22,23} Although the reports of dengue virus infection in vitro, ex vivo, and in vivo models have been studied, the mechanism behind the reduction in platelet cell number causing thrombocytopenia has not yet been clearly understood. 20,24,25

Virus-mitochondria interaction is being revealed in several reports suggesting mitochondrial dysfunction. ^{26,27} Reports also indicate that the virus-coded proteases cleave the mitochondrial proteins. In the case of dengue virus also NS proteins like NS4B and NS2BNS3 target the mitochondrial membranes. ¹⁸ NS3 is reported to target the mitochondrial matrix and cleaves the GrpE Like 1 (GrpEL1), a co-chaperone of mitochondrial heat shock protein (mtHSP70). ²⁸ The cleavage sites in the dengue virus polyprotein and the nature of the protease activity appear to yield two forms of the protease, i.e., NS2BNS3 and NS3 alone. ¹² In addition to the mitochondrial targeting by the dengue virus protease, it was also detected in the host nucleus. ^{16,29} But whether it is NS2BNS3 or NS3 or both is not known. Hence this study gave an attempt to reveal the localization of NS2BNS3 and NS3, identification of substrates, and consequences with reference to cell homeostasis.

Thrombocytopenia, i.e., reduced platelets is a health disorder that occurs during different ill health conditions including many viral infections which led to the death of millions of people across the globe. Dengue virus infections are known from ancient times which cause "thrombocytopenia" as the primary symptom. Platelet activation, their clearance, and plasma leakage are proposed as the reasons for the platelet reduction in dengue virus patients. $^{30-34}$ But, to the best of our knowledge, there is no clear study explaining the mechanism involving the virus components in thrombocytopenia. The studies on dengue virus protease (including our report published in the Journal of Virology, 2020²⁸) puzzle the scientific community regarding its role in disease pathogenesis. The findings of our present study suggest the localization of dengue virus protease in two subcellular organelles of a cell, i.e., nucleus and mitochondria. There is no such instant indicating the dual localization of a single protein coded by a virus genome. A crucial nuclear transcription factor called EDRF1 (erythroid differentiation regulatory factor 1) is found as the another substrate for this protease. Ex vivo and in vivo (dengue virus-infected clinical samples) analyses clearly supported the above observation. EDRF1, in turn, regulates another two factors (GATA1 and Spectrins) of the cells (play a key role in proplatelet and platelet formation) which are also downregulated in protease-transfected or virus-infected conditions. Dengue virus-infected K562 cells (megakaryocyte derived) show reduced cell number as the number of days progressed. Mitochondrial dysfunction of the protease-transfected cells was observed which also accounts for the reduction in cell number. Therefore, we felt that this study gave the molecular-level explanation for thrombocytopenia and facilitates focused therapeutic development.

RESULTS

Identification of nuclear localization signals (NLSs) and development of recombinant constructs

Using *in silico* method, NLS sequences were identified in both NS2BNS3 (594 a.a) and NS3pro-helicase (464 a.a). In NS2B (130 a.a), three basic amino acid residues 1471 KKKQR 1475 at position 1471–1475 were identified

iScience Article



A NS2BNS3

LNEGIMAVGIVSILLSSLLKNDVPLAGPLIAGGMLIACYVISGSSADLSLEKAAEVLWEEEAEHSGASHNILVEVQDDGTMKIKDEERDDTLTILLKATLLAVSGV YPMSIPATLFVWYFWQKKKQRSGVLWDTPSPPEVERAVLDDGIYRILQRGLLGRSQVGVGVFQDGVFHTMWHVTRGAVLMYQGKRLEPSWASVKKDLISY GGGWRLQGSWNTGGEVQVIAVEPGKNPKNVQTTPGTFKTPEGEVGAIALDFKPGTSGSPIVNREGKIVGLYGNGVVTTSGTYVSAIAQTKASQEGPLPEIED EVFKKRNLTIMDLHPGSGKTRRYLPAIVREAIKRKLRTLILAFTRVVASEMAEALKGMPIRYQTTAVKSEHTGREIVDLMCHATFTMRLLSPVRVPNYNMIIMDE AHFTDPASIAARGYISTRVGMGEAAAIFMTATPPGSVEAFPQSNAVIQDEERDIPERSWNSGYDWITDFPGKTVWFVPSIKSGNDIANCLRKNGKRVIQLSRK TFDTEYQKTKNNDWDYVVTTDISEMGANFRADRVIDPRRCLKPVILKDGPERVILAGPMPVTVASAAQRRGR

B NS3pro-helicase

MLDDGIYRILQRGLLGRSQVGVGVFQDGVFHTMWHVTRGAVLMYQGKRLEPSWASVKKDLISYGGGWRLQGSWNTGEEVQVIAVEPGKNPKNVQTTP GTFKTPEGEVGAIALDFKPGTSGSPIVNREGKIVGLYGNGVVTTSGTYVSAIAQTKASQEGPLPEIEDEVF*KKR*NLTIMDLH*P*GSGKTRRYLPAIVREAI*KRK* LRTLIAPTRVVASEMAEALKGMPIRYQTTAVKSEHTGREIVDLMCHATFTMRLLSPVRVPNYNMIIMDEAHFTDPASIAARGYISTRVGMGEAAAIFMTATP PGSVEAFPQSNAVIQDEERDIPERSWNSGYDWITDFPGKTVWFVPSIKSGNDIANCL*RK*NGKRVIQLSRKTFDTEYQKTKNNDWDYVVTTDISEMGANFR ADRVIDPRRCLKPVILKDGPERVILAGPMPVTVASAAQRRGR

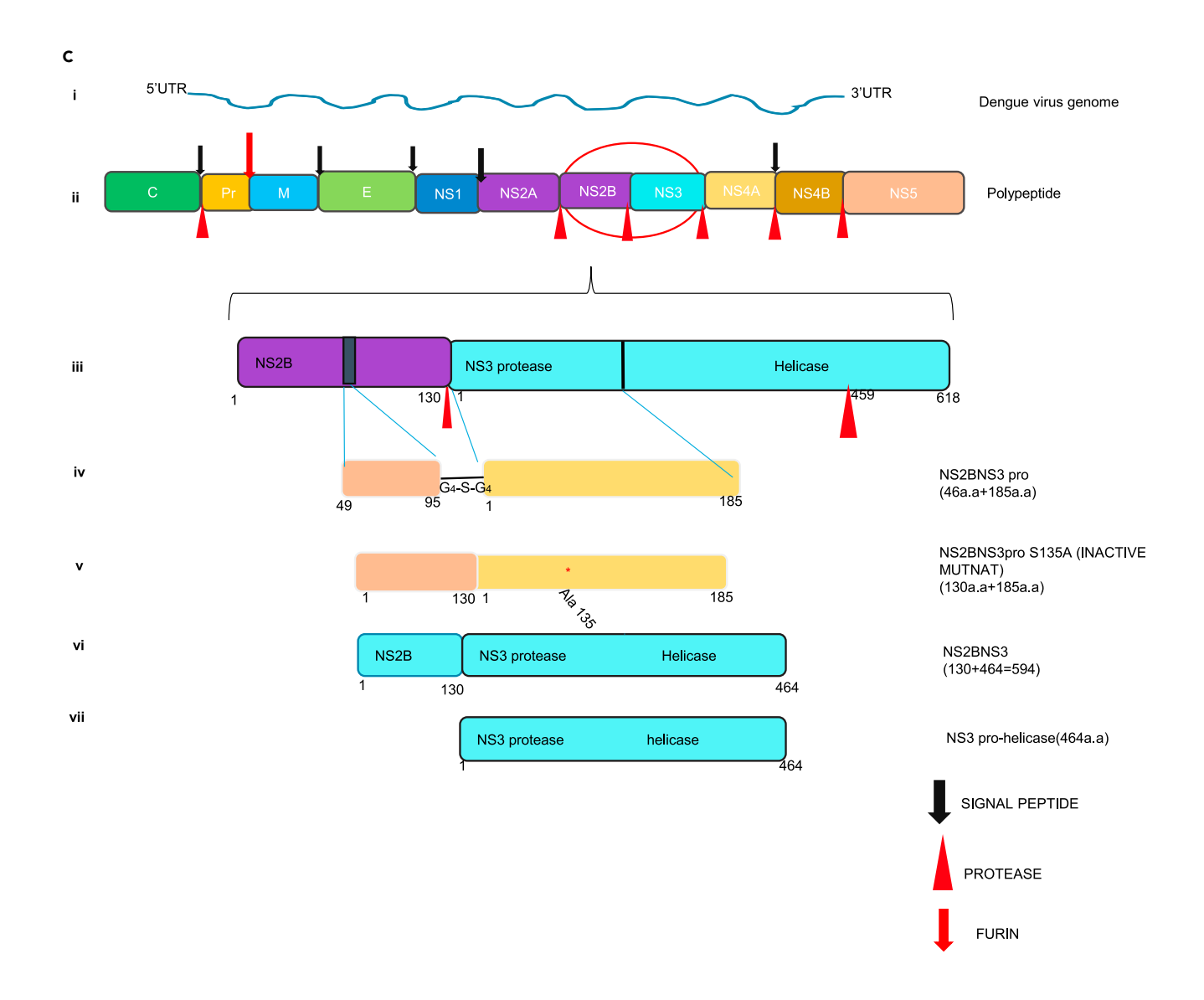






Figure 1. Amino acid sequence of protease and genome organization

(A and B) NS2BNS3 (NS2B-130+NS3-464 = 594 a.a) (B) NS3pro-helicase (464 a.a). Amino acid sequence showing the nuclear localization sequence (NLS) in green and mitochondrial targeting sequence (MTS) in red. Full-length NS2B sequence in (blue) and NS3 sequence in (black). (C) (i) Dengue virus genome (RNA) (ii) Dengue virus mature polypeptide showing structural proteins (capsid, pre-membrane, and envelope) and non-structural proteins (NS1 – NS5). (iii) Dengue virus full-length protease with NS2B and NS3 fragments. (iv) NS2B (46 a.a) Glycine linked (G4-S-G4) NS3 protease (185 a.a). (v) Mutant form of NS2BNS3pro (S135A) (NS2B – 130 a.a and NS3pro-185 a.a). (vi) NS2BNS3 (130 + 464 a.a) (vii) NS3 pro-helicase (464 a.a).

which are similar to classical monopartite NLS stretch that consists of basic amino acid residues with motif K (K/R) X (K/R). In NS3 sequence, two stretches of bipartite signal (2–3 positively charged amino acid followed by 9–12 linker sequence containing proline residue) were identified at positions (a.a 1656–1716 and 1839–1856) with a score of 4–4.1 (Figures 1A and 1B). The mitochondrial targeting sequence (MTS) was identified in NS3 during our earlier study. Based on these analyses the recombinant constructs NS2BNS3pro (46 + 185 a.a), NS2BNS3pro (S135A) mutant (130 + 185 a.a), NS2BNS3 (594 a.a), and NS3pro-helicase (464 a.a) were generated (Figure 1C) as detailed in methods.

Protease localization studies

We performed transfections in K562 cells and analyzed at 20 x magnification for the transfection efficiency, and the data suggested that 50–60% of the cells are positively transfected (Figure S1). Further, the data indicated that the expressed proteins (GFP-tagged) of all three constructs (NS2BNS3pro, NS2BNS3pro (S135A) mutant, and NS2BNS3) localized to the nucleus compared to vector alone as the GFP was found to merge with the Hoechst stain (nucleus) (Figure 2A [viii, xi and xvi]). In the enhanced green fluorescent protein plasmid N-terminal (pEGFP-N1) vector, the intensity of the green peak is low and does not merge with blue peak, but in case of pEGFP-N1 NS2BNS3pro, pEGFP-N1 NS2BNS3pro (S135A) mutant and pEGFP-N1 NS2BNS3 show merged green peaks with blue peaks of varying intensities indicating the GFP expression in nucleus (Figure 2B [i-ivi]). The bar graphs further support the above observation with the high GFP/blue expression ratios which represent the percentage mean arbitrary intensity in the nucleus (Figure 2C).

The NS2BNS3 also possesses the MTS along with NLS; hence we intended to analyze the possibility of its localization to the mitochondria also. In this direction, the NS2BNS3 was transfected along with mitochondria red fluorescent protein (MitoRFP), stained with Hoechst stain and analyzed for the localizations. The data suggested GFP and the MitoRFP expression are not merged suggesting no localization of NS2BNS3 to the mitochondria (Figure 3A [viii]). This observation is further supported by the graphical analysis showing that the red peaks are completely separated from the green peaks (Figure 3B ii). It was further confirmed that NS2BNS3 localized in nucleus as indicated with a high-intensity peak of GFP (green peak) in the nuclear region (Figure 3C [ii]). But NS3 alone was reported to be localized to the mitochondrial matrix which shows both the MTS and NLS. In order to properly understand the localization of NS3 also, we carried out the transfections along with MitoRFP, stained with Hoechst stain, and analyzed the localizations in mitochondria and nucleus. The results show that NS3pro-helicase enters both mitochondria and nucleus as indicated by the intensity profiles where the GFP expression (green) is merging with red (mitochondria) and high GFP intensity in blue peak region (nucleus) (Figures 3A [xiii]; 2B [iiii]). The bar graphs which represent the percentage mean arbitrary intensity of each channel in the nucleus indicated the GFP expression in nucleus supporting the above observations (Figure 3D).

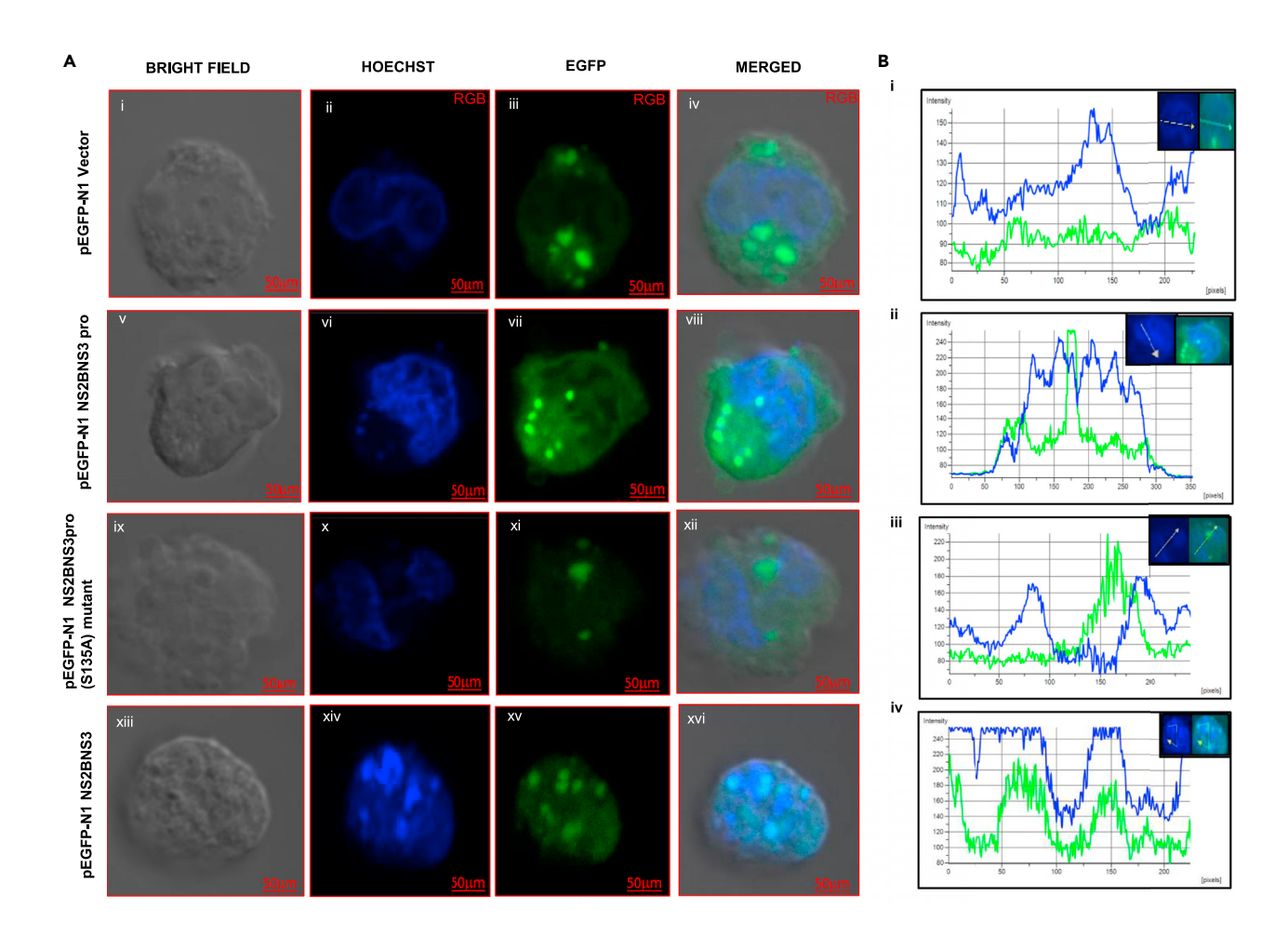
With the cell lysates of the above experiments, we have carried out the western blotting analysis (anti-NS2BNS3pro antibody) to verify the presence of protease forms that localize to nucleus or mitochondria or both. The immunoblotting results were found to be consistent with the above localization experiments suggesting that the NS3pro-helicase (75 kDa) localized to both cytoplasm (mitochondria) and nucleus (Figure 3E ii), whereas NS2BNS3 (92 kDa) localized only to the nucleus (Figure 3E i). We also observed a 70 kDa band in the nucleus (Figure 3E ii), possibly due to an internal self-cleavage site in NS2BNS3. Absence of actin (Figure 3E iii) and less GFP (Figure 3E iv) in nuclear fraction support the fractionations.

Identification of protease-interacting proteins

To identify the host factors interacting with NS2BNS3 protease, we performed *in vitro* nickel-nitrilotriacetic acid (Ni-NTA) pull-down assay with purified NS2BNS3pro incubating with K562 whole cell lysate (Figures 4A, 4B, S2A and S2B). Protein bands that appeared in elutes (E1-E4) were identified by matrix-assisted laser desorption ionization-time of flight (MALDI-TOFF) mass spectrometry. The identified bands







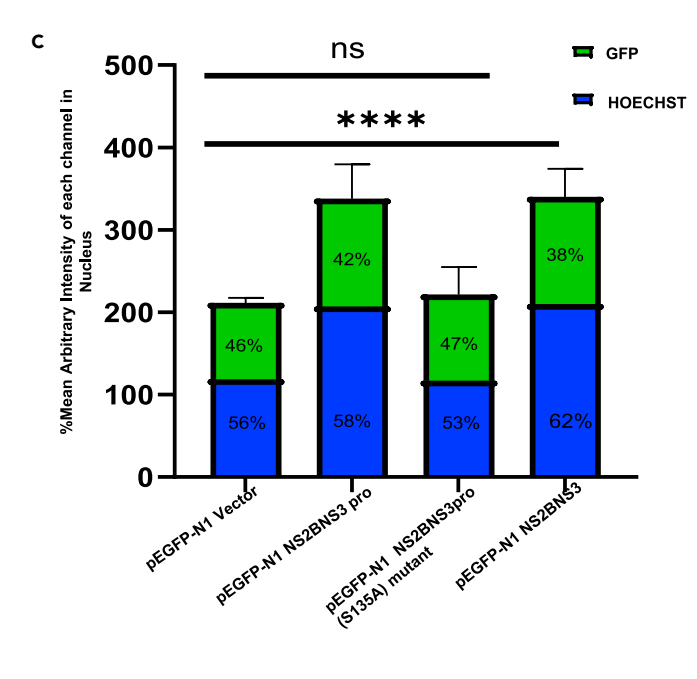






Figure 2. Localization of expressed dengue virus protease in K562 cells

(A) pEGFP-N1 vector (i-iv), pEGFP-N1 NS2BNS3pro (v-viii), pEGFP-N1 NS2BNS3pro (S135A) mutant (ix-xii), and pEGFP-N1 NS2BNS3 (xiii-xvi) were transfected transiently and observed after 28 h post transfection. The images represent the bright field (Gray), Hoechst33342 (nuclear staining blue), GFP (green) and merged at 100X (scale bar = $50\mu m$) magnification using Carl Zeiss confocal microscopy. See also Figure S1.

(B) i. Fluorescence intensity profiles using NIS Elements AR software of pEGFP-N1 vector showing GFP expression (green) in cytoplasm. ii-iv. pEGFP-N1 NS2BNS3pro, pEGFP-N1 NS2BNS3pro (S135A) mutant, and pEGFP-N1 NS2BNS3 show the expression in nucleus with different intensities.

(C) The bar graphs represent the percentage arbitrary mean intensity of each channel (Green and Blue) in nucleus of transfected cells presented as mean values (\pm) SD plotted in graph pad prism 9. The percentage was calculated using (mean intensity of each channel/total intensity in nucleus X100). ρ values indicated p < 0.0001, **** = significant, ns = non-significant.

from the above elutes were found to be EDRF1 (Figures 4C and 4D). Also, the Mascot search result supported the above finding that the identified protein EDRF1 has a score of 57 which is the highest among the list (Figure 4E). Western blot analysis using anti-EDRF1 antibody showed the presence of EDRF1 in elutes and beads thus confirming EDRF1 as a protease-interacting host protein (Figures 4F and 4G).

Identification of protease cleavage sites in EDRF1 using in silico methods

ProP-1.0 server identified a total of five cleavage sites (dibasic amino acid residues, i.e., Arg/Lys in P1/P2 position) at different amino acid sequence positions of EDRF1 (50,100,152,926,987) (Figure S2C). In order to know which of the above cleavage site is located near the catalytic triad of protease, we performed *in silico* docking method for analyzing the interactions of protease and EDRF1 by superimposed models (Figure S3A). It was observed that the cleavage site at a.a 985–988 of EDRF1 (cyan) interacted with the catalytic triad of protease (H-51, D-75, S-135) (green) (Figure S3B). Thus, we have developed a recombinant plasmid cloning DNA 3.1 (pcDNA3.1) c-myc vector containing the c-terminal end from amino acid 798 to 1238, approximately 50 kDa of EDRF1 (encompassing a.a 985–988 cleavage site) as described in STAR Methods.

EDRF1 cleavage in co-expressed conditions

The cell extracts co-expressed with both EDRF1 and protease were resolved on 10% SDS PAGE and transferred onto the hydrophilic polyvinylidene fluoride (PVDF) membrane. Western blot analysis was done to detect the levels of EDRF1 using anti-Myc tag antibody. The blot showed no band in co-transfected vectors as the Myc tag is only 1.2 kDa (very small to detect) (Figure 4H lane 1). In pcDNA3.1 c-myc containing EDRF1 as an insert, the EDRF1 band was detected as intact showing the presence of overexpressed EDRF1 alone (Figure 4H lane 2). As expected, no expression was observed in pcDNA3.1-myc vector alone (Figure 4H lane 3). Importantly, EDRF1 completely disappeared in presence of protease in co-transfected pcDNA3.1 c-myc EDRF1 and pEGFP-N1 NS2BNS3pro, suggesting EDRF1 as a substrate of protease (Figure 4H lane 4). pEGFP-N1 vector alone and pEGFP-N1 NS2BNS3pro lysates were loaded as controls (Figure 4H lanes 5 and 6).

To confirm the expression of NS2BNS3pro in the above experiment, we have checked the expression of protease using anti-GFP antibody (pEGFPN1-NS2BNS3pro) after stripping the same membrane. It was observed that, in co-transfected vectors and pEGFP-N1 vector alone, GFP was expressed (Figure 4J lanes 13 and 17). No band was observed in pCDNA3.1 c-myc EDRF1 and pCDNA3.1 c-myc vector alone using anti-GFP antibody (Figure 4J lanes 14 and 15). In co-transfected pcDNA3.1 c-myc EDRF1 and pEGFP-N1 NS2BNS3pro cell lysates, the protease was detected thus confirming the expression of NS2BNS3pro in the co-transfected conditions (Figure 4J lane 16). pEGFP-N1 NS2BNS3pro was also found to be expressed alone as a control (Figure 4J lane 18).

Analysis of levels of EDRF1, GATA1, and spectrins in protease-transfected and virus-infected cell lysates

The GATA1 expression and activity were reported to be regulated by EDRF1. 35-37 GATA1 in turn controls the synthesis of spectrin proteins which are required for pro-platelet and platelet formation. 38 EDRF1, a 138 kDa protein, is reported to be expressed in megakaryocytic (K562) and erythroid cell lineages. 35,36 Hence, we intended to analyze the levels of EDRF1, GATA1, and spectrins in protease-transfected and virus-infected K562 cells. For this purpose, total cell lysates of transfected/infected were resolved on 10% SDS PAGE followed by western blot analysis with anti-EDRF1 antibody. It was observed that EDRF1 levels were deteriorated significantly in presence of pEGFP N1 NS2BNS3pro as compared to the vector, concluding that EDRF1 was being cleaved by dengue virus protease (Figures 5A–5D). The same cell lysates were used to check the endogenous levels of GATA1 and spectrins. It was observed that, compared to pEGFP N1 vector alone, GATA1 and spectrin levels were found to be reduced (Figures 5A–5D). To confirm



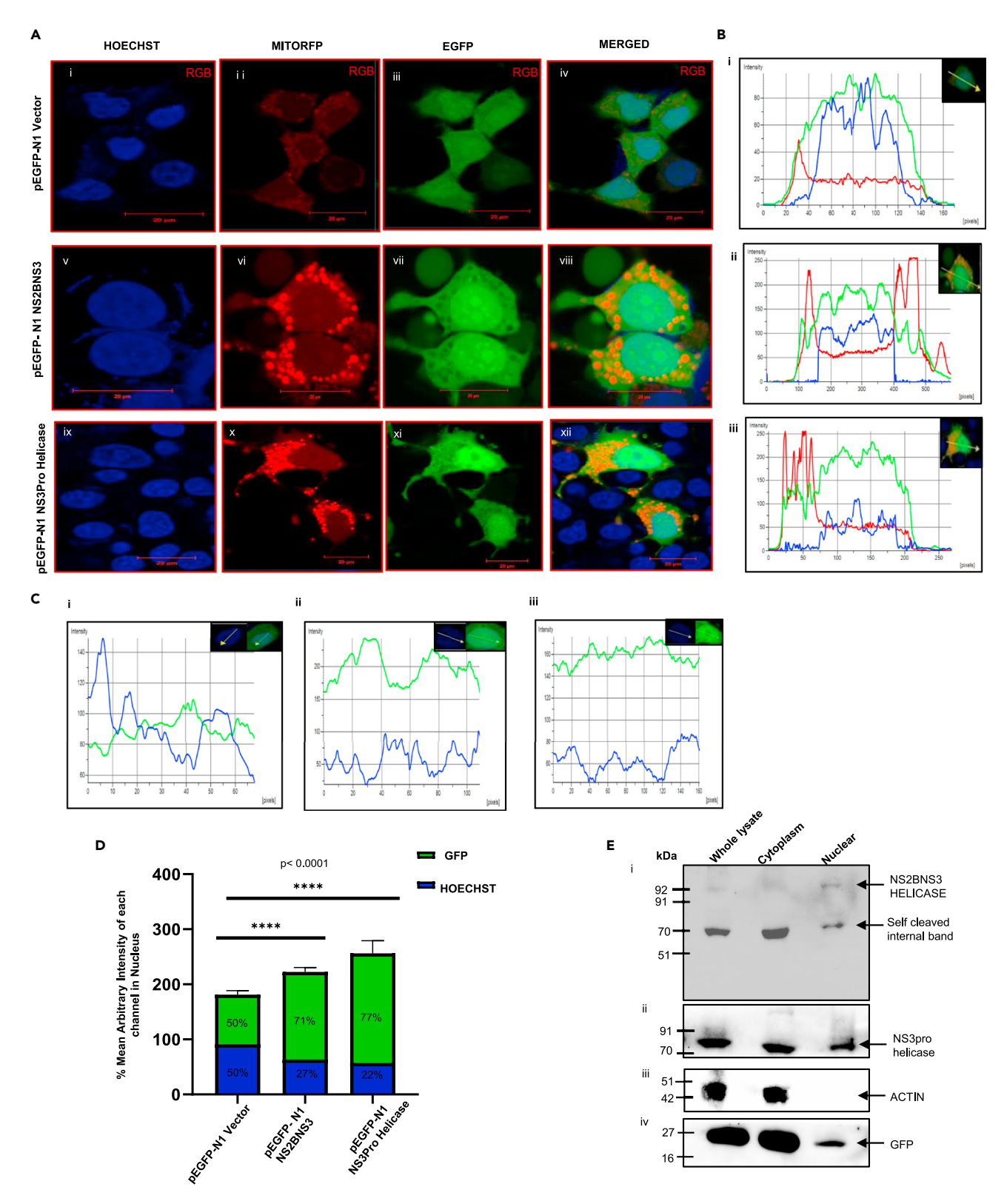


Figure 3. Localization of NS2BNS3 and NS3pro-helicase

(A) Confocal images at 60X (scale bar = $20\mu m$) showed the localization of pEGFP-N1 vector (i-iv); pEGFP-N1 NS2BNS3 (v-viii); and pEGFP-N1 NS3prohelicase (ix-xii), with both localization markers, i.e., MitoRFP and Hoechst.





Figure 3. Continued

- (B) i. Fluorescence intensity profiles were generated using NIS Elements AR software of pEGFP-N1 vector, ii. pEGFP-N1 NS2BNS3, iii. pEGFP-N1 NS3prohelicase.
- (C) i-iii Represent the intensity profiles of GFP (green) in nucleus (blue).
- (D) The bar graph representing the arbitrary mean intensity of each channel (green and blue) in nucleus of transfected cells as calculated in Figure 2C.
- (E) pEGFP-N1 NS2BNS3 and NS3pro-helicase subcellular fractions of transfected HEK cell lysates probed with NS2BNS3pro antibody.

the above data, we have transfected pEGFP N1 NS2BNS3 (594 a.a) which represents one of the forms of naturally existing dengue virus protease. A mutant of NS2BNS3pro (NS2BNS3pro S135A) carrying the mutation in the catalytic triad was also included. The data suggest that the levels of EDRF1 and GATA1 were drastically reduced in presence of pEGFP N1 NS2BNS3, compared to the mutant and the vector (Figures 5E–5G).

To further confirm the above result, we extended our study using the K562 virus-infected cell lysates (7 days post infection) as mentioned in STAR Methods. Supporting the transfection analyses, the levels of EDRF1, GATA1, and spectrin proteins were compromised significantly, clearly depicting the role of protease in EDRF1 cleavage (Figures 5H–5K). It was observed that the reduction of EDRF1 levels is clear in virus-infected cell lysates compared to the above transfection studies.

Analysis of EDRF1 and GrpEL1 levels in clinical samples

Total forty-four albumin out clinical samples with different grades of infections, i.e., DF, DHF, and DSS were included for the analysis (Table S1). Other febrile-infected samples were used as controls. SDS PAGE followed by western blotting was done to analyze the levels of EDRF1. It was observed that EDRF1 levels were reduced in DF, DHF, and DSS samples, but a significant difference was observed in DHF and DSS samples (Figures 5L [upper panel] and 5M; Figure S4). GrpEL1 was also included in this study as this protein was identified as a substrate of NS3 in our earlier studies. ²⁸ The GrpEL1 levels were also found to be reduced (consistent with our earlier report) in the samples in which the EDRF1 levels were reduced, i.e., in case of DF and DHF (Figure 5L [lower panel] and N).

Effect of protease on mitochondrial functions

NS3 was shown to target the mitochondrial matrix and cleave GrpEL1, a co-chaperone of mitochondrial Hsp-70 (mtHsp-70), in our previous study. ²⁸ In the present study also it was observed that NS3 localizes to mitochondria as well as into the nucleus (Figure 3A [ix-xii]). In this direction, to analyze the functional activities of mitochondria we have used HepG2 cell lines (hepatocytes) that have moderate energetic demand and are frequently used for several mitochondrial studies. ³⁹ They are also reportedly permissible for dengue virus infections. ⁴⁰ Thus, in this study we have performed cell mitostress assays for pEGFP-N1 vector and pEGFP N1 NS3pro-helicase-transfected HepG2 cells, and six parameters were measured as described below.

Basal respiration

Oxygen consumption rate (OCR) is a measure of the total cellular respiration in cells that meet the cellular ATP demand of the cell under baseline conditions. Basal levels of OCR in NS3pro-helicase-transfected cells were found to be decreased compared to vector-transfected cells which suggested low mitochondrial respiration in transfected cells (Figure 6C i).

ATP production-coupled respiration

On the addition of oligomycin, F0/F1 ATPase (complex V) shuts off, which relates to the activity of mitochondria generating the ATP linked to basal respiration. It was observed that in presence of oligomycin, the ATP production was compromised in NS3pro-helicase-transfected cells when compared to vector (Figure 6C ii). A decrease in ATP production-coupled respiration results in low ATP demand indicating damage to the electron transport chain (ETC).

Maximal respiration

On the addition of Carbonyl cyanide p-(trifluoromethoxy) phenylhydrazone (FCCP) (uncoupler), the movement of protons (H+ ions) will be allowed. This phenomenon leads to sudden increase in maximal respiration indicating high substrate availability and good integrity of the ETC as observed in vector-transfected





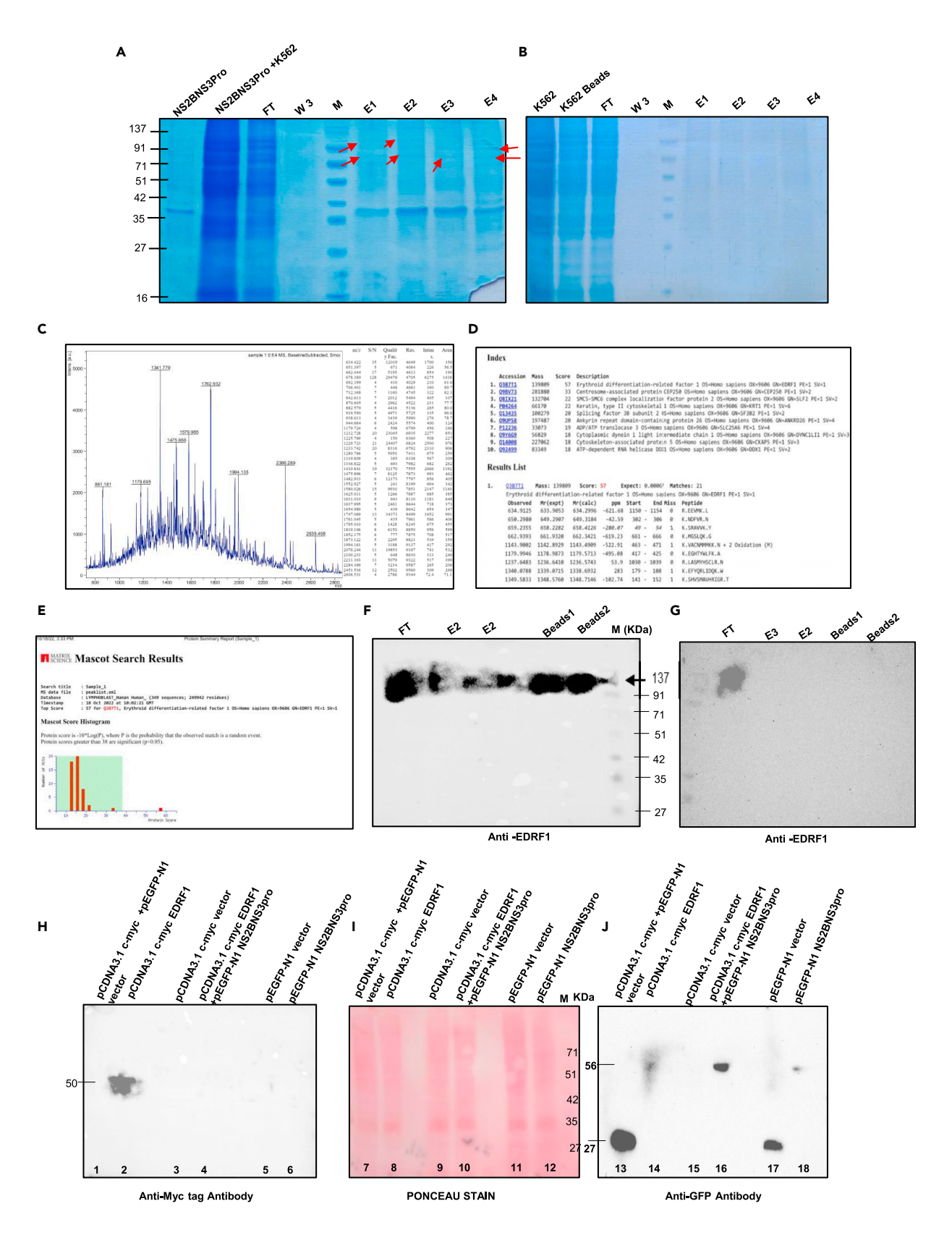






Figure 4. Identification of EDRF1 as another substrate of dengue virus protease

(A and B) In vitro pull-down assay from K562 cell lysate with pRSET-A NS2BNS3pro purified protein and (B) negative control. The arrows indicate the bands used for identification. See also Figures S2A and S2B.

(C and D) Identification data of the protein bands obtained from above in vitro pull-down assay.

(E–G) The graph represents the Mascot search result showing the identified protein as EDRF1 with the top score 57. Western blotting analysis of the fractions of pull-down assay by using anti-EDRF1 antibody, experimental (F), and negative control (G).

(H) Western blot analysis after 48 h of co-transfection. HEK cells were transfected with single or co-transfected with recombinant vectors as indicated on the blots and probed with anti-myc tag antibodies.

- (I) Ponceau S staining of the above membrane Lanes: 7–12 and M (protein marker).
- (J) The above membrane was stripped and probed with anti-GFP antibodies.

cells. However, there was no increment in maximal respiration in NS3-pro helicase-transfected HepG2 cells (Figure 6C iii) indicating the defective mitochondrial ETC.

Spare respiratory capacity

It is a measure of the difference between maximal respiration and basal respiration and represents the cell fitness and the cell response due to high energy demand. In NS3pro-helicase-transfected cells, maximal respiration was found to be low compared to vector; thus there was low spare respiratory capacity compared to the vector. Low respiratory capacity indicates low fitness of the cell (Figure 6Civ).

Proton leak

Basal respiration that is not linked to ATP production indicates the proton leak. There was no significant change in proton leak due to low energy demand or low substrate availability in transfected cells (Figure 6C v).

Non-mitochondrial oxygen consumption

Addition of antimycin and rotenone inhibits complex III leading to low cellular respiration. Non-mitochondrial oxygen consumption is the measure of the cells recovering their energy demand through other cellular processes. In the NS3pro-helicase-transfected cells, there was no increase in non-mitochondrial OCR as compared to the vector indicating the damage to mitochondria (Figure 6C vi).

Reduction in cell number during dengue virus infection in K562 cells

In order to analyze the effect of virus infection on K562 cells (megakaryocyte-derived cell line), we performed a cell counting method to analyze the cell number during virus infection. For this purpose, K562 cells with dengue-infected or uninfected were analyzed day wise (0, 3, 5, and 7) for morphological changes. Fourth day post infection onwards, visible cell morphological changes (deformed shape, reduced size, and tiny appearance) occurred. Total cell count starts decreasing after day 3. The rounded cell morphology of K562 cells was changed, a visible reduction in cell size on seventh day was observed, and the changes were imaged under an inverted bright-field microscope (magnification at 10X) (Figures 7 A and 7B). The virus infection was confirmed by RT-PCR on the fifth day (Figure 7C).

DISCUSSION

Dengue virus infections occupied the top of the list of emerging infectious diseases at present, but there is no specific drug or vaccine until now. All four serotypes cause similar disease manifestations individually or in combination with other serotypes. Flaviviruses target many host cellular proteins for efficient viral replication. The proteases of dengue and other flaviviruses (West Nile virus [WNV], Japanese encephalitis virus [JEV], and Zika virus) are known to cleave self-polyprotein and host proteins. All The polyprotein cleavage sites in case of dengue virus and its nature of activity suggest the possibility of existence of two forms of protease, i.e., NS3 alone and along with NS2B, i.e., NS2BNS3. NS2BNS3 is reported to target the mitochondrial membrane whereas NS3 alone targets the mitochondrial matrix in which the MTS was identified. The protease was also found in the nucleus without referring to any of the above two forms. Hence as a first step in this study, we have searched for the NLSs in both the NS2BNS3 and NS3. The data suggested the presence of NLS in both the above two forms (Figures 1 A and 1B). A similar stretch with (KKKRK) was found to be reported in simian virus 40 (SV40) large T-antigen. Transfection experiments carried out in order to verify the above observation with the developed recombinant constructs indicated the localization of NS2BNS3 into the nucleus and NS3pro-helicase localization into both the mitochondria and the nucleus (Figures 2 and 3). The mitochondrial localization of NS3 is consistent with our earlier

iScience Article



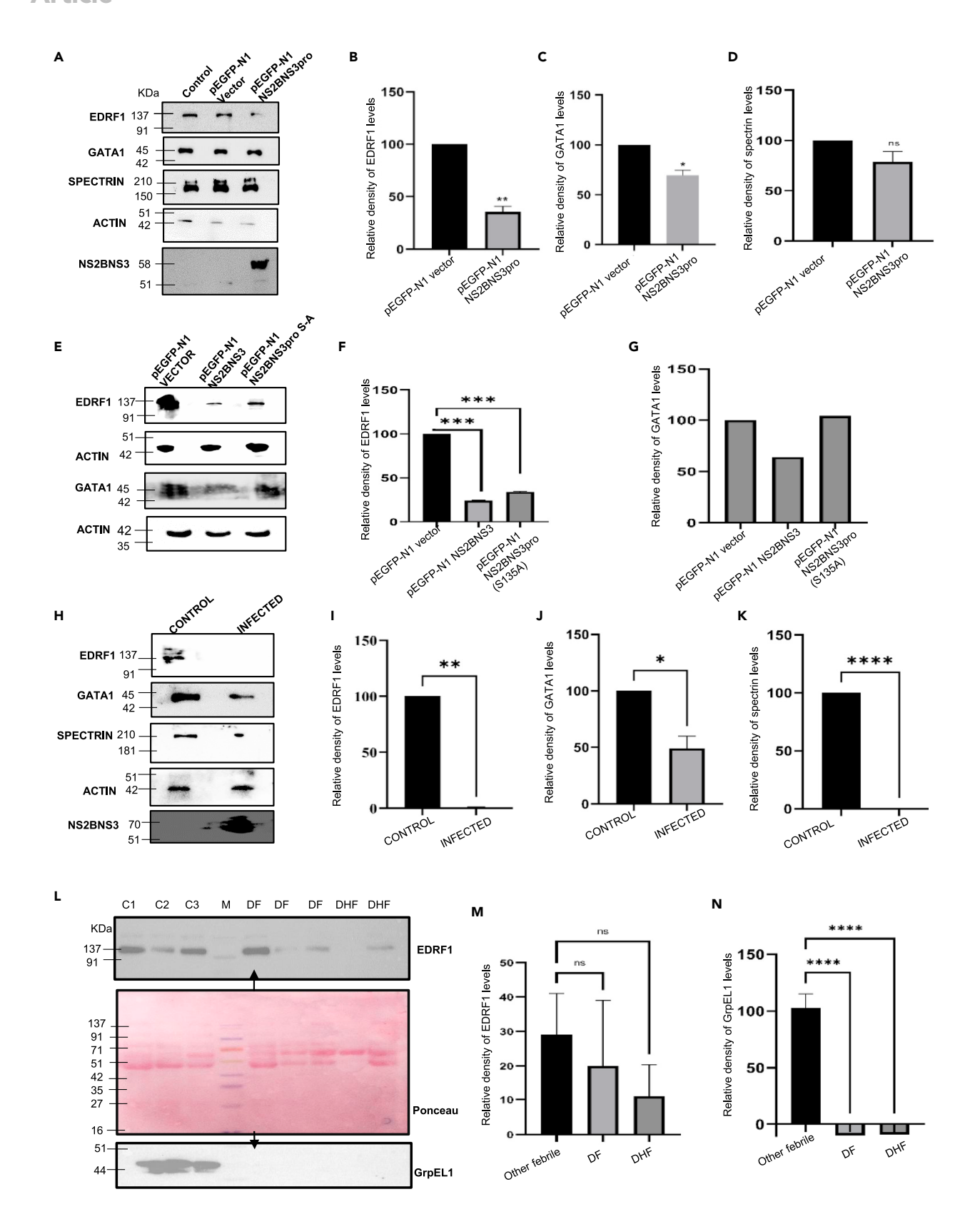






Figure 5. Analysis of levels of EDRF1, GATA1, spectrin, and GrpEL1 in ex vivo and in vivo (clinical samples). Western blot analysis of K562 transfected cell lysate

(A) pEGFP-N1 vector and pEGFP-N1 NS2BNS3pro for 28 h of transient transfections with indicated antibodies on the left.

(B-D) Bar diagram represents the means of 3 independent sets of experiments for proteins indicated.

(E) Western blot analysis of K562 cell lysate transiently transfected with pEGFP-N1 NS2BNS3 and pEGFP-N1 NS2BNS3pro (S135A) mutant analyzed after 28 h of transfection with indicated antibodies.

(F-G) Bar diagram represents the means of three sets of independent experiments for the indicated proteins.

(H) Western blot analysis of DENV-infected and uninfected in K562 cell lysates after 7 days with indicated antibodies.

(I–K) Bar diagram of respective proteins of 3 sets of independent experiments.

(L) Albumin out other febrile (C1, C2, C3) and dengue-infected serum samples (DF and DHF). The samples were separated on 10%SDS PAGE, and western blotting was done with anti-EDRF1 (top) and anti-GrpEL1 (bottom) antibodies and Ponceau stained membrane (Middle).

(M and N) Bar diagrams represent the relative densities of EDRF1 and GrpEL1 proteins in clinical samples. See also Figure S4 and Table S1.

observations.²⁸ In order to further confirm the above observations, we have carried out the transfection experiments using the mitochondrial (MitoRFP) and nuclear (Hoechst stain) localization markers for both NS2BNS3 and NS3. The results show that, while the NS3pro-helicase localized with the Hoechst stain (nucleus), NS2BNS3 did not colocalize with the MitoRFP (mitochondria) which supports the above observations (Figure 3). It was speculated that the NS2BNS3 could not enter the mitochondria as the MTS present at the N-terminal end of the NS3 is masked by NS2B. Both NS2BNS3 and NS3 localized to the nucleus due to multiple NLSs present in both forms. The western blot analysis carried out to detect the protease in the nuclear or the cytoplasmic (mitochondria) extracts indicates the presence of the NS3 (75 kDa) in cytoplasmic (mitochondria) fraction whereas both NS2BNS3 and NS3 (92 & 75 kDa) were present in the nucleus (Figure 3E). A 70 kDa band observed in the nucleus of NS2BNS3-transfected extracts may be due to the internal self-cleavage site (Figure 3E [i]).¹² The above observations suggest the localization of both the NS2BNS3 and NS3 into the nucleus.

In order to identify the substrates of NS2BNS3/NS3, if any, from the nucleus, we have carried out the pull-down experiment consisting of total cell extracts with NS2BNS3pro. The co-eluted protein bands were identified by mass spectrometry analysis and were found to be EDRF1 (Figures 4A–4E, S2A, and S2B). Western blotting analysis of the elutes of the above experiment using anti-EDRF1 antibodies confirms the interaction of NS2BNS3 with EDRF1 (Figures 4F and 4G). In continuation, the amino acid sequence of ERDF1 was searched for the cleavage sites, and we found five sites at amino acid sequences 50,100,152,926,987 (Figure S2C). Structural superimposition of EDRF1 and protease suggested that the cleavage site (RK/A) (985–988) is located in the catalytic triad of protease (Figure S3). Hence, we have generated the EDRF1 recombinant construct from the amino acids 798–1238 of EDRF1. Co-transfection experiments carried out with the above EDRF1 and the NS2BNS3pro constructs suggested the complete disappearance of EDRF1 but not in controls (Figure 4H, lane 4). This observation suggested EDRF1 as another substrate of dengue virus protease, which reportedly regulates the expression and activity of GATA1.

GATA1 is involved in differentiation, proliferation, and maturation of megakaryocytes (platelet lineage), and its activity is modulated by the EDRF1 protein. EDRF1 has been reported to play a major role in transcriptional regulation and expression of GATA1 and globin gene expression, a key factor in megakaryopoiesis. 43 Based on these reports we framed the hypothesis that EDRF1, GATA1, and spectrins might be affected during the dengue virus infection. In order to test the same, the NS2BNS3 transfection experiments carried out in K562 cells suggested the reduced levels of EDRF1, GATA1, and spectrin proteins in the expressed conditions of protease (Figures 5A-5G). Similar analysis carried out using the cell extracts of the dengue virus-infected cells supported the above observations (Figures 5H-5K). Both the above two conditions strongly suggest the cleavage of EDRF1 and as a result the downregulation of GATA1 and spectrin proteins. Further, the EDRF1 and the GrpEL1 levels were analyzed in the dengue virus-infected clinical samples. GrpEL1 was also chosen, as it was shown to be the substrate of NS3 in our earlier studies. 28 The levels of both the above proteins were significantly reduced in dengue virus-infected samples which are drastic in case of the severe disease (DHF and DSS), indicating the cleavage of ERDF1 (Figures 5L-5N and S4). The effect on the EDRF1 levels is more and more clear from ex vivo to in vivo (clinical samples) conditions (Figures 5 and S4). Reports indicate that EDRF1 plays a key regulatory role in GATA1 mRNA expression and DNA binding activity. 35,36 Importantly, GATA1 is known to be involved in erythrocyte and megakaryocytic precursor development; disruption of any of the above-mentioned two functions of GATA1 leads to thrombocytopenia and anemia. 43,44 Several lines of reports indicate that defects in GATA1 activity lead to thrombocytopenia, structural abnormalities in megakaryocytes, and impairment of platelet activation. ^{22,43,44} GATA1 is also known to involve in spectrin mRNA synthesis, and the spectrin proteins are reportedly needed for pro-platelet and platelet formation. 45 Several lines of research indicated that





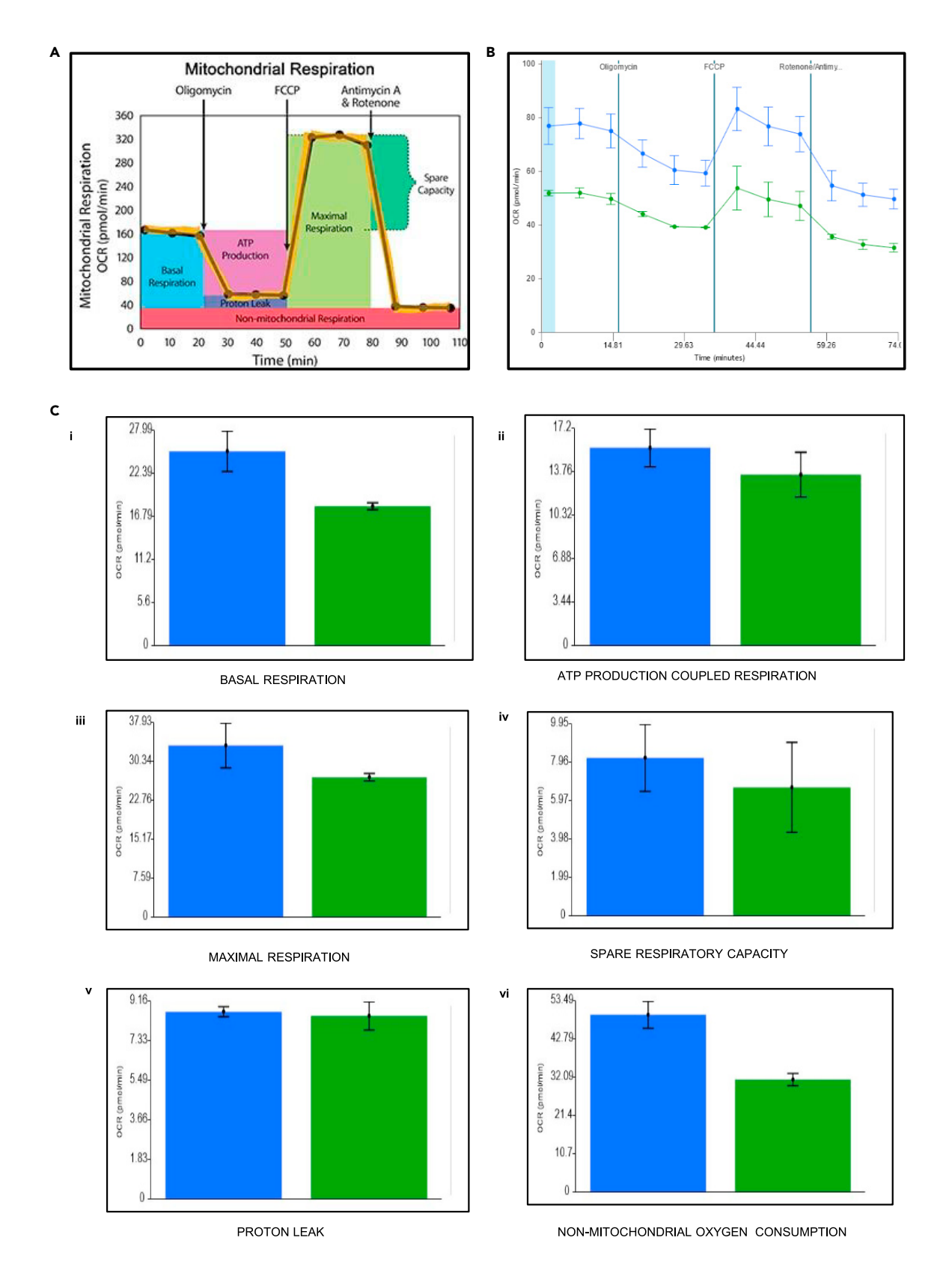






Figure 6. Mitochondrial function analysis in protease-transfected cells

(A) Represents the reference model for the analysis of mitochondrial bioenergetics in mitostress assay.

(B) Agilent Seahorse XFp cell mitostress assay showing bioenergetics of mitochondria in cells transfected with pEGFP-N1 vector and pEGFP-N1 NS3prohelicase with respect to oxygen consumption rate vs. time.

(C) The graphs represent the oxygen consumption rate vs. time during injection of the three drugs (Oligomycin, FCCP, and Rotenone/Antimycin). (i) Basal respiration (ii) ATP production-coupled respiration (iii) Maximal respiration (iv) Spare respiratory capacity (v) Proton leak (vi) Non-mitochondrial oxygen consumption. The parameters measured are shown in representative bar graphs with error bars of at least two experiments (n = 3, i.e., triplicates in each experiment).

alpha and beta spectrins are essential proteins involved in cytoskeleton formation, particularly in erythrocytes, in association with actin. 46 Interesting function of spectrin proteins, as far as the present study concerned, is their involvement in the pro-platelet and platelet formation. Hence the cleavage of EDRF1 observed in the present study led to decreased levels of GATA1 and subsequently to fewer spectrins and finally to the reduced number of platelets, i.e., thrombocytopenia. The proposed mechanisms of thrombocytopenia in dengue virus infections 30–34 and present observations are possibly parts of a cascade of events of a single mechanism. However, further research is required to indicate whether they are interlinked or different and which is predominant, if different. Non-functional platelets without the number change (thrombopathy) are another possible disorder to be considered in dengue virus-infected patients. But, as the current literature including the present study support the reduction in platelet number, the "thrombopathy" may need to be further assessed.

Reports suggest defective mitochondrial quality and dysfunctioning during viral infections including dengue virus.^{26,34} Reports also indicate that the dengue virus NS2BNS3 targets the mitochondrial membrane proteins and NS3 enters the mitochondrial matrix and cleaves the matrix protein (GrpEL1), a cochaperone of the mtHSP70.²⁸ In all the above cases, the role of the above proteins in mitochondrial activity is not clear. Hence, we have analyzed the activities of mitochondria (basal respiration, ATP productioncoupled respiration, maximal respiration, spare respiratory capacity, proton leak, and non-mitochondrial oxygen consumption) in the cells transfected with NS3. These activities were found to be reduced (except proton leak) significantly compared to the controls (Figure 6). This observation supported the hypothesis that the mitochondrial dysfunction/defectiveness is due to the effect of the dengue virus-coded protease. The above findings related to mitochondria were supported by the earlier studies carried out by virus infections. 40 Mitochondrial dysfunctions are also reported to be leads to impaired platelet formation. 34 Hence, we proceeded with the analysis of cell numbers under dengue virus infections using the megakaryocyte-derived K562 cells. The results showed a reduction in the number which is more prominent as the number of days progressed (Figure 7). Platelets are the cell types that are required in a huge number in the blood at a given point of time. In order to produce a large number of cells, the platelet lineage cells have to undergo vigorous growth and differentiation which require a high input of ATP. But the mitochondrial damage occurred during dengue virus infections (due to protease as described above), and the cells are incapable of dividing fast to yield enough platelet number because of less ATP generation by mitochondria. Hence, it is concluded that cleavage of the EDRF1, a nuclear transcription factor, by NS2BNS3 of dengue virus, and the NS3-mediated mitochondrial dysfunction contribute to the reduced number of platelet formation (thrombocytopenia) during dengue virus infections.

Ethics statement

This study was approved by the Institutional Ethics Committee, University of Hyderabad (UH/IEC/2021/1).

Limitations of our study

The present study carried out is completely around the dengue virus protease and its effect on cell homeostasis. Availability of a specific anti-protease molecule would have shed light more clearly on the observations. But the reported two anti-protease drugs quercetin and Nordihydroguaiaretic acid (NDGA) are highly cell toxic and hence were not used in this study. Hence the availability of a specific anti-protease molecule could be considered as the limitation in the present study.

STAR*METHODS

Detailed methods are provided in the online version of this paper and include the following:

- KEY RESOURCES TABLE
- RESOURCE AVAILABILITY





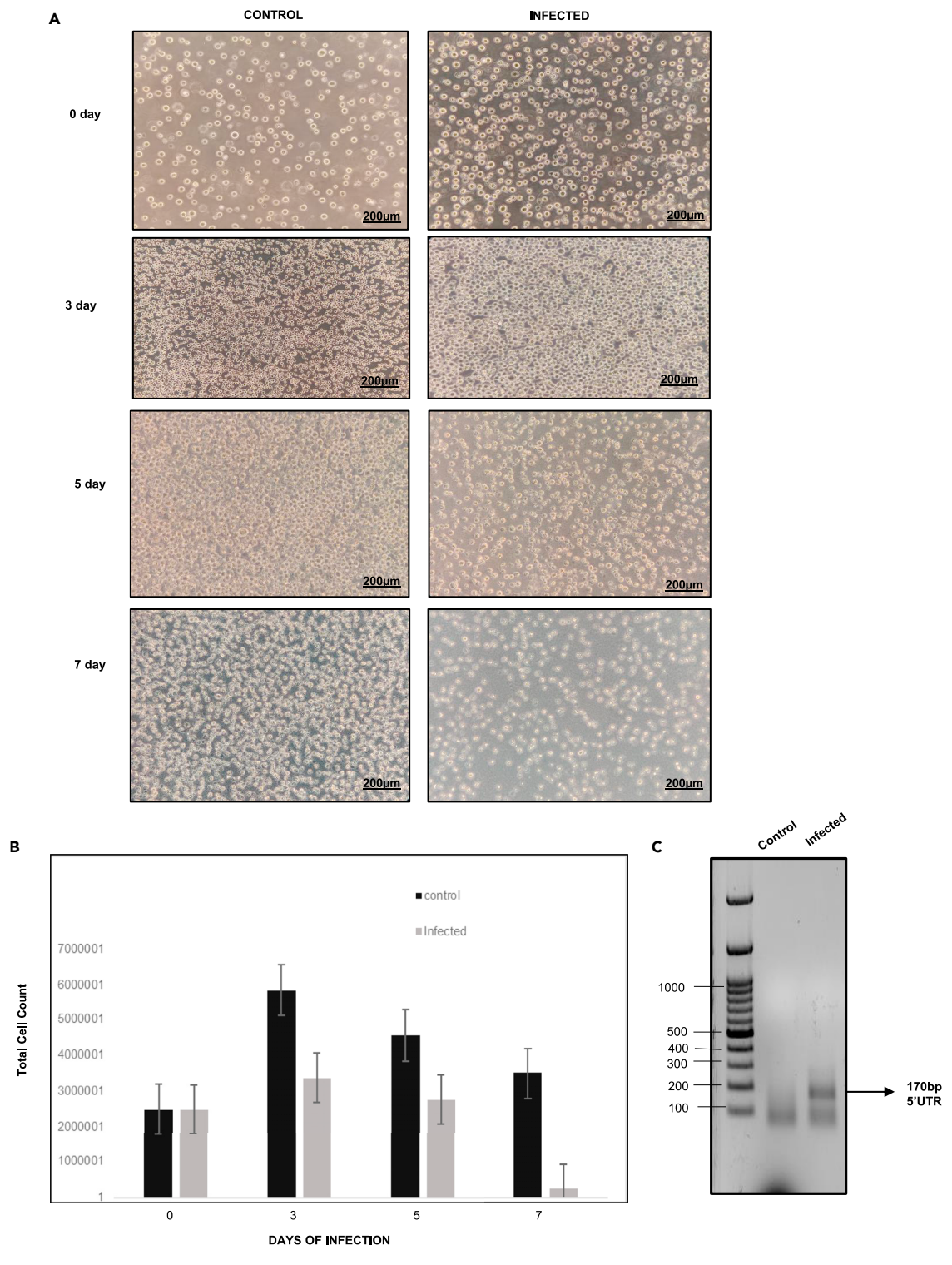


Figure 7. Analysis of cell number during dengue virus infection

(A) Morphological analysis at 10X (scale bar = $200\mu m$) of infected and uninfected K562 cells observed at different days post infection from 0 to seventh day. (B) Bar graph showing the total cell count of uninfected and infected K562 cells. The error bars represent the average total cell count of at least two independent experiments.

(C) RT-PCR analysis of amplified fragment of 5'UTR (170 bp) during dengue infection on the fifth day.





- Lead contact
- Materials availability
- O Data and code availability
- EXPERIMENTAL MODEL AND STUDY PARTICIPANT DETAILS
 - Cell lines
- METHOD DETAILS
 - O Prediction of nuclear localization signal (NLS)
 - O Dengue virus constructs
 - O Cloning of EDRF1 in pcDNA3.1 c-myc vector
 - O Dengue virus protease localization analysis
 - O Detection of dengue virus protease in subcellular fractions
 - O In vitro pulldown assay and protein identification
 - O Identification of proteins obtained in the above pull-down experiment
 - O Identification of protease cleavage sites in EDRF1 using in silico methods
 - O EDRF1 cleavage analysis with co-transfection studies
 - O Analysis of EDRF1 levels in transfected cell extracts
 - O Analysis of EDRF1 levels in virus infected cell extracts
 - O EDRF1 and GrpEL1 levels in clinical samples
 - O Bioenergetics of mitochondria in transfected cells
 - O Cell number analysis during dengue virus infection
- QUANTIFICATION AND STATISTICAL ANALYSIS

SUPPLEMENTAL INFORMATION

Supplemental information can be found online at https://doi.org/10.1016/j.isci.2023.107024.

ACKNOWLEDGMENTS

The authors acknowledge the DBT (BT/PR14240/MED/29/985/2015) and STARS-MoE-IISc (STARS/APR2019/BS/584/FS) for the financial support. The authors also acknowledge the DBT-BUILDER program of the School of Life Sciences (No BT/INF/22/SP41176/2020), UOH, India, for the Agilent Seahorse XFP mini analyzer and Indian Council of Medical Research (ICMR) for providing fellowship to L.G.

AUTHOR CONTRIBUTIONS

Conceptualization, L.G. and M.V.; Methodology, L.G. and M.V.; Investigation, L.G., D.M, D.R., P.C., and A.B; Writing-Original Draft, L.G. and M.V.; Writing-Review & Editing, L.G. and M.V.; Funding Acquisition, M.V.; Resources, M.V.; Supervision, M.V.

DECLARATION OF INTERESTS

The authors declare no conflict of interest.

INCLUSION AND DIVERSITY

We support inclusive, diverse, and equitable conduct of research.

Received: January 18, 2023 Revised: April 7, 2023 Accepted: May 30, 2023 Published: June 5, 2023

REFERENCES

- 1. World Health Organization. (2012). Global Strategy for Dengue Prevention and Control. https://apps.who.int/iris/bitstream/handle/10665/75303/9789241504034_eng.pdf.
- Zeng, Z., Zhan, J., Chen, L., Chen, H., and Cheng, S. (2021). Global, regional, and national dengue burden from 1990 to 2017: a systematic analysis based on the global
- burden of disease study 2017. EClinicalMedicine 32, 100712. https://doi. org/10.1016/j.eclinm.2020.100712.
- 3. Malavige, G.N., Fernando, S., Fernando, D.J., and Seneviratne, S.L. (2004). Dengue viral infections. Postgrad. Med. *80*, 588–601. https://doi.org/10.1136/pgmj.2004.019638.
- Martina, B.E.E., Koraka, P., and Osterhaus, A.D.M.E. (2009). Dengue virus pathogenesis: an integrated view. Clin. Microbiol. Rev. 22, 564–581. https://doi.org/10.1128/CMR. 00035-09.
- 5. Gebhard, L.G., Filomatori, C.V., and Gamarnik, A.V. (2011). Functional RNA Elements in the dengue virus. Viruses 3,

iScience

Article



- 1739–1756. https://doi.org/10.3390/ v3091739.
- Luo, D., Wei, N., Doan, D.N., Paradkar, P.N., Chong, Y., Davidson, A.D., Kotaka, M., Lescar, J., and Vasudevan, S.G. (2010). Flexibility between the protease and helicase domains of the dengue virus NS3 protein conferred by the linker region and its functional implications. J. Biol. Chem. 285, 18817–18827. https://doi.org/10.1074/jbc. M109.090936.
- Li, Q., and Kang, C. (2022). Structures and dynamics of dengue virus nonstructural membrane proteins. Membranes 12, 231. https://doi.org/10.3390/ membranes12020231.
- Luo, D., Vasudevan, S.G., and Lescar, J. (2015). The flavivirus NS2B-NS3 proteasehelicase as a target for antiviral drug development. Antivir. Res. 118, 148–158. https://doi.org/10.1016/j.antiviral.2015. 03.014
- Li, J., Lim, S.P., Beer, D., Patel, V., Wen, D., Tumanut, C., Tully, D.C., Williams, J.A., Jiricek, J., Priestle, J.P., et al. (2005). Functional profiling of recombinant NS3 proteases from all four serotypes of dengue virus using tetra peptide and octapeptide substrate libraries. J. Biol. Chem. 280, 28766– 28774. https://doi.org/10.1074/jbc. M500588200.
- Chiang, P.Y., and Wu, H.N. (2016). The role of surface basic amino acids of dengue virus NS3 helicase in viral RNA replication and enzyme activities. FEBS Lett. 590, 2307–2320. https://doi.org/10.1002/1873-3468.12232.
- Shiryaev, S.A., Kozlov, I.A., Ratnikov, B.I., Smith, J.W., Lebl, M., and Strongin, A.Y. (2007). Cleavage preference distinguishes the two-component NS2B–NS3 serine proteinases of Dengue and West Nile viruses. Biochem. J. 401, 743–752. https://doi.org/10. 1047/BJ20061136.
- Constant, D.A., Mateo, R., Nagamine, C.M., and Kirkegaard, K. (2018). Targeting intramolecular proteinase NS2B/3 cleavages for trans-dominant inhibition of dengue. Proc. Natl. Acad. Sci. USA 115, 10136–10141. https://doi.org/10.1073/pnas.1805195115.
- Lin, K.H., Nalivaika, E.A., Prachanronarong, K.L., Yilmaz, N.K., and Schiffer, C.A. (2016). Dengue protease substrate recognition: binding of the prime side. ACS Infect. Dis. 2, 734–743. https://doi.org/10.1021/acsinfecdis. 6b00131
- Lennemann, N.J., and Coyne, C.B. (2017). Dengue and Zika viruses subvert reticulophagy by NS2B3-mediated cleavage of FAM134B. Autophagy 13, 322–332. https:// doi.org/10.1080/15548627.2016.1265192.
- Lin, J.C., Lin, S.C., Chen, W.Y., Yen, Y.T., Lai, C.W., Tao, M.H., LIN, Y.L., Mlaw, S.C., and Wu-Hsieh, B.A. (2014). Dengue viral protease interaction with NF-κB inhibitor α/β results in endothelial cell apoptosis and hemorrhage development. J. Immunol. 193, 1258–1267. https://doi.org/10.4049/jimmunol.1302675.

- De Jesús-González, L.A., Cervantes-Salazar, M., Reyes-Ruiz, J.M., Osuna-Ramos, J.F., Farfán-Morales, C.N., Palacios-Rápalo, S.N., Pérez-Olais, J.H., Cordero-Rivera, C.D., Hurtado-Monzón, A.M., Ruíz-Jiménez, F., et al. (2020). The nuclear pore complex: a target for NS3 protease of dengue and Zika viruses. Viruses 12, 583. https://doi.org/10. 3390/v12060583.
- Yu, C.Y., Chang, T.H., Liang, J.J., Chiang, R.L., Lee, Y.L., Liao, C.L., and Lin, Y.L. (2012).
 Dengue virus targets the adaptor protein MITA to subvert host innate immunity. PLoS Pathog. 8, e1002780. https://doi.org/10. 1371/journal.ppat.1002780.
- Yu, C.Y., Liang, J.J., Li, J.K., Lee, Y.L., Chang, B.L., Su, C.I., Huang, W.J., Lai, M.M.C., and Lin, Y.L. (2015). Dengue virus impairs mitochondrial fusion by cleaving mitofusins. PLoS Pathog. 11, e1005350. https://doi.org/ 10.1371/journal.ppat.1005350.
- Noisakran, S., Onlamoon, N., Songprakhon, P., Hsiao, H.M., Chokephaibulkit, K., and Perng, G.C. (2010). Cells in dengue virus infection in vivo. Adv. Virol. 2010, 164878. https://doi.org/10.1155/2010/164878.
- Diamond, M.S., Edgil, D., Roberts, T.G., Lu, B., and Harris, E. (2000). Infection of human cells by dengue virus is modulated by different cell types and viral strains. J. Virol. 74, 7814–7823. https://doi.org/10.1128/jvi.74. 17.7814-7823.
- Balsitis, S.J., Coloma, J., Castro, G., Alava, A., Flores, D., McKerrow, J.H., Beatty, P.R., and Harris, E. (2009). Tropism of dengue virus in mice and humans defined by viral nonstructural protein 3-specific immunostaining. Am. J. Trop. Med. Hyg. 80, 416–424.
- 22. Vogt, M.B., Lahon, A., Arya, R.P., Spencer Clinton, J.L., and Rico-Hesse, R. (2019). Dengue viruses infect human megakaryocytes, with probable clinical consequences. PLoS Neglected Trop. Dis. 13, 00078377–e7923. https://doi.org/10.1371/journal.pntd.0007837.
- Shivdasani, R.A. (2001). Molecular and transcriptional regulation of megakaryocyte differentiation. Stem Cell. 19, 397–407. https://doi.org/10.1634/stemcells.19-5-397.
- Huang, K.J., Li, S.Y.J., Chen, S.C., Liu, H.S., Lin, Y.S., Yeh, T.M., Liu, C.C., and Lei, H.Y. (2000). Manifestation of thrombocytopenia in dengue-2-virus-infected mice. J. Gen. Virol. 81, 2177–2182. https://doi.org/10.1099/0022-1317-81-9-2177.
- Lahon, A., Arya, R.P., and Banerjea, A.C. (2021). Dengue virus dysregulates master transcription factors and PI3K/AKT/mTOR signaling pathway in megakaryocytes. Front. Cell. Infect. Microbiol. 11, 715208. https://doi.org/10.3389/fcimb.2021.715208.
- Saxena, R., Sharma, P., Kumar, S., Agrawal, N., Sharma, S.K., Awasthi, A., and Awasthi, A. (2023). Modulation of mitochondria by viral proteins. Life Sci. 313, 121271. https://doi. org/10.1016/j.lfs.2022.121271.

- Singh, B., Avula, K., Sufi, S.A., Parwin, N., Das, S., Alam, M.F., Samantaray, S., Bankapalli, L., Rani, A., Poornima, K., et al. (2022). Defective mitochondrial quality control during dengue infection contributes to disease pathogenesis. J. Virol. 96, e0082822. https:// doi.org/10.1128/jvi.00828-22.
- Gandikota, C., Mohammed, F., Gandhi, L., Maisnam, D., Mattam, U., Rathore, D., Chatterjee, A., Mallick, K., Billoria, A., Prasad, V.S.V., et al. (2020). Mitochondrial import of dengue virus NS3 protease and cleavage of GrpEL1, a cochaperone of mitochondrial Hsp70. J. Virol. 94, 011788-20–e1220. https:// doi.org/10.1128/JVI.01178-20.
- Palacios-Rápalo, S.N., De Jesús-González, L.A., Del, Á.R.M., Osuna-Ramos, J.F., Farfan-Morales, C.N., Gutiérrez-Escolano, A.L., and Del Ángel, R.M. (2021). Nuclear localization of non-structural protein 3 (NS3) during dengue virus infection. Arch. Virol. 166, 1439–1446. https://doi.org/10.1007/s00705-021-05026-w.
- Looi, K.W., Matsui, Y., Kono, M., Samudi, C., Kojima, N., Ong, J.X., Tan, C.A., Ang, C.S., Tan, P.H.Y., Shamnugam, H., et al. (2021). Evaluation of immature platelet fraction as a marker of dengue fever progression. Int. J. Infect. Dis. 110, 187–194. https://doi.org/10. 1016/j.ijid.2021.07.048.
- Alonzo, M.T.G., Lacuesta, T.L.V., Dimaano, E.M., Kurosu, T., Suarez, L.A.C., Mapua, C.A., Akeda, Y., Matias, R.R., Kuter, D.J., Nagata, S., et al. (2012). Platelet apoptosis and apoptotic platelet clearance by macrophages in secondary dengue virus infections.
 J. Infect. Dis. 205, 1321–1329. https://doi.org/ 10.1093/infdis/jis180.
- 32. Ojha, A., Nandi, D., Batra, H., Singhal, R., Annarapu, G.K., Bhattacharyya, S., Seth, T., Dar, L., Medigeshi, G.R., Vrati, S., et al. (2017). Platelet activation determines the severity of thrombocytopenia in dengue infection. Sci. Rep. 7, 41697. https://doi.org/10.1038/ srep41697.
- Chao, C.H., Wu, W.C., Lai, Y.C., Tsai, P.J., Perng, G.C., Lin, Y.S., and Yeh, T.M. (2019). Dengue virus nonstructural protein 1 activates platelets via Toll-like receptor 4, leading to thrombocytopenia and hemorrhage. PLoS Pathog. 15, e1007625. https://doi.org/10.1371/journal.ppat. 1007625.
- 34. Hottz, E.D., Oliveira, M.F., Nunes, P.C.G., Nogueira, R.M.R., Valls-de-Souza, R., Da Poian, A.T., Weyrich, A.S., Zimmerman, G.A., Bozza, P.T., and Bozza, F.A. (2013). Dengue induces platelet activation, mitochondrial dysfunction and cell death through mechanisms that involve DC-SIGN and caspases. J. Thromb. Haemostasis 11, 951–962. https://doi.org/10.1111/jth.12178.
- 35. Wang, D., Ma, S., Wang, S., and Shen, B. (2002). Antisense EDRF1 gene inhibited transcription factor DNA-binding activity in K562 cells. Sci. China C Life Sci. 45, 289–297. https://doi.org/10.1360/02yc9032.
- 36. Wang, X., Wang, D., Chen, X., Hu, M., Wang, J., Li, Y., Guo, N., and Shen, B. (2001). cDNA cloning and function analysis of two novel





- erythroid differentiation related genes. Sci. China C Life Sci. 44, 99–105. https://doi.org/10.1007/BF02882078.
- Wang, D., Li, Y., and Shen, B. (2001). Initial function analysis of a novel erythroid differentiation related gene EDRF1. Sci. in. China. 44, 489–496. https://doi.org/10.1007/ BF02882391.
- Boulanger, L., Sabatino, D.E., Wong, E.Y., Cline, A.P., Garrett, L.J., Garbarz, M., Dhermy, D., Bodine, D.M., and Gallagher, P.G. (2002). Erythroid expression of the human alpha-spectrin gene promoter is mediated by GATA-1- and NF-E2-binding proteins. J. Biol. Chem. 277, 41563–41570. https://doi.org/10.1074/jbc.M208184200.
- Hill, B.G., Benavides, G.A., Lancaster, J.R., Ballinger, S., Dell'Italia, L., Jianhua, Z., and Darley-Usmar, V.M. (2012). Integration of cellular bioenergetics with mitochondrial quality control and autophagy. Biol. Chem. 393, 1485–1512. https://doi.org/10.1515/hsz-2012-0198.
- El-Bacha, T., Midlej, V., Pereira da Silva, A.P., Silva da Costa, L., Benchimol, M., Galina, A., and Da Poian, A.T. (2007). Mitochondrial and bioenergetic dysfunction in human hepatic cells infected with dengue 2 virus. Biochim. Biophys. Acta 1772, 1158–1166. https://doi. org/10.1016/j.bbadis.2007.08.

- 41. Wahaab, A., Mustafa, B.E., Hameed, M., Stevenson, N.J., Anwar, M.N., Liu, K., Wei, J., Qiu, Y., and Ma, Z. (2021). Potential role of flavivirus NS2B-NS3 proteases in viral pathogenesis and anti-flavivirus drug discovery employing animal cells and models: a review. Viruses 14, 44. https://doi. org/10.3390/v14010044.
- Lu, J., Wu, T., Zhang, B., Liu, S., Song, W., Qiao, J., and Ruan, H. (2021). Types of nuclear localization signals and mechanisms of protein import into the nucleus. Cell Commun. Signal. 19, 60. https://doi.org/10. 1186/s12964-021-00741-y.
- Kuhl, C., Atzberger, A., Iborra, F., Nieswandt, B., Porcher, C., and Vyas, P. (2005). GATA-1mediated megakaryocyte differentiation and growth control can be uncoupled and mapped to different domains in GATA1. Mol. Cell Biol. 25, 8592–8606. https://doi.org/10. 1128/MCB.25.19.
- Goldfarb, A.N. (2007). Transcriptional control of megakaryocyte development. Oncogene 26, 6795–6802. https://doi.org/10.1038/sj. onc.1210762.
- 45. Patel-Hett, S., Wang, H., Begonja, A.J., Thon, J.N., Alden, E.C., Wandersee, N.J., An, X., Mohandas, N., Hartwig, J.H., and Italiano, J.E. (2011). The spectrin-based membrane skeleton stabilizes mouse megakaryocyte membrane systems and is essential for proplatelet and platelet formation. Blood

- 118, 1641–1652. https://doi.org/10.1182/blood-2011-01-330688.
- Ghalloussi, D., Dhenge, A., and Bergmeier, W. (2019). New insights into cytoskeletal remodeling during platelet production.
 J. Thromb. Haemostasis 17, 1430–1439. https://doi.org/10.1111/jth.14544.
- Gandikota, C., Gandhi, L., Maisnam, D., Kesavulu, M.M., Billoria, A., Prasad, V.S.V., and Venkataramana, M. (2021). A novel anti-NS2BNS3pro antibody-based indirect ELISA test for the diagnosis of dengue virus infections. J. Med. Virol. 93, 3312–3321. https://doi.org/10.1002/jmv.26024.
- Gu, X., Ma, Y., Liu, Y., and Wan, Q. (2021). Measurement of mitochondrial respiration in adherent cells by Seahorse XF96 cell mito stress test. STAR Protoc. 2, 100245. https:// doi.org/10.1016/j.xpro.2020.100245.
- Agilent, Technologies.. Agilent Seahorse XF cell mitostress kit. https://www.agilent.com/ CS/library/UserManual/Public/XF-cell-Mitostress-Test-kit-user-guide.pdf.
- Vaddadi, K., Gandikota, C., Jain, P.K., Prasad, V.S.V., and Venkataramana, M. (2017). Cocirculation and co-infections of all dengue virus serotypes in Hyderabad, India 2014. Epidemiol. Infect. 145, 2563–2574. https:// doi.org/10.1017/S0950268817001479.





STAR*METHODS

KEY RESOURCES TABLE

REAGENT or RESOURCE	SOURCE	IDENTIFIER
Antibodies		
EDRF1 Rabbit Polyclonal Antibody	Proteintech, USA	Cat# 21883-1-AP, RRID: AB_11042452
MYC tag Mouse Monoclonal Antibody	Proteintech, USA	Cat# 60003-2-lg, RRID: AB_2734122
Alpha-1 Spectrin Rabbit Polyclonal Antibody	ImmunoTag	Cat# ITT13417 RRID: N/A
GATA-1 Rabbit Polyclonal Antibody	ImmunoTag	Cat# ITT06184 RRID: N/A
GFP (D5.1) Rabbit mAB(monoclonal antibody)	Cell Signaling Technology	Cat# 2956, RRID:AB_1196615
Actin mouse Monoclonal Antibody	Santa Cruz Biotechnology	Cat#sc8432
Rabbit Anti-Mouse-IgG HRP conjugated Antibody	GeNei	Cat# 1140580011730 RRID:N/A
Mouse Anti-Rabbit- IgG HRP Conjugated Antibody	Santa Cruz Biotechnology	Cat# sc-2357, RRID:AB_628497
NS2BNS3pro Rabbit Antibody (raised in housed)	(Gandikota et al. ⁴⁷)	N/A
Bacterial and virus strains		
Escherichia coli. (BL21 competent cells)	N/A	N/A
Dengue Virus Type 1(in-house serotyped)	(Vaddadi et al. ⁵⁰)	
Biological samples		
Clinical serum samples (Dengue Infected patient serum)	Lotus Hospital for Women and Children, Lakdikapul-500004, Hyderabad,	N/A
	Telangana State, India.	
Chemicals, peptides, and recombinant proteins		
DMEM	Gibco	Cat#11995-065
RPMI	Gibco	Cat#11875-093
FBS	Gibco	10270106
Anti-Anti (Antibiotic)	Gibco	Cat#15240062
Trypsin-EDTA (1X) solution	Himedia	Cat#TCL007
Paraformaldehyde	Sigma	Cat#P6148
Triton-X100	Himedia	Cat#TC286
RIPA Buffer	Sigma Aldrich	Cat# R0278
Hoechst stain 33342	Molecular probes by Life Technologies	Cat#H21492
Ni-NTA beads	Qiagen	Cat# 30210
NS2BNS3pro (recombinant protein)	(Gandikota et al. ⁴⁷)	N/A
Femto LUCENT™ PLUS-HRP	G-Biosciences	Cat. # 786-003
Lipofectamine reagent 2000	Invitrogen	Cat#11668-027
Critical commercial assays		
Midi prep plasmid isolation kit	Thermofischer Scientific	Cat#K0482lk
Gel Extraction Kit	Thermofischer Scientific	Cat# K0691

(Continued on next page)





Continued		
REAGENT or RESOURCE	SOURCE	IDENTIFIER
Experimental models: Cell lines		
Human Embryonic Kidney 293 cells (HEK 293)	National Centre for Cell Science [NCCS], Pune, India.	N/A
Vero cells (monkey kidney cell),	National Centre for Cell Science [NCCS], Pune, India.	N/A
Hepatocellular carcinoma (HepG2)	National Centre for Cell Science [NCCS], Pune, India.	N/A
Megakaryocyte derived cells (K562)	National Centre for Cell Science [NCCS], Pune, India.	N/A
Oligonucleotides		
NS2B FP- 5'TATGGGATCCGCTGATTTATC ATTGGAGAAA 3'	(Gandikota et al. ⁴⁷)	https://doi.org/10.1002/jmv.26024.
NS2B RP-5'CCCGCCTCCACCACTACCTCCGCC CCCGAGCGTGTCATCTCTCTCTTCAT 3'	Gandikota et al. ⁴⁷)	https://doi.org/10.1002/jmv.26024.
NS2B FP- 5'GCCCCTCAATGAAGGAATTATGG 3'	This paper	N/A
NS2B RP- 5'TGATCTCTGTTTCTTTTTCTGCCA 3'	This paper	N/A
NS3 FP-5'TATG <u>CTCGAG</u> ATGGGATGGTATCTATAGA 3'	This paper	N/A
NS3 RP- 5' GGATGTAGGTCCATTATTGTTAGGT 3'	This paper	N/A
Helicase FP-5'ACATCCAGGATCAGGAAAAACA 3'	This paper	N/A
Helicase RP-5'TATC <u>GGATCC</u> CCCATGTAAATA TACTGG 3' primers.	This paper	N/A
Overlapping Extension PCR NS2B FP 5'GCCCCTCAATGAAGGAATTATGG3'	This paper	N/A
Overlapping Extension PCR NS3 RP 5' GGATGTAGGTCCATTATTGTTAGGT 3'	This paper	N/A
EDRF1 FP-5'TATC <u>GAATTC</u> GCCATGGCTGATT TGTCTACAGACTT 3'	This paper	N/A
EDRF1 RP-5'TATG <u>CTCGAG</u> CTGAAC GGCATTGCTGCT 3'	This paper	N/A
Recombinant DNA		
pRSET-NS2BNS3pro	Gandikota et al. ⁴⁷)	
pEGFP-N1 NS2BNS3pro	This paper	N/A
pEGFP-N1 NS2BNS3helicase	This paper	N/A
pEGFP-N1 NS3prohelicase	(Gandikota et al. ²⁸)	https://doi.org/10.1128/JVI.01178-20.
pCDNA 3.1 c-myc EDRF1	This paper	N/A
mitoRFP vector	(Gandikota et al. ²⁸)	https://doi.org/10.1128/JVI.01178-20.
pEGFP-N1 Vector	(Gandikota et al. ²⁸)	https://doi.org/10.1128/JVI.01178-20.
Software and algorithms		
Image J	ImageJ	https://imagej.nih.gov
Graph pad Prism version.9	Graph pad	https://www.graphpad.com
NIS ELEMENTS AR SOFTWARE	Nikon Microscopes	N/A
cNLS mapper software		https://nlsmapper.iab.keio.ac.jp

RESOURCE AVAILABILITY

Lead contact

Further information and reasonable requests for resources and reagents should be directed to the lead contact, Dr. Musturi Venkataramana (mvrsl@uohyd.ernet.in).

iScience Article



Materials availability

The recombinant constructs developed in the study will be available upon request.

Data and code availability

- All original data reported in this paper will be shared by the lead contact upon request.
- This paper does not report original code.
- Any additional information required to reanalyze the data reported in this paper is available from the lead contact upon request.

EXPERIMENTAL MODEL AND STUDY PARTICIPANT DETAILS

Cell lines

Human Embryonic Kidney 293 cells (HEK 293), Vero cells (monkey kidney cells), Hepatocellular carcinoma (HepG2) and Megakaryocyte derived cells (K562) were obtained from National Centre for Cell Science [NCCS], Pune, India. HEK, HepG2 and Vero cells were maintained in Dulbecco's Modified Eagle's medium (DMEM, Gibco, Invitrogen, USA). K562 cells were maintained in RPMI media (RPMI + L-Gluatamine, Gibco, Invitrogen, USA) at 37°C in a humidified incubator with 5% CO2. Both DMEM and RPMI were supplemented with 10% Fetal Bovine Serum (FBS) and 1% antibiotic containing (vol/vol) penicillin and streptomycin.

METHOD DETAILS

Prediction of nuclear localization signal (NLS)

To identify the nuclear localization signal in NS2BNS3 and NS3, the amino acid sequences were retrieved from the NCBI data base of the in-house characterized DENV1 with Accession no. KX618706.1, Protein id. ASD49618.1. NLS in both the sequences were determined using the cNLS mapper software with a cutoff score of 0.4 and also identified the residues that show the monopartite and bipartite NLS sequences based on classical nuclear localization signal.⁴²

Dengue virus constructs

All the constructs were generated from the in-house characterized DENV1 serotype . pRSET-A NS2BNS3pro (46a.a+185a.a.) clone was generated earlier in our previous study.⁴⁷ NS2BNS3pro consists of hydrophilic domain of NS2B (46a.a) and protease domain of (NS3 185a.a) were linked via a G4-S-G4 linker sequence. NS2B was amplified using NS2B Forward- 5' TATGGGATCCGCTGATTTATCATTGGA GAAA and NS2B Reverse - 5 CCCGCCTCCACCACTACCTCCGCCCCGAGCGTGTCATCTCTCT TCAT 3' primers. NS3pro was amplified using NS3 Forward-5'GGGGGGGGGGTAGTGGTGGAGGCGG GAGAGCAGTTCTTGATGATGGTA and NS3 Reverse 5'ATCGAGAATTCTTACCTAAACACCTCGTCCT CAATC3' primers. The obtained gene products were used as templates with external primers (the above forward primer of NS2B and the reverse primer of NS3) for overlap extension PCR to generate NS2B-G4-S-G4-NS3pro. This amplified DNA was digested with ECoRI and BamHI enzymes and then ligated to the pRSET-A vector. The clone was confirmed by sequencing. In order to develop pEGFP-N1 NS2BNS3pro, the above pRSET-A NS2BNS3pro was used as a template with forward 5' TATGCTCGAGATGGCTGATT TATCATTGGAC 3' and reverse 5' TATCGGATCCGTAAACACCTCGTCCTC 3' primers. The amplified fragment (696 bp) and pEGFP-N1 vector were digested with Xhol/BamHI enzymes and gel purified by gel extraction kit (Thermofisher Scientific). The digested products were ligated using T4 ligase enzyme. Ligated product was transformed into E. Coli. DH5 α competent cells and the isolated plasmid was confirmed with restriction digestion using Xhol/BamHI enzymes. The positive clone pEGFP-N1 NS2BNS3pro was further confirmed by sequencing. pEGFP-N1 NS3pro-helicase (464a.a) construct was also developed during our previous study.²⁸ To develop this construct, NS3pro (185a.a) was amplified using the NS3 forward 5' TATGCTCGAGATGGGATGGTATCTATAGA3' and reverse 5' GGATGTAGGT CCATTATTGTTAGGT 3' primers. Helicase was amplified using forward F 5'ACATCCAGGATCAG GAAAAACA 3' and reverse 5'TATCGGATCCCCCATGTAAATATACTGG 3' primers. The reaction was performed in a final volume of 25 μ l containing 0.5 μ l cDNA template, 2.5 μ l reaction buffer, 0.5 μ l of 10mM dNTPs, 0.25U of Tag polymerase enzyme, 0.5 µl of each of 10 µM forward and reverse primers. Cycling conditions were followed with an initial denaturation step at 95°C for 4 minutes, followed by 35 cycles of 94°C for 30 seconds, 53°C for 30 seconds and 72°C for 1 minute, and final extension at 72°C for 10 minutes. The final products were electrophoresed on 1% agarose gel and purified by gel extraction method. Further





overlapping extension PCR was carried to generate NS3pro-helicase (464a.a) using forward primer of NS3 protease containing *XhoI* restriction site at 5′ end and reverse primer of helicase containing *BamHI* restriction site at 3′ end as mentioned above. The plasmid construct, NS3pro-helicase consists of 185 amino acids protease domain of NS3 and 283 amino acids of helicase domain. The obtained clone was ligated into pJET 1.2 vector and further subcloned into pEGFP-N1 vector using *XhoI/BamHI* restriction sites to obtain pEGFP-N1 NS3pro-helicase (464a.a).

In order to develop pEGFP-N1 NS2BNS3 (130+464=594 a.a), NS2B fragment was amplified using NS2B forward 5' GCCCCTCAATGAAGGAATTATGG 3' and NS2B reverse 5' TGATCTCTTTTTCTGCCA 3' primers. The reaction was performed in a final volume of 25µl containing 0.5µl of cDNA template, 2.5µl reaction buffer, $0.5\mu l$ of 10mM dNTP mix, 0.25U of Taq polymerase enzyme, $0.5\mu l$ of each 10 μM forward and reverse primers. The pTZ57RT-NS2BTA construct that existed in lab was used as a template. Cycling conditions were followed with an initial denaturation step at 95°C for 4 minutes, followed by 35 cycles of 94°C for 30 seconds, 53°C for 30 seconds, 72°C for 1 minute, and final extension at 72°C for 10 minutes. The final products were electrophoresed on 1% agarose gel and purified by gel extraction method and used as templates for overlapping extension PCR. The reaction mixture was prepared by adding the templates, NS2B and NS3pro-helicase (100ng each), 1X buffer, 10mM dNTP and Q5 polymerase. Two step overlapping extension PCR was carried out to join NS2B at the 5' end of NS3pro-helicase: 94°C for 4 minutes, (94°C for 30 seconds, 55°C for 40 seconds, 72°C for 1.4 minutes) 10 cycles followed by 72°C for 15 minutes as a final extension. Later, external primers (NS2B forward & helicase reverse) were added and followed by 35 cycles of second round of PCR, 94°C for 30 seconds, 53°C for 30 seconds, 72°C for 1.4 minutes, and final extension at 72°C for 10 minutes. The obtained fusion fragment was electrophoresed on 0.8% agarose gel and purified by gel extraction method. The overlapping extension PCR amplified product of NS2BNS3 (594 a.a) was ligated into pJET 1.2 using T4 DNA ligase. The ligated product was transformed into E. coli. DH5 α competent cells. Plasmid was isolated, and insert was confirmed by restriction digestion. To sub-clone pJET 1.2 NS2BNS3 into pEGFP-N1 vector, pJET 1.2 NS2BNS3 and pEGFP-N1 vector were subjected to Xhol/HindIII restriction enzyme digestion. 1.8 kbp digested product from pJET1.2 clone was obtained and further ligated to linearized pEGFP-N1 vector. The ligated recombinant was transformed into E. coli. DH5 α competent cells. Plasmid was isolated, and insert was confirmed by restriction digestion and further by sequencing. To clone NS2BNS3pro (S135A) mutant (130+185a.a), NS3pro (S135A) was generated by site directed mutagenesis. The dengue virus NS3 protease inactive mutant was generated by amino acid substitution Ser135 in catalytic triad with Ala using the primers Forward, 5'-TTTTA AACCCGGCACAGCTGGATCTCCC 3' and Reverse, 5'-TCACGATGGGAGATCCAGCTGTGCCGG 3'. Above amplified NS2B (130a.a) and NS3pro (S135A) (185a.a) were overlapped with overlapping extension PCR using forward 5' GCCCCTCAATGAAGGAATTATGG 3' of NS2B at 5' end and reverse 5' GGA TGTAGGTCCATTATTGTTAGGT 3' primers of NS3 at 3' end as described above. The obtained fusion fragment was electrophoresed on 0.8% agarose gel and purified by gel extraction method. NS2BNS3pro (S135A) mutant was ligated to pJET 1.2 blunt end vector using T4 ligase and clone was confirmed using Xhol/HindIII restriction digestion. The digested NS2BNS3pro (S135A) mutant was further subcloned to pEGFP-N1 vector as described above. NS2BNS3 (594 a.a) and NS3pro-helicase (464a.a) are the naturally existing forms of dengue virus infections.¹²

Cloning of EDRF1 in pcDNA3.1 c-myc vector

From K562 cell pellet, total RNA was isolated using Trizol as per manufacturer's protocol. For cDNA synthesis, total isolated RNA was mixed with oligo(dT) primers in sterile RNase free water and reaction was followed up with mixing: total RNA (1µg), oligo(dT) random primer mix (0.5µg/µl), 10 mM dNTP, and RNase free water. The RNA was denatured for 5 minutes at 65°C. Then 10X AMV buffer, AMV Reverse Transcriptase (10U/µl), RNase inhibitor (40U) and RNase free water were added. Total RNA was reverse transcribed using the reaction cycle: 45°C for 50 minutes, 80°C for 5 minutes. The cDNA generated was used as template for amplification of EDRF1 with forward 5′ TATC<u>GAATTC</u>GCCATGGCTGATTTGTCTACAGACTT 3′ and reverse 5′ TATG<u>CTCGAG</u>CTGAACGGCATTGCTGCT 3′ primers. The primers were designed based on the EDRF1 sequence available with accession no NP_001189367.1. The PCR mix contains 10X buffer, 10mM dNTP, forward and reverse primers (10µM each), cDNA (100ng), Taq Polymerase (0.25U) and water. Cycling conditions were followed with an initial denaturation step at 94°C for 5 minutes, followed by 35 cycles of 94°C for 1 minute, 58°C for 30 seconds, 72°C for 1.5 minutes, and final extension at 72°C for 10 minutes. The amplified fragment was run on 1% agarose gel and 1.3 kbp amplified product was obtained. To further clone the amplified fragment in pcDNA3.1 c-myc vector, both the vector and insert were digested





with restriction sites Xhol/ECoRI, ligated and transformed into E. Coli. DH5 α competent cells. The recombinant plasmid was isolated and further confirmed with restriction digestion and sequencing.

Dengue virus protease localization analysis

Transient transfections were performed using the constructs pEGFP-N1 vector, pEGFP-N1 NS2BNS3pro (46a.a+185a.a), pEGFP-N1 NS2BNS3pro (S135A) mutant (130 a.a + 185 a.a) and pEGFP-N1 NS2BNS3 (130 a.a + 464 a.a) in K562 cells. Briefly, one day before transfection, approximately 10^5 cells were seeded in 6-well plate. Transfection was performed with the above mentioned constructs using Lipofectamine 2000 reagent as per manufacture's protocol in ratio (1.5 μ g plasmid and 3μ l Lipofectamine). After 28 hours the cells were harvested, washed with 1X PBS and fixed using 4% paraformaldehyde for 20 minutes. Then the cells were permeablized with 0.25% Triton-X 100 in 1X PBS for 5 minutes, washed with 1X PBS followed by nuclear staining with Hoechst 33342 stain (Molecular probes). The cells washed and resuspended in 1X PBS and Glycerol (1:1) and mounted on to glass slide with a coverslip. The cells were analyzed using laser scanning confocal microscope (Carl Zeiss) at 20X and 100X magnifications. The images were merged in order to observe the co-localizations. The localization color (green/blue) intensity profiles were prepared using NIS Elements AR software program to analyze the GFP (green peak) in nucleus along with Hoechst stain (blue). The fluorescence percentage was calculated using (Mean intensity of each channel/total intensity in nucleus X100). p- values indicated p<0.0001, **** = significant, ns = non-significant.

In order to analyze the cross localizations of NS2BNS3 (in mitochondria) and NS3pro-helicase (in nucleus), we have used MitoRFP vector and Hoechst satin for both the constructs. In this direction, transient transfections were performed in HEK cells using the constructs pEGFP-N1 vector, pEGFP-N1 NS2BNS3 (594 a.a) and pEGFP-N1 NS3pro-helicase (464 a.a) along with MitoRFP vector. HEK cells were seeded onto coverslips in 12 well plate and the plasmid constructs were transfected along with mitoRFP vector (1 μ g to 2 μ Lipofectamine). After 48 hours, the cells were washed with 1X PBS and fixed using 4% paraformaldehyde for 20 minutes and permeablized with 0.25% Triton-X 100 in 1X PBS for 5 minutes, followed up with staining with Hoechst stain (nucleus) and mounting the coverslip with glycerol on to glass slide. The cells were analyzed using laser scanning confocal microscope at 60X magnification and the images were merged for the analysis. The localization intensity profiles were prepared using NIS Elements AR software program. The fluorescence percentage was calculated as above.

Detection of dengue virus protease in subcellular fractions

Similar transfections were performed (pEGFP-N1 vector, pEGFP-N1 NS2BNS3 (594 a.a) and pEGFP-N1 NS3pro-helicase (464 a.a)) as described above in HEK cells. For preparing whole cell lysates, cells were harvested and washed with 1XPBS by centrifuging at 3000rpm for 5 minutes. The cell pellet was resuspended in RIPA buffer, incubated on ice and vortexed 2-3 times in intervals for 15 minutes. The solubilized lysate was centrifuged at 14000rpm for 15 minutes and the supernatant was collected as whole cell lysate. For preparing cytoplasmic and nuclear fractions, cells were washed with ice-cold 1X PBS, mildly homogenized in hypotonic buffer (20mM HEPES, 10mM KCl, 1mM EDTA, 10% glycerol and 0.5% Triton-X100) and incubated for 10 minutes. The homogenized lysate was centrifuged at 2000g at 4°C for 10 minutes. The supernatant collected as cytoplasmic fraction and the pellet was used for nuclear extraction. The pellet was further washed twice with 1XPBS and resuspended in RIPA buffer. The resuspended pellet was incubated for 30 minutes on ice and vortexed at 5 minute intervals. The completely dissolved pellet was allowed for centrifugation at 20,000g for 15 minutes. The supernatant was collected as a nuclear fraction. The lysates were quantified using Bradford reagent and resolved on 10%SDS PAGE and immunoblotted with NS2BNS3pro antibody (1:1000), anti-GFP antibody (1:1000) and actin (1:2500).

In vitro pulldown assay and protein identification

K562 cells were cultured in 100mm dishes. The cells were harvested and lysed with RIPA buffer. The lysate was quantified by Bradford reagent (Bio-Rad) and 250-300μg protein (500μl) lysate was used for pulldown. pRSET-A NS2BNS3pro purified protein (200μg) was allowed for binding to Ni-NTA His beads for 3 hours with gentle rocking and centrifuged for 1 minute at 4° C to remove the unbound protein. K562 cell lysate incubated with the protein bead complex overnight with gentle rocking at 4° C. The complex was centrifuged for 1 minute and unbound proteins were collected as flow through (FT), followed by washes of 10-50mM imidazole (500μl each). The interacting proteins were eluted from washed bead complex using imidazole (100-300mM).





Identification of proteins obtained in the above pull-down experiment

Elutes, FT washes and the bead complex were mixed with 4X Laemmli buffer and boiled for 10 minutes, centrifuged for 1 minute and resolved on 10% SDS PAGE. A similar procedure was followed up with Ni-NTA beads bound to K562 cell extract without purified protein (control). The gel containing the bands were eluted and followed up by MALDI TOFF mass spectrometry analysis (Galaxy International /Sandor Life Sciences Pvt. Ltd.). Further, the above-mentioned flow through, washes and elutes were resolved on 10% SDS PAGE, transferred onto PVDF membrane and probed with anti-EDRF1 antibody (1:3000). The anti-rabbit secondary HRP conjugated antibody was used (1:10000) and the developed image was recorded (Chemidoc, Bio-Rad).

Identification of protease cleavage sites in EDRF1 using in silico methods

Full length EDRF1 protein sequence accession no: Q3B7T1.1, was retrieved from NCBI data base. Protease cleavage sites were identified by using ProP-1.0 Server-DTU Health Tech. Further, the protease and EDRF1 structures were superimposed using auto docking tool to identify the cleavage sites for the protease catalytic triad.

EDRF1 cleavage analysis with co-transfection studies

HEK cells were seeded and allowed to grow up to 80% confluency. pEGFP-N1 NS2BNS3pro (46 a.a + 185 a.a) was transiently co-transfected with pcDNA3.1 c-myc EDRF1. Transfection was done using Lipofectamine 2000 reagent (1:3 ratios) as per the manufacturer's protocol. After 48 hours, cells were harvested and proceeded for western blotting and the cleavage was analyzed using anti-Myc tag (1:1000) and anti-GFP antibodies (1:1000). Secondary HRP-conjugated anti-mouse and anti-rabbit antibodies (1:10000), respectively were used.

Analysis of EDRF1 levels in transfected cell extracts

Cells were seeded at conc. of $5x10^5$ cells/ml in 6 well plates prior to the day of transfection in RPMI growth media with 10% FBS without antibiotic and incubated at 37°C with 5% CO₂. After 12 hours, cells were transfected with pEGFP-N1 vector, pEGFP-N1 NS2BNS3pro, pEGFP-N1 NS2BNS3pro (S135A) mutant, pEGFP-N1 NS2BNS3 (1-5 μ g/ μ l) and allowed to grow for 24 hours. Cells were analyzed for GFP expression using fluorescence microscope. Then the cells were harvested and cell extracts prepared, resolved on 10% SDS PAGE and probed with anti-GFP (1:1000) or anti-NS2BNS3pro (1:5000) or anti-EDRF1 (1:3000) or anti-GATA1 (1:5000) or anti-alpha1 spectrin (1:2500) antibodies (one blot with anti-GFP or anti-NS2BNS3pro or anti-EDRF1; the other blot with anti-GATA1 or anti-alpha1 spectrin). The secondary anti-rabbit HRP-conjugated antibody (1:10000) was used and anti-actin (1:2500) was used and probed with HRP-conjugated anti-mouse secondary antibody (1:10000). The blot was developed and imaged using Chemidoc (Bio-Rad).

Analysis of EDRF1 levels in virus infected cell extracts

Virus infection in Vero cells was performed as described in our earlier studies. ²⁸ For infection of K562 cells, Vero cells propagated viral supernatant was used. A day before infection four dishes of size 100mm were seeded with 10⁶ cells. On the day of infection, cells were harvested and counted using a hemocytometer. Suspension cells were seeded again in 60mm (10⁵) cells per dish and inoculated with viral supernatant in ratio 1:4 dilutions with MoI of 0.09 in serum free RPMI media. The virus was allowed for adsorption for 2-3 hours with mild agitation in 15 minutes' intervals. After the adsorption, the media was replaced with RPMI media containing 5% FBS and cells were allowed to grow for up to 7 days. Uninfected K562 cells were used as control which were also allowed to grow for 7 days. Infection was confirmed with NS2BNS3pro antibody (1:1000). The cells were harvested, cell lysate was prepared and western blotting was carried using anti-EDRF1, anti-GATA1 and anti-alpha1 spectrin antibodies as described above.

EDRF1 and **GrpEL1** levels in clinical samples

Clinical samples (n=44) were classified as DF, DHF and DSS as per WHO guidelines (Table S1). The samples were processed for albumin depletion. Briefly, in 100μ l of serum sample, 1M NaCl was added to final conc of 0.1M and incubated for 60 min at 4°C on rocking. Ice cold ethanol was added to the sample to a 42% concentration and further incubated for 60 min at 4°C. The sample was centrifuged at 14,000 rpm for 45 min at 4°C, and the pellet was stored. Using 0.8 M cold sodium acetate (pH 4.0), the pH of the supernatant was lowered to 5.7 and incubated for 30 min at 4°C. Again, the sample was centrifuged at 14,000 rpm

iScience Article



for 30 min, and the supernatant containing albumin was separated. Both pellets were re-suspended and mixed in 10 mM Tris, pH 6.8 and 1 M urea. The protein concentrations of obtained albumin-depleted samples were estimated by Bradford assay. Samples (10µg) were resolved on a 10% SDS-PAGE gel and immunoblotted with anti-EDRF1 antibody (1:3000) followed by stripping and probed with anti-GrpEL1 antibodies (1:2500). Anti-rabbit secondary HRP-conjugated antibodies (1:10000) were used and the blot was developed as described above.

Bioenergetics of mitochondria in transfected cells

Transient transfection was performed in HepG2 cells with plasmid constructs pEGFP-N1 vector and pEGFP-N1 NS3pro-helicase as per manufacturer's protocol. 28 hours post transfection 7000-8000/well cells were seeded in Agilent Seahorse XFp mini culture plates (8-wells) up to 70% confluency and allowed to grow at 37°C in 5% CO2 incubator, as per the manufacturer's protocol. For the cell mitostress assay, the sensory cartridge was hydrated with milli-Q water one day before at 37°C incubator without CO2. Next day, sensory cartridge is equilibrated with XFp Calibrant solution for 2 hours. Later, the sensory cartridge was filled with three drugs [Oligomycin (1.5 μ M), FCCP (0.5 μ M), Rotenone/Antimycin (0.5 μ M)] as per protocol and XFp cell mitostress assay was performed using Seahorse XFp Analyzer with the in-built software program. ^{48,49}

Cell number analysis during dengue virus infection

2 sets of 60mm dish (10⁵) K562 cells (control, infected) were infected with viral supernatant for 0, 3, 5 and 7 days, harvested and counted manually with trypan blue dye (Sigma) using a hemocytometer. The virus infection was confirmed by RT-PCR of 5' UTR on 5th day. The experiments were performed for three times, the total cell count after each day of infection was taken and an average of two experiments were considered using Microsoft Excel software.

QUANTIFICATION AND STATISTICAL ANALYSIS

The graphs were presented using graph pad prism 9. Experiments were performed at least 3 times and data were represented as means and standard deviations and were statistically analyzed by Student's t-tests and one-way ANOVA analysis. (*), (***), (***) signifies p-values of 0.05,0.005 and 0.0001. (ns) signifies non-significant. All densitometry analysis was done using Image J software.



lekha gandhi <lekha10292@gmail.com>

Fwd: Editorial Decision on STAR Protocols manuscript STAR-PROTOCOLS-D-23-00419R1

1 message

Dr. Musturi Venkataramana <mvrsl@uohyd.ac.in>

Tue, Sep 12, 2023 at 9:26 PM

To: lekha gandhi <lekha10292@gmail.com>

----- Forwarded message ------

From: STAR Protocols <em@editorialmanager.com>

Date: Tue, 12 Sept, 2023, 9:19 pm

Subject: Editorial Decision on STAR Protocols manuscript STAR-PROTOCOLS-D-23-00419R1

To: Musturi Venkataramana <mvrsl@uohyd.ac.in>

Dr. Musturi Venkataramana University of Hyderabad Prof C R Rao Road, Gachibowli Hyderabad 500046 INDIA

Simultaneous detection of dual subcellular localized dengue virus protease by co-transfection STAR-PROTOCOLS-D-23-00419R1

Sep 12, 2023

Dear Dr. Venkataramana,

I am pleased to let you know that, based on your revisions and the reviewer comments below, your Protocol has now been "accepted in principle" as at STAR Protocols.

Before we can formally accept your manuscript, we require that the final files are uploaded according to our production guidelines as outlined in our Final Files Checklist. We will not be able to accept your paper until all the steps have been followed accurately. Please email us at starprotocols@cell.com if you have any questions. We would like to have your final materials within 10 days, but please let us know if you need more time. If you need additional time to address the concerns that came up in the review process, please let us know so we can discuss a plan for moving your paper forward.

Please include your responses to these items as your response to reviewers when you upload the final files.

- Please address the minor reviewer comments appended below.
- Go through the full final files checklist as well as the items below to prevent delays in publication.
- Please see our most recent article template to help you in preparing your final manuscript.
- Timing must be included with each major step. It is also possible to include additional timing notes for sub steps, but only if the total time for the major step is included.

Title page and Summary

- On the title page of the manuscript, please indicate who will serve as the **lead contact and technical contact**; **include email addresses for both contacts**. For more information on the responsibilities of each, please refer to our information for authors page.
- The summary is a paragraph no longer than 80 words and should describe the protocol. The background should ideally only take up one sentence while the rest of the summary should focus on each of the major steps using an active voice and present tense.

1 of 4 9/28/2023, 11:11 AM

REVIEW Open Access

Check for updates

Respiratory illness virus infections with special emphasis on COVID-19

Lekha Gandhi, Deepti Maisnam, Deepika Rathore, Preeti Chauhan, Anvesh Bonagiri and Musturi Venkataramana*

Abstract

Viruses that emerge pose challenges for treatment options as their uniqueness would not know completely. Hence, many viruses are causing high morbidity and mortality for a long time. Despite large diversity, viruses share common characteristics for infection. At least 12 different respiratory-borne viruses are reported belonging to various virus taxonomic families. Many of these viruses multiply and cause damage to the upper and lower respiratory tracts. The description of these viruses in comparison with each other concerning their epidemiology, molecular characteristics, disease manifestations, diagnosis and treatment is lacking. Such information helps diagnose, differentiate, and formulate the control measures faster. The leading cause of acute illness worldwide is acute respiratory infections (ARIs) and are responsible for nearly 4 million deaths every year, mostly in young children and infants. Lower respiratory tract infections are the fourth most common cause of death globally, after non-infectious chronic conditions. This review aims to present the characteristics of different viruses causing respiratory infections, highlighting the uniqueness of SARS-CoV-2. We expect this review to help understand the similarities and differences among the closely related viruses causing respiratory infections and formulate specific preventive or control measures.

Keywords: COVID-19, Respiratory virus infections, Influenza viruses, SARS, MERS

Introduction

Studies on viruses and viral diseases have been carried out in science, medicine, and agriculture for hundreds of years, leading to the emergence of virology as a separate branch of microbiology. Viral epidemics and pandemics occur periodically throughout the world. Virologists have contributed well to virus research to understand the structural organization, cellular mechanisms, vaccination, and antiviral molecules against many viruses. In the 1900s, WHO eradication efforts of some viruses such as smallpox, cowpox, measles, rabies and poliomyelitis brought significant advancement in controlling and preventing the diseases and understanding the viral replication, transmission,

pathogenesis, cellular functions and disease manifestation. Despite large diversity, they share common principles to enable the infection. Another conserved feature between viruses is activating cell signalling processes when interacting with cells [1]. In this direction, studies are required to decipher the characteristics of many viruses causing diseases [2]. Viruses infect almost all living organisms, including bacteria, fungi, fish, birds, plants, animals, and humans. There are different ways of virus transmission, such as vector borne, blood borne, aerosol borne, etc. [3]. The compatible receptors mostly decide this host range on the tissues or the cells [4]. Similarly, within the host organ/ tissue, tropism is also directed by the presence of specific receptors for different viruses. As another aspect of viruses, the Baltimore system of classification of viruses divides the viruses into seven different classes based on the messenger RNA (mRNA) formation from

Department of Biotechnology and Bioinformatics, School of Life Sciences, University of Hyderabad, Hyderabad 500046, Telangana, India



© The Author(s) 2022. **Open Access** This article is licensed under a Creative Commons Attribution 4.0 International License, which permits use, sharing, adaptation, distribution and reproduction in any medium or format, as long as you give appropriate credit to the original author(s) and the source, provide a link to the Creative Commons licence, and indicate if changes were made. The images or other third party material in this article are included in the article's Creative Commons licence, unless indicated otherwise in a credit line to the material. If material is not included in the article's Creative Commons licence and your intended use is not permitted by statutory regulation or exceeds the permitted use, you will need to obtain permission directly from the copyright holder. To view a copy of this licence, visit http://creativecommons.org/licenses/by/4.0/. The Creative Commons Public Domain Dedication waiver (http://creativecommons.org/publicdomain/zero/1.0/) applies to the data made available in this article, unless otherwise stated in a credit line to the data.

^{*}Correspondence: mvrsl@uohyd.ernet.in





Mitochondrial Import of Dengue Virus NS3 Protease and Cleavage of GrpEL1, a Cochaperone of Mitochondrial Hsp70

Chaitanya Gandikota, Fareed Mohammed, Lekha Gandhi, Deepti Maisnam, Ushodaya Mattam, Deepika Rathore, Arpan Chatterjee, Katyayani Mallick, Arcy Billoria, V. S. V. Prasad, Naresh Babu Venkata Sepuri, Musturi Venkataramana

^aDepartment of Biotechnology and Bioinformatics, School of Life Sciences, University of Hyderabad, Hyderabad, Telangana, India

ABSTRACT Dengue virus infections, which have been reported in nearly 140 countries, pose a significant threat to human health. The genome of dengue virus encodes three structural and seven nonstructural (NS) proteins along with two untranslated regions, one each on both ends. Among them, dengue protease (NS3) plays a pivotal role in polyprotein processing and virus multiplication. NS3 is also known to regulate several host proteins to induce and maintain pathogenesis. Certain viral proteins are known to interact with mitochondrial membrane proteins and interfere with their functions, but the association of a virus-coded protein with the mitochondrial matrix is not known. In this report, by using in silico analysis, we show that NS3pro alone is capable of mitochondrial import; however, this is dependent on its innate mitochondrial transport signal (MTS). Transient-transfection and protein import studies confirm the import of NS3pro to the mitochondrial matrix. Similarly, NS3pro-helicase (amino acids 1 to 464 of NS3) also targets the mitochondria. Intriguingly, reduced levels of matrix-localized GrpE protein homolog 1 (GrpEL1), a cochaperone of mitochondrial Hsp70 (mtHsp70), were noticed in NS3pro-expressing, NS3pro-helicase-expressing, and virus-infected cells. Upon the use of purified components, GrpEL1 undergoes cleavage, and the cleavage sites have been mapped to KR81A and QR92S. Importantly, GrpEL1 levels are seriously compromised in severe dengue virus-infected clinical samples. Our studies provide novel insights into the import of NS3 into host mitochondria and identify a hitherto unknown factor, GrpEL1, as a cleavage target, thereby providing new avenues for dengue virus research and the design of potential therapeutics.

IMPORTANCE Approximately 40% of the world's population is at risk of dengue virus infection. There is currently no specific drug or potential vaccine for these infections. Lack of complete understanding of the pathogenesis of the virus is one of the hurdles that must be overcome in developing antivirals for this virus infection. In the present study, we observed that the dengue virus-coded protease imports to the mitochondrial matrix, and our report is the first ever of a virus-coded protein, either animal or human, importing to the mitochondrial matrix. Our analysis indicates that the observed mitochondrial import is due to an inherited mitochondrial transport signal. We also show that matrix-localized GrpE protein homolog 1 (GrpEL1), a cochaperone of mitochondrial Hsp70 (mtHsp70), is also the substrate of dengue virus protease, as observed *in vitro* and *ex vivo* in virus-infected cells and dengue virus-infected clinical samples. Hence, our studies reveal an essential aspect of the pathogenesis of dengue virus infections, which may aid in developing antidengue therapeutics.

KEYWORDS dengue virus, NS3, GrpEL1, GrpEL2, mtHsp70, mitochondria

Citation Gandikota C, Mohammed F, Gandhi L, Maisnam D, Mattam U, Rathore D, Chatterjee A, Mallick K, Billoria A, Prasad VSV, Sepuri NBV, Venkataramana M. 2020. Mitochondrial import of dengue virus NS3 protease and cleavage of GrpEL1, a cochaperone of mitochondrial Hsp70. J Virol 94:e01178-20. https://doi.org/10.1128/JVI.01178-20.

Editor Susana López, Instituto de Biotecnologia/UNAM

Copyright © 2020 American Society for Microbiology. All Rights Reserved.

Address correspondence to Naresh Babu Venkata Sepuri, nareshuohyd@gmail.com, or Musturi Venkataramana, mvrsl@uohyd.ernet.in.

Received 12 June 2020 Accepted 13 June 2020

Accepted manuscript posted online 24 June 2020

Published 17 August 2020

^bDepartment of Biochemistry, School of Life Sciences, University of Hyderabad, Hyderabad, Telangana, India

^cLotus Children's Hospital, Lakdikapul, Hyderabad, Telangana, India

> J Med Virol. 2021 Jun;93(6):3312-3321. doi: 10.1002/jmv.26024. Epub 2020 Sep 30.

A novel anti-NS2BNS3pro antibody-based indirect ELISA test for the diagnosis of dengue virus infections

Chaitanya Gandikota ¹, Lekha Gandhi ¹, Deepti Maisnam ¹, Muppuru Muni Kesavulu ², Arcy Billoria ³, Vankayalapati Sri Venkateswara Prasad ³, Musturi Venkataramana ¹

Affiliations + expand

PMID: 32418268 DOI: 10.1002/jmv.26024

Abstract

Dengue virus reportedly circulates as four genetically distinct serotypes for which there is no widely accepted vaccine or drug at present. Morbidity and mortality caused by this virus are alarming for the possible increased threat to human health. A suitable diagnostic test is the prerequisite for designing and developing control measures. But, the tests being employed at present possess one or the other drawback for this disease diagnosis. During the dengue virus infections, NS2B is essential for the stability and catalytic activity of the NS3 protease. N-terminal 185 amino acids of NS3 protease domain along with hydrophilic portion of NS2B (NS2BNS3pro) is being used to screen dengue inhibitors but not for diagnosis until now. In the present study, we have used purified NS2BNS3pro as an antigen to trap anti-NS2BNS3pro antibodies of the clinical samples. Antibodies were detected successfully in both Western blot analysis and enzyme-linked immunosorbent assay (ELISA) tests. In ELISA, antibodies were detected in both primary and secondary infections of all serotypes.

Medicinal Chemistry Research https://doi.org/10.1007/s00044-020-02660-y

ORIGINAL RESEARCH





Design, synthesis, and evaluation of different scaffold derivatives against NS2B-NS3 protease of dengue virus

Lata R. Ganji¹ · Lekha Gandhi² · Venkataramana Musturi² · Meena A. Kanyalkar o¹

Received: 17 June 2020 / Accepted: 27 October 2020 © Springer Science+Business Media, LLC, part of Springer Nature 2020

Abstract

The number of deaths or critical health issues is a threat in the infection caused by Dengue virus, which complicates the situation, as only symptomatic treatment is the current solution. In this regard we have targeted the dengue protease NS2B-NS3 that is responsible for the replication. The series was designed with the help of molecular modeling approach using docking protocols. The series comprised of different scaffolds viz. cinnamic acid analogs (CA1–CA11), chalcone (C1–C10) and their molecular hybrids (Lik1–Lik10), analogs of benzimidazole (BZ1-BZ5), mercaptobenzimidazole (BS1-BS4), and phenylsulfanylmethylbenzimidazole (PS1-PS4). Virtual screening of various natural phytoconstituents was employed to determine the interactions of designed analogs with the residues of catalytic triad in the active site of NS2B-NS3. We have further synthesized the selected leads. The synthesized analogs were evaluated for the cytotoxicity and NS2B-NS3 protease inhibition activity and compared with known anti-dengue natural phytoconstituent quercetin as the standard. CA2, BZ1, and BS2 were found to be more potent and efficacious than the standard quercetin as evident from the protease inhibition assay.

Keywords Dengue virus · NS2B-NS3 protease · Molecular modeling · Protease inhibition

Introduction

Dengue virus (DENV) is categorized as a pandemic, affecting most of the population in India and the globe. DENV belongs to *Flaviviridae* and the infection is transmitted by mosquitoes' specifically *A. aegypti*. DENV exists in five different serotypes (DENV 1–5) [1] and protection against all these types is a real challenge. DENV consists of positive single-stranded RNA virus that encodes a polyprotein with ten viral proteins, out of which three are structural (cap, envelope and membrane) and seven are nonstructural (NS1, NS2A, NS2B, NS3, NS4A, NS4B, and NS5).

Supplementary information The online version of this article (https://doi.org/10.1007/s00044-020-02660-y) contains supplementary material, which is available to authorized users.

Meena A. Kanyalkar meenatul@gmail.com

Published online: 17 November 2020

- Department of Pharmaceutical Chemistry, Prin. K. M. Kundnani College of Pharmacy, Plot 23, Jote Joy Building Rambhau Salgaonkar Marg, Cuffe Parade, Mumbai 400005, India
- Department of Biotechnology and Bioinformatics, School of Life Sciences, University of Hyderabad, Hyderabad, Telangana, India

Several scientists targeted some of the above vital DENV proteins generating important synthetic leads with variable degree of antiviral activity. Similarly, some natural phytoconstituents are reported as potential anti-DENV agents. Among all the targets available, NS2B-NS3 is considered as an important target of DENV. NS3 protease is associated with co-factor NS2B via a Gly-Ser linker, together believed to be involved in the DENV replication activity. NS3 is a trypsin-like serine protease and composed of two domains, N-terminal and C-terminal, consisting together of 618 amino acids. The N-terminal known as protease domain, consists of 1-180 residues whereas C-terminal is known as helicase domain with 180-618 residues. Although, NS3 with NS2B is believed to be responsible for the activity but the catalytic triad (His51, Asp75, and Ser135) is located in the NS3 protease domain [2-4]. It is reported that, only a part of NS2B is known to be important for NS2B-NS3 protease activity. Molecules that directly or indirectly inhibit this protease activity can hinder DENV infection. In India, during recent outbreak, Carica papaya leaves extract emerged as one of the therapeutic options and is believed to increase the platelet count in dengue-infected patients [5, 6]. The chief constituents of papaya leaves extract include quercetin (i), caffeic acid (ii), p-coumeric acid (iii), kaempferol (iv),



(19) INDIA

(22) Date of filing of Application :12/04/2019 (43) Publication Date : 16/10/2020

(54) Title of the invention: DESIGN, SYNTHESIS AND EVALUATION OF B4N (DUHSLBTMV16072018-1) AND T4N (DUHSLBTMV16072018-2), THE DERIVATIVES OF NORDIHYDRO GUAIRETIC ACID (NDGA) AS POTENTIAL INHIBITORS OF DENGUE VIRUS PROTEASE

	:A61K0031050000,	(71)Name of Applicant:
	A61K0031090000,	1)UNIVERSITY OF HYDERABAD
(51) International classification	A61K0031404000,	Address of Applicant :Prof. C.R Rao Road, Gachibowli-
	A61K0045060000,	500046, Hyderabad, Telangana, India Telangana India
	C07C0043230000	(72)Name of Inventor:
(31) Priority Document No	:NA	1)CHAITANYA .G
(32) Priority Date	:NA	2)LEKHA GANDHI
(33) Name of priority country	:NA	3)PROF. NARESH BABU SEPURI
(86) International Application No	:NA	4)Y. RAVIKUMAR
Filing Date	:NA	5)Dr. MUSTURI VENKATARAMANA
(87) International Publication No	: NA	
(61) Patent of Addition to Application	:NA	
Number	:NA	
Filing Date	.INA	
(62) Divisional to Application Number	:NA	
Filing Date	:NA	
(57) A1		I .

(57) Abstract:

The present invention relates to derivatives of Nordihydroguaiaretic acid (NDGA), especially heterocyclic derivatives of NDGA of compound of formula (I) where R is as described herein in the description. The present invention also relates to the pharmaceutically acceptable salts and solvates of these compounds. In addition the present invention also relates to the method of inhibiting dengue viral protease to treat dengue viral infections.

No. of Pages: 39 No. of Claims: 8





क्रम सं/SL No :044154208



सत्यमेवा जयते य भारत सरकार.

पेटेंट कार्यालय, भारत सरकार च केवल पेटेंट प्रमाण पत्र

The Patent Office, Government Of India

Patent Certificate

(Rule 74 of The Patents Rulese)

ामगरित **सि** मिरिटे " एंगिमिः एस प्रि प्रस्ति हिंगीना

पेटेंट सं. / Patent No.

دفتر، هندستان, बौद्धिक सम्पत्ति व(पेदेंदर्गनेयमुवकारनियम,74)

आवेदन सं. / Application No. : 201941014858

भारत सरकार, Intellectual Property Office, Government of India. বৌদ্ধিক সম্পত্তিৰ কাৰ্যালয়, ভাৰত

भारत स फाइला करने की तारीख / Date of Filingnen of Initia, वि12/04/2019

पेटेंटी / Patentee केंक्टार्क बोद्धिक संपदा कार्यालय: भारत UNIVERSITY OF HYDERABAD एउ

एतद्वारा प्रमाणित किया जाता है कि पेटेंटी को उपरोक्त आवेदन में यथाप्रकटित DESIGN, SYNTHESIS AND EVALUATION OF B4N (DUHSLBTMV16072018-1) AND T4N (DUHSLBTMV16072018-2), THE DERIVATIVES OF NORDIHYDRO GUAIRETIC ACID (NDGA) AS POTENTIAL INHIBITORS OF DENGUE VIRUS PROTEASE नामक आविष्कार के लिए, पेटेंट अधिनियम, 1970 के उपबंधों के अनुसार आज तारीख अप्रैल 2019 के बारहवें दिन से बीस वर्ष की अविध के लिए पेटेंट अनुदत्त किया गया है।

It is hereby certified that a patent has been granted to the patentee for an invention entitled DESIGN, SYNTHESIS AND EVALUATION OF B4N (DUHSLBTMV16072018-1) AND T4N (DUHSLBTMV16072018-2), THE DERIVATIVES OF NORDIHYDRO GUAIRETIC ACID (NDGA) AS POTENTIAL INHIBITORS OF DENGUE VIRUS PROTEASE as disclosed in the above mentioned application for the term of 20 years from the 12th day of April 2019 in accordance with the provisions of the Patents Act,1970.

अनुदान की तारीख : 02/06/2023 Date of Grant : **टिप्पणी** - इस पेटेंट के नवीकरण के लिए फीस, यदि इसे बनाए रखा जाना है, अप्रैल 2021 के बारहवें दिन को और उसके पश्चात प्रत्येक वर्ष मे उसी दिन देय होगी।

Note. - The fees for renewal of this patent, if it is to be maintained, will fall / has fallen due on 12th day of April 2021 and on the same day

सरकार, घेंपिव मंपडी स्टउत, ਭातउ मतवात, Ф७७७७ ७२८७८ ७२८७७ ७७८७७, ७७७०७७.८, Ф७७०७०, बौद्धिक संपदा चा कार्यालय, भारत सरकार, ବୌଦ୍ଧିକ ସମ୍ପଦ

in every year thereafter







International Conference on Virus Evolution, Infection and Disease Control (ICVEIDC)

Dept. of Biotechnology & Bioinformatics, School of Life Sciences, University of Hyderabad, Hyderabad - 500046, India.

15th to 17th December 2022

Certificate

This is to certify that Mr / Ms / Mrs. Lekha Landhi from University of Hyderahae has been awarded the Best Oral / Poster award for the presentation entitled. Differential localization
The regite virus providences and convequences
in "International Conference on Virus Evolution, Infection and Disease Control (ICVEIDC)" organized by
Department of Biotechnology and Bioinformatics (DoBB), School of Life Sciences, University of Hyderabad, Hyderabad during December 15-17, 2022.
Convener.

ICVEIDC-2022



International Conference of Virology

(VIROCON 2020)

on

Evolution of Viruses and Viral Diseases

February 18-20, 2020

Organized by Indian Virological Society

in collaboration with

Indian National Science Academy

Certificate of Participation

This is to certify that

Lekha Gandhi

University of Hyderabad, Hyderabad, Telangana has presented a Poster / Oral / Lead Talk entitled

Idetification and evaluation of novel dengue virus (DENV 1) ns2bns3 (protease) inhibitors

in the International Conference of Virology

held at Indian National Science Academy, New Delhi, India

Prof. V K. Baranwal

Organizing Secretary

VIROCON 2020

Dr. Govind P Rao

Secretary General, IVS

VIROCON 2020



International Conference on Innovations in Pharma and Biopharma Industry:



"Challenges and Opportunities for Academy and Industry"

20th - 22nd December 2017

Certificate of Participation

This is to certify that Pr	of. / Dr. /Mr. / Ms	Lekha	Fandhi .		
talk / Oral / Poster Bioinformatics, School from 20-22 Dec 2017.	session of ICI	PBI-2017 hel	d in Departme	ent of Biotechnol yderabad – 500 04	

Prof. P. Prakash Babu Convener

Prof. Anand K. Kondapi

Prof. K.P.M.S.V. Padmasree



AS-UoH Joint Workshop on **Frontiers in Life Sciences**



Septemeber 16-17, 2016



This is to certify that Dr/Ms/Mr. Lekha yandhi

has

participated/presented a poster in AS-UoH Joint Workshop on Frontiers in Life Sciences organized during Septemeber 16-17, 2016 at SLS Auditorium, University of Hyderabad, Hyderabad, India.

Sue L-CL Dr. Sue Lin-Chao Coordinator Academia Sinica

Dr. J.S.S. Prakash Coordinator

University of Hyderabad





Department of Biotechnology and Bioinformatics School of Life Sciences University of Hyderabad Hyderabad 500046

Plagiarism Free certificate

This is to certify that similarity index of this thesis has been checked by the library of University of Hyderabad is 38%. Out of this 30% (26 &14%) similarity has been found to be identify from the candidate own publications which forms the major part of the thesis. The details of student publications are as follows:

- Differential localisation of dengue virus protease affects cell homeostasis and triggers to thrombocytopenia (Similarity index 16% and 14%)
- Mitochondrial import of dengue virus NS3 protease and cleavage of GrpEL1, a cochaperon of mtHSP70 (Similarity index<1).

About 8% similarity was identified from the external source in the present thesis which is according to prescribed regulations of the university. All the publications related to thesis have been appended at the end of thesis. Hence, the present thesis considered to be plagiarism free.

Dr. Musturi Venkataramana
Dr. Musturi Venkataramana
Dept. of Blote Shoology
School of Life Sciences
Supervisor Hyderabad
Gachibowii, Hyd-500 046. India.

Studies on subcellular localization of dengue virus protease, consequential effects on cell homeostasis and evaluation of anti-protease molecules.

by Lekha Gandhi

Submission date: 27-Sep-2023 02:32PM (UTC+0530)

Submission ID: 2178376624

File name: Lekha Gandhi.docx (30.58M)

Word count: 24167

Character count: 139343

Librarian

Indira Gandhi Memorial Library UNIVERSITY OF HYDERABAD Central University P.O. HYDERABAD-500 046. studies on subcellular localization of dengue virus protease, consequential effects on cell homeostasis and evaluation of anti-protease molecules.

ORIGINALITY REPORT

33% INTERNET SOURCES

35% **PUBLICATIONS**

STUDENT PAPERS

e. Ne Printestu

PRIMARY SOURCES

- Lekha Gandhi, Deepti Maisnam, Deepika Rathore, Preeti Chauhan, Anvesh Bonagiri, Musturi Venkataramana. "Differential localization of dengue virus protease affects 1 6. B. Kuinstelling cell homeostasis and triggers to thrombocytopenia", iScience, 2023 Publication
 - www.ncbi.nlm.nih.gov Internet Source
- Submitted to University of Hyderabad, Hyderabad Student Paper

Chaitanya Gandikota, Fareed Mohammed, Lekha Gandhi, Deepti Maisnam et al. "Mitochondrial import of dengue virus NS3 protease and cleavage of GrpEL1, a cochaperone of mtHsp70", Journal of Virology, Venkataram d-500 046. Indla.

5	www.mdpi.com Internet Source	<1%
6	www.biorxiv.org Internet Source	<1%
7	Nikita Nanaware, Anwesha Banerjee, Satarupa Mullick Bagchi, Parikshit Bagchi, Anupam Mukherjee. "Dengue Virus Infection: A Tale of Viral Exploitations and Host Responses", Viruses, 2021	<1%
8	discovery.ucl.ac.uk Internet Source	<1%
9	pdfs.semanticscholar.org Internet Source	<1%
10	ir.ymlib.yonsei.ac.kr Internet Source	<1%
11	etheses.whiterose.ac.uk Internet Source	<1%
12	core.ac.uk Internet Source	<1%
13	elifesciences.org Internet Source	<1%
14	link.springer.com Internet Source	<1%

15	dokumen.pub Internet Source	<1%
16	Submitted to Higher Education Commission Pakistan Student Paper	<1%
17	www.nature.com Internet Source	<1%
18	doras.dcu.ie Internet Source	<1%
19	"Dengue and Zika: Control and Antiviral Treatment Strategies", Springer Science and Business Media LLC, 2018 Publication	<1%
20	"Emerging Human Viral Diseases, Volume I", Springer Science and Business Media LLC, 2023 Publication	<1%
21	Submitted to University of Sydney Student Paper	<1%
22	Prabhudutta Mamidi, Tapas Kumar Nayak, Abhishek Kumar, Sameer Kumar et al. "MK2a inhibitor CMPD1 abrogates chikungunya virus infection by modulating actin remodeling pathway", Cold Spring Harbor Laboratory, 2021 Publication	<1%

23	hdl.handle.net Internet Source	<1%
24	livrepository.liverpool.ac.uk Internet Source	<1%
25	nagoya.repo.nii.ac.jp Internet Source	<1%
26	pure.tue.nl Internet Source	<1%
27	repository.helmholtz-hzi.de Internet Source	<1%
28	research-information.bris.ac.uk Internet Source	<1%
29	www.trademarkelite.com Internet Source	<1%
30		<1 _%
_	Internet Source www.zhb.uni-luebeck.de	<1% <1% <1%
30	www.zhb.uni-luebeck.de Internet Source edepositireland.ie	<1% <1% <1% <1%
31	www.zhb.uni-luebeck.de Internet Source edepositireland.ie Internet Source pubmed.ncbi.nlm.nih.gov	<1% <1% <1% <1% <1% <1%

35	Laura Mónica Álvarez-Rodríguez, Angel Ramos-Ligonio, José Luis Rosales-Encina, María Teresa Martínez-Cázares et al. "Expression, Purification, and Evaluation of Diagnostic Potential and Immunogenicity of a Recombinant NS3 Protein from All Serotypes of Dengue Virus", Journal of Tropical Medicine, 2012 Publication	<1%
36	Nunes Duarte dos Santos, C "Determinants in the Envelope E Protein and Viral RNA Helicase NS3 That Influence the Induction of Apoptosis in Response to Infection with Dengue Type 1 Virus", Virology, 20000901	<1%
37	aem.asm.org Internet Source	<1%
38	eprints.qut.edu.au Internet Source	<1%
39	sbv.org.br Internet Source	<1%
40	swat.tamu.edu Internet Source	<1%
41	Balasubramanian, Anuradha, Mark Manzano, Tadahisa Teramoto, Rajendra Pilankatta, and Radhakrishnan Padmanabhan. "High- throughput screening for the identification of	<1%

small-molecule inhibitors of the flaviviral protease", Antiviral Research, 2016.

Publication

42	Kavithambigai Ellan, Ravindran Thayan, Jegadeesh Raman, Kazuya I. P. J. Hidari, Norizah Ismail, Vikineswary Sabaratnam. "Anti-viral activity of culinary and medicinal mushroom extracts against dengue virus serotype 2: an in-vitro study", BMC Complementary and Alternative Medicine, 2019 Publication	<1%
43	diposit.ub.edu Internet Source	<1%
44	journals.plos.org Internet Source	<1%
45	jvi.asm.org Internet Source	<1%
46	msbmb.org Internet Source	<1%
47	www.freepatentsonline.com Internet Source	<1%
48	Submitted to University of KwaZulu-Natal Student Paper	<1%
49	Wang, T "Biotin-ubiquitin tagging of mammalian proteins in Escherichia coli",	<1%

Protein Expression and Purification, 200307

Publication

50	bdpsjournal.org Internet Source	<1%
51	Submitted to Brunel University Student Paper	<1%
52	Submitted to Monmouth University Student Paper	<1%
53	d-nb.info Internet Source	<1%
54	dea.lib.unideb.hu Internet Source	<1%
55	www.hindawi.com Internet Source	<1%
56	www.umweltbundesamt.at Internet Source	<1%

Exclude quotes On Exclude bibliography On Exclude matches < 14 words